NASA CP-2244

THE SPACE TELESCOPE OBSERVATORY

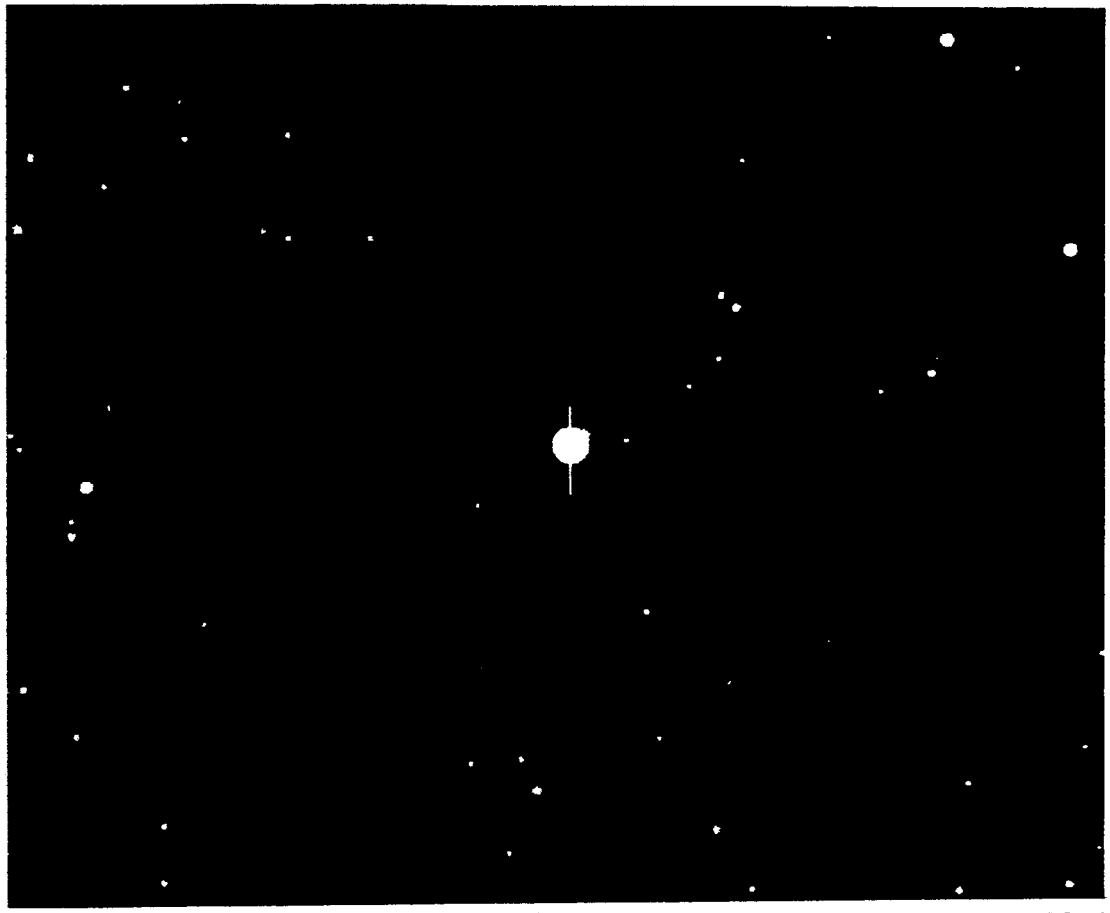

SPECIAL SESSION OF COMMISSION 44, IAU 18TH GENERAL ASSEMBLY • PATRAS, GREECE • AUGUST, 1982

ORGANIZED BY

THE EUROPEAN SPACE AGENCY AND THE NATIONAL AERONAUTICS AND SPACE ADMINISTRATION

SPACE TELESCOPE SCIENCE INSTITUTE

NASA
National Aeronautics and Space Administration

NASA CP-2244

THE SPACE TELESCOPE OBSERVATORY

SPECIAL SESSION OF COMMISSION 44, IAU 18TH GENERAL ASSEMBLY • PATRAS, GREECE • AUGUST, 1982

ORGANIZED BY

THE EUROPEAN SPACE AGENCY AND THE NATIONAL AERONAUTICS AND SPACE ADMINISTRATION

Edited by
Donald N.B. Hall
Space Telescope Science Institute

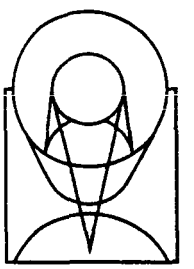

SPACE TELESCOPE SCIENCE INSTITUTE

Operated by the Association of Universities for Research in Astronomy Inc., for the National Aeronautics and Space Administration under Contract NAS5-26555

National Aeronautics
and Space Administration

**Scientific and Technical
Information Branch**

1982

CONTENTS

PREFACE

The Space Telescope, the first large-aperture, long-term optical and ultraviolet observatory to be launched into space, is rapidly approaching realization. By the next IAU General Assembly in 1985, the telescope should be available for scheduling of observations by general observers.

The overall Space Telescope Project operates under the direction of the National Aeronautics and Space Administration's George C. Marshall Space Flight Center, with Goddard Space Flight Center managing the focal plane instruments, mission operations, and the Space Telescope Science Institute contract.

The present volume consists of the ten papers presented at a special session of IAU Commission 44 held in Patras, Greece, during the 18th General Assembly, August 1982. The session was jointly sponsored by the European Space Agency and NASA. The papers, authored by individuals or groups who have played a major role in the development of the observatory, deal with the performance of the telescope and instruments and with plans for observations and data reduction and analysis. The papers are particularly significant, because, in most cases, the projected performance of the observatory is extrapolated from measurements of properties of actual components. Together, they represent an up-to-date overview of the observatory's scientific potential as perceived by the scientists currently involved in its development.

The editor wishes gratefully to acknowledge the numerous contributions that have made this volume possible. All of the authors provided camera-ready copy on schedule, far enough in advance of the actual session to allow printing of this volume for distribution at the General Assembly. The cover image is a simulation, by Dr. J. Kristian, of a 3000-second V band integration with the wide-field mode of the wide field/planetary camera, in which sources as faint as $m_v = 28$ are discernible. Goddard Space Flight Center undertook the printing and shipping of the volume, and Professor C. L. Goudas and the IAU Local Organizing Committee in Patras arranged its distribution to participants at the General Assembly. Ms. Kimberly Apple of the Space Telescope Science Institute coordinated arrangements with the authors, Goddard Space Flight Center, and the Local Organizing Committee.

N82 33297

Science Operations with Space Telescope

Riccardo Giacconi

Space Telescope Science Institute
Homewood Campus
Baltimore, Maryland 21218

Introduction

When Space Telescope begins operations in 1985, it will provide a major improvement in observational capabilities for optical astronomy. It will, in some sense, represent the first qualitative improvement in telescope capabilities in the optical domain since the completion in 1948 of the 200" Hale Telescope at Palomar Mountain.

The unique capabilities of Space Telescope derive from the fact that the Observatory will be placed into orbit around the earth, and, therefore, its "seeing" will be unaffected by the obscuring and distorting effects of the earth's atmosphere. This will allow the attainment of an angular resolution, a sensitivity, and a wavelength coverage unachievable from the ground.

Space Telescope (ST) is provided with a diverse complement of focal plane instruments, including cameras and spectrometers, which can be changed and improved over time. It will be used as a general purpose observatory available to astronomers from all over the world to carry out studies impinging on all areas of current astronomical interest.

Space Telescope will be inserted into orbit and serviced by the National Aeronautics and Space Administration (NASA) Space Transportation System (Fig. 1). It is the insurance provided by this system--that a payload can be delivered into orbit in working condition and can be repaired and maintained as necessary over two decades--which justifies the large capital investment in this facility.

Communications to and from Space Telescope will occur through the Tracking and Data Relay Satellite System (TDRSS), a system of geostationary communication satellites which are currently being installed.

After reception at Goddard Space Flight Center (GSFC), the data will be transmitted to a newly created Space Telescope Science Institute (ST ScI) which will have responsibility for science operations. The ST ScI will select observations, prepare observing plans, issue (through GSFC) commands to the spacecraft, receive, reduce, analyze, and archive the data and distribute it to the observers. It will also be a first rank research institution with a resident staff of astronomers charged with the task of maximizing the scientific return from Space Telescope. Although this mode of operation is conventional in ground-based observatories, it represents a first for NASA.

Space Telescope will, therefore, be the first major user of many of the general space systems capabilities which are now being developed as well as the first major orbiting observatory whose scientific management has been delegated by NASA to an independent institute managed by the astronomers themselves.

In addition, therefore, to its intrinsic interest, the ST Project is an important first step in the establishment of permanent observational capabilities for astronomy in space; ST is a test bed for developing the necessary technology and operational experience that will permit implementation of the full array of spaceborne radio, infrared (IR), optical, ultraviolet (UV), and X-ray telescopes, which are anticipated to follow in the next two decades.

It should be stressed that even in this context, Space Telescope is a bold and significant first step, and we are quite confident in our expectation that observations with Space Telescope will be at the cutting edge of much of the astronomical research of the next decade.

The purpose of this symposium is to acquaint the international community of potential users with the design and performance characteristics of the Space Telescope and its first generation complement of instruments, with some detail of current operation plans and with some aspects of the expected scientific returns.

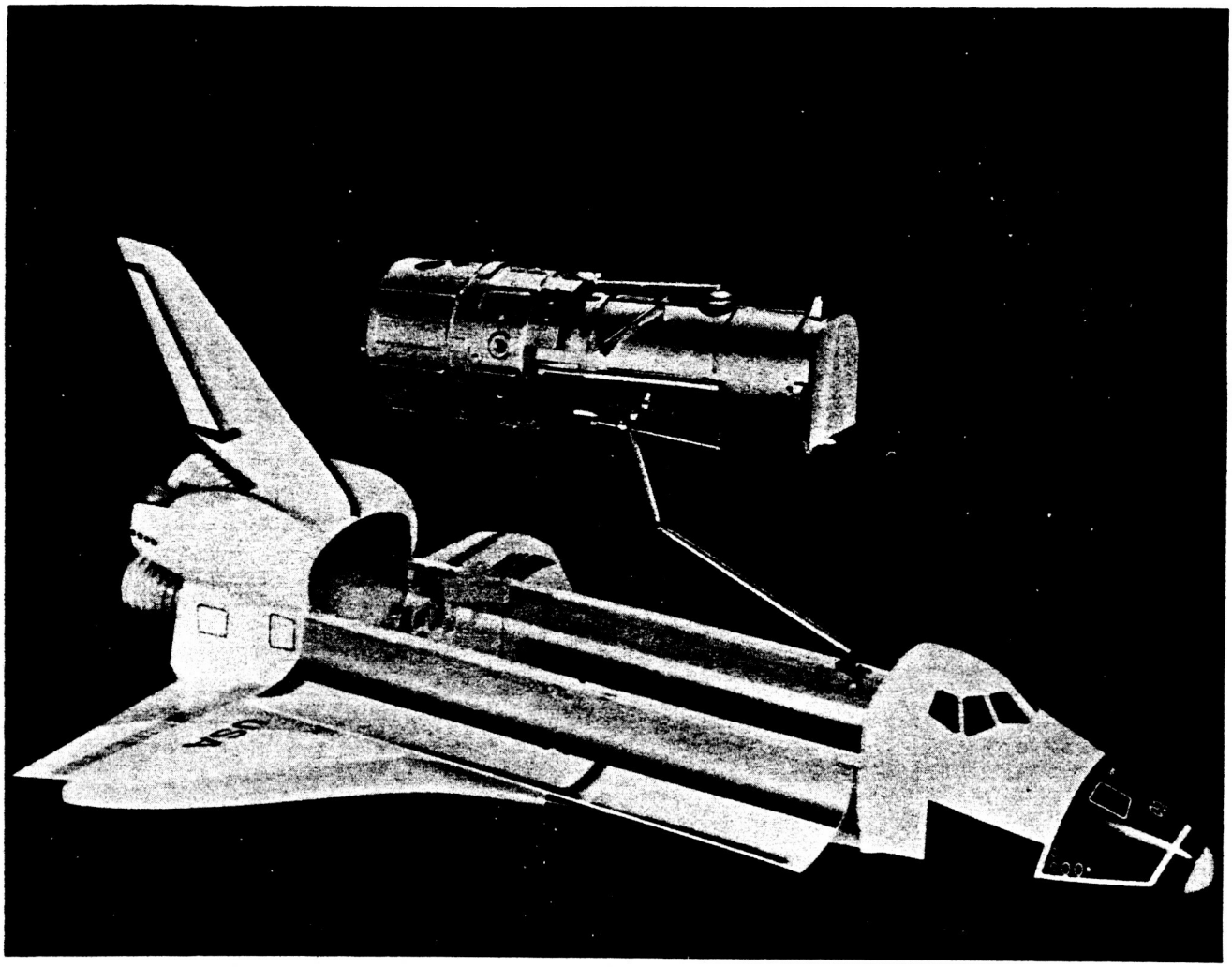

Figure 1. The space telescope being deployed by shuttle.

This symposium will include presentations by the NASA and European Space Agency (ESA) project scientists and by the leaders of the Investigation Definition and Experiment Development Teams, which will give us an up-to-date description of the ST system and of the focal plane instruments, as well as their performance characteristics and some of their application to specific observational objectives.

In view of the above, I have taken as my main task today a discussion of the user aspects of the ST system. Given the existence of the ST ScI which is charged with the responsibility for the science operations, most of the interactions between the General Observers (GOs) with ST will occur through the Institute. After a brief summary of the ST capabilities, I will discuss, therefore, the nature of the ST ScI and some of the Science Operation Concepts currently being developed. I will conclude with some aspects of the expected impact of ST on astronomy.

The telescope and focal plane instruments

A rather complete description of the scientific and political history as as well as of the early development of the Space Telescope is contained in articles by R. O'Dell[1] and J. Bahcall and Lyman Spitzer, Jr.[2] As currently being developed, ST Observatory (Fig. 2) consists of a mirror of 2.4-meter (94-inch) aperture, of Ritchey-Chretien optical design with an f/24 Cassegrain configuration.

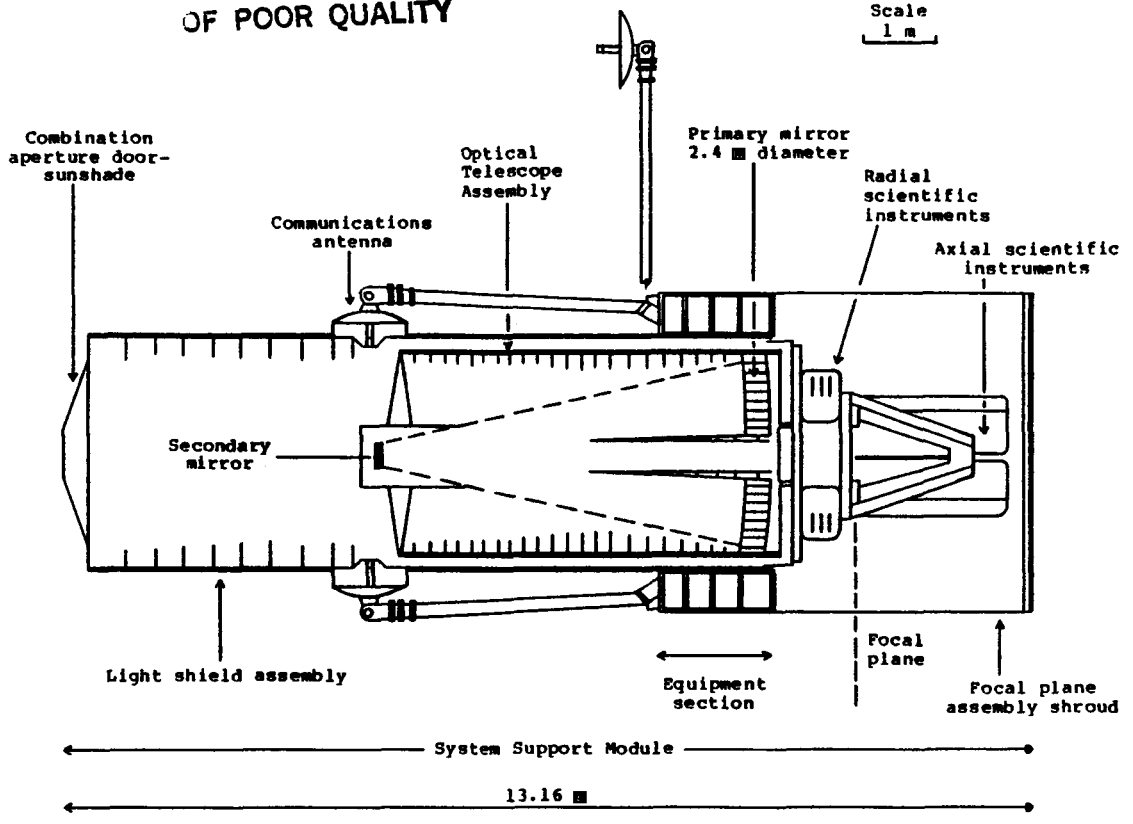

Figure 2. Space telescope conceptual drawing.

One of the most important characteristics of ST is the high quality of the image formed by this mirror at the focal plane. The Mirror has now been constructed by Perkin-Elmer (a second mirror of almost identical characteristic was constructed by Eastman Kodak) under the scientific guidance of the Telescope Scientists, William G. Fastie of The Johns Hopkins University and Daniel J. Shroeder of Beloit College. The optical surface has been measured to have a system wave front error of less than 1/60 of a wavelength RMS at 632.8 nm. Seventy per cent of the energy from a star falls in a radius at the focal plane of less than 25 microns at 632.8 nm, corresponding to less than 0.1 arc seconds. At 121.6 nm, the fraction of the encircled energy remains larger than 40%. The reflection efficiency of the aluminized (ULE), MgF_2-coated surfaces is found to be better than 70% at 121.6 nm and better than 85% at 632.8 nm.

With appropriate focal plane instrumentation, the telescope will, therefore, ultimately cover the range of wavelengths from the far ultraviolet to the far infrared.

The field of view includes approximately 14 arc minutes; the central 11 arc minutes have the highest resolution and are viewed by 5 focal plane instruments; three Fine Guidance Sensors (FGS) view three 90° segments of an annulus of inner and outer radii approximately 11 and 14 arc minutes respectively as seen in Fig. 3. The central 2.7 x 2.7 arc minutes are reflected off to one side by a diagonal mirror to the Wide-Field and Planetary Camera (WF/PC); four quadrants about 6 arc minutes wide around this central area are used by four axial instruments.

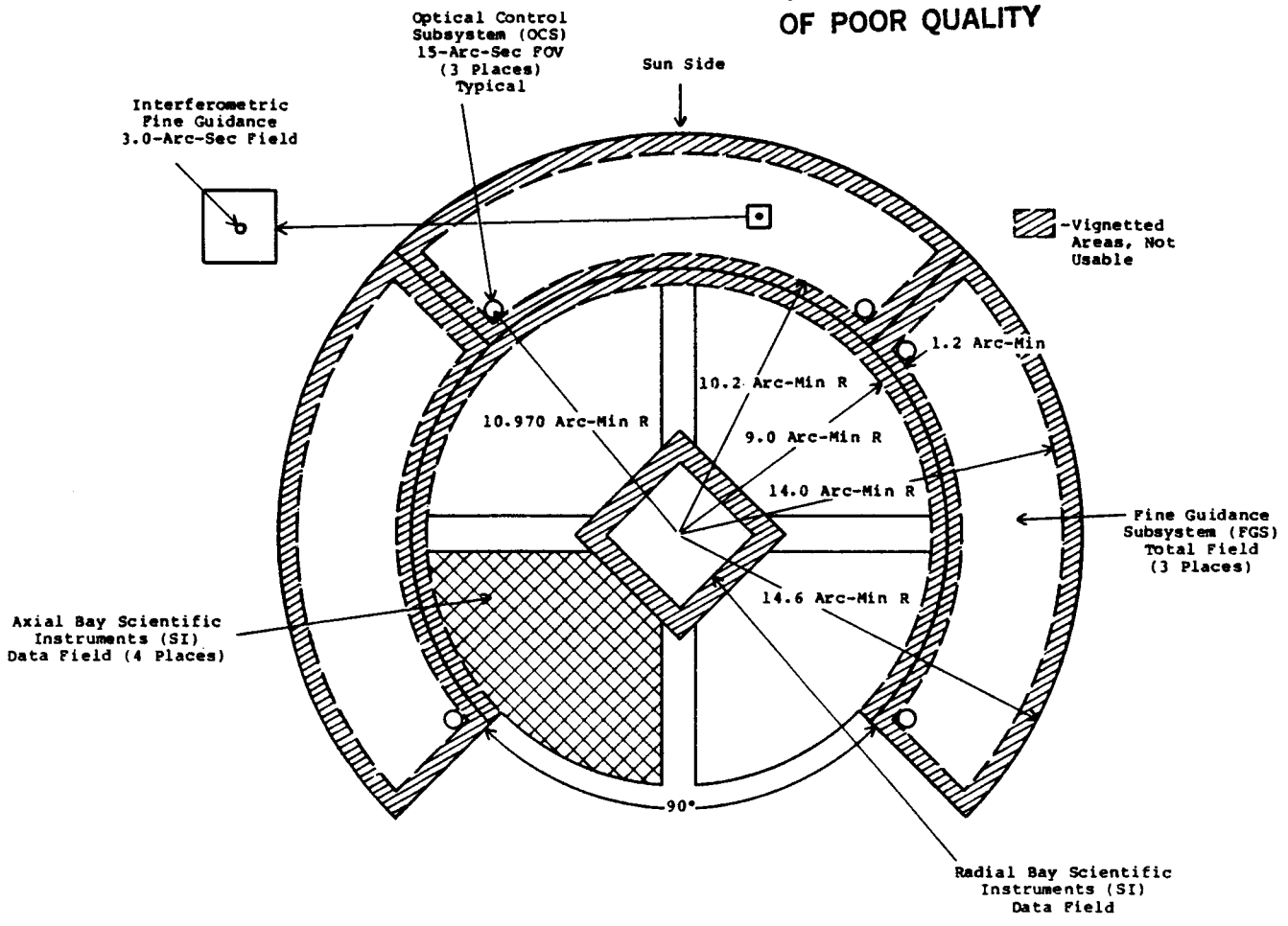

Figure 3. Space telescope field of view.

The complement of scientific instruments[3] includes, in addition to the Wide Field and Planetary Camera and Fine Guidance Sensors, a Faint Object Camera (FOC), a Faint Object Spectrograph (FOS), a High Resolution Spectrograph (HRS), and a High Speed Photometer (HSP). Basic characteristics of the instruments are summarized in Table 1.

The Wide Field and Planetary Camera[4] can be operated in two modes corresponding to focal ratios of f/12.9 or f/30. The first gives a 2.7 x 2.7 arc min^2 field of view (Wide Field); the second, a 68.7 x 68.7 arc sec^2 field (planetary). The detector consists of a mosaic of four CCD arrays of 800 x 800 pixels each. The pixel size in WF mode corresponds to 0.1/arc sec and in the PC mode to 0.043 arc sec. The first mode yields the largest field of view available on ST at the expense of some resolution; the second attains nearly the full resolution of the optics. The camera is sensitive in the range 115.0 to 1100.0 nm and will yield a photometric accuracy of better than 1 percent over a wide dynamic range. It is equipped with 48 special purpose filters to yield color information. Recent measurements of extremely low noise characteristics insure that the instrument can achieve sensitivity of better than m_v=28, for point sources in one hour exposure. It will certainly be one of the most versatile and widely used instruments on ST. The instrument is being developed under the leadership of J. A. Westphal of the California Institute of Technology.

The Faint Object Camera[5] is being developed by the European Space Agency under the leadership of F. Duccio Macchetto (Project Scientist) and H. C. Van den Hulst (Team Leader). It is intended as a complementary instrument to the WF/PC, which exploits the full performance of ST by attaining the highest angular resolution and sensitivity in a narrower wavelength band (120 nm to 500 nm). It can operate in two modes, which produce images of 11 x 11 arc sec^2 or 22 x 22 arc sec^2 onto Westinghouse television tubes with MgF_2 intensifiers. Pixel sizes of 25 microns correspond in the two modes to 0.02 and 0.04 arc sec respectively. The instrument records individual photons and, as a special feature, the instrument can achieve very high angular resolution (0.007 arc sec) in very

narrow fields, thereby permitting the use of post facto image reconstruction techniques. It is also equipped with filters, dispersing elements, polarimeters, and an occulting disk which will enhance its versatility for special observations.

Table 1. Instruments on the f/24 2.4-m Ritchey-Chretien SPACE TELESCOPE

		Field	Res.	Band-pass	Limits	
WF/PC	Wide Field Camera, f/12.8	2.7 x 2.7	0.1	1150-11000Å	$9.5 \leq m_v \leq 28$mag.	
	Planetary Camera, f/30	1.2 x 1.2	0.04	1150-11000	$8.5 \leq m_v \leq 28$	
	4,800 x 800 CCD detectors, 15μ square					
FOC	Faint Object Camera, f/96	11" x 11"	0.02	1200-6000Å	$21 \leq m_v \leq 28$mag.	occulting
	f/48	22 x 22	0.04	1200-6000	$21 \leq m_v \leq 28$	disk also
						spectra &
	MgF_2 image intensifier, Westinghouse TV tube					polarimeter
FOS	Ft Obj Spectrograph, R=10^3	0.1 to 4.3	3Å	1150-7000Å	$19 \leq m_v \leq 22$mag.	polarimeter
	R=10^2	0.1 to 4.3	30	1150-7000	$22 \leq m_v \leq 26$	polarimeter
	SiO_2 & MgF_2 512-diode Digicon detectors, 50-μsec resolution					
HRS	Hi Res Spectrograph, R=10^5	0.25 to 2.0	0.03Å	1100-3200Å	$m_v \leq 11$mag.	exp = 0.025 sec
	R=2x10^4	0.25 to 2.0	0.15	1100-3200	$m_v \leq 14$	exp = 0.025
	R=2x10^3	0.25 to 2.0	1.5	1100-1700	$m_v \leq 17$	exp = 0.025
	CsTe/MgF_2 and CsI/LIF 512-diode Digicons, 5 blazed gratings, 1 echelle					
HSP	Hi Speed Photometer, filters	0.4,1.0,10"	16μsec	1200-8000Å	$m_v \leq 24$mag.	polarimeter
	2, S-20 & 2, CsTe/MgF_2 photomultiplier detectors					
FGS	Fine Guidance System, 3 star selectors	69(arcmin)^2	0.003	4670-7000Å	$4 \leq m_v \leq 20$mag.	
	Koester prism interferometer and image dissector					

Compilation from Thornton Page,
Dudley Lecturer, Dudley Observatory
Schenectady, New York

The Faint Object Spectrograph is a sensitive, medium-resolution (10^2 - 10^3) spectrometer, which is being developed under the leadership of Richard J. Harms of the University of California, San Diego.[6] The images formed by concave gratings (for short wavelengths) or by a prism (for long wavelengths) are detected by Digicon arrays. The spectrograph will be sensitive from about 115 nm to 800 nm. The different modes can furnish spectral resolution $\lambda/\Delta\lambda$ of 10^2 or 10^3 corresponding to the ability to resolve 30 A, or 3 A, respectively. The smallest slit size is 0.1 arc second. The instrument can also be used to study the polarization of the incoming light and to study time variability in the spectra of bright sources with a resolution of 10 millisec. The system is designed to have adequate resolution for the study of very faint objects. It is anticipated, therefore, that it will be widely used for much of the spectroscopic work in which sensitivity is the basic consideration.

The High Resolution Spectrograph, which is being developed under the leadership of John C. Brandt of Goddard Space Flight Center,[7] is primarily intended for use in the 110.0- to 320.00-nm region with resolution of 2 x 10^4 or 1.0 x 10^5. The highest resolution corresponds to 0.05 A, and will be one of the finest in astronomical use. Of course, such resolution is obtainable only for relatively bright objects. The dispersing elements are

concave gratings and the detectors are Digicon systems similar to the FOS. Sensitivity of this instrument will be some 100 times better than the International Ultraviolet Explorer (IUE), with finer spectroscopic resolution and photometric accuracy.

The High Speed Photometer/Polarimeter is being developed under the leadership of Robert C. Bless of the University of Wisconsin.[8] The instrument is designed to carry out high time resolution studies of sources over a wide band of wavelengths, from 120 to 700 nm, over intervals as short as 10 microsec for the brightest sources. A number of filters can be used for broad-band spectroscopy. Apertures from 0.1 to 2.8 arc seconds can be used. The detectors are magnetically focused image dissectors with no mechanically moving parts. Polarimetry of the focused radiation can be carried out in the near ultraviolet. The instrument is designed to be simple, precise, and rugged. It can be used to study, for instance, time variability of some of the optical counterparts of collapsed objects such as stellar mass black holes or neutron stars. More generally, it will be used to establish photometric standards and time variability for a number of stellar objects.

The guidance system and the fine guidance sensors

ST can be pointed to any desired position in the sky by means of reaction wheels, which are unloaded by means of magnetic torquing against the Earth's magnetic field.

Error signal reference for the reaction wheels is provided by precise gyros on all three axes. Gyro reference is characterized, in very low noise systems, by small drift rates; that is, gyros are sensitive to rate of angular motion with time. Gyros are not, however, accurate enough to determine a precise absolute pointing direction or to maintain it over long periods of time.

In order to derive absolute pointing direction and to correct for drift, ST relies on fixed head star trackers and fine guidance sensors. The first have wide fields of view, which insure the acquisition of bright catalogued stars ($mv \leq 8$), but are capable of establishing direction to no better than a few arc seconds. This precision is sufficient for coarse altitude determination but is totally inadequate to place the small slits (.1 arc sec) of the ST spectrometers on the desired objects or to permit long-term exposures and integration at the high angular resolution of which the optical system and detector are capable. Fine guidance sensors are used to determine to high precision the position of reference stars with respect to the system axis. They consist of a Koester's prisms interferometers/photomultipliers combination which can determine stellar positions to an accuracy of a few to several milliarc seconds within a field of view of 15 milliarc seconds. They are being developed at the Perkin-Elmer Corporation.

Two of the three FGS (only two are needed) are caused to scan the 69 arc min^2 field of view for stars of previously known coordinates (guide stars), and the difference between the actual and predicted position of these reference objects is used to update the gyros each second of time. Estimates based on structural models of the ST, and on measured noise characteristic of the gyros, yield an estimated pointing stability of 0.007 arc seconds for the ST system.

The third FGS can be used to carry out astrometric measurements of designated objects with respect to the reference objects. An Astrometry Science Team, chaired by W. Jefferys of the University of Texas at Austin, is studying the very significant capability which ST opens up for astrometric measurements of objects as faint as m_v=17 to a precision of 0.002 arc seconds.[9]

In order to ensure that guide stars are present everywhere in the sky ST is pointed, within the relatively small angular field of view of the FGSs, it is necessary to measure guide stars with precise positions (0.3 arc sec) to m_v=14.5 magnitude.[10] Since no suitable star catalogue exists, it is one of the important tasks of the Space Telescope Science Institute to develop the required capability prior to ST launch. More precisely, pointing of ST requires knowledge of the target position with respect to guide stars brighter than 14.5 magnitudes and visible within the field of view of the FGSs, to a precision finer than the desired minimum slit size. In particular cases, such as for the 0.1 arc second slit of the FOS, small area scans must be performed to locate the slit within the uncertainity of 0.33 arc seconds which is foreseen for guide star position determinations.

Ground control of ST

The great flexibility and complexity of operation of the ST observatory and of each instrument requires on board computer control of most functions. The rather low orbit (28.5, degrees inclination, 500 km) permits only infrequent communication access from ground stations. Use of the geostationary TDRSS communication satellites ensures accessibility for about 85% of the orbit, but sharing the TDRSS capability with other missions will limit the time available to ST ground control for issuance of commands to about 20%. ST will, therefore, be operated in a far more automated mode than most astronomical observatories.

Observations will be, in general, preprogramed, meaning that for each observation a series of ground commands will have to be worked out well in advance, as is necessary to place the telescope in the required viewing orientation, to acquire guide stars, to select the specific focal plane instrument to be used and its specific operating mode, to obtain any necessary calibration sequences, and to store the data onboard until TDRSS is available.

In addition, time varying viewing constraints are imposed by the necessity to avoid the sun ($\geq$ 50°), the bright limb of the earth ($\geq$ 70°), and the moon ($\geq$ 15°); therefore, observations of a specific object cannot, in general, be carried out except at specific times during the "season." Moreover, the required time for slewing from one pointing direction to another is not negligible (18 minutes for 90°), and the settling time, that is, the time required to identify and lock on to guide stars is also substantial (minutes).

Most observations, therefore, will be strung together into an observing sequence well in advance (6 months) of observing in an effort to optimize efficiency of use of ST by minimizing instrument cycling and calibration times, slewing times, and settling times, and to take into account all viewing constraints or effects which might alter background rates--for instance, scattered zodiacal light or particle background as a function of geomagnetic coordinates.

Real time control of the observatory will be possible for only a small fraction of all observations and will, in general, allow only for small positioning corrections or for selection of one among a few preprogrammed options by the observer. Transmission of data at a rate of one megabit/sec will be available about 20% of the time; for most of the time available, the rate is 4 kilobit/sec. The volume of data to be received from ST, while not unusually large for typical space missions, is a substantial and continous stream which requires highly automated procedures for data receipt and editing as well as for first-cut data reduction, processing, and archiving.

The scientific planning and operation of Space Telescope is a demanding task which has been entrusted to the Space Telescope Science Institute.

Space Telescope Science Institute

Space Telescope Science Institute (ST ScI) is an independent research institute operated by the Association of Universities for Research in Astronomy, Inc. (AURA) on behalf of NASA.

The charter of this institute requires ST ScI to:

- Establish ST science program guidelines
- Select ST observers and archival researchers
- Provide direct technical support to observers before, during, and after their observation
- Fund U.S. users
- Develop science observations, procedures, and capability
- Develop an integrated observing schedule to be used by the operations control center
- Process, archive, and publicize the scientific data derived with the ST, making this information accessible
- Evaluate the scientific performance of the ST observatory and its individual scientific instruments and advise NASA on observatory status
- Sponsor ST-related research necessary for efficient use of the ST observatory
- Conduct a program to encourage writing scientists
- Promote international participation
- Establish a scientific staff of the first rank to perform the above functions and conduct their own research related to ST.

The Institute began its existence in April 1981. Staff is being recruited and a permanent facility to house it is being constructed on the campus of The Johns Hopkins University (JHU) in Baltimore, Maryland. Staff complement now stands at 50. Several of the long-lead-time activities have been initiated, in particular the definition of technical management and operation concepts, the development of a guide star selection system (GSSS) and the development of a science data reduction and analysis system (SDAS). These plans and concepts are described in a series of formal documents, including a technical management plan (MA-03),[11] a GSSS design concept (SO-04),[12] a Science Data Analysis System (SDAS) concept (SO-03),[13] and Science Operations Concepts (SO-07).[14] These documents will be revised and refined as more is learned in the program, but they form the basis of our plans for implementation. The discussion that follows summarizes information contained in those documents.

ST ScI will be an institute with a staff of approximately 200, including some 50 astronomers at the Ph.D. level. Some 40 of these astronomers are AURA staff, 10 will be ESA staff. Support staff will consist of AURA personnel as well as subcontractor support personnel provided by Computer Science Corporation (CSC) (under an AURA-CSC subcontract arrangement), and of five ESA employees.

ST ScI activities are organized by functional responsibilities into: Office of the Director, Program Management Division, Business Management Division, Data and Operations Division, Scientific Instrument Support Branch, Research Support Branch, General Observer Support Branch, Academic Affairs Branch, and two project offices for GSSS and for SDAS.

Operations by the ST ScI staff will be conducted at two locations--the ST ScI facility (on the JHU campus) and the Science Support (SSC) Center at GSFC. Both facilities will operate on a 24-hour/day schedule (Fig. 4).

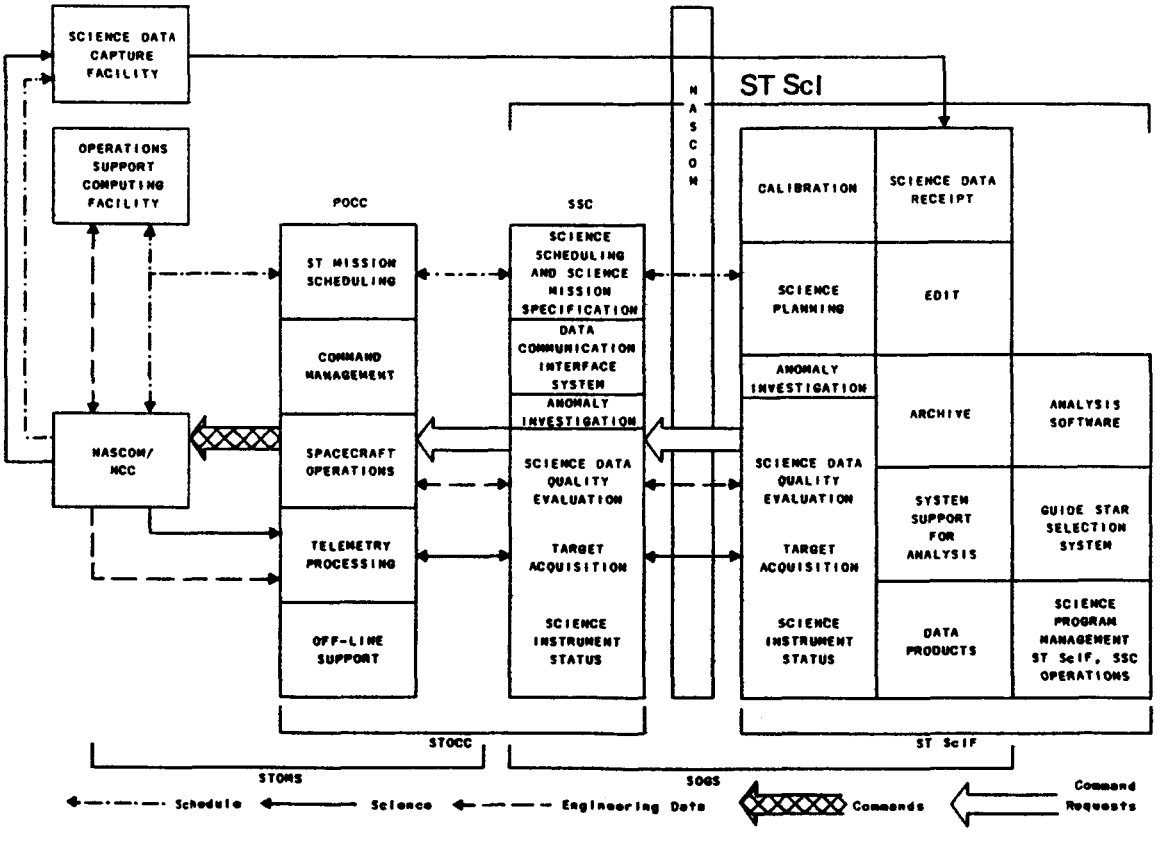

Figure 4. Space Telescope Science Institute relation to other project elements.

Computational capabilities will be provided at one or the other of the facilities to support guide star selection, mission planning and scheduling, mission specifications and target acquisitions, science data quality evaluation, science instrument status and anomaly investigation, calibration activities, science data editing and archiving, science data analysis, and hard copy data generation.

The bulk of the hardware and software to support these activities is being developed for the ST ScI under a NASA contract to TRW to provide a Science Operations Ground System (SOGS). The hardware is expected to consist of six VAX computers, two at the SSC and four at the ST ScI with appropriate peripherals. Additional computers for use by the Guide Stars Selection System and for supporting the Scientific Data Analysis System are being acquired by ST ScI directly. Much of the software for calibration of the data and for first-cut data reduction and analysis is being provided by the Instrument Development Teams and by the SDAS Project of the ST ScI. Data analysis capabilities will support interactive analysis efforts by the Institute staff for its own research as well as computational requirements of the General Observers (GOs) and Archival Researchers (ARs) as required. Copies of the data on magnetic tapes will be furnished to the GOs and ARs to permit further elaboration of the data at their home institution.

Community participation in the activities of the ST ScI and in its guidance will occur through several mechanisms (Fig. 5). In addition to solicitation and support of GOs and ARs, the Institute will sponsor a program of Visiting Scientists and Post Doctoral Fellows. Members of the scientific community will be asked to serve on the internal commmittees of ST ScI such as the Time Allocation Committee and the Users Committee. An external Search Committee under the chairmanship of Jeremiah Ostriker is currently being used to review applicants for scientific positions at the Institute. AURA exercises its management oversight responsibilities of the Institute through a Space Telescope Institute Council (STIC), chaired by Lyman Spitzer, Jr. A Visiting Committee drawn from the astronomical community will annually assess the performance of ST ScI and report to AURA Board of Directors and to the Associate Administrator for Science and Application of NASA.

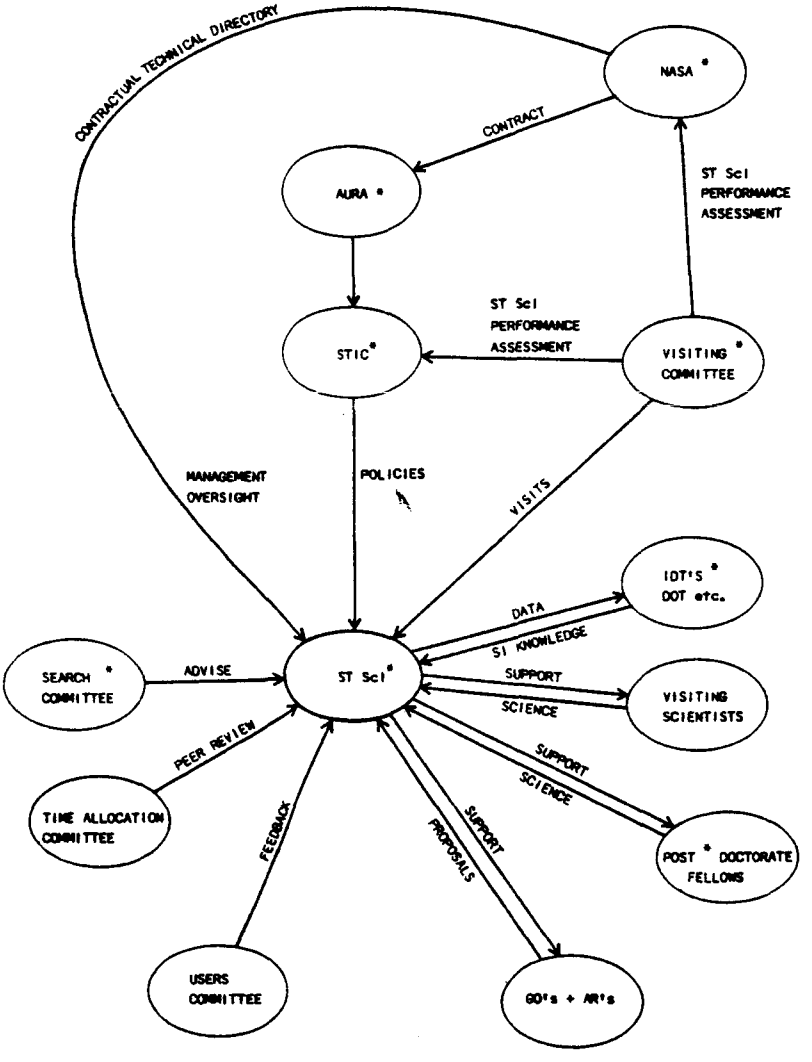

Figure 5. Interaction of community with Space Telescope Science Institute.

Allocation of observing time

After launch and an initial system check out and science verification activity lasting three months, observing time has been assigned to the scientists associated with the development of ST and the Science Instruments, for a steadily decreasing fraction of available time: 100% for two months, 50% for an additional six months, 25% for the next year and 10% for the next ten months. This amounts to an average use of 30% time during the first two and one-half years of the mission; correspondingly an increasingly large fraction of the time, amounting to 70% in the first two and one-half years, will be devoted to openly solicited, peer-reviewed, and competitively selected proposals. Scientific Staff members of the ST ScI will also obtain observing time through this competitive procedure. It is expected that on the average, scientists from ESA member states will capture at least 15% of available time for GOs.

A Director's discretionary time, consisting of a fraction between 0% and 15% of available time, is reserved for non-peer-reviewed observations that may become necessary for scientific support activities, for acquisition of targets of opportunity, and for high-risk or long-term programs not amenable to peer review. Actual utilization of this time will be reported periodically by the Director to STIC.

According to recent NASA guidelines, the scientists involved in the early development of ST and ST Instruments must specify particular observing targets for the first two-and-one-half-year period, two years prior to launch. Listing of these targets as well as planned times of observations and instrument and mode selection will be made available to potential proposers at the time of an open selection (12 months before launch).

A users' guide containing detailed descriptions of the ST, the science instruments (SI) and ground systems will also be provided by the ST ScI. This guide will contain instrument parameters, filter/grating selection, exposure/integration times and data format, instrument sensitivity, background, wavelength range, resolution, and other relevant parameters. (These parameters will be updated as orbital data are accumulated.) The users' guide will also contain target acquisition modes, calibration requirements, and lists of standard calibration targets--in short, the necessary information to design a scientific observation.

It is anticipated that proposals will be solicited every six months to allow for an efficient cycle of review and scheduling.

Proposals, formats, and contents will be specified in the solicitation. Typically they will require:

- A title
- Name and address of proposer
- Sponsoring institution
- Abstract of scientific justification
- Scientific justification
- Observing list
- Target identification for determination of guide stars
- Detailed observing sequence
- Special calibration requirements
- Special planning problems
- Previous ST experience
- Other commitments affecting scheduling
- Required data reduction and data products
- Budgetary requests

Proposals will be analyzed by ST ScI staff for technical feasibility and scheduling constraints. They will be submitted to expert outside reviewers for comments on scientific merit. Results of the evaluation will be made available to a Time Allocation Committee (TAC) which will advise the Director on priorities. The TAC will be composed of eight to twelve scientists broadly representative of astronomical disciplines, will be chaired by a senior ST ScI scientist, and will have a NASA and an ESA observer.

Priority allocation is the responsibility of the Director.

It is a process more complex than assignment of time at a ground based facility, since the available time is not fully known in advance and operational requirements impose in general the selection of a number of targets greater than can be accommodated in the available time. Thus, about 20% of the available time can be devoted to a high priority category of observations which will be carried out if at all possible, 65% of the time to medium priority observations which are carried out on a best effort basis, and 20 to 50% of the time to supplemental targets which will be used to fill the schedule when high and

medium priority targets are unavailable. In general, an observation of a high priority target will be planned to occur within six months of proposal approval, although target crowding and seasonal effects may push the observation to the next observing season (12 months). Targets of lower priority will be acquired on a best effort basis.

Upon scientific selection the mission operation and scheduling group will begin to prepare an integrated observing plan six months prior to execution. This is required to prepare for Guide Star selection, for full identification of instrument modes and calibration requirements and for detailed sequencing of observations. The process must take into account viewing restraints, ST constraints, viewing requirements, etc., and will be iterated to maximize scientific returns. In general, individual targets from several GO programs will be intermixed in the sequencing process.

Some planning constraints are related to earth fixed phenomena, such as the location of the South Atlantic Anomaly, TDRSS visibility and location of ground based observatories. The ephemeris of ST will be known some 60 to 30 days in advance of observation with sufficient accuracy to set absolute times for events. At this point, monthly operating plans can be forwarded for comments and successive interactions to the SSC which will generate Science Missions Specifications, and transmit them to the Payload Operations Control Center (POCC), some 24 days prior to observations. Interactions with POCC are anticipated to take into account further operational requirements and better knowledge of satellite ephemerides. Unanticipated events such as the insertion of targets of opportunity or operational problems such as failed commands may still alter the program which will be finally fixed in detail some 24 hours prior to observations.

I have gone into some detail in the above to give the reader a flavor of the reasonably complex sequence of steps required for observation scheduling. It is clear that under these conditions real time interaction with ST becomes difficult to implement. We anticipate that approximately 20% of the observations will be carried out with real time observer participation. Real time participation will consist of target acquisition assistance or of a choice among a few alternative modes of instrument use, each of which will have to be analyzed and planned in detail.

Data rights policies and access

Data from ST will be transmitted by GSFC to the ST ScI where data reduction will be performed. Data analysis capabilities will be provided at ST ScI to GOs and ARs as well as to Institute staff. In addition, ST ScI will perform the archival and distribution functions of the National Space Science Data Center (NSSDC) and the World Data Center - A for Rockets and Satellites for ST data.[15]

Observational data obtained by ST for scientific research either as a result of the peer review proposal process or as a result of the time assigned to development phase scientist, will be considered proprietary for a one-year period, after the data is reduced to a form suitable for analysis. For astronomical research programs requiring a series of observations, the one-year period will start from the time that the program is substantially completed. In special circumstances, the one-year period can be extended for compelling scientific reasons by the ST ScI Director, but extensions beyond two years will be granted only in the most compelling cases and will have to be approved in each instance by the STIC.

After the proprietary period, ST data will be made available to the community at large as well as to the public. Archival Researchers need only submit proposals if they need financial or technical support from ST ScI. Otherwise, data requests will be honored on a cost reimbursable basis, although small requests by qualified scientists may be honored at no charge as has been the practice of NSSDC.

Requests for significant portions of the archives will be dealt with, by referring them to NASA, since they may impose a substantial burden on ST ScI capabilities. At the moment there exists an ESA-NASA agreement which provides for transfer on a cost reimbursable basis of archived, nonproprietary data from ST ScI to a European Coordinating Facility (ECF), which will be described by F. Duccio Macchetto.[16]

As computer and data storage technology improves, we expect to establish remote computer access to the ST ScI data base for the convenience of users. This may initially take the form of a browse capability and later be extended to direct access to the archive. These possibilities are not part of the current NASA plans and are just beginning to be explored. Ultimately we would expect that ST archival data may be as easily accessible and as widely used as was the case for the National Geographic Society Mount Palomar Sky Survey.

Impact of ST on astronomy

The broad wavelength coverage, angular resolution and sensitivity of the ST observatory will allow us to perform a number of observations currently unfeasible with ground-based instruments. Several scientific symposia and workshops[17,18,19] have addressed the potential scientific returns to be expected from ST in each subdiscipline of astronomy, and further discussions of specific applications will occur at this Symposium.

It is clear that use of ST promises significant advances in the pursuit and extension of many of the outstanding astrophysical problems of current interest.

ST will make a fundamental contribution to the determination of the distance scale and age of the Universe, by providing an extension of a factor of ten in the distance over which we can measure the properties of the standard candles, used in the logical ladder leading to the determination of the Hubble constant.

Study of clusters of galaxies and individual galaxies at larger redshifts, then possible from the ground, will provide significant tests of world models and cosmic evolution.

The extension of morphological classification of galaxies to redshifts of order of 1 and the extension of stellar population studies at very faint levels will provide important clues on the formation, dynamics, and evolution of galaxies.

Study of the central regions of active galactic nuclei and quasars (QSOs) can provide the basic data necessary to understand the physics of the nuclear regions of galaxies, and the source of the tremendous energies released there, possibly giant collapsed objects.

ST promises the extension of stellar studies in our own galaxy to the faint population of stars which populate the corona. Studies of physical conditions and chemical composition of the interstellar medium and studies of the injection of material through stellar winds, evolution of outer atmospheres of stars, coronal winds, circumstellar shells, planetary nebulae and supernova remnant can be extended with ST to the UV range of wavelengths.

An area of great potential for ST observations relates to the study of the birth and evolution of single and binary stars and globular star clusters. Future extensions of ST capabilities to longer wavelength in the infrared will further improve the capabilities for this type of research.

Astrometric measurements with ST promise also an improvement in precision of a factor ten. This will have a dramatic effect on many fundamental problems of astronomy. Parallaxes can be obtained with the same precision for objects ten times more distant than possible from the ground. Visual orbits of some spectroscopic binaries can be obtained with a substantial improvement in our knowledge of stellar masses. A search can be carried out for planetary systems of other stars. Finally a link can be forged between optical, radio, and dynamical reference frames, and the inertial reference frame can be tied down by measurement of star motions relative to QSOs.

In planetary astronomy ST will play a major role in the coming decade in part because of the decreased commitment of NASA to major planetary flyby missions, but also because of the possibility of performing synoptic studies of planetary atmospheres, high resolution and UV studies of comets, and astrometric studies of the motions of the moons of the outer planets.

This list has no claim to completeness. One of the benefits which will result from the improvement in sensitivity provided by ST, that I find personally most interesting, is that it will permit observations of faint optical counterparts of objects of primary interest to radio and high energy astronomy.

One of the fundamental problems in X-ray astronomy, for instance, still remains the source of the diffused extragalactive X-ray background. Although a large fraction of the individual sources which produce it have been shown to be quasars, many of the faintest sources in the deep X-ray surveys[20] carried out with the "Einstein" satellite remain unidentified (Fig. 6). This situation will worsen with the advent of Advanced X-ray Astronomy Facility (AXAF) which will detect sources 100 times fainter than "Einstein" in the 0.25 to 7 kev domain.[21] This is not surprising if one considers the following example: 3C273 emits an X-ray flux of 6×10^{-11} erg cm^{-2} sec^{-1} and has an apparent visual magnitude $m_v = 13$. The Einstein survey reached a limit of 2×10^{-14} erg cm^{-2} sec^{-1} and AXAF will reach a limit of 2×10^{-16} erg cm^{-2} sec^{-1} for faint sources. The corresponding apparent luminosity of 3C273, if placed at the large Z corresponding to the limits of detectability in X-rays for the two observatories, would be $m_v=22$ and $m_v=27$ respectively (Fig. 7).

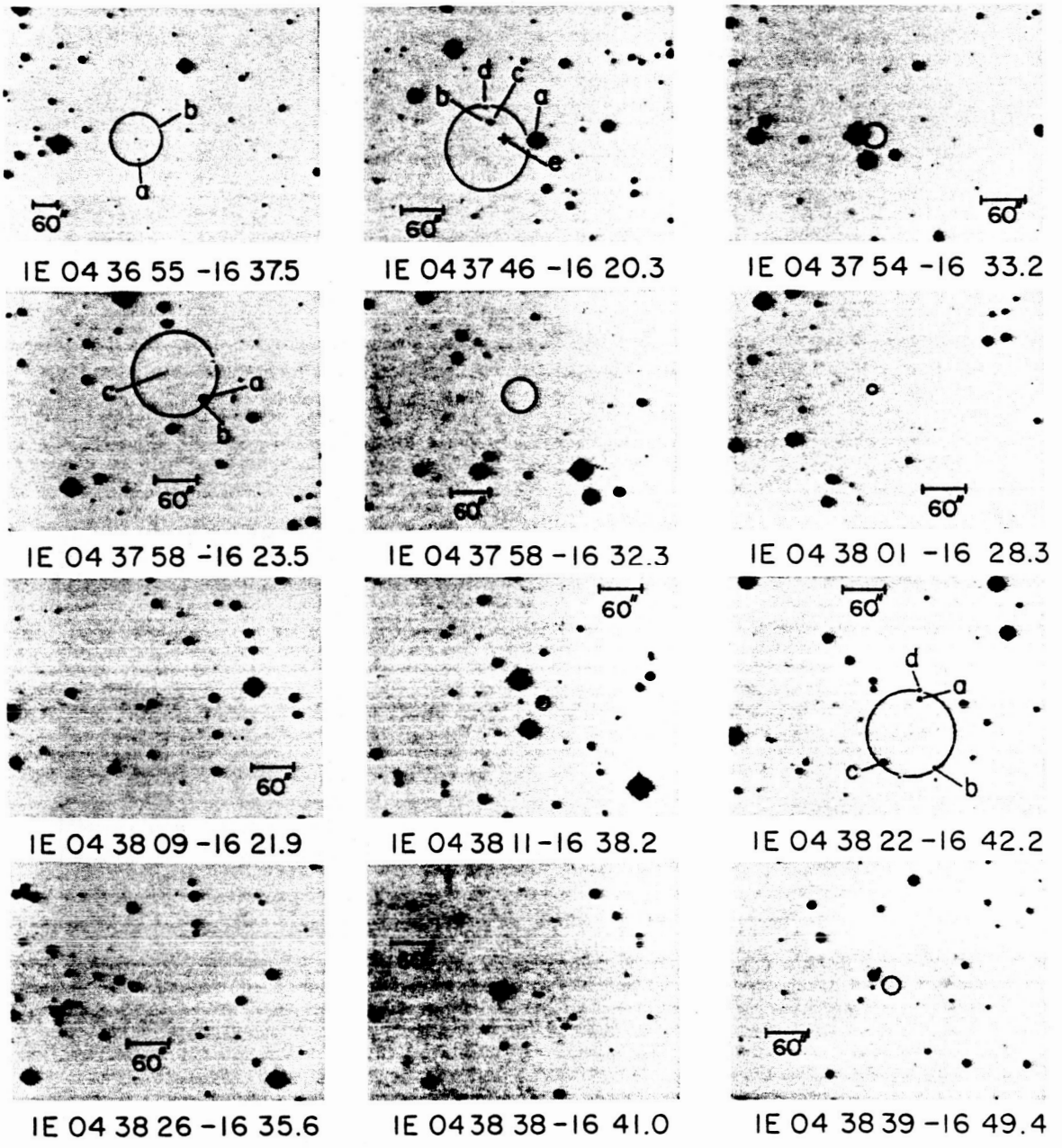

Figure 6. Deep surveys--Einstein.

Of course it is entirely possible that many of the unidentified objects in the X-ray surveys are not QSO at all, but perhaps protogalaxies or other exotic objects which could be discovered and studied with ST.

The point of these remarks is that ST is not only desirable but essential if we wish to continue carrying out the study of cosmic objects over the entire range of wavelengths available, from radio waves to X-rays, an approach which has proven so powerful in the recent past. It may well be, in fact, that this approach will be the one which will provide the most unexpected and startling returns from ST: the discovery of new classes of astrophysical objects with unsuspected physical properties.

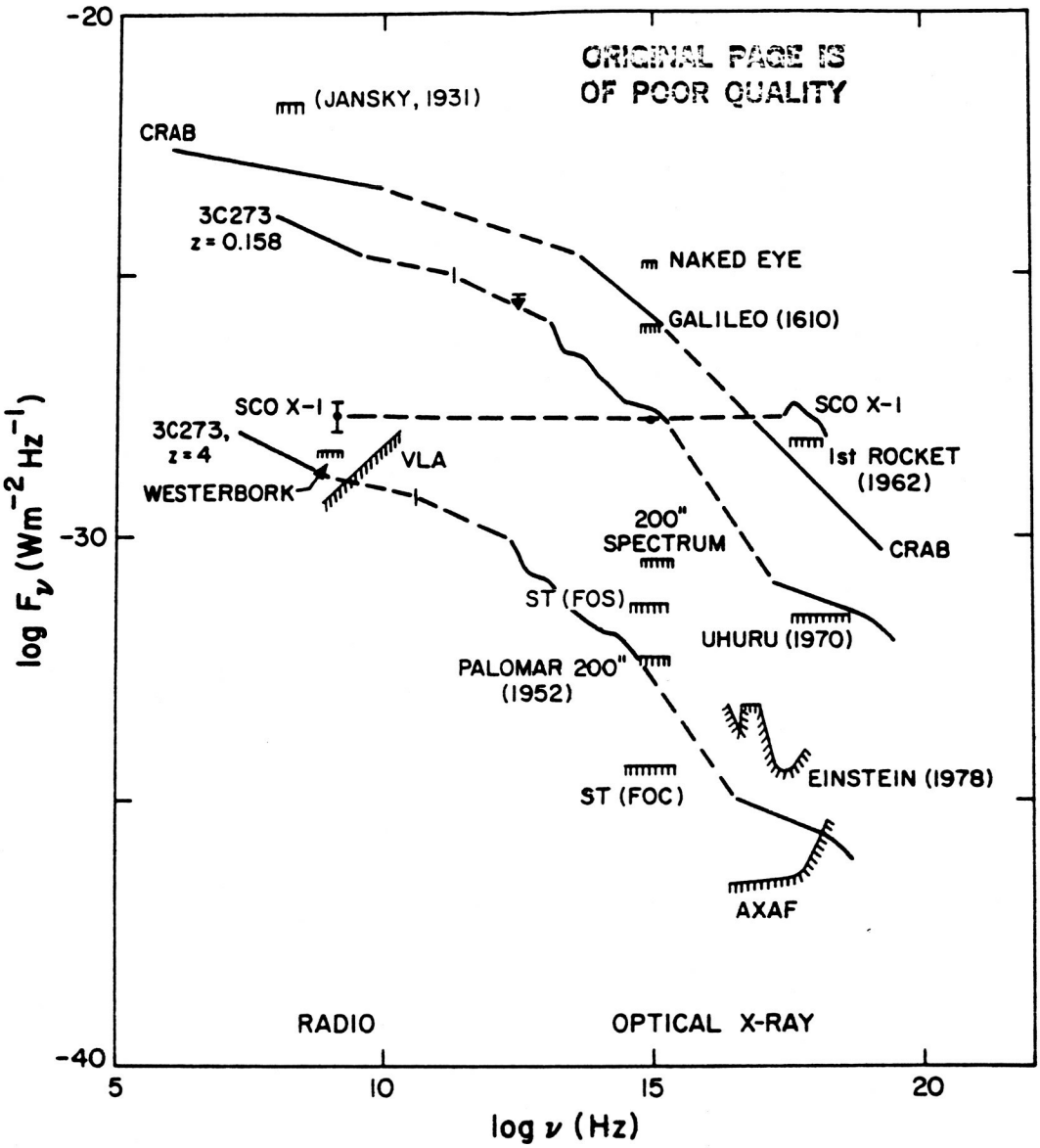

Figure 7. Detectability of 3C273.

Finally, I would like to note that the impact of ST on astronomy will manifest itself in many aspects of the research enterprise besides the intrinsic value of the scientific data. It will be the first time that a national or international optical observatory will have capabilities clearly superior to privately developed telescopes, a fact which may influence the career development of many young astronomers. It is hoped that the data handling and archival capability which will have to be provided will be used as a tool in many other astronomical applications. The substantial development effort which will culminate in ST will provide the astronomical community not only with newly developed technology which already has found application in ground-based observatories, but even more significantly with a new generation of astronomers which has developed the skills and self-confidence to undertake the construction of very substantial new observational facilities. After a period of hiatus in which astronomers seemed to be most involved in the digestion of the results flowing from the capital investment of the previous generation, it may well be that the next two decades will be remembered as the heroic construction phase for observational astronomy.

References

1. O'Dell, C. R. 1980, The space telescope, in Annual Reviews Monograph: Telescopes for the 1980's, ed. G. Burbidge and A. Hewitt. Palo Alto, California: Annual Reviews, Inc., pp. 129-193.

2. Bahcall, J., and Spitzer, L. 1982, The space telescope. Sci. Am. 247(1): 40-51.

3. Leckrone, D. S. 1980, Publ. Astron. Soc. Pac. 92:5.

4. Westphal, J. A., and the Wide Field Planetary Team. 1982, The wide field and planetary camera, in The Space Telescope Observatory. Baltimore: Space Telescope Science Institute, pp. 28-39.

5. Macchetto, F. D., *et al.* October 1980, The Faint Object Camera for the Space Telescope. ESA SP-1028.

6. Harms, R. J., and the FOS Science and Engineering Team. 1982, Astronomical capabilities of the faint object spectrograph on space telescope, in The Space Telescope Observatory. Baltimore: Space Telescope Science Institute, pp. 55-75.

7. Brandt, J. C., and the HRS Investigation Definition and Experiment Development Teams. 1982, The high resolution spectrograph for the space telescope, in The Space Telescope Observatory. Baltimore: Space Telescope Science Institute, pp. 76-105.

8. Bless, R. C., and the HSP Investigation Definition Team. 1982, The high speed photometer for space telescope, in The Space Telescope Observatory. Baltimore: Space Telescope Science Institute, pp. 106-113.

9. Jefferys, W. H. 1980, Celestial Mechanics, 22. Dordrecht, Holland, and Boston, Massachusetts: D. Reidel Publishing Co., pp. 175-181.

10. Benedict, George F. 10 October 1979, Space Telescope Astrometry Team Guide Selection System Specifications and Design. Austin: The University of Texas.

11. 24 March 1982, MA-03 Technical Management Plan (SCI 82004C). Baltimore: Space Telescope Science Institute.

12. 3 May 1982, SO-04 Guide Star Selection System Documentation, Vol. 2: System Design Specification and Description, Preliminary (SCI 82017B). Baltimore: Space Telescope Science Institute.

13. 15 March 1982, SO-03 Science Data Analysis Software Documentation, Vol. 2: Requirements, Preliminary (SCI 82015B). Baltimore: Space Telescope Science Institute.

14. ST Data Management Plan Document.

15. Macchetto, F. D. 1982, European astronomy and the space telescope: the space telescope coordinating facility, in The Space Telescope Observatory. Baltimore: Space Telescope Science Institute, pp. 16-19.

16. Longair, M. S., and Warner, J. W. 1979, Scientific Research with the Space Telescope. IAU Colloquium #54 (NASA CP-2111) Princeton, New Jersey.

17. Macchetto, F. D., Pacini, F., Tarenghi, M. 1979, ESA/ESO Workshop on Astronomical Uses of the Space Telescope. Geneva, Switzerland.

18. February 1981, Optical jets in galaxies, in Proceedings of the Second ESO/ESA Workshop on the Use of the Space Telescope and Co-ordinated Ground Based Research. (ESA-SP-162) Munich, Germany.

19. Giacconi, R., *et al.* 1979, Astrophys. J. Lett 239, L 1.

20. Giacconi, R., *et al.* 1979, The Einstein Observatory and future x-ray telescopes, in Annual Reviews Monograph: Telescopes for the 1980's, ed. G. Burbidge and A. Hewitt. Palo Alto, California: Annual Reviews, Inc., pp. 195-278.

N82 33298

European Astronomy and the Space Telescope: The Space Telescope European Coordinating Facility

F. Macchetto

Astronomy Division
Space Science Department of ESA
Keplerlaan 1
2200 AG Noordwijk
The Netherlands

Abstract

To allow European astronomers to make full use of the extraordinary capabilities of the Space Telescope, ESA has decided to establish the European Coordinating Facility. Its role is described in this paper.

I Introduction

The Space Telescope will play the dominant role in astronomy for the rest of this century. For the first time in history astronomers will have access to a large telescope whose performance will be diffraction limited in the optical waveband. The Space Telescope will lead to major advances in our understanding of the Universe. In addition, as it has been the case in the past when large new instruments were brought into astronomy it is expected that the Space Telescope will lead to the discovery of new astronomical phenomena which will give a more complete picture of the Universe we live in.

The perception of the major importance of the Space Telescope and the absolute necessity to be closely associated with it have been evident to the European astronomers since the early study phases of the project. This led eventually to the agreements that brought the European Space Agency into the Space Telescope programme.

This participation consists of three major elements:

a) the provision of the solar arrays which supply the electrical power to the spacecraft

b) the provision of the Faint Object Camera, described elsewhere in this volume

c) the provision of 15 astronomers and data reduction specialists to the Space Telescope Science Institute.

In return for these contributions, European astronomers are guaranteed a minimum of 15% observing time on the ST, although it is confidently expected that a larger share will be obtained based on the scientific merit of the proposals.

What is the position of the European astronomers with regard to the Space Telescope observatory? What are the special needs that its very existence implies for the European astronomers? These are the questions that are addressed in this paper.

II European participation in the Space Telescope Science Institute

As part of its overall participation in the ST programme ESA makes substantial contributions to the Science Institute. This participation has been agreed at two main levels. In the overseeing structure European astronomers are expected to serve in the AURA Board of Directors and in the Space Telescope Institute Council. At least two European astronomers will be members of the Telescope Allocation Committee and one a member of the Visiting Committee.

Within the Science Institute itself ESA provides 15 persons who will fill a variety of staff positions. About two thirds of these positions will be reserved to astronomers and the ESA provided staff will be fully integrated within the Science Institute.

It is foreseen that most appointments will be made for periods of up to 4 years duration after which the astronomers will return to their home institutions thus ensuring that the know-how gained in the ST is eventually brought back to Europe.

From the point of view of the European users of the Space Telescope, there should be no

significant difference in the way they interface with the Science Institute. Proposals will be solicited from the Science Institute and the European proposals will not be subjected to any pre-selection procedure, although a copy of the proposal must be sent to ESA for accounting purposes. The selection procedure will be the same as for all other proposals. Funding however will not be provided by NASA or ESA; rather it is expected that all funding required will be obtained through the national institutions.

Access by European astronomers to the Science Institute facilities, will be granted on the same basis as any other astronomer. From a practical point of view it is likely that travel funds restrictions will be the limiting factor in deciding the extent and frequency of the visits to the Science Institute. These restrictions will be even more apparent when requesting funds to carry out extensive data analysis or archival research as opposed to the primary observations.

III Space Telescope and ground-based astronomy in Europe

It is obvious that ST will play a major role in making the forefront observations of the future, certainly those that cannot be made in any other way from the ground because of spatial resolution or wavelength coverage or that require inordinate amounts of observing time. It is equally obvious that ground based telescopes will be essential in preparing the scientific ground for the ST observations and in following up these observations with complementary ones, in addition to carrying out their normal observing programmes.

In assessing the impact that the Space Telescope is likely to make upon the European astronomical community, it is instructive to examine the other observatory facilities that will be available to the European astronomers.

European astronomers are guaranteed at least 15% observing time on the ST. In comparison the amount of observing time available to European astronomers from large ground-based telescopes is about one order of magnitude greater. Europeans have access to the ESO telescopes at La Silla, the Anglo-Australian Telescope, the French-Canadian Telescope and the UK Infrared Telescope in Hawaii. The German telescopes are now operational in Calar Alto Spain and the French Pic-du-Midi telescope is producing high resolution images. A number of Schmidt telescopes at Siding Springs, La Silla, in France and in Italy are surveying the sky and producing large amounts of data. Plans are well under way for the La Palma observatory with its 4.2m telescope, for the installation in La Silla of a twin to the German telescope of Calar Alto and for the construction of the ESO New Technology Telescope also in La Silla.

In step with these developments modern instruments have been and are being developed, most of which utilize up-to-date detectors such as panoramic photon-counting devices, CCD and other digital detectors. It is now a common requirement of all telescopes, to be able to handle two dimensional arrays of digital data of the same type of that produced by the Space Telescope instruments.

It is clear from all this that most astronomy will still be done with ground based telescopes during the Space Telescope lifetime, and it is evident that very few, if any, European astronomers will be full time Space Telescope astronomers.

It is equally clear that the type of data produced by the ground-based telescopes, e.g. digital images and spectra, is of the same nature as that produced by the Space Telescope. There is therefore a need throughout Europe to solve an image and data processing problem for ground-based astronomy as a whole to which the Space Telescope needs will be a limited addition.

This has been recognized already some years ago and perhaps brought to a sharp focus because of the Space Telescope requirements in the ESA ST Working Group, a team composed of distinguished European astronomers. The problem was then recognized to be how to provide the most effective mechanisms for pursuing image processing in general.

Several groups who have reviewed this problem have concluded that, even within individual countries, large centralised systems are not what the astronomers need. The essence of image-processing in the Space Telescope era and beyond will be interactive computing. In interactive analysis of data, thinking time between operations is the most important part of the scientific analysis and for a major project may extend over several weeks, possibly months. Thus, every astronomer will want to have ready access to such a system close to his own institute which automatically means a distributed network of small computers. The rapid progress in computer technology has brought such systems within the financial reach of an increasing number of institutes in Europe.

As a matter of fact considerable progress has already been made in Europe at the

national level. Sophisticated data analysis packages have been developed in France under the coordination of the CDCA in Nice and operate in a number of laboratories utilizing different computers. In the United Kingdom a distributed network of computers, Starlink, comprising seven centres has been established. In Italy a similar concept has been adopted for Astronet, which will link eight centres within this year. The European Southern Observatory has developed a major data analysis centre which serves many users of the ESO telescopes. Similar facilities exist or are planned in many other countries.

There remains however one danger, namely that software development will be fragmented at the individual centres. This is a good thing from the point of view that every research programme has its own special requirements. On the other hand a large amount of unnecessary duplication of effort will result. In addition a considerable number of basic software programmes are required by every centre which do not need to be developed over and over again at a large cost.

In this light it is clear that a requirement exists for the role of one of these centres to be expanded to cover the tasks of provision of basic software and coordination of the software development effort. There would be distinct advantages in coordinating software on a European scale. This would be a positive contribution towards fostering collaboration not only in Space Telescope astronomy but also in astronomical data reduction in general.

The requirement is then to establish a central facility which ensures the coordination within Europe, and with the Science Institute, of astronomical software development. This assumes the existence of a well designed flexible software system capable of accepting new software programmes as they are developed by the users in their local data analysis centres. These programmes would then be fully tested and documented at the "coordinating facility" and made available to the user community. In this sense it will act as a "clearing house" for astronomical software. In addition software development of its own should take place at this centre.

IV The European Coordinating Facility

The first task of the ECF as has emerged naturally from the analysis of the previous section is therefore that of carrying out the coordination of the development of scientific analysis software throughout Europe.

Just as important, European astronomers need to have easy access to all ST observations after these are no longer proprietary data belonging to the original guest observer. As a rule this is expected to occur one year after the observing program has been completed. These data archives will grow as time progresses and will become a scientific resource of major importance. The nature of the research carried out on data archives is such that it would be extremely difficult for most European astronomers to obtain the necessary travel funds to the United States. Even if these funds were forthcoming serious logistic limitations would be found at the ST Science Institute whose priority task will always be to support the on-going observations. To allow European astronomers to be in a position to fully exploit the enormous potential provided by the data archives, ESA has agreed with NASA that a full copy of these archives will be deposited in the ECF.

The second major task of the ECF is then to provide an efficient means for archiving, cataloguing, retrieving and disseminating all the ST observations to the astronomers from ESA member states.

Another consideration is that it is by no means certain that all the astronomical institutes in Europe will be able to afford or have easy access to an image processing centre of the right kind. In this context a central facility will ensure some support to these ST users. This support will of course have to be limited by the availability of resources such as computer time and number of terminals but it will undoubtedly be of considerable interest to the European ST users.

Finally it is important that this facility should provide for detailed know-how on ST and its complement of scientific instruments. This will ensure that the European scientists will have easy access to the information needed for the preparation of their observing proposals and best exploitation of the data.

After extensive consultation with the European scientists ESA has decided that to establish a Space Telescope European Coordinating Facility which will carry out the tasks outlined above, will greatly enhance the scientific return expected from the Space Telescope. To help in this task ESA will provide a team of about seven people and a nominal sum towards the start up costs. Such a small team cannot possibly be expected to function in isolation and the scheme will only be effective if the Facility is located in a "Host-Institute" which provides an excellent scientific environment and a considerable

number of supporting services.

A call for proposals for the "Host-Institute" was issued two years ago and amongst the excellent proposals received, a peer review team chose the European Southern Observatory, Germany, as the location for the ECF.

In addition to its dynamic scientific environment, ESO will provide the physical location, dedicated personnel, the computer facilities etc. and will establish the ECF as a new division reporting directly to its Director General while ESA will issue broad policy guidelines and maintain overall monitoring of the ECF performance. This will ensure that the required visibility and autonomy of functioning will be maintained by the ECF.

At present a Memorandum of Agreement and other lower level documents are being negotiated between ESA and ESO. It is expected that these negotiations will be concluded before the end of the current year with a view to begin work in earnest in establishing the ECF in 1983.

We are confident that the existence of the European Coordinating Facility will provide the European astronomers with the means to submit first rate observing proposals and to fully exploit the wealth of data produced by the Space Telescope and will therefore greatly contribute to the scientific success of the mission.

N82 33299

The Space Telescope Observatory

C. R. O'Dell

Marshall Space Flight Center
Marshall Space Flight Center, Alabama 35812

Abstract

The Space Telescope will be the first long-lived, versatile astronomical observatory in space. The wide wavelength range and emphasis on high image quality of its design will make it a unique facility. The history of the observatory is briefly described, as is the overall system design. The principal design features that are important to the scientific user are described. The final section reports on the present status of preparation for launch in the spring of 1985.

1. Introduction

The Space Telescope observatory concept goes back to the epochal writings of Herman Oberth[1] and Lyman Spitzer,[2] which described the basic advantages of a space observatory. When the National Aeronautics and Space Administration (NASA) was formed in 1959, astronomy became a natural scientific discipline to be pursued from space. In the early 1960's the first of a series of recommendations that a large, diffraction limited telescope be built was made.[3] Even as the Orbiting Astronomical Observatory spacecraft were being built, technology and design studies were conducted of a more ambitious instrument that has come to be called the Space Telescope.

In the autumn of 1971 NASA began detailed study of the Space Telescope, then of 3-m aperture and called the Large Space Telescope, to determine the feasibility of such a project. The answer was a strong yes and the preliminary design began in 1972. This design study was extended as construction funds eluded the program leaders until late in 1977 when approval was given by the Congress to actually build and operate the observatory. By this time a decision had been made to enter into a 15% partnership with the European Space Agency, who would provide a key Scientific Instrument, the solar array, and operation and staff support.

Considering the level of technological challenge involved with the Space Telescope, the program has adhered remarkably well to the original schedule, although money availability has caused some delays beyond the original development plan. The Space Telescope is now scheduled for launch in the spring of 1985, some 13 years after the first formal studies, a long time but an interval commensurate with the expected scientific return.[4]

2. System description

The optical design is the Ritchey-Chretien variation of the Cassegram configuration, providing a coma-free wide field which is astigmatic in its outer portions.[5] With a 2.4-m clear aperture and F24 focal ratio, the scale in the focal surface is 3.6 arcsec/mm. The Scientific Instruments are located in five separate bays, which allows them to operate and be replaced independent of one another. The services that must be provided to the telescope are furnished by a Support Systems Module, which encircles the primary mirror. This system is the most complex part of the spacecraft and provides the power, control, and communication functions that are essential to operation.

The attitude control function is very important and is done through a series of mechanisms. Actual motions are caused by speed variations in spinning reaction wheels. The signal for these wheels comes from a variety of sources; a course Sun sensor; fixed head star trackers, gyroscopes, interferometric star trackers. The functional combination of these will be described in the section on the Pointing and Control System.

Spacecraft power originates in the articulating solar arrays being provided by the European Space Agency. A power system, which includes storage batteries, then provides electrical power through orbital day or night.

Control of the spacecraft is done from the ground command signals generated at the control center at Goddard Space Flight Center near Washington, D.C., and sent to the Space Telescope via the Tracking and Data Relay Satellite System, which geometrically allows direct access about 85% of each orbit. The scientific and engineering data come to earth via the same system, at a maximum rate of one megabit/second. Since the Tracking and Data Relay Satellite is shared by many other users, it will be available only a portion of each

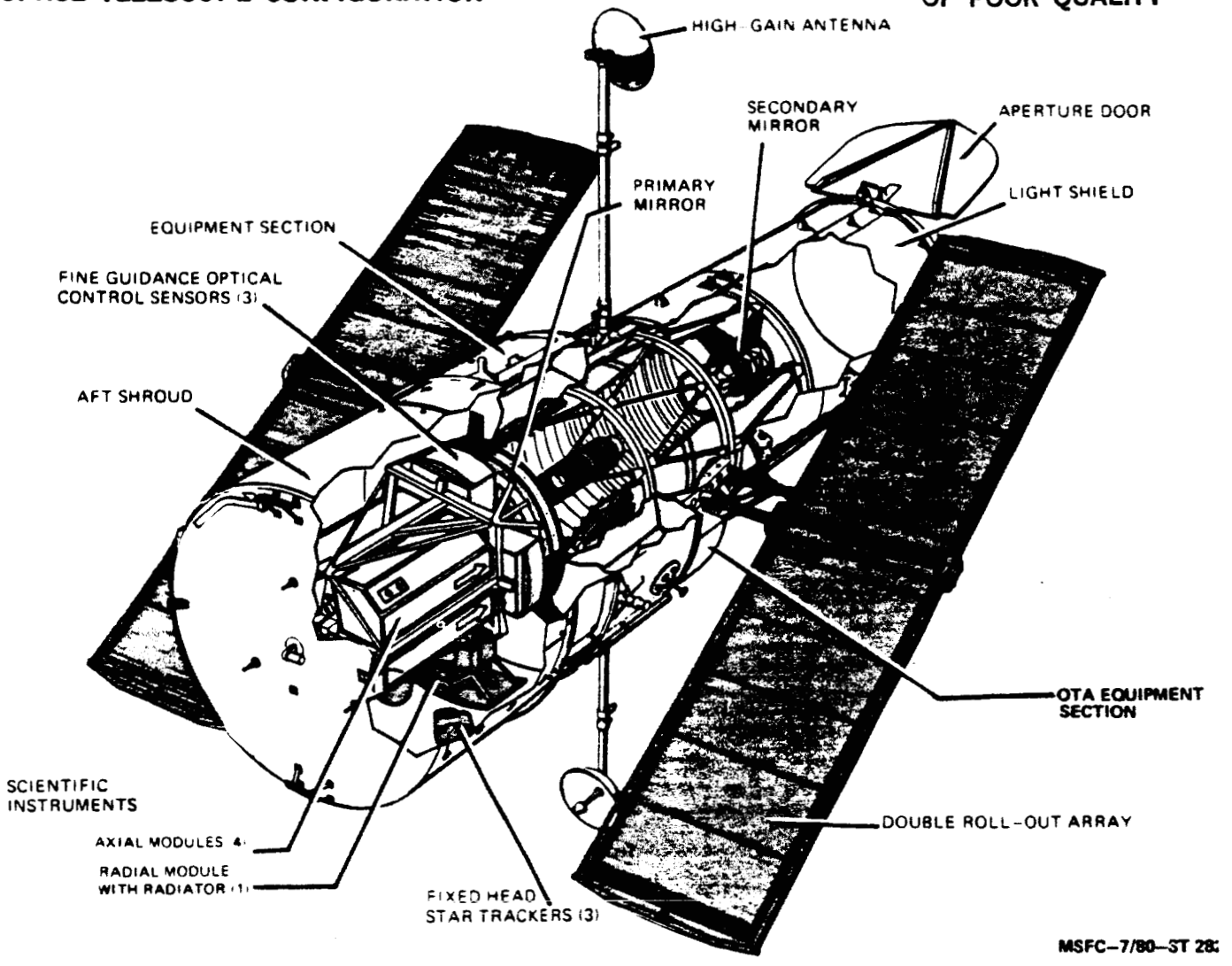

Figure 1. This cutaway drawing shows the major components of the Space Telescope Observatory.

orbit. This means that we will be able to do real-time control of the spacecraft about 20 percent of the time, an important scheduling constraint.

3. Images

The Ritchey-Chretien telescope system presents an image of excellent quality at the focal surface. In common with other two mirror systems it represents a balance between image characteristics. By going to the Ritchey-Chretien design we have essentially complete freedom from coma, but, at the expense of astigmatism at the edge of the useful field of view. This trade-in characteristic is appropriate since the astigmatic images are still useful for pointing reference.

The Space Telescope is being developed to meet certain minimum performance requirements, e.g., resolution of 0.1 arcseconds, full width of the image at half of maximum intensity of 0.06 arcseconds, and 70% of the total image energy encircled within 0.1 arcseconds radius (all figures specified at 633 nm). At this point in the program we expect to meet and probably exceed these requirements. Figure 2 shows how the image should vary across the field of view. The reference wavelength (633 nm) is used because it is conveniently provided in the optical laboratory. We expect high reflectivity from the MgF overcoated aluminum reflecting surfaces from about 115 nm to 1 mm wavelength.

We expect that the image quality will improve at shorter wavelengths as the wavelength/

Figure 2. The Ritchey-Chretien optical design of the Space Telescope is coma free, but has off-axis astigmatism. This illustration gives the approximate effect of astigmatism at the circle of least confusion.

aperture ratio improves; however, at some point the telescope begins to fail the near diffraction limit criteria and the image fails to improve with decreasing wavelength. Our current best estimate for this wavelength dependence is shown in Table 1. It is important to note that this prediction does not include pointing stability contributions, unlike Figure 2.

Table 1

Full Width at Half Maximum for a $\lambda/20$ System

Wavelength (nm)	0.12	0.20	0.35	0.63
FWHM (arcseconds)	0.011	0.018	0.030	0.054

The image surface is divided into eight segments, as shown in Figure 3. This division into fixed segments gives the central field and the inner parts of the axial Scientific Instruments' field an image of high quality.[6] The outer parts of the axial Scientific Instruments' fields are distorted by astigmatism and are not used by any of the initial Scientific Instruments. The outer three portions are fed to the Fine Guidance Sensors that are described in the next section. This division into fixed subsections was determined to be the most cost effective solution to the problem of providing access for several Scientific Instruments. A highly reliable moving structure would have been too expensive. This awkward division has not, at present, been a serious impact on the design of individual Scientific Instruments. There may be a limitation in the future Scientific Instruments if very wide field detectors become available. An added benefit of this approach is that the central Scientific Instrument (the Wide Field/Planetary Camera) and one of the axial Scientific Instruments can be operated simultaneously for some observations.

Another important characteristic of the telescope design is straylight control. The Space Telescope will be operating under continuously changing exposure to three bright sources: the sun, the moon, and the illuminated earth. The design was to minimize the impact of these sources on Space Telescope science. The result of our straylight control design is to reduce straylight to a surface brightness of 23^{m} arcsec^{-2} (which is the same as the darkest part of the zodiacal cloud surrounding the earth's orbit) at 50° from the sun, 15° from the moon, and 70° from the bright limb of the earth. When these constraints

FOCAL PLANE MAP

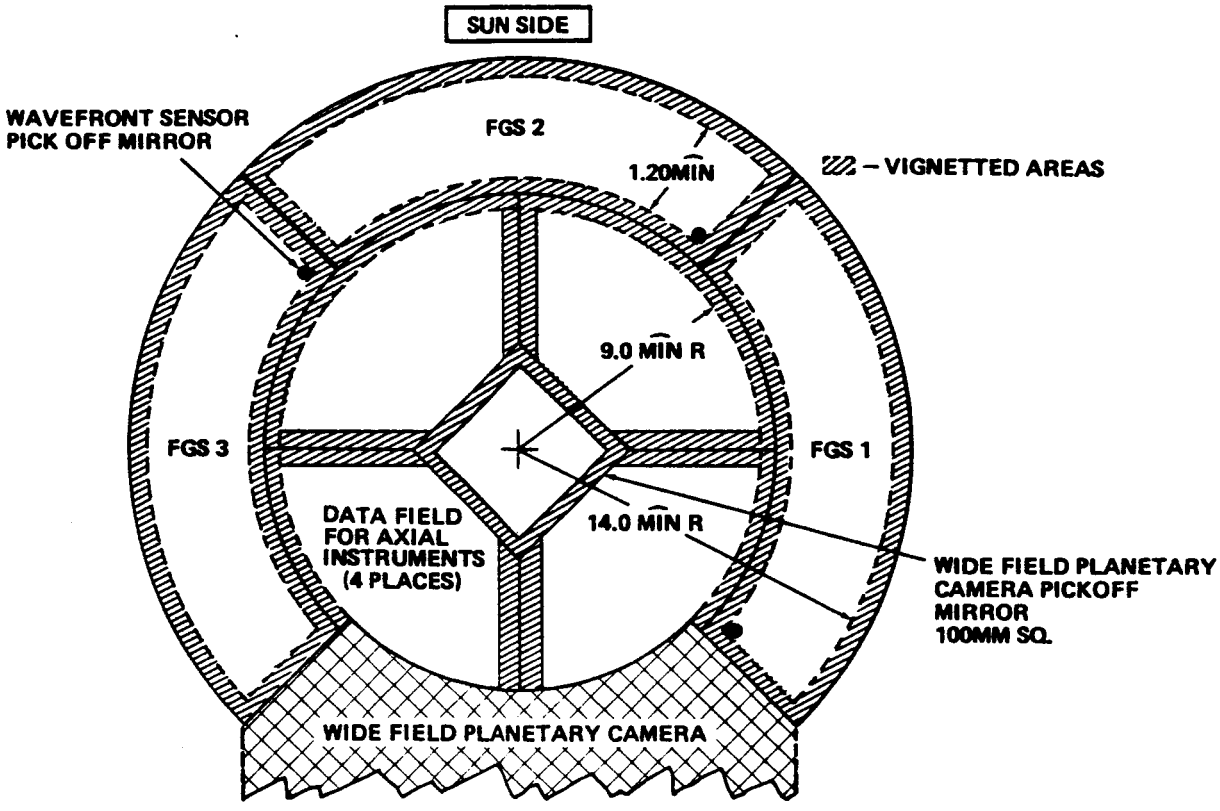

Figure 3. The focal surface is divided into eight dedicated segments, each supporting a specific scientific instrument or fine guidance sensor.

are violated the straylight increases in a complex fashion which allows observations of sources not at the faint light limit. The impact on operations of the constraints are discussed later.

4. The Pointing and Control System

The greatest technical challenge in building the Space Telescope (next to the precision optics) has been the Pointing and Control System. The Pointing and Control System is used for every astronomical observation and it is important that potential users understand the functions of this system. During routine operation three position indicators are used: Fixed Head Star Trackers, which are independent of the main telescope optics and can locate bright stars to a precision of about one arcminute; Rate Gyroscopes which drift with an uncertainty of about 0.01 arcseconds/second; the Fine Guidance Sensors, which derive their signals from stars imaged near the edge of the Space Telescope's field of view.

The process of a typical acquisition of an object begins with a slew of the telescope (15 degrees/minute maximum rate) to a predetermined spot. Since the uncertainties of position due to gyro drift and the inaccuracies (especially roll angle) of the initial direction increase with displacement, slews will be as short as possible. The uncertainty can be several arcminutes after a 90^{o} slew. The Fixed Head Star Trackers are used to determine the rough position as necessary. Then the coordinates of a candidate guide star are fed into each of two Fine Guidance Sensors (FGS). One FGS begins searching for the first guide star, using a spiral search pattern with a 2 arcsecond aperture. Upon finding a star in the correct brightness range it stops and the other FGS searches for its guide star. When the second star is found, the relative positions provide the final confirmation of position. If the confirmation is not made, the search resumes. The search can be made over three arcminutes. The sensitivity of the system is that it will operate adequately at 14.5^{m}, a brightness level that statistically will produce two guide stars for 85% of the fields at the Galactic Poles. The acquisition cycle will typically take about three minutes.

Once the guide stars are acquired, the images are fed to a Koesters prism interferometer

which provides a tracking signal. The basic stability reference is the set of rate gyros, with their positions being updated every second by the FGS signal. The resulting stability should be 0.007 arcsecond rms. This pointing stability is quite adequate for visual and near ultraviolet images, but could become a limiting feature if very good far ultraviolet images are realized.

The sequence described above refers to the frame of reference of the FGS's which should be known to about 0.01 arcseconds accuracy. Unfortunately, few celestial objects' locations are known with this accuracy, so that the previously known positions become the limiting feature for an initial observation with the Space Telescope. The easily available ground determinations (about one arcsecond) suffice for the wide field instruments (the Wide Field/Planetary Camera and the Faint Object Camera) but are too crude for the other instruments. Each instrument has a method of automatically centering the science object or sending down a real time signal which will allow the observer located at the Space Telescope Science Institute to make the final decision on the exact pointing. In addition, the Wide Field/Planetary Camera and Faint Object Camera can often be used to make a quick image from which the position of the science target with respect to the guide stars can be determined, either in near real time or later on in the observing schedule.

It is obvious that a tremendous amount of astrometric data is needed for operation of the Space Telescope. The Space Telescope Science Institute is developing a system to provide positions of candidate guide stars and the most commonly observed science objects. The need for positions of objects not appearing on the available survey material will be met on a case by case basis.

We are not able to predict exactly how the Pointing and Control System will perform in orbit, so some procedures may change. We do expect that internal motions within Scientific Instruments may cause the FGS's to lose lock. The worst offenders will be identified and a gyro reference only mode will be used until the vibrations subside. If a random loss of lock occurs, a stop taking data indication will be given until the automatic reacquisition process has been completed. Since the spacecraft will not have moved very far and the relative positions have been determined accurately, this cycle should be short.

5. Operations

The Space Telescope is a complex machine, as such, it has many operational constraints imposed by the spacecraft design. We have tried to minimize these constraints, within the available development budget; unfortunately, many still remain. The primary constraints are imposed by the rapidly changing viewing conditions that come from the low earth orbit (500 km). The Space Telescope will be passing through a full cycle of sun/earth/moon illumination every 100 minutes and the straylight constraints discussed above will apply. Upon any one orbit we will have a condition very much like that shown in Figure 4, where some regions of the sky are continuously observable and others are entirely excluded. Of course, there will be some operation procedures, such as looking over the dark limb of the earth in order to observe comets or interior planets, which will be pursued only after experience is gained.

The basic science schedule is generated by the Space Telescope Science Institute and provided to the operations center at the Goddard Space Flight Center near Washington, D.C. This center then generates a set of spacecraft commands that are procedurally safe and still carry out the desired science. These commands are then sent to the Space Telescope via the Tracking and Data Relay Satellite System. Up to 24 hours of commands can be stored on board. The resulting data can be sent down immediately on stored on tape recorders and broadcast down later. Upon receipt at the Goddard Space Flight Center the data is repackaged and sent on to the Space Telescope Science Institute for reduction. Most of the observations will be automatic, but the system is designed to permit real time interaction with the observer. This operational flexibility is intended to allow the best scientific use of the Space Telescope.

The Space Telescope is the first "permanent" space observatory, i.e., it is intended to have a very long functional life due to the ability to service and modify it. This will be done through a program called maintenance and refurbishment. It is expected that we may visit the Space Telescope on orbit with the Space Shuttle about every 2½ years for orbital servicing and that at intervals of about five years the observatory will be returned to earth for changes and repairs that cannot be made on orbit. This flexibility means that the Space Telescope should continue indefinitely, as long as the returns justify the cost. The design life is 15 years on orbit.

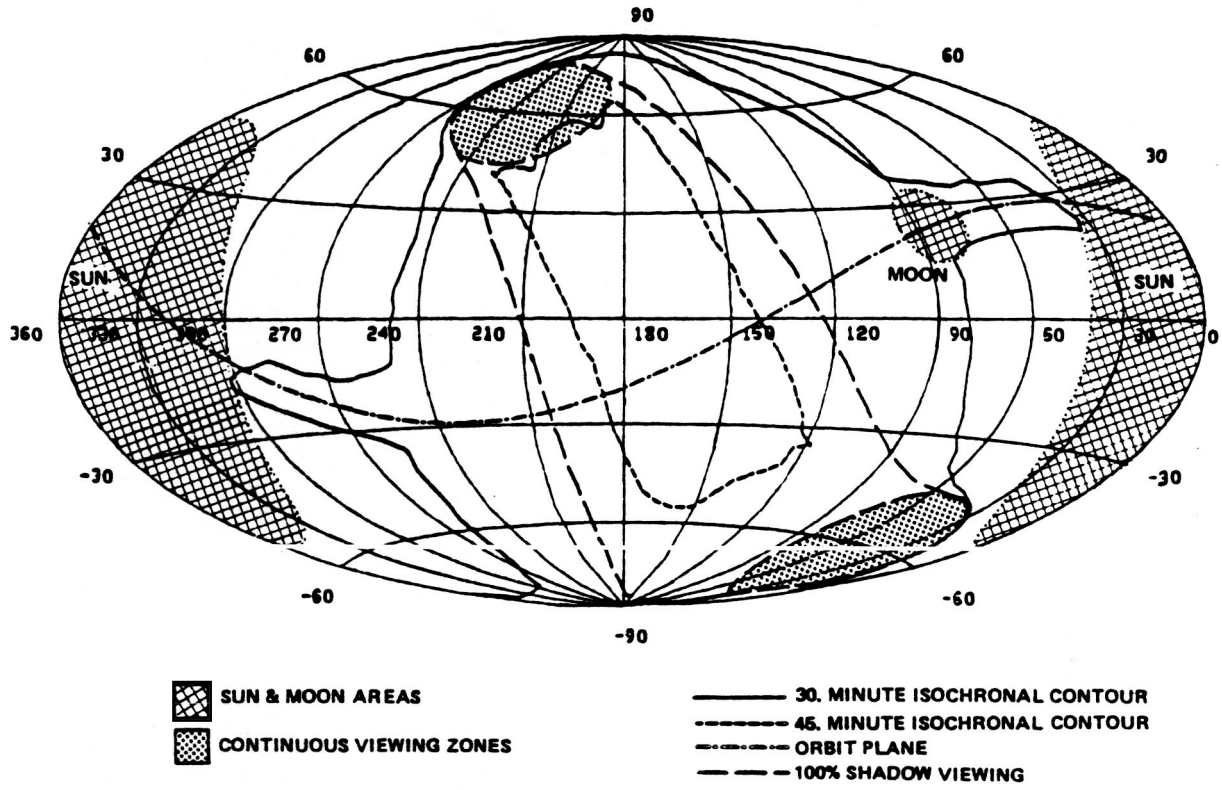

Figure 4. Like a ground observatory, the Space Telescope has preferred viewing zones on the sky. This figure shows regions excluded because of straylight considerations. The other contours describe regions of optimum viewing.

New Scientific Instruments will be needed as the Space Telescope program matures. These instruments may reflect changing scientific priorities or improved technologies, or both. The present plan is to begin study of second generation Scientific Instruments in late 1983, with the start of construction to begin about a year after launch. We expect that three to four instruments will be studied and one or two will be constructed. The latter would then be ready for installation about five years after launch. A similar cycle would then be repeated periodically throughout the lifetime of the observatory.

6. Status

The Space Telescope is well into construction, with launch anticipated in the spring of 1985. Although many components are built simultaneously, the basic plan is that it is built from the inside to the outside. The telescope portion will be completed first. Figures 5, 6, and 7 show the finished primary mirror and the structures that hold the optical mirrors and the Scientific Instruments. Many other major components, including the ESA provided solar array are almost complete. The Scientific Instruments will be delivered by the summer of 1983, and 1984 will see the integration of all parts and testing of the system. The operations preparations parallel this, climaxing in operation readiness just before launch.

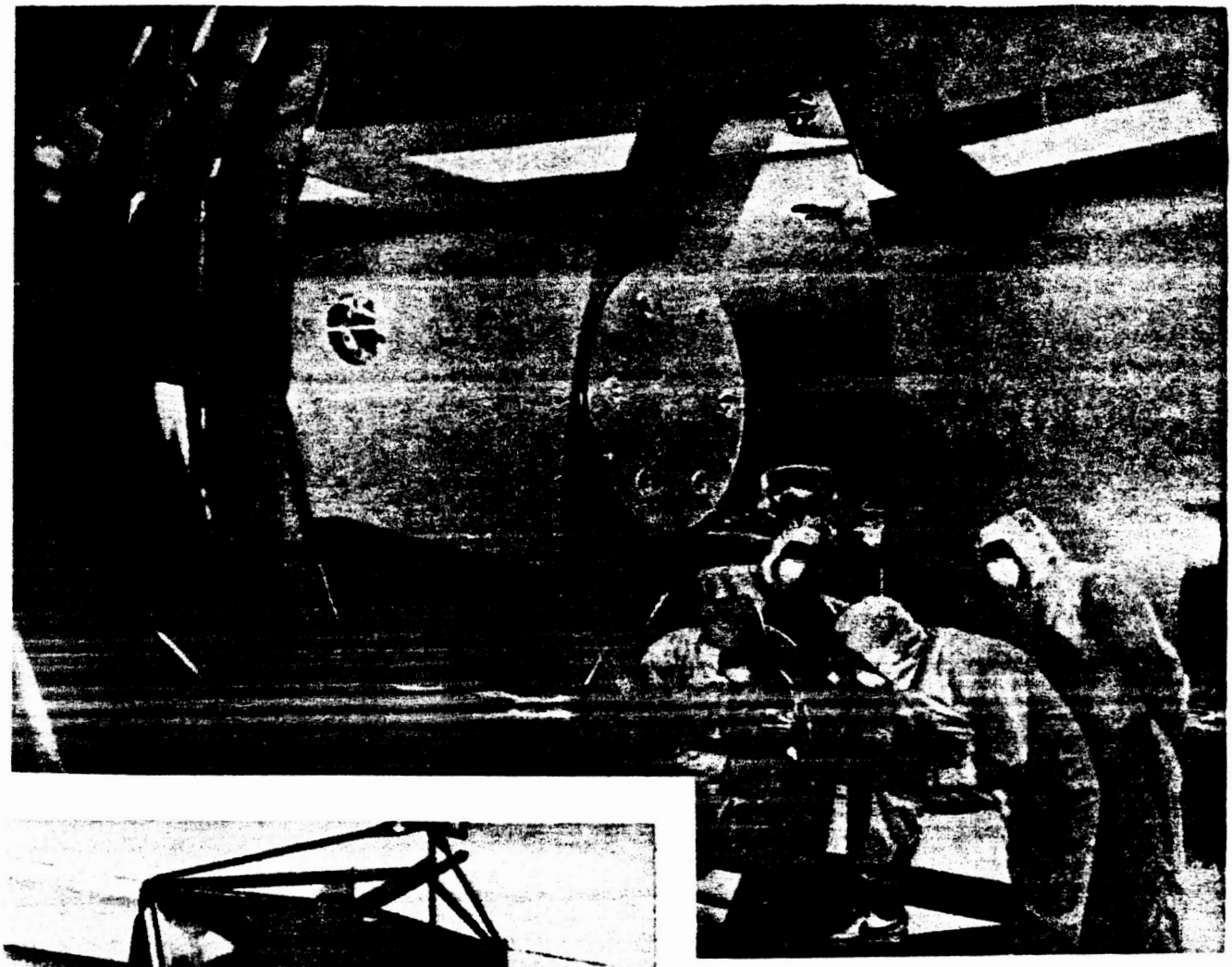

Figure 5. Figuring and coating of the primary mirror has been completed. The mirror is now receiving the attachment that will hold it in correct alignment.

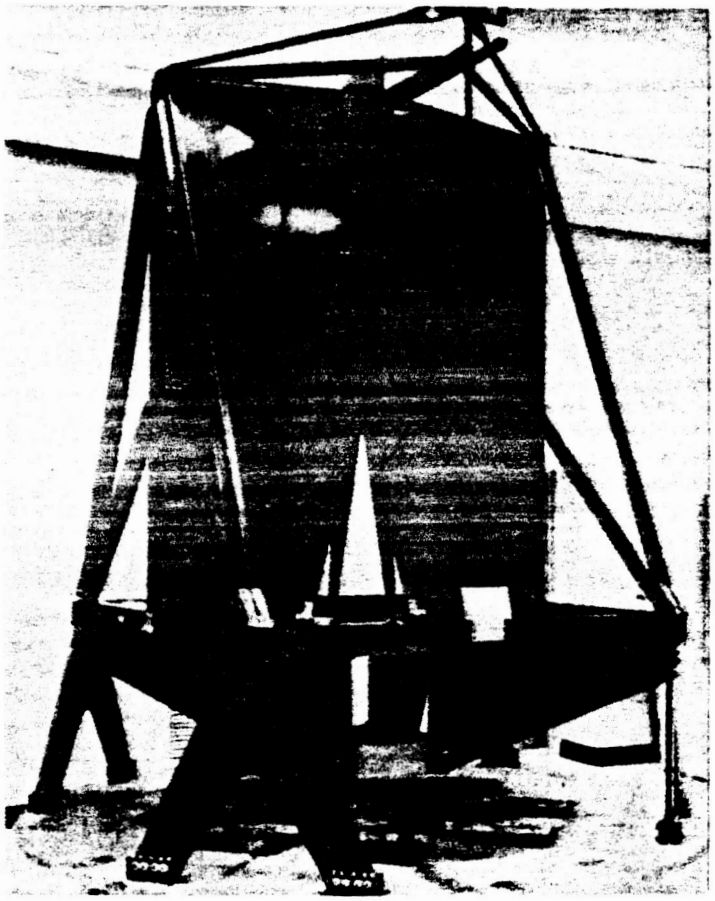

Figure 6. The focal plane structure attaches to the aft side of the main ring and holds the scientific instruments, fine guidance sensors, and several other major components. Its principal material is graphite-epoxy.

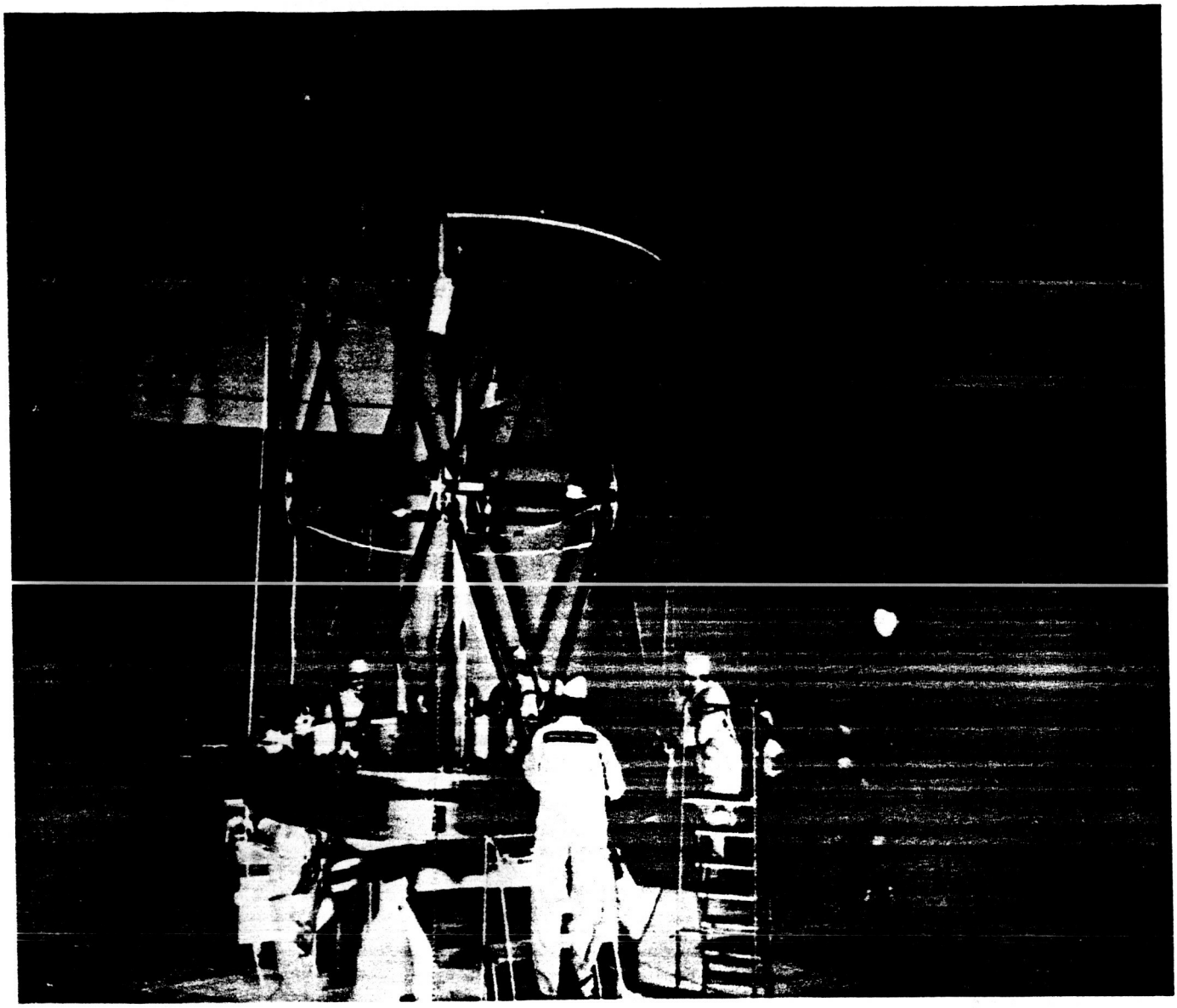

Figure 7. The principal structure for the telescope is shown. The titanium ring is the main structural component of the observatory. The graphite-epoxy truss structure holds the primary and secondary mirrors in alignment.

References

1. Oberth, H. 1923 Die Rakete zu den Planetraümen, Munich: R. Oldenbourg
2. Spitzer, L. 1946 Astronomical Advantages of an Extraterrestrial Observatory, Project RAND Report, Douglas Aircraft Co., Sept. 1
3. National Academy of Sciences 1962 A Review of Space Research. Publ. 1079, Chap. 2, Astronomy. Natl. Acad. Sci., Natl. Res. Council
4. Bahcall, J. N. and O'Dell, C. R. 1979 The Space Telescope Observatory. In: Scientific Research with the Space Telescope, NASA CP-2111 (M. S. Longair and J. W. Warner, editors)
5. O'Dell, C. R. 1981 The Space Telescope. In: Telescopes for the 1980s, Annual Reviews Inc., Palo Alto, California (G. Burbridge and A. Hewitt, editors)
6. Leckrone, D. S. 1980 Publ. Astron. Soc. Pac., 92: 5-21

D4

N82 33300

The Wide Field/Planetary Camera

James A. Westphal

WF/PC Principal Investigator
California Institute of Technology
Mail Stop 170-25, Pasadena, California 91125
and the
WF/PC Investigation Definition Team*

Abstract

A wide suite of potential astronomical and solar system scientific studies using the Wide Field/Planetary Camera on Space Telescope are described. The expected performance of the camera as it approaches final assembly and testing is also detailed.

Introduction

As we near the final assembly and testing of the Wide Field/Planetary Camera (WF/PC) for Space Telescope (ST) we can more confidently predict its performance in orbit. This seems a good time to widely publish this data and some of the scientific programs that are especially attractive to our Investigation Definition Team (IDT).

The Camera

The WF/PC will be placed in a "radial" bay of ST where an attached mirror will deflect the central 3x3 arc min field into the WF/PC housing. The incoming f/24 ST beam will pass through a shutter and a filter wheel arrangement allowing certain combinations of filters, polarizers and transmission gratings to be inserted in the optical path. The f/24 beam then comes to focus on the surface of a shallow four faceted mirrored pyramid which splits the field of view into four quadrants. The four now-diverging f/24 beams are folded into the entrances of four small Cassegrain reimaging telescopes which convert the f/24 beam to f/12.9 for the Wide Field Camera (WFC) mode. These form new images, through MgF_2 field lenses onto the four WFC solid state CCD silicon detectors.

Alternately, by ground or stored command, the pyramid can be rotated 45^{o} about the optical axis and the four diverging beams routed into four different Cassegrain repeaters which form f/30 images on the four Planetary Camera (PC) CCDs. Thus the Wide Field/Planetary Camera has two different spatial resolutions which can be selected to optimize the trade-off between spatial resolution and field coverage appropriate for each target.

The CCDs must be cooled by thermoelectric coolers to below $-95^{o}C$ to reduce the "dark current" to acceptable levels. Appropriate electronics process and finally digitize each 800x800 pixel CCD output to allow the data to be transmitted to the ground and delivered within 24 hours to the Space Telescope Science Institute for use by the observer. The technical details useful for a WF/PC user to begin to plan this program are given to the best of our present knowledge and prediction near the end of this paper.

Our Investigation Definition Team (IDT) was selected by NASA in a competition in 1977 to conduct a scientific investigation using the WF/PC instrument we proposed in response to an Announcement of Opportunity. The IDT bears the responsibility for the conceptual design, procurement, testing, and calibration of the WF/PC. We selected the Jet Propulsion Laboratory in Pasadena, California to design and build the WF/PC.

In the following sections we have included excerpts of our original science proposal to illustrate some of our IDT's special interests. These studies are obviously only a tiny fraction of the possible uses of ST with the WF/PC but are illustrative of most of its capabilities.

Cosmology

Nothing else in astronomy so captures the general imagination or has deeper implications for human philosophy than the large-scale nature and history of the universe, and it is here that the Space Telescope offers its greatest promise. The WF/PC will be a prime

---

*W. A. Baum, A. D. Code, D. G. Currie, G. E. Danielson, J. E. Gunn (Deputy P. I.), T. F. Kelsall, J. A. Kristian, C. R. Lynds, P. K. Seidelmann, and B. A. Smith

ST instrument for cosmological exploration on three major fronts: the calibration of the distance scale, the measurement of evolutionary changes, and the testing of models of the Universe as a whole.

The cosmic distance scale

In the last twenty-five years, our knowledge of the distance scale has improved dramatically. This improvement has been largely due to a single instrument: the 200-inch Hale telescope. Beginning with Baade and Swope's investigation of the Cepheids in M31, this effort has continued through the most recent work by Sandage and Tammann. The increased light gathering power of the 200-inch over earlier telescopes offered a major increase in observational capability.

With its high resolution and freedom from atmospheric effects, the Space Telescope will offer a similar quantum leap in capability. With exposures of a few thousand seconds, the limiting magnitude of our Wide Field Camera on ST will be 100 times fainter than the 200-inch photographic limit, and we will be able to see similar objects 10 times farther away with the same resolution and photometric accuracy. For the problem of the distance scale, this factor of 10 is crucial, since it will allow us to observe Cepheid variables in galaxies of the Virgo cluster. This means that we will be able, for the first time, to tie local measurements of these primary distance indicators to the distant realms of the great clusters, without the need for poorly known secondary distance indicators. Having directly established the distance to Virgo, we will then have a large sample of galaxies which can be used to decrease the uncertainties of the secondary distance indicators (brightest stars, HII regions, integrated galaxy magnitudes, etc.). With improved accuracy of the secondary indicators and the ability to detect them 10 times farther away, we are then in an excellent position to investigate the details of the Hubble flow at distances where it is unaffected by the perturbing effects of the local supercluster, and to examine the gravitational effect of the local supercluster itself. This latter line of investigation leads directly to an estimate of the local mass density, which is a central and very poorly known datum for cosmology.

At Virgo's distance a 20-day cepheid with $\langle M_V \rangle = -5.5$ is expected to be an object of about V = 26 magnitude. In a 3000-second exposure with the Wide Field Camera, such a cepheid will be observed with a signal-to-noise ratio of about 10.

It is perhaps instructive to compare the WFC capability with the work that has been done on cepheids from the ground. Baade and Swope fairly easily detected cepheids in M31 (distance modulus 24.2) with periods less than 3 days (absolute visual magnitude = -3), and measured 350 cepheids in selected areas covering a small fraction of the area of the galaxy. More recently, Sandage and Tammann have pushed the present capability to very nearly its limit in their study of NGC 2403 (distance modulus 27.6). In a very intensive search over the entire galaxy, they detected and measured seventeen cepheids with periods from 20 to 90 days (M_V = -5 to -7).

The ease of measuring cepheids in Virgo (distance modulus 31.5) with the Wide Field Camera on ST, taking into account the increase of 5 in limiting magnitude, lies between these two cases. It should be similar to measuring cepheids M31 from the ground at 3 times its real distance, or NGC 2403 at 60% of its real distance. A single WFC exposure will cover about 1/4 of the area of a giant galaxy in Virgo and we would expect to be able to measure roughly 100 cepheids, with periods greater than 10 days, with about 30 optimally spaced exposures.

Beyond the Virgo Cluster, and therefore beyond the domain of redshift anomalies caused by the local supercluster, the diameters of HII regions will provide one of the methods for establishing distances of galaxies as far as the Coma Cluster, whose redshift is 0.022. On the basis of present distance estimates for Coma, the largest HII regions would be expected to subtend about 0.4 arcsecond or 9 pixels at f/30. Only a few images, one or two per selected galaxy, should be needed to establish the distance scale out to redshifts of order 0.025.

Globular clusters are another valuable indicator for establishing relative distances. At the distance of Coma, they should still be identifiable objects, and the brightest are expected to be about V = 26 magnitude. The brightest stars in galaxies, as bright as M_V = -8, can be distinguished to distances of at least 50 Mpc with the WFC, and will provide ancillary distance information. All these indicators except the cepheids require only one image per galaxy or, at most, images in a few colors. Enlargement of the statistical base for such distance indicators is perhaps as important as simply reaching farther. The improved statistics obtained from the distant sample will allow returning to the local supercluster and accurately mapping the velocity anomalies, if any. These anomalies provide probably the best test for the mean mass density of the universe.

From these ST studies, it seems likely that the Hubble constant can be determined within the accuracy of our knowledge of the distance to M31. This can then, in due course, be refined through other investigations carried out with the same camera, by, for example, accurate photometry of RR Lyrae stars in M31's globular clusters ($V \simeq 25$).

Evolution

For galaxies of very large redshifts the enormous look-back times provide both the opportunity and the need for investigating evolutionary changes. Differences in the spectral energy distributions of galaxies at different redshifts yield data with which evolutionary models can be compared.

The broad wavelength response of CCDs, together with the large number of filter positions in the WF/PC design, provide an ideal spectrophotometric instrument for quantitative investigation of population differences out to the largest observable redshift, i.e., as far back in time as possible. The entire spectral response of interest from 3400Å to 11000Å can be covered by thirteen spectrally adjacent filters having bandwidths about 10 percent of their central wavelengths. We intend to initially investigate ten clusters of galaxies distributed over the full span of accessible look-back times.

Evolutionary inferences can also be drawn serendipitously from images of non-selected fields recorded by the camera while the telescope is being used by the other instruments. Counts of galaxies to various limiting magnitudes will provide useful data for the evolutionary correction to magnitudes of galaxies in the field, and so yield important information about the history of star formation in bright spirals.

Recently obtained data from several sources suggests that near the magnitude limit of ground-based telescopes, a population of very blue extended objects is appearing. The exciting possibility exists that these are very young galaxies being seen at large redshifts. While this issue may be resolved before ST flies, the galaxy count exposures will surely record many of these objects to fainter levels than are possible from the ground, and information on their spatial structure and distribution can be obtained.

Measurements of the diameters of bright cluster ellipticals, which can be done to very large redshifts with the WF/PC, provide information on the evolutionary correction to the magnitudes of these objects which are needed for the test of the dynamical evolution of these systems. These data, together with the population evolution discussed above and a great deal of theoretical work, will yield the cosmological world models.

Tests of world models

In a qualitative sense, the expanding Universe lends itself to a number of possible interpretations, and it is the ultimate goal of observational cosmology to identify the correct world model from among the theoretical possibilities. The key discriminant derivable from observations of very bright galaxies is the deceleration parameter q_o which quantifies the slowing down of the expansion. It not only distinguishes one type of Universe from another (say, Big Bang versus Steady State, or Open versus Closed), but it also assays the total amount of matter in the Universe and translates the Hubble constant into a value for the age of the Universe. Comparison of the matter density so obtained with that from relatively local measurements provides one of the most crucial tests of conventional General Relativity on a size scale larger than physical laws have ever heretofore been tested.

The observables for distinguishing world models and for deriving q_o are the redshifts, magnitudes, and diameters of galaxies belonging to clusters. Members of clusters can be ranked so that intrinsically similar galaxies at various distances can be selected for measurement. For specifying the type, age, and mass of the Universe with confidence, the accuracy in the determination of q_o needs to be pushed below ± 0.1. In an open Big Bang Universe with $0 < q_o < +0.5$ and $\Lambda = 0$, an accuracy of ± 0.1 in q_o requires integrated magnitudes (with all corrections) to ± 0.1 or metric diameters to $\pm 5\%$ at a redshift $z = 1$. For a giant EO at $z = 1$ about half the light will fall within a radius of 1 arcsec, and with the WF/PC the surface brightness of the galaxy at 1 arcsec radius will be measurable to 3-percent accuracy. The resulting profile of the galaxy can then be well enough determined to yield its integrated magnitude and metric diameter. Since the dispersion in absolute magnitude is about $0^m.4$ for such systems, twenty such clusters will provide a large enough data base for determination of q_o to 0.1, provided one understands the evolution.

Data of this quality will provide not only a good measurement of q_o, but also a fundamental test of the Doppler interpretation of the redshift, i.e., a test of the expanding Universe concept itself. If the expansion is real, the bolometric surface brightnesses of galaxies, corrected for evolution, should be dimmed by a factor of $(1+z)^4$. For comparison, the "tired light" model implies a dimming factor of only (1+z). Although present data appear to support the Doppler models, the WF/PC makes possible a much more definitive test.

The same multi-color spectrophotometry obtained for investigating evolutionary changes will also yield redshifts by location of the 4000Å "break" in the spectrum, and this method can probably be used as far out as clusters of galaxies can be found. The obtainable accuracy, $\Delta z \sim 5\%$, is compatible with that of the magnitudes and diameters with which redshifts will be plotted. Although eight to ten images at stepped wavelengths will be required for each selected cluster, our camera yields redshifts for all galaxies in the field of view simultaneously, thereby distinguishing cluster members from non-members.

Galaxies

The extraordinary spatial resolution, faint magnitude threshold, and broad wavelength coverage of the camera open dramatic opportunities for extending our knowledge of galaxies, the fundamental aggregates of matter in the large-scale Universe. Clues to the origin and evolution of galaxies lie in their structure and content. The Space Telescope will reach members of the Local Group almost as effectively as large ground-based telescopes now reach the Magellanic Clouds, while ST studies of the Clouds can approach in detail those now made in parts of our own Galaxy. Studies of relatively distant galaxies, e.g., peculiar or active ones, will also be important.

QSOs and active galaxies

The extreme distances at which QSOs and active galaxies can be detected make them important potential probes of early epochs and remote parts of the observable Universe. The initial observations of these objects will be aimed at better understanding the physical processes in them and the manner in which they have evolved.

Using the visible-light grating, the CCD camera is ideally suited for identifying very faint QSOs and measuring redshifts. For brighter and nearer QSOs, the camera's high spatial resolution and high signal-to-noise ratio will permit associated nebulosities to be examined and their relationship to galaxies to be investigated. Polarization observations of QSOs, Seyfert galaxies, and galaxies with active nuclei can be made at high spatial resolution to put tighter constraints on physical models. The WF/PC includes polarizing filters allowing three axis polarization measurements with any of the available filters between 2500Å and 7000Å.

Stellar populations

Color-magnitude diagrams, color-color diagrams, and luminosity functions need to be derived in nearby galaxies of differing morphological type and in various regions within those galaxies. Within M31 and its companions, for example, 2000-second broad-band exposures will provide adequate magnitudes and color indices down to $M_V \sim +3$, which is near the main-sequence turnoff for even the oldest stellar populations. Using the techniques already familiar from studies of star clusters in our own Galaxy, color-color diagrams will permit corrections for interstellar reddening and will yield relative metallicity indices of the stars. Populations in M31 can be studied in the outskirts, across spiral arms, in inter-arm regions of the disk, and (with a less faint threshold) in the nuclear bulge. The rate of movement of material through spiral arm regions should be especially well measured from this work. Indeed, we should be able to learn more about stellar populations from studies of M31 than from studies of our own Galaxy.

For comparing populations in galaxies of various types, fields would be needed in each of several members of the Local Group. These should particularly include at least two dwarf galaxies like the Draco and Leo II systems. Incipient resolution of dwarf galaxies as far out as the Virgo Cluster would test for homogeneity of that important population type.

Counts and luminosity classifications of planetary nebulae provide a measure of the rate at which a population is returning mass to the interstellar medium of a galaxy. That, in turn, affects the potential for new star formation. WF/PC images through [O III] λ 5007 and Hα filters, when compared with images in the adjacent continuum, will enable planetary nebulae to be detected and differentiated from ordinary H II regions throughout the Local Group making use of resolution, luminosity and excitation criteria. Most of the same fields observed for color-magnitude studies would be good candidates for Hα and

[O III] imaging and might in some instances be selected to include other nebulosities for which high resolution is of particular interest.

The narrow [O III] filter will permit the detection of bright planetaries to very large distances; the brightest planetaries, of which there should be several hundred in an elliptical galaxy at $M_{pg} \sim -19$, can be detected at the distance of the Virgo Cluster. These objects provide a tool for the study of the stellar population of normal ellipticals, and also provide unique dynamical tests for mapping the random motions of stars in ellipticals to large radii.

The stellar population near the poles of our own Galaxy can be analyzed statistically in WF/PC images obtained for studying other high galactic latitude objects such as QSOs. However, additional images on a suitable color system would permit luminosities and distances to be sorted out with less risk of ambiguity. Such an investigation is of fundamental importance for probing the intergalactic sea beyond (or perhaps intermingled with) the bound population of the galactic halo. Stars of solar luminosity, if they exist at such distances, can easily be identified to more than 100 kpc.

Star counts to the very faint magnitudes observable with the WF/PC, together with rough luminosity classifications obtainable from broad-band photometry, will provide data on the spatial distribution of the galactic halo at distances of this order.

Nuclei of galaxies

Historically, one of the most discussed needs for a large Space Telescope has been to obtain luminosity profiles at high resolution in the nuclei of nearby galaxies. Ground-based and balloon observations have not yet been able to tell us whether the nuclei of galaxies contain single large masses of unknown character or whether ordinary objects are merely distributed very densely. With our WF/PC camera operating at f/30 deep in the red and with modest deconvolution of the image, we expect to probe the sharpness of the central peak to less than 0.05 arcsec, a much better limit than now available. At M31, 0.05 arcsec amounts to 0.15 pc.

An important part of the puzzle is the rapid light variation observed in some active galactic nuclei. This phenomenon is difficult to understand on the basis of conventional models. High-resolution data on nearby Seyferts, combined with spectra, will allow separation of the emission region, which will be well resolved for the closer objects (e.g., NGC 1068 and NGC 4151). We intend, as a very high priority endeavor early in the mission, to obtain images of the nuclei of at least ten galaxies, including M31, M32, M33, NGC 1068, NGC 4151, NGC 4278, NGC 5128 (Cen A), M101, M81, and M87.

For comparison with the nuclear bulge population of nearby galaxies, some images will be obtained of the nuclear bulge of our own Galaxy through Baade's window. Solar-type stars (of 21st magnitude) are near the limit that can be dealt with from the ground due to crowding.

Extremely distant radio sources

We propose to search for extremely distant quasars and radio galaxies by taking deep exposures of fields in which there are radio sources having accurately known positions, but where nothing is visible to the limit of ground-based observations. Many such fields now exist; a few even among the bright sources of the 3CR Catalog.

It is well established that strong radio galaxies fall within a fairly narrow range of absolute magnitude, at the bright end of the galaxy luminosity function, and that quasars are all brighter than the brightest galaxies. If a radio source cannot be seen at a given apparent magnitude, it sets a fairly well-determined lower limit to its distance. This means that the optically empty radio fields will lead us immediately to an extremely distant class of objects and a very early sample of the universe, which would otherwise take much more time to find with random searches in the serendipity mode.

Ground-based observations are now pressing their extreme limit for radio galaxies at $z = 1$, and the great improvement in limiting magnitude of ST will enable us to see radio galaxies at much larger redshifts. These very faint radio sources may shed light upon a number of questions, including the behavior of quasar counts at large redshifts.

Cosmological studies of relevance to galaxies

Many of the WF/PC observations we have proposed under Cosmology are also of value in understanding galaxies and their contents. For example, distance indicators (cepheids, H II regions, globular clusters, and brightest stars) may exhibit population-dependent

differences from one galaxy to another. Any differences can be tested not only by comparing one distance indicator with another but also by comparing such characteristics as the distribution of cepheid periods from one type of galaxy to another.

In the Cosmology section we have proposed to obtain spectrophotometric measurements of highly redshifted clusters of galaxies in order to derive evolutionary corrections to magnitudes and diameters used in the testing of cosmological models. In the process, of course, we will acquire excellent material for refining the population models and evolutionary history of elliptical galaxies which predominate in rich clusters and which are of key importance to understanding the early history of the Universe.

Observations of QSOs, Seyfert galaxies, and galaxies with active nuclei have also been proposed in the Cosmology section in order to understand their use as potential tools for exploring the remotest parts of the Universe, but they are of great interest in themselves as enigmatic objects where extraordinary physical processes are taking place. WF/PC photometric, spectrophotometric, and polarimetric observations of QSOs will contribute to a definitive physical model, and may be one of the major achievements of the Space Telescope.

Stars, clusters, and nebulae

There are a number of important problems involving the study of galactic objects which are ideally suited to the high-resolution capability of the camera.

Globular star clusters

The WF/PC will allow detection and photometry of stars intrinsically much fainter than is possible from the ground, well into the crowded centers of the clusters. For the bright clusters with moduli near 15, white dwarfs and lower main sequence stars can be found and photometered to absolute magnitude +12. Using the visible transmission grating with a spectral resolution ~50, energy distributions can be obtained for these objects to $M_V \sim \pm 10$. For the very centrally condensed X-ray clusters, the nearest example of which is M15, the details of the luminosity distribution in the core can be mapped, to compare with theoretical efforts in order to discover whether the X-ray sources are really associated with massive condensed objects.

Images of globular star clusters can be compared to determine the extent of mass segregation in these objects, for which there are now detailed theoretical models but no convincing observations. All these data bear on the very interesting question of whether the initial mass function is the same in globular clusters, possibly the site of all population II star formulation, as it is in the solar neighborhood today. There are indirect indications to the contrary from present data, but the WF/PC will be able to settle the question directly.

Dwarf ellipticals like Draco, Sculptor, Leo II, and Fornax have moduli of order 20, so the WF/PC will reach to well below their main-sequence turnoffs, and crude spectra can be obtained with the gratings to about the turnoff. Critical comparison of their stellar populations can be made with those of globular clusters, which are presumably similar.

H II regions and planetary nebulae

The WF/PC will allow the study of the fine-scale structure of H II regions and planetaries with unprecedented detail; the resoultion in Orion will correspond to a linear distance of about 10 AU with modest deconvolution (0.05 arcseconds). Combined with the λ3727, λ5007 [O III], λ6300 [O I], and narrow Hα and Hβ filters, studies of excitation and ionization structure, as well as maps of dust distribution, can be made on these scales. It has always been clear that these objects are exceedingly inhomogeneous, with important structure well beyond the resolution of ground-based telescopes.

Supernova remnants

The same remarks apply to the line-emitting filaments and knots in SNRs. In the important special case of the Crab Nebula, we will resolve features as small as the gyroradius of the most energetic electrons of the synchrotron-emitting population and thus perhaps to the smallest scale of structure in the synchrotron continuum. The relation of the mysterious wisps to the pulsar may well be clarified; the "thin wisp" passes within about one arcsec of the pulsar but is not centered on it. It is clear that the rapid movement seen in the wisps is connected with energy transport from the pulsar into the nebula, but the mechanism is unclear, partly because the geometry is obscure. WF/PC images will certainly clarify the picture.

Novae

The high spatial resolution of the WF/PC and its monochromatic imaging capability will allow the detailed development of a nearby nova shell to be studied. The density and excitation conditions can be followed during early stages using the nebular line filters. Nature, of course, needs to supply the nova. Several pictures at different times and several wavelengths will be required, but the exposures will be very short.

The galactic center

The bulge near the center can be studied, as already mentioned, through Baade's "window". We will be limited by crowding to the study of stars of about the sun's luminosity and brighter, but the application of techniques like Scheuer's P(D) formalism will allow the determination of the luminosity function, and mass function, to considerably smaller masses. Again the question is whether or not the initial mass function in the bulge, which presumably formed under conditions not unlike those in elliptical galaxies, is the same as it is elsewhere.

Star formation

The high resolution capability of the WF/PC allows study of several processes related to the early evolutionary history of stars. In the Taurus dark cloud, there is star formation going on at a distance of about 100 pc. The 0.05 arcsec resolution of deconvolved high S/N images from the f/30 system corresponds to only about 5 AU at this distance, and to dynamical times for a one solar mass object of only about three years. Thus the motions of matter into (or out of) protostars can be watched at these scales with the expectation of things happening on interesting timescales! The important question of whether protostars have large accretion discs which might eventually be connected to the development of planetary systems can perhaps be settled by direct observation of the discs. These observations are quick (the exposures are short, and even fairly complete spectral coverage can be accomplished in quite a short time and the results potentially very exciting.

Solar system

We believe that the ST will prove to be no less important for planetary science than spacecraft targeted to individual planets. Observations with the WF/PC can contribute in a major way to our knowledge about individual Solar System objects, including the dynamics of outer planet atmospheres, rudimentary compositional classification of airless bodies, the detection of circumplanetary matter, and many of the processes occurring in comets. In the course of time, it offers the exciting possibility of detecting planets of other stars. The f/30 camera will exploit almost the full optical resolution of the Space Telescope and at the same time cover more than a 1 arcmin field. Planetary studies will usually not be in competition with other ST programs, since planets can be observed at times when the ST is unable to work on fainter objects in the presence of sunlight and earthlight. Planetary observational needs fall into several general classes:

Planetary atmospheres

At f/30 the camera can image Uranus and Neptune with two or three times the resolution of detail now seen in the best ground-based photographs of Jupiter and Saturn, respectively. Our resolution of detail on Jupiter will approach that in Voyager flyby images. Differences in cloud structure and in the cloud flow pattern will be analyzed with reference to theoretical models that describe the various dynamic instability modes by which heat is transported in planetary atmospheres. Although the banded structure of Jupiter's atmosphere clearly shows that dynamic forces play an important role on that planet, very little is known, observationally, about atmospheric structure on the other outer planets.

Monochromatic images of the outer planets in the methane bands will enable us to draw inferences concerning composition and vertical structure of the atmospheres above the cloud tops and concerning relative heights of the cloud tops in various regions of each planet. Observations of Uranus from year to year over the lifetime of ST will be particularly interesting, as the subsolar latitude on Uranus will progress much of the way from the pole to the equator.

Measurements of the optical oblateness of Uranus and Neptune, when combined with J_2 will place constraints on the radial mass distributions in their interiors. Systematic global views of Mars and Venus will provide information about some atmospheric phenomena that have been frustratingly difficult to study from flybys and orbiters. Flybys catch only a quick glimpse, and orbiters tend (for good reasons) to be myopic. Aeolian transport of dust is a major factor in the surface geology of Mars, and the Planetary

Camera will enable us, during critical intervals, to observe the dynamics of dust storms and condensate clouds with more than ten times the resolution typically available in synoptic observations with ground-based telescopes.

Ground-based ultraviolet images of Venus indicate that the slowly circulating cloud pattern undergoes major changes in form and contrast in the course of days. The PC can dramatically increase the length of the data base for such UV data. Indeed, all of the planets need to be explored at wavelengths below 2900Å.

We also note that a number of complex organic molecules, some of biological significance, have absorption bands in the range 2200-2600Å. If such absorbers exist in the atmospheres of Jupiter and Saturn, their global distribution and, in particular, their relationship to atmospheric convective structure is of great interest and bears on questions relating to the origin of life in the solar system.

Surfaces

The Planetary Camera will be quite effective in distinguishing photometrically different compositional provinces on airless bodies of the Solar System. Twelve of these will have diameters between 3 and 30 pixels at f/30. Ground-based photometry of asteroids has already demonstrated that albedo differences may be of cosmogonic origin. On the other hand, some airless bodies are known to have non-uniform albedo and color, particularly the synchronously rotating satellites of outer planets. We will be able to resolve the surfaces of the larger asteroids and satellites adequately to detect any inhomogeneity. The diameter and albedo of Pluto will be measured accurately for the first time, and its density estimated. The details of the newly discovered satellite of Pluto will also be easily observed. The PC will also be very effective for searching for possible satellites of minor planets. The rings of Uranus will be of great intrinsic interest.

Emissions

The distribution of molecules, ions, and radicals near the nucleus of a comet tells how and at what rate they are formed, and it puts constraints on the composition of the nucleus. The high resolution of the Planetary Camera will permit the domain of parent molecules in the inner coma to be mapped to within the distance they will have reached only one minute after evaporating from the nucleus. For some comets, both f/12 and f/30 will be useful. Although our f/30 camera cannot be expected to resolve the disk of the nucleus, it can isolate the nucleus photometrically so that its size and the number density of dust particles in its vicinity may be estimated. Parabolic comets are, of course, objects of opportunity. When a favorable one is discovered, one would want to schedule ST observations at various heliocentric distances before and after perihelion passage. For comparison, one would want to obtain similar observations of a periodic comet such as Encke and, of course, of Halley which will be in the vicinity of the Sun near the presently planned launch date. The innermost Galilean satellite of Jupiter, Io, is surrounded by emission clouds of sodium, potassium, and sulfur emitted from its active volcanos. With the WF/PC, the distribution of these emissions in the immediate vicinity of the surface of Io can be investigated.

Planets of other stars

Whether the Universe abounds with planets is an exceedingly important question both scientifically and philosophically. Detection of planets around nearby stars by direct imaging would be extremely difficult, because the reflected light of even a major planet will typically be less than 10^{-8} as bright as its parent star. The planet image will be overpowered by photon noise in the wings of the star image. Although this problem may, in principle, be overcome by the use of an apodizing screen in front of the telescope, the required precision of the optical figure ($\sim\lambda/1000$) is far beyond ST specifications.

Astrometric detections, however, appear feasible. Among nearby stars which are not known doubles, a large number would be expected to exhibit positional oscillations exceeding 0.002 arcsecond peak-to-peak if each possesses a planet of Jupiter's mass and orbital radius. The oscillation of the Sun, for example, would have that amplitude if observed from a distance of 5 parsecs. A proper search for planetary systems will require periodic observations of candidate stars over the lifetime of the ST. We have developed a technique to modify a portion of one quadrant of the camera to allow bright candidate stars to be measured astrometrically against the faint star background in a single exposure. A low reflectance (about 0.05% at 6500Å) spot of 1.38 arcseconds diameter has been placed on the "pyramid" mirror near the ST f/24 focus within the WF/PC. This allows attenuation of a star (or other object) by more than 7 stellar magnitudes without disturbing its astrometic location in the CCD image. Combined with the large dynamic range of the WF/PC, a single exposure should allow astrometric location of the

bright star to about 1-2 milliarcseconds. This technique is totally independent of spacecraft pointing, guiding and thermal stability, as well as the mechanical and optical stability of the WF/PC itself, and depends only on the geometric stability of a single CCD silicon membrane which is operating at constant temperature. We believe the possibility of detecting planets and low density companions of nearby stars by this technique is one of the most exciting uses of ST.

Predicted WF/PC performance

We now have procured and measured the flight optics, filters, polarizers and gratings, and selected and characterized the flight CCDs. Based on these data we can predict the performance in orbit of the WF/PC within about 20% uncertainty. Since the ST flight primary and secondary mirrors are finished and coated we can combine the ST and WF/PC data to predict overall performance. Table 1 shows our expectations for certain general characteristics. Of special interest is the low noise and large dynamic range of the CCDs.

Table 1. General Characteristics

Readout noise	-	13.9-17.8 electrons
Dark current	-	less than 0.01 electrons/sec
Digitization level bits	-	12
Electrons/bit	-	7.5
Exposure time	-	0.12-100,000 seconds
Intrascene dynamic range	-	1500

Table 2 gives the run of detective quantum efficiency we expect and illustrates the very large spectral coverage available.

Table 2. Detective Quantum Efficiency

(nm)	WF/PC (%)	WF/PC + OTA (%)
115	0.2	0.05
120	5	2
125	6	2.5
140	6	2
160	7	3
200	10	5
250	10	5
300	10	5
350	10	6
400	6	4
500	20	12
600	30	18
700	32	18
800	20	12
900	16	9
1000	10	7
1100	3	2

Table 3 gives other interesting properties and predictions indicating that stars should be detectable down to m_V = 28 during a single orbit exposure.

Table 3. Camera Specific Characteristics

	WFC	PC
Field of view	2.63x2.63 arcmin	68x68 arcsec
Pixel size	0.1 arcsec	0.043 arcsec
Overall dynamic range	(0.12 - 3000 seconds) $10.0<m_V<28.5$	$9.0<m_V<28.0$

Predicted Performance for Stars

m_V	S/N WFC	S/N PC
	t = 0.12 second	
9.1	-	320
10.0	210	
13.7		20
14.3	20	
14.7		10
15.0	10	
15.8		3
16.4	3	
17.0		1
17.6	1	
	t = 3000 seconds	
20.1	-	320
20.9	210	
24.6		20
25.1	20	
25.5		10
26.0	10	
26.8		3
27.4	3	
28.0		1
28.6	1	

Table 4 shows filter, polarizer and grating transmission properties. Unfortunately "red leaks" in the UV filters will be significant when observing cool or red sources due to the high QE in the red.

Table 4. Filter Properties

Filter No.	Center Wavelength Å	Width Å	Comment
1	1216	150	Wide Lyman Alpha
2	1450	290	20%
3	1800	360	20%
4	2250	450	20%
5	2800	560	20%
6	3300	600	U
7	4350	900	B
8	5525	950	V
9	6800	1400	R
10	8150	1700	I
11	10000	(9000 to CCD cutoff)	Long λPass
12	5950	2500	Wide V
13	9100	(7200 to CCD cutoff)	Wide R
14	1280 to blocker cutoff	Long λPass	Wide UV (CaF_2)
15	-	1280 to 2000	UV blocker
16	-	1280 to 3200	UV blocker
17	Polarizer		0^o Orientation
18	Polarizer		60^o Orientation
19	Polarizer		120^o Orientation

Table 4. Filter Properties (Cont'd.)

Filter No.	Center Wavelength Å	Width Å	Comment
20	UV Grating		CaF_2 substrate
21	B Grating		on BG-38 substrate
22	R Grating		on OG-570 substrate
23	3300	330	10%
24	3700	370	10%
25	4100	410	10%
26	4500	450	10%
27	4900	490	10%
28	5450	545	10%
29	6000	600	10%
30	6600	660	10%
31	7250	725	10%
32	8000	800	10%
33	8750	875	10%
34	9650	965	10%
35	10500	1050	10%
36	3750	80	3727 redshifted
37	4686	20	He II
38	4363	20	O III
39	4870	30	Hβ
40	5017	30	O III redshifted
41	5160	100	C_2 (comets) and Mg II
42	5890	40	HeI, NaD
43	6310	30	O I redshifted
44	6563	20	Hα
45	6660	150	Hα redshifted
46	8890	50	CH_4 (planetary)
47	10830	100	HeI
48	6585	20	NII, redshifted Hα Virgo

There are three "objective" gratings available which cover the far UV (1300-4000Å in two cross-dispersed orders), the blue (3000-6000Å) and the red IR (6000-12000Å). The dispersions are given in Table 5. We expect some of the most interesting "serendipity" images will come from these gratings where each compact source will have a short spectrum along with a "zero order" image which can be used as a wavelength fiducial. We expect that 3000 second exposures will yield usable spectra to $m_V = 24$ and hope that it will be possible to calibrate these spectra photometrically. Ground-based efforts are underway using a small telescope and appropriate gratings with a WF/PC reject CCD to develop the necessary "flat fielding" and other calibration techniques as well as software to reduce WF/PC-like grating images spectrophotometrically.

Table 5. Grating Dispersions (Å/pixel)

	WFC	PC
UV at 2400Å		
1st Order	12.1	5.2
2nd Order	15.0	6.4
Blue at 5000Å	55.5	23.8
Red at 7800Å	110.8	47.6

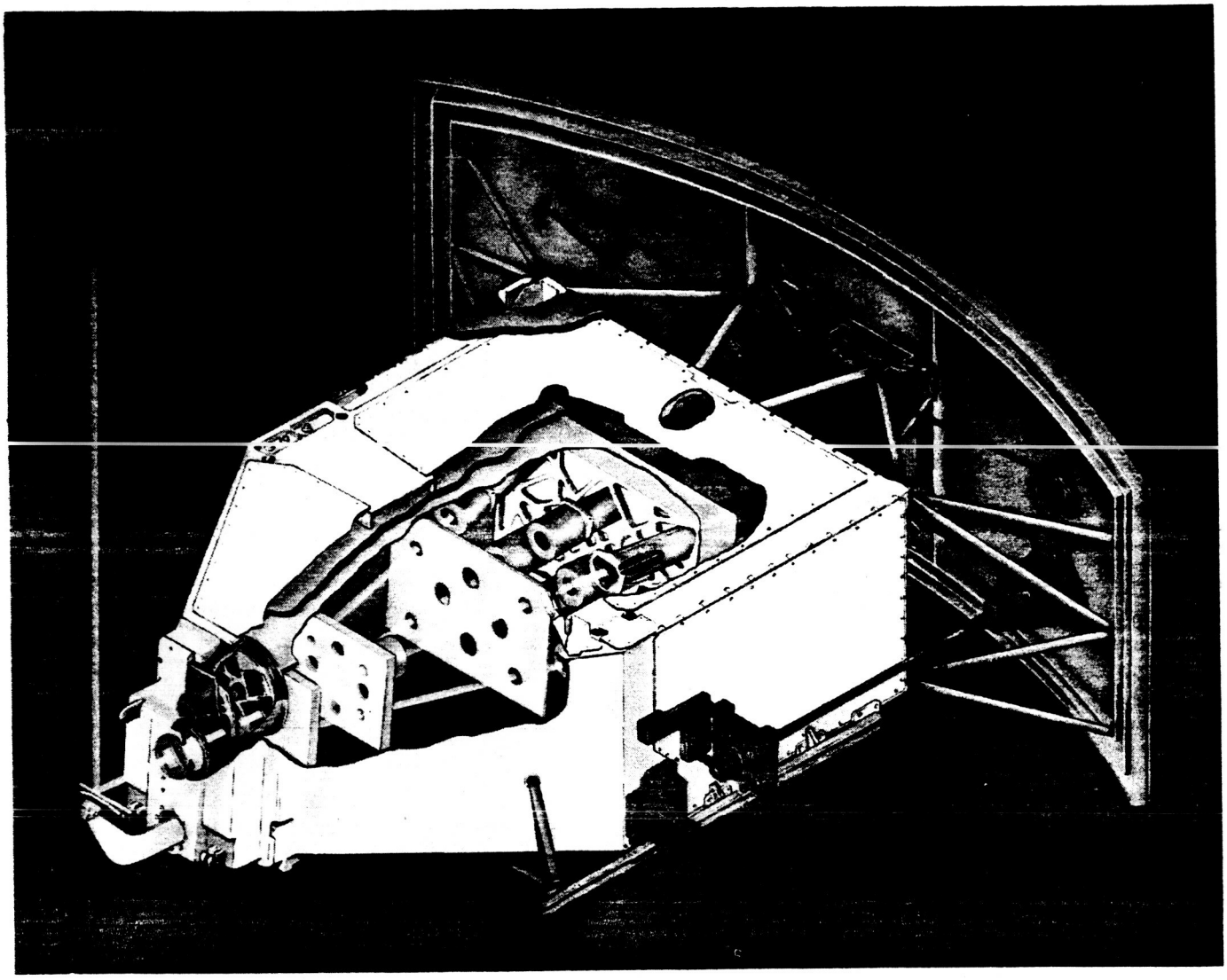

Figure 1. The Wide Field/Planetary Camera

N82 33301

THE FAINT OBJECT CAMERA

F. Macchetto*, and the Faint Object Camera Instrument Science Team

Astronomy Division, Space Science Department of ESA, ESTEC,
Noordwijk, The Netherlands

ABSTRACT - The Faint Object Camera will fully exploit the spatial resolution capability of the Space Telescope on the very faintest detectable objects over a broad wavelength range. A full complement of filters, objective prisms and polarizers, a choice of coronographic masks, and a variety of scan formats extend the scientific versatility of the direct imaging mode. In addition, the Faint Object Camera provides the unique facility of long-slit spectroscopy to Space Telescope observers.

1. MAIN CHARACTERISTICS

The FOC is one of the four axial scientific instruments located at the focal plane of the ST and has overall dimensions of about $0.9 \times 0.9 \times 2.2 m^3$. Its design is modular and allows for interchange with the other axial scientific instruments; this ensures that removal and re-installation can be achieved in-orbit by a suited astronaut.. The total weight of the FOC is about 318 kg and the average power consumption over a 95-min orbit will be less than 140 W.

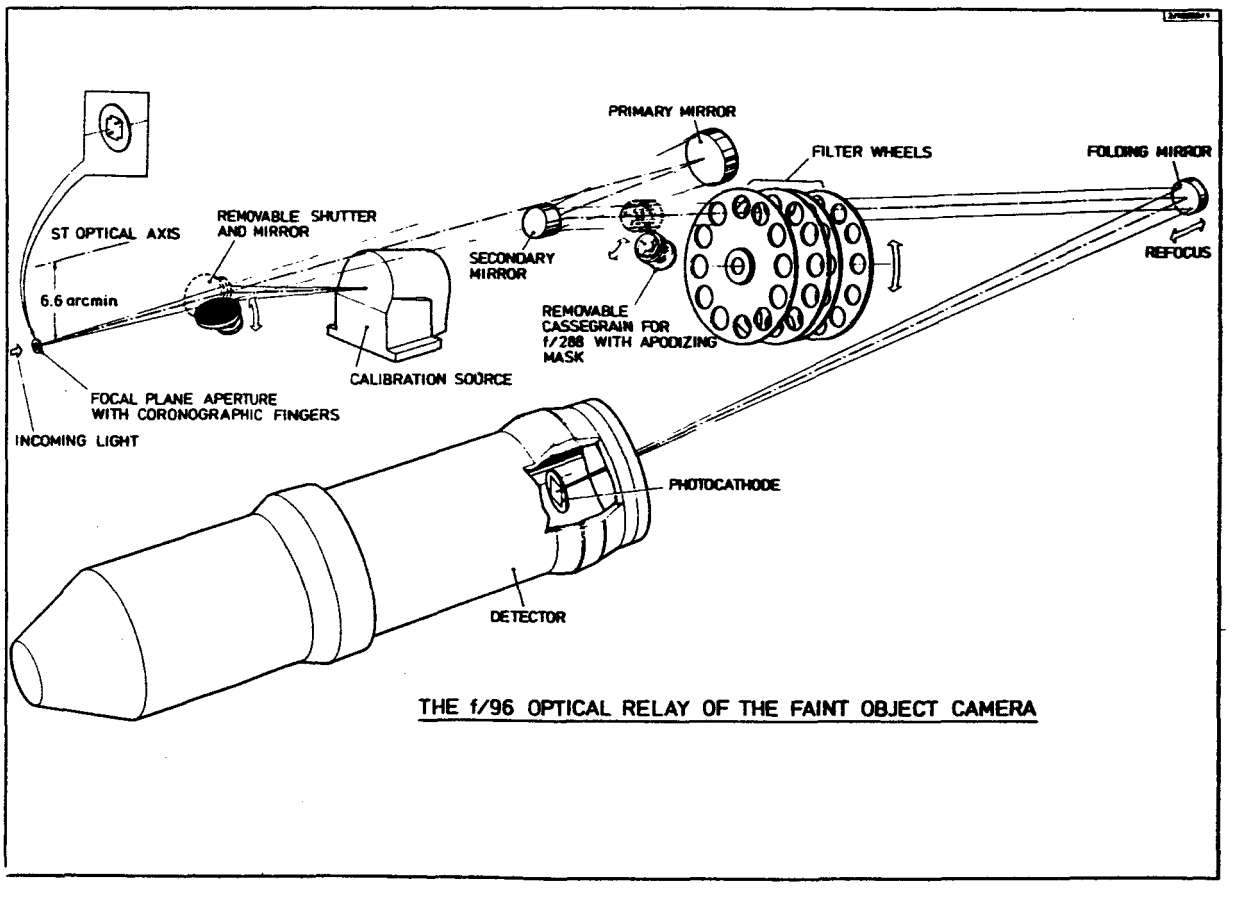

THE f/96 OPTICAL RELAY OF THE FAINT OBJECT CAMERA

FIG. 1 The f/96 optical relay

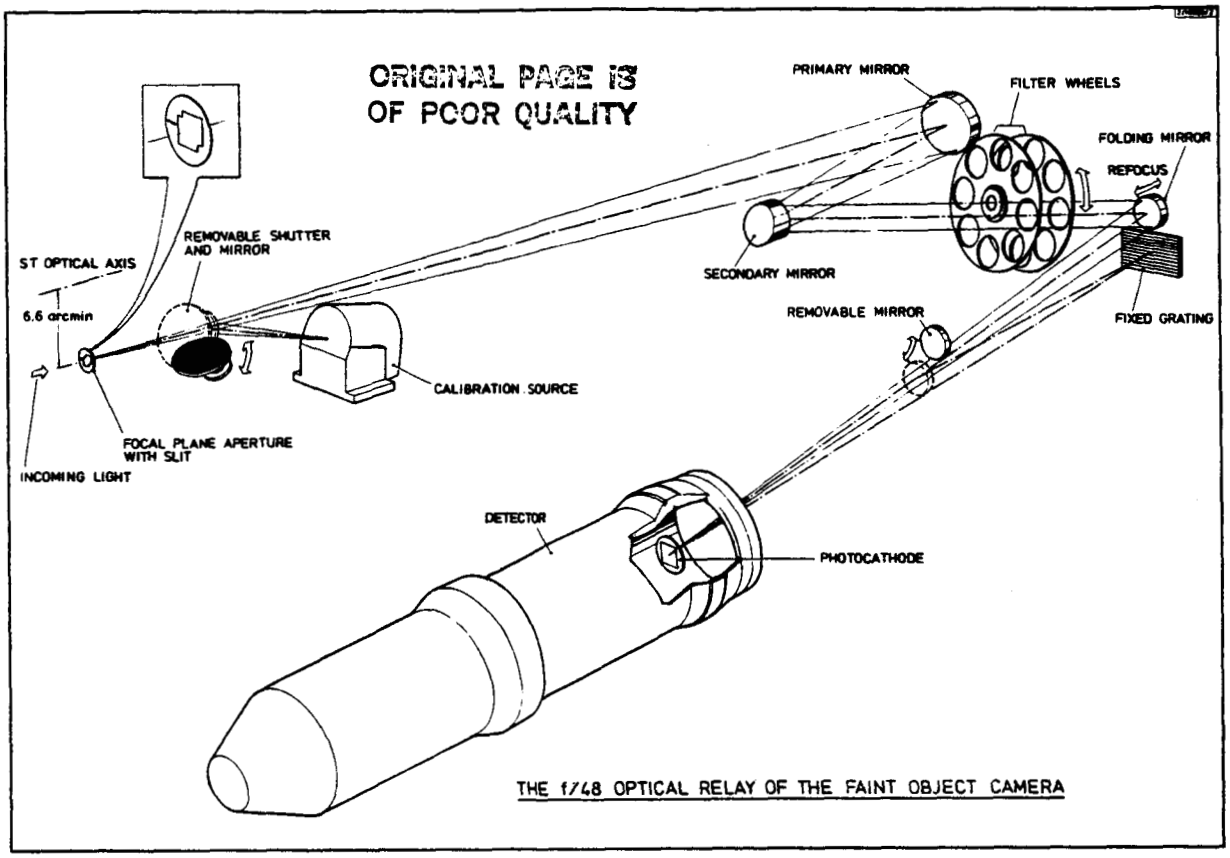

FIG. 2 The f/48 optical relay

1.2. The optical system

The FOC contains two complete and independent cameras, each with its own optical path and detector system. The purpose of the f/96 and f/48 optical relays is to transfer the images from the f/24 focal plane of the ST to the detector photocathodes, matching their pixel sizes with the least possible image degradation and light loss, while correcting for the astigmatism of the ST optics.

A number of additional components are provided, such as filters, objective prisms and polarisers, and facilities for long-slit spectroscopy and coronography, to enhance the scientific capabilities of the instrument.

All the optical elements and both detectors are supported on an optical bench, which is rigidly connected to the focal-plane structure of the ST. The optical bench is contained within the load-carrying structure which provides a light-tight enclosure. To meet the image stability requirements, the internal surfaces of the load-carrying structure which enclose the optical bench are actively thermally controlled with a stability of better than 0.5°C. The relevant elements of the optical systems are shown in physical layouts in Figures 1 and 2 and as a functional block diagram in Figure 3.

1.2.1. The f/96 and f/48 optical relays

The primary optical relay of the FOC has a focal ratio of f/96 and is designed to exploit fully the resolution capabilities of ST. The second optical relay has a focal ratio of f/48 for a larger field of view. The normal pixel size (25 μm) corresponds to 0.022 arcsec at f/96 and 0.044 arcsec at f/48. As the centres of both FOC entrance apertures are 6.6 arcmin away from the ST optical axis, the relays must also correct the residual astigmatism and field curvature of the ST Ritchey-Chretien optics.

Each relay consists of an aplanatic system. Beyond the aperture, the beam is relayed from a spherical concave primary mirror, to an elliptical convex secondary mirror and then to a cylindrical concave folding mirror, which focusses the image onto the detector's first-stage photocathode. The folding mirrors can be moved for in-flight refocussing. In the

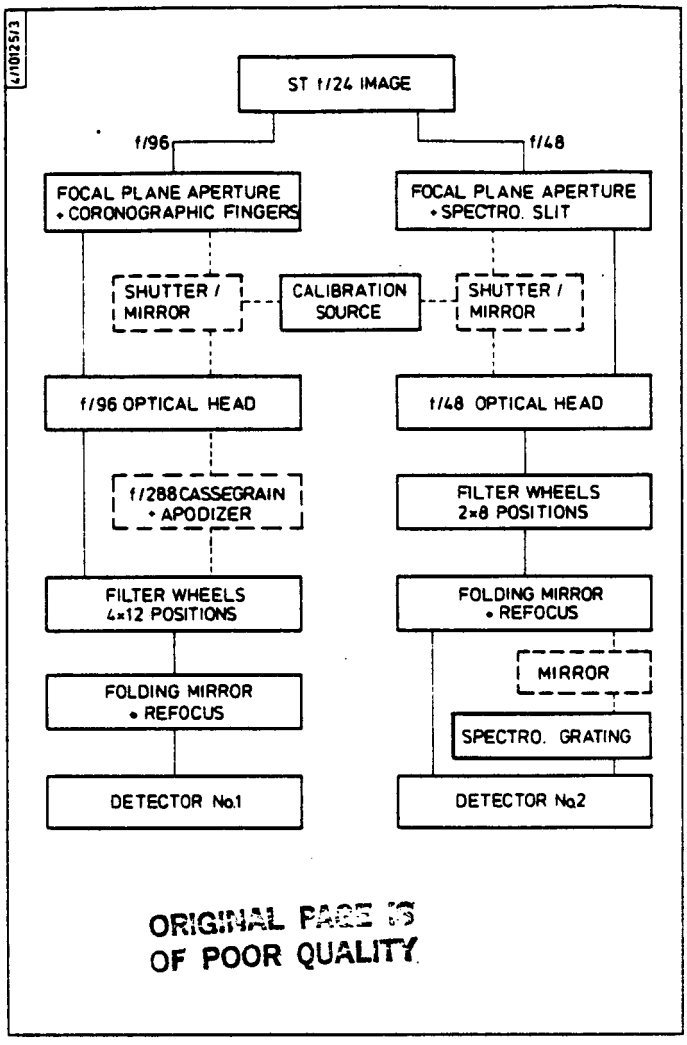

FIG. 3 Optical block diagram. Removable elements are shown in dashed lines.

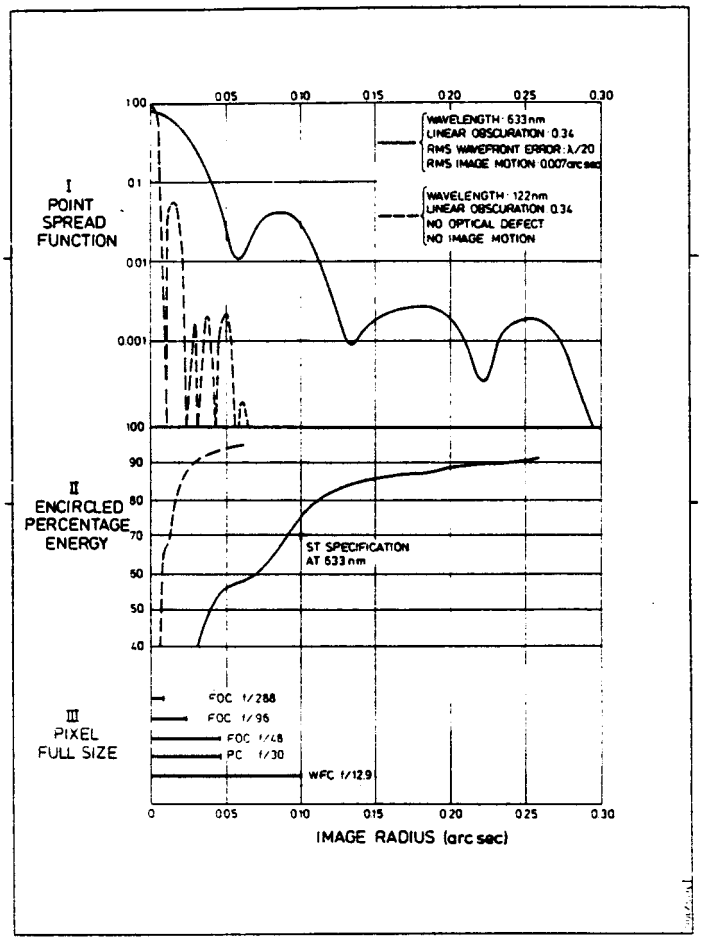

FIG. 4 Expected image quality of the Space Telescope. The image properties are described by the point spread function (I) and the encircled energy fraction (II) and compared with the adopted pixel size for FOC and WFC/PC (III).

event of light overload, each focal-plane aperture can be closed by a shutter in less than 0.2s. With the shutter closed, a mirror behind it reflects the light from a calibration source into the optical path.

1.2.2. The very high resolution apodizer (f/288 mode)

The theoretical Rayleigh limit (1.22 λ/D) for the angular resolution of the ST is 0.066 arcsec at 633 nm and 0.013 arcsec at 125 nm. The optical quality of the ST guarantees near diffraction-limited performance at 633 nm; the FOC imaging at f/96 exploits this resolution capability. There is a reasonable probability that near diffraction-limited performance will be reached by the ST at shorter wavelengths but, even at wavelengths where the diffraction limit cannot be reached by the overall optical quality, the telescope aberrations will probably produce a stationary speckle pattern. Deconvolution of this pattern may then be possible, thereby yielding diffraction-limited images at the shortest detectable wavelengths. To exploit this exceptional resolution capability, a facility for imaging at f/288 can be inserted into in the f/96 optical path, giving a pixel size of 0.007 arcsec (corresponding to the rms guiding error of ST): this is sufficient to sample the speckle pattern even at 125 nm (Figure 4).

The f/288 facility is a compact Cassegrain assembly which produces a magnification of x3 and can be inserted at the pupil location in the f/96 optical path between the secondary mirror and the filter wheels (Figures 1 and 3). The total f/288 field of view will then be 7.5x7.5 arcsec and its centre will be offset from the centre of the f/96 field of view by 6.4 arcsec in the x direction and by 7.1 arcsec in the y direction, therefore including the 0.8 arcsec wide coronographic finger (see Section 1.2.3).

1.2.3. Coronography

Faint structure close to bright objects may be studied with a coronographic facility included in the f/96 relay. It consists of a fixed mask placed at the ST focal plane and of an apodizing mask located on the f/288 removable Cassegrain at the ST pupil. The focal-plane mask (Figure 1) contains two fingers, 0.4 and 0.8 arcsec wide respectively, either of which can obscure the central spot and up to three Airy rings of the bright source depending on wavelength. The apodizing mask has been designed to remove the light scattered and diffracted by the ST secondary mirror and spider and by the three supports of the ST primary mirror. Since the mechanisms are independent it is possible to use either one of the coronographic fingers alone at f/96 or the 0.8 arcsec coronographic finger and the apodizing mask at f/288, thus realising a Lyot-type coronograph.

The performance of this coronograph will depend strongly on the optical quality of the ST. Assuming this to be good, the coronograph will allow, by direct imaging, the detection of features of 2×10^{-7} relative intensity (16.7 magnitudes fainter) at an angular separation of 1 arcsec from a bright point object.

1.2.4. Long-slit spectrography

The f/48 focal plane aperture contains a rectangular slit of dimension 20x0.1 arcsec^2 on one side of the main aperture (Figure 2). When the spectrographic mode is selected, the light passing through the slit is transferred through the f/48 relay and is reflected onto a fixed plane grating by a removable convex mirror placed between the folding mirror and the detector (Figures 2 and 3). From there the spectrally dispersed and spatially resolved image is focussed onto the photocathode of the f/48 detector. The convex mirror corrects the additional astigmatism introduced by the spectrographic elements. Both mirror and grating work with a magnification of unity.

The spectrograph works with three orders of the grating at fixed wavelength ranges and fixed slit width (see Table 1). The efficiencies in the various orders without filters are given in Table 2 and Figure 5. The f/48 wide-band and long-pass filters can be used to select a particular order. Selection of position angle is possible only by rolling ST. This ability is severely limited by the required orientation of the solar arrays to sunlight. Depending on the object position and time of the year, it may take several months before an observation at a particular position angle is feasible.

Table 1. The three orders of the spectrograph.

Order	Spectral range	Projected slit width	Pixel size
1st	360-540 nm	0.40 nm	0.18 nm
2nd	180-270 nm	0.20 nm	0.09 nm
3rd	120-180 nm	0.13 nm	0.06 nm

1.2.5. Transmission elements

The f/96 relay includes four wheels each with 12 positions, comprising a total of 34 filters (4 long-pass, 3 wide-band, 6 broad-band, 19 narrow-band, 2 interference), five attenuators, three polarisers, two objective prisms and four empty holes. The f/48 relay contains two wheels each with eight positions, comprising 12 filters (3 long-pass, 3 wide-band, 6 broad-band), two objective prisms and two empty holes.

The five neutral density filters of the f/96 wheels (Δm = 1, 2, 4, 6, 8) provide possible attenuations of 1,2,3...9 magnitudes. In the manufacture of the attenuators very good uniformity in transmission has been achieved over the spectral range from 120 to 700 nm.

The f/96 polarisers are oriented in three different position angles (0°, 60°, 120°) and their spectral range will extend from 130 to 600 nm. The angular separation of the ordinary and extraordinary beam is sufficient to achieve a 512x512 pixel format (25x25 μm^2 pixel) without overlap of the images. The transmission of the plane-polarised light is 10% at 130 nm, 50% at 180 nm and 85% at 250 nm.

Each relay has two objective prisms: one single prism of magnesium fluoride for operation in the far UV (spectral resol-

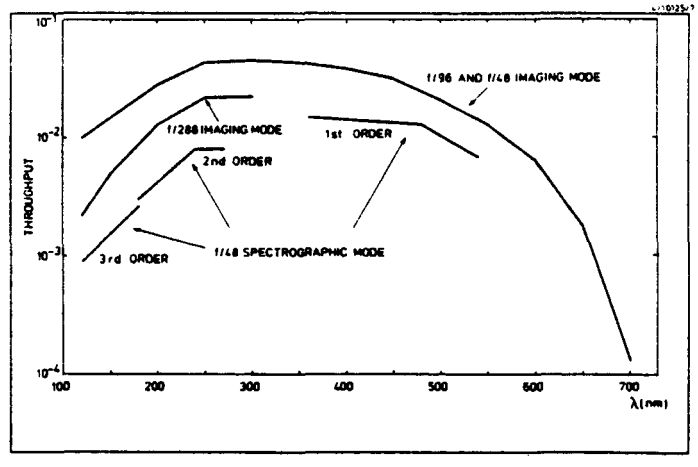

FIG. 5 ST + FOC total efficiency

ution $\lambda/\Delta\lambda$ = 50; efficiency of 90% at 150 nm) and one double prism of magnesium fluoride and silica for operation in the near UV (spectral resulution $\lambda/\Delta\lambda$ = 100 at f/96 and $\lambda/\Delta\lambda$ = 50 at f/48; efficiency of 80% at 250 nm). The pass-band of the objective prisms is 120-700 nm for the far UV and 200-700 nm for the near UV. The orientation of the objective prisms is such that the 1-D zoom option doubles the pixel size only in the direction perpendicular to the dispersion, thus maintaining full spectral resolution but doubling the field of view.

1.3. The Detectors

To exploit fully the ST resolution whilst preserving a reasonable field of view, the detector should have as large a number of separated resolution elements as possible. Furthermore, to reach the faintest objects, the highest sensitivity is required over a wide wavelength range, with the lowest possible instrumental noise. To achieve these goals, an imaging detector working in the photon-counting mode (Figure 6) has been chosen.

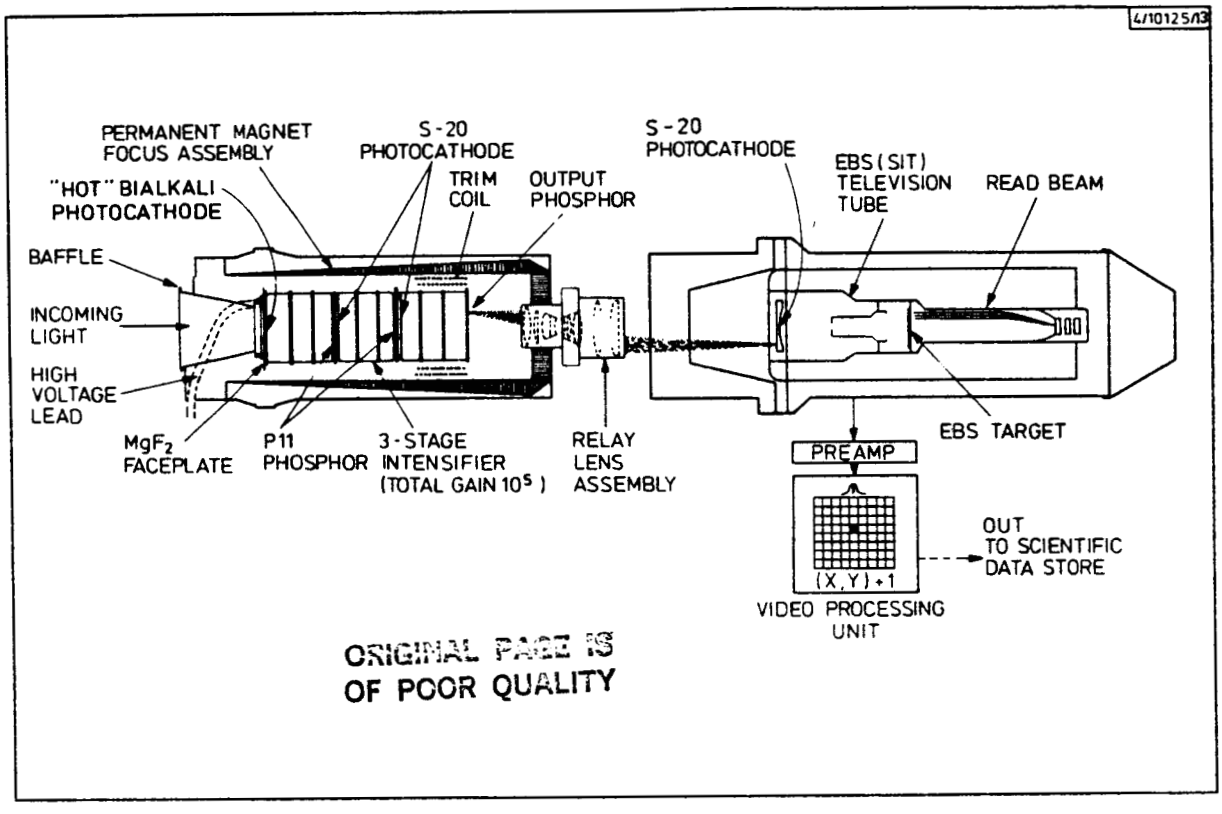

FIG. 6 Schematic drawing of the FOC photon-counting detector

The two identical detectors consist of a three-stage image intensifier, which is optically coupled by a relay lens system to a television tube. The TV tube detects the scintillations at the output of the intensifier, corresponding to the arrival of individual photons at the first-stage photocathode. The central x-y position of each burst is measured by a Video-Processing Unit, and the memory cell in the Scientific Data Store associated with that position (or pixel) is incremented by one. The image gradually builds up during exposures of up to several hours, and can be read in a non-destructive way at any intermediate time.

The pixel size is normally 25x25 μm^2 on the photocathode plane, but a one-dimensional (1-D) zoom option can be selected giving 25x50 μm^2 pixels, with the long dimension perpendicular to the dispersion of the objective prisms and of the spectrographic grating.

The useful photocathode area is 25.6x25.6 mm^2, which corresponds to 1024x1024 normal size pixels. Mass and power constraints limit the capacity of the Scientific Data Store to 262.144 (512^2) words of 16 bits (or twice as many words of 8 bits). The normal data store format is 512x512 pixels with 16-bit digitisation. Other 16-bit imaging formats are selectable: 1024x256, 256x256, 128x128 and 64x64 pixels, and each of these available formats can be positioned anywhere within the useful photocathode area. A 1024x512 pixel format

is also available with 8-bit digitisation, and with the 1-D zoom option it covers the whole useful area of the photocathode.

1.4. Performance of the FOC

A summary of the FOC modes is shown in Figure 7. Tables 2 and 3 give the ST and FOC efficiencies at several wavelengths for imaging and spectroscopy without filters. The bottom lines in this Table give the total probability that a photon which enters the 2.4-m circular aperture is actually detected. These values (see also Figure 5) allow the determination of the system performance at any wavelength, taking into account the detector background (less than 3×10^{-4} counts pixel^{-1} s^{-1}). ST stray light (m_V > 23 mag arcsec^{-2}) and the sky brightness. Some examples of the total system performances (Table 4) have been computed in magnitudes for a point source over a circle of 0.1 arcsec in radius, or magnitudes per arcsec^2 for extended objects over a resolution element of 2x2 pixels. In each case the spectrum of the source has been taken to be equivalent to that of an A0 V star and the integration has been carried out over a bandpass of 100 nm centred around the U-band for the imaging mode and around the B-band for the spectroscopic mode. The calculations assume that a star of $m_B = 25$ gives 6.1 photons s^{-1} nm^{-1} in the 2.4-m circular aperture at 435 nm.

The finite speed of the TV tube readout and videoprocessing system limits the linear range of pulse counting, this range depend-ind on the selected format. For the full 512x512 format, a maximum count rate of 0.6 counts pixel^{-1} s^{-1} results in non-linearity at the single pixel level of better than 10%, correctable to a photometric accuracy of about 1%. Higher rates of up to 3 counts pixel^{-1} s^{-1} can be corrected with decreasing accuracy. The limit of 0.6 counts pixel^{-1} s^{-1} corresponds to the central part of a point source of $m_V = 21$, or to an extended source of 15 mag arcsec^{-2}, for the f/96 full format. Nevertheless it is expected that even for bright point sources with heavily saturated centres, good photometry can still be obtained by extrapolating the outer parts of the point spread function, since this will extend over a hundred pixels or more.

Bright objects may also be observed by insertion of neutral density filters into the f/96 beam or by reducing the field format so that a given pixel can be sampled more frequently.

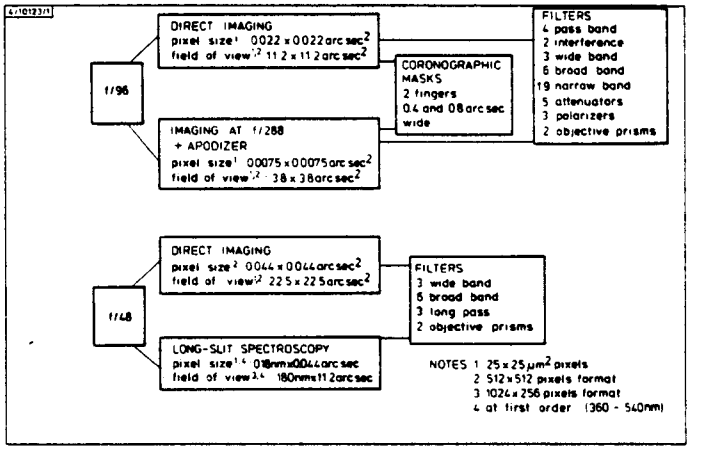

FIG. 7 Summary of the FOC modes

Table 2. Minimum efficiencies in the f/96 and f/48 imaging modes (without filters). (Final values may differ slightly from those tabulated).

Wavelength (nm)	120	150	200	250	300	350	400	450	500	550	600	650	700
ST throughput	0.41	0.43	0.52	0.57	0.58	0.61	0.63	0.64	0.64	0.62	0.62	0.62	0.60
FOC optics throughput	0.50	0.50	0.53	0.57	0.61	0.65	0.69	0.70	0.70	0.70	0.70	0.70	0.70
Detector spectral response	0.05	0.07	0.10	0.13	0.13	0.11	0.09	0.07	0.05	0.03	0.015	0.004	0.0003
Total ST + FOC	0.010	0.015	0.028	0.043	0.045	0.043	0.039	0.032	0.021	0.013	0.0065	0.0018	0.00013

Table 3. Minimum efficiency in the f/48 spectrographic mode (without filters).

	Third order			Second order			First order		
Wavelength (nm)	120	160	180	180	240	270	360	480	540
FOC optics throughput*	0.046	0.057	0.064	0.072	0.12	0.11	0.22	0.35	0.32
Total ST + FOC efficiency	0.0009	0.0018	0.0026	0.003	0.008	0.008	0.015	0.013	0.007

* These values include the efficiencies of the grating and of the folding mirror.

Table 4. Nominal Performances.

Magnitude	Time (s) for S/N = 10	S/N in 1000 s	S/N in 10 h
m_L	*f*/96 (*point sources*)		
21	25	64	380
22	63	40	240
23	160	25	150
24	420	15	93
25	1 200	9.3	56
26	3 600	5.3	32
27	13 000	2.7	16
28	61 000	1.3	7.7
29	330 000	0.55	3.3
30	1 900 000	0.23	1.4

Magnitude	Time (s) for S/N = 10	S/N in 1000 s	S/N in 10 h
m_L arcsec^{-2}	*f*/96 (*extended objects*)		
15	35	58	320
16	89	34	200
17	220	21	130
18	560	13	80
19	1 400	8.4	50
20	3 700	5.2	31
21	9 800	3.2	19
22	18 000	1.9	11
23	91 000	1.1	6.3
24	360 000	0.53	3.2
25	1 800 000	0.24	1.4

Magnitude	Time (s) for S/N = 10	S/N in 1000 s	S/N in 10 h
m_L	*f* 48 (*point sources*)		
21	25	64	380
22	62	40	250
23	160	25	150
24	410	16	94
25	1 100	9.5	57
26	3 300	5.5	33
27	12 000	2.9	18
28	49 000	1.4	8.5
29	250 000	0.63	3.8
30	1 400 000	0.26	1.6

Magnitude	Time (s) for S/N = 10	S/N in 1000 s	S/N in 10 h
m_L arcsec^{-2}	*f*/48 (*extended objects*)		
17	14	84	500
18	36	53	320
19	91	33	200
20	230	21	120
21	610	13	77
22	1 700	7.7	46
23	5 300	4.4	26
24	20 000	2.3	14
25	90 000	1.1	6.3
26	480 000	0.46	2.7
27	2 800 000	0.19	1.1

Magnitude	Time (s) for S/N = 10	S/N in 1000 s	S/N in 10 h
m_g	*f* 48 *spectrographic mode* (*A0 point sources*)		
12	5	140	830
13	13	87	520
14	33	55	330
15	83	35	210
16	210	22	130
17	520	14	83
18	1 300	8.7	52
19	3 400	5.4	33
20	8 900	3.4	20
21	25 000	2.0	12
22	77 000	1.1	6.8
23	290 000	0.59	3.5

Magnitude	Time (s) for S/N = 10	S/N in 1000 s	S/N in 10 h
m_g arcsec^{-2}	*f* 48 *spectrographic mode* (*A0 extended objects*)		
8	8	120	690
9	19	73	440
10	47	46	280
11	120	29	170
12	300	18	110
13	750	11	69
14	1 900	7.2	43
15	4 900	4.5	27
16	13 000	2.7	17
17	38 000	1.6	9.7
18	130 000	0.89	5.3

For example, in the 64x64 pixel format at full resolution, the limiting rate for about 10% photometric accuracy would be 190 counts pixel^{-1} s^{-1}. These higher data rates raise the possibility of using small-field formats in a time-resolution imaging mode (for example, in searches for optical counterparts of radio pulsars or variable X-ray sources).

Table 5 summarises the angular pixel sizes, the fields of view and the bright limiting magnitudes corresponding respectively to 1% and about 10% photometric accuracy on a single pixel for the various FOC modes, formats and pixel sizes. An on-board uniform intensity source and a grid of reseau marks on the detector photocathode will allow in-flight calibration of photometric response and of geometric distortion at the single pixel level.

Table 5 FOC modes and performances

FOC mode: / Pixel size: / FOC format	f/96 Imaging 0.022 × 0.022 (0.044)	f/288 Imaging 0.0075 × 0.0075 (0.015)	f/48 Imaging 0.044 × 0.044 (0.088)	f/48 Spectroscopy 0.18 nm × 0.044 (0.088) (first order)
512 × 512 pixels	11.2 × 11.2 (22.5)	3.8 × 3.8 (7.6)	22.5 × 22.5 (45)	90 nm × 20
	21.0 *V*	18.3 *V*	22.5 *V*	15.5 *B*
	15.2 *V*	12.5 *V*	17.7 *V*	10.7 *B*
1024 × 256 pixels	22.5 × 5.6 (11.2)	7.6 × 1.9 (3.8)	45 × 11.2 (22.5)	180 nm × 11.2 (20)
	21.0 *V*	18.3 *V*	22.5 *V*	15.5 *B*
	15.2 *V*	12.5 *V*	17.7 *V*	10.7 *B*
256 × 256 pixels	5.6 × 5.6 (11.2)	1.9 × 1.9 (3.8)	11.2 × 11.2 (22.5)	45 nm × 11.2 (20)
	19.5 *V*	16.8 *V*	21.0 *V*	14.0 *B*
	13.7 *V*	11.0 *V*	15.2 *V*	9.2 *B*
128 × 128 pixels	2.8 × 2.8 (5.6)	0.95 × 0.95 (1.9)	5.6 × 5.6 (11.2)	22.5 nm × 5.6 (11.2)
	18.0 *V*	15.3 *V*	19.5 *V*	12.5 *B*
	12.2 *V*	9.5 *V*	13.7 *V*	7.7 *B*
64 × 64 pixels	1.4 × 1.4 (2.8)	0.47 × 0.47 (0.95)	2.8 × 2.8 (5.6)	11.2 nm × 2.8 (5.6)
	16.6 *V*	13.9 *V*	18.1 *V*	11.1 *B*
	10.8 *V*	8.4 *V*	12.3 *V*	6.3 *B*
1024 × 512 pixels (8 bit)	22.5 × 11.2 (22.5)	7.6 × 3.8 (7.6)	45 × 22.5 (45)	180 nm × 20
	21.8 *V*	19.1 *V*	23.3 *V*	16.3 *B*
	16.0 *V*	13.3 *V*	18.5 *V*	11.5 *B*

NOTE: In this table the first row gives the field of view (arcsec), the second row gives the upper magnitude for point sources with 1% photometric accuracy on the central pixel; the third row gives the corresponding magnitude per arcsec² for extended sources. Upper magnitudes for about 10% photometric accuracy on the central pixel are about 1.7 magnitude brighter. Numbers in brackets refer to the extended axis of the 1-D zoom mode. In the f/48 spectrographic mode the format is limited by the slit length of 20 arcsec.

1.5. Comparison of the FOC with other ST instruments

In deciding whether or not to use the FOC for a particular observation, it is useful to make a comparison with the other ST instruments with similar capabilities. For imaging applications, the FOC provides the highest angular resolution at all wavelengths and the Wide-Field Camera/Planetary Camera (WFC/PC) the largest field of view (up to 2.67 x 2.67 arcmin²). The FOC will have an advantage in speed over the WFC at wavelengths less than about 450 nm. The two systems will be about equal in speed at 500 nm, while the WFC/PC is more advantageous than the FOC for $\lambda >$ 550 nm.

For imaging of faint objects two advantages of the FOC become important. Firstly, dark current generation in the CCD cameras amounts to about 0.1 events pixel^{-1}s^{-1}, whereas that in the FOC is about three orders of magnitude smaller. This advantage is particularly attractive in the UV where the sky background is darker and the FOC efficiency good. Secondly, every time a CCD image is read out, it is accompanied by amplifier read-out noise which amounts to about 12 electrons rms per pixel. There is no read-out noise in the FOC. When the above differences are taken into account, the relative speeds of the cameras

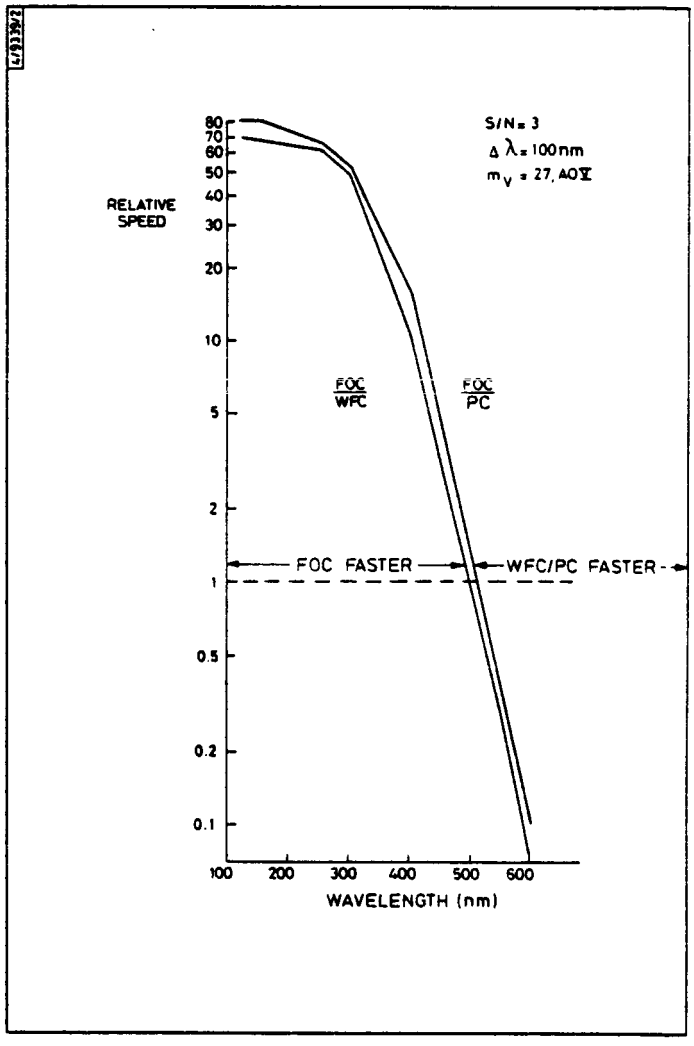

FIG. 8 Relative specals of the FOC and the WFPC

in detecting faint objects can be compared. Figure 8 shows the comparison in speed between the FOC (f/96 configuration) and the WFC/PC configurations for the detection of a star with a flat spectrum having $m_V = 27$ with S/N = 3 with a band-pass of 100 nm.

The long-slit spectrograph of the FOC does not pretend to be a complete spectrographic facility but represents a natural extension of the high-resolution imaging capability of the FOC. The spectral resolution of the FOC spectrograph is $2x10^3$, intermediate between that of the Faint Object Spectrograph and the High Resolution Spectrograph. The FOC spectrograph will be the only choice for problems requiring simultaneous spatial resolution perpendicular to the dispersion direction. This unique facility will enable spectroscopic profiles of extended objects to be made with an angular resolution of the order of 0.1 arc-sec; this operation will be very useful in measuring velocity dispersions as well as temperature, density and composition distributions in comets, nebulae and galaxies. Unlike the Faint Object Spectrograph, the FOC spectrograph field of view will extend well beyond the target in many cases, thus producing simultaneous data for sky subtraction purposes. The limitations of the FOC spectrograph are its fixed spectral ranges and slit width. Wavelength calibration will be carried out by observations of astronomical sources.

2. SURVEY OF SCIENCE OPPORTUNITIES

This Chapter presents a wide range of scientific opportunities available to potential users of the FOC. Table 6 summarizes some of the exciting projects that might be undertaken, illustrating diagrammatically the application of the different FOC operational modes to different types of astrophysical problems. This survey is valid today, but even more exciting problems may present themselves by the time ST is launched.

Table 6. A survey of science opportunities for the FOC.

Optical train	Operating modes	Examples of scientific objectives
f/96	Normal imaging (with or without wide- or narrow-band filters)	High-resolution imaging especially in the ultraviolet-planets, binary stars, globular clusters. Detection of jets, optical emission from radio lobes. Morphological classification of distant galaxies. Proper motion studies of stars in globular clusters, Magellanic Clouds and of supernovae filaments.
	" with polarizer	Polarisation in young stars, circumstellar shells, radio jets.
	" with objective prisms	Detection of low-redshift quasars by Lyα emission. Determination of the redshifts of X-ray clusters.
	f/288 VHRA	Diffraction-limited ultraviolet observations.
	f/288 VHRA (in coronographic mode)	Detection of planets around nearby stars; mass loss from stars; nebulosity around quasars.
	Coronograph without apodizer	Binary star observations.
f/48	Normal imaging (with or without filters)	As above, but where a larger field of view is desirable, and/or when lower resolution is acceptable, e.g. following supernovae light curves up to 6 years after the explosion.
	" with objective prisms	As above.
	Long-slit spectroscopy	Spectroscopy across extended systems - globular cluster and galaxies. Determination of the velocity dispersion in the nuclei of galaxies and across the arms of spiral galaxies.

2.1. The distance scale

Measuring the distances to astronomical objects is of fundamental importance, since knowledge of the luminosities of stars and galaxies depends on estimates of their distance, and the age of the Universe is deduced from the distance scale assigned to galaxies which experience the general cosmological expansion. Because of its high angular resolution, the FOC will contribute to direct geometrical distance determinations, and its limiting magnitude will make it capable of greatly extending the range of distances over which presently employed distance indicators ('standard candles') can be used.

Parallaxes with 10% accuracy should be measurable to distances of at least 100 pc, bringing the Hyades within range. For the nearest stars, the ability to obtain more accurate parallaxes will correspondingly increase the accuracy to which the luminosity of main-sequence stars are known. Measurement of the proper-motion dispersions of stars in the nearest globular clusters, such as 47 Tuc and ωCen, coupled with accurate radial-velocity dispersions being made with new ground-based techniques, could give distances of these clusters. Accurate distances to expanding nebulae can also be measured by relating radial-velocity measurements to angular expansion rates.

A coordination of observational programmes with the Hipparcos astrometry mission will make the best use of this powerful combination of instruments. FOC observations of selected fields will enable a rotation free proper motion system for the Hipparcos observations to be established. Similarly, using the reference frame determined by Hipparcos, relative proper motions and parallaxes obtained by the FOC and by the other ST instruments can be converted to absolute ones.

The classical distance indicators - RR Lyrae stars, Cepheid variables, the brightest stars, globular clusters and HII regions - can all have their absolute magnitudes calibrated through knowledge of the distance to the Magellanic Clouds. RR Lyrae stars will easily be seen in Local Group galaxies; the brighter Cepheid variables likewise in the Virgo cluster. A single sequence of a dozen exposures spaced three days apart will make it possible to determine the light curves directly. At these distances the Hubble flow is unaffected by the perturbing effects of the local supercluster, and primary distance indicators would be tied to the great galaxy clusters without the need for poorly known secondary distance indicators. The brightest stars and globular clusters will be resolved at redshifts up to $z \lesssim 0.06$, a distance range including several N-type galaxies. Giant HII regions would be detectable to redshifts of about one.

Photometric measurements of Type-I supernovae provide a well-known cosmological test. Following the discovery of such a supernova in a remote galaxy at maximum light, it will be important to measure its magnitude at about 60 days and again at about 250 days after maximum. Standard light curves predict that the supernova will then be about 3 and 6 magnitudes fainter than at maximum respectively. An understanding and determination of the supernova's physical conditions then enables the ratio of the scale factors of the Universe at the present epoch and at the epoch of the supernova explosion to be deduced. For better discrimination, the 'fast' supernovae (Type Ia) are preferred - these have a decline of 0.016 magnitude per day instead of 0.012 for the slower type, and a slightly brighter absolute magnitude. The FOC, reaching considerably fainter limiting magnitudes than ground-based observations, provides an excellent opportunity to perform the test. The small field size is not a disadvantage, the supernovae being discovered by surveys from the ground. The absolute photographic magnitude is predicted to be about M = -19 magnitudes, and at $m_{pg} = 19.5$ (probably a realistic magnitude for discovery) the distance modulus is 38.5 and the corresponding redshift is 0.15, large enough to provide cosmological data.

2.2. Stars and stellar evolution

Observation and theory provide few indications of the way in which stars actually form and how the stellar birth rate depends on time, stellar mass, etc. A profitable line of attack on these problems would be to observe systems that are active in star formation at the present epoch - for example at different locations in nearby galaxies of various morphological types.

In our own Galaxy optical observations of the giant HII regions are impeded by interstellar absorption. Many young stars are surrounded by thick dust clouds which absorb most of the stellar energy and reemit it in the infrared spectral region. The extremely faint limiting magnitudes of the FOC may make it possible to detect the central star in some cases despite this large attenuation. For external galaxies, insufficient angular resolution prevents detailed observations of known giant HII regions. Not only high resolution, but also a faint limiting magnitude is required to reach these interesting regions. A typical observing proposal may call for exposures of several such regions in nearby galaxies (LMC, M33, M101) in order to look for the individual OB stars expected between $-10<M<-2$. Observations in the U and V bands, and an ultraviolet band would enable colour-magnitude diagrams and luminosity functions for the stars to be determined, and allow comparisons between galaxies, and locations within galaxies, to be made.

There is much current interest in the evolution of stellar population and in elemental abundances in our own Galaxy. With the FOC these studies can be further extended to other galaxies. Studies of stellar populations from the distribution of stars in the HR diagrams

for different parts of other galaxies can be persued to distances of the order of 10 Mpc and will include galaxies of all types. Within our Galaxy, observations should lead to an improved understanding of the central regions by enabling us to penetrate the absorbing clouds in those directions.

Studies of M31 have shown that curious variations of stellar populations occur close to the nucleus - they appear as variations in the strengths of metallic lines or other photometric indices such as CN. It is desirable to extend such a study to galaxies of different morphological types where, again, ground-based observations do not have sufficient angular resolution for systems more distant than M31. Line and continuum observations in the ultraviolet will provide confirmation of the existence of hot stars suspected from earlier studies.

Observations of very young supernova remnants have already been discussed in the context of establishing the cosmological distance scale. The youngest supernova remnant known in a nebular phase. Cas A, has an age of 300 years - there is therefore a great gap in our knowledge at all wavelengths for the age range 700 days after maximum light (in the case of SN 1972e in NGC 5253) to 300 years. Extrapolation of a typical light curve suggests that one might be able to follow such an object spectroscopically in both the UV and the visible with the FOC to an age of 6-7 years, far beyond the transitional period between the opaque and the nebular stages. Reliable abundance estimates can then be made for the material that is still largely uncontaminated debris from the parent star. For older supernovae in our Galaxy (Vela, IC443 etc.) proper motion measurements of the filaments can be made, leading to a more complete dynamical picture of these objects.

Most planetary nebulae and HII regions of high surface brightness have sufficiently high electron densities that the 2s state of hydrogen is collisionally de-excited. But in the Cygnus Loop and Vela regions a significant band of enhanced optical continuum appears to be two-photon emission. These objects therefore provide a good opportunity of confirming the existence of long-standing theoretical prediction in atomic physics. It is important to understand these features since continuum observations provide the only direct practical way of determining the hydrogen recombination temperatures.

Only two optical pulsars are known at the present time. In the case of the Crab, the pulsar is known to be rotating about the magnetic field axis near the centre of the nebula, although the significance of these observations is not known. The thin wisps close to the pulsar are also mysterious - although the rapid movement seen in these wisps suggests a connection with the energy transport from the pulsar into the nebula, the relevant mechanism is unclear. For the other optical pulsar in Vela, Figure 9 shows the potential of the time-resolution imaging mode from observations made at the Anglo-Australian Telescope.

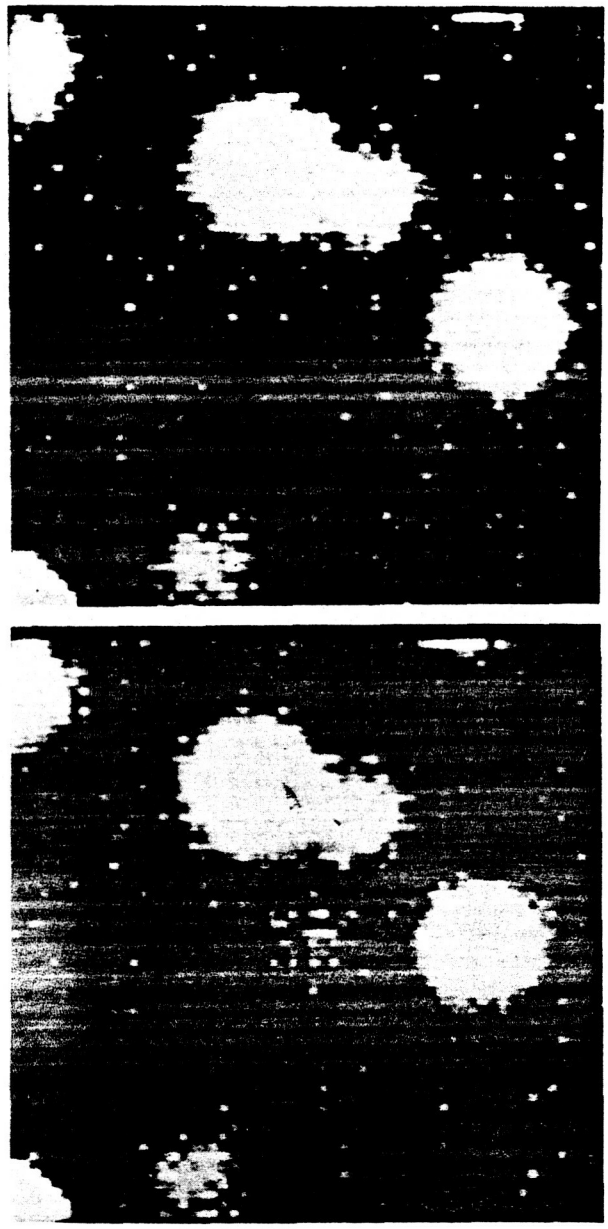

FIG. 22 Time resolution imaging of the Vela pulsar. Two pictures of a series of eight continuously cycled in 89 ms. The pulsar is low in (a) and bright in (b) (m_B = 24.4 mag). Total field is 12 x 12 arcsec^2 (IPCS used direct at the Cassegrain focus of the AAT).

2.3. Stellar systems - globular clusters and normal galaxies

Globular clusters are a very common component of the past and present Universe, and are strongly connected with the halos of both spiral and elliptical galaxies. Some 150 globular clusters are known to orbit our own Galaxy, many hundreds are known in M31, some thousands around M87, etc. Although the globular-cluster population of

a galaxy is largely dependent on its luminosity, there are some notable exceptions, and the phenomenon deserves further study.

At the distance of the Virgo cluster, globular clusters will have diffuse images at f/96 resolution and will be easily distinguishable from stars. Out to the Coma cluster the brighter globular clusters will still be countable, and their UBV colours can be determined with a respectable S/N in about an hour.

The brightest globular clusters of a galaxy are a precarious distance indicator, whereas the luminosity function of the whole cluster population may be a more stable indicator. The faint limiting magnitude of the FOC will enable this determination to be made for many Virgo galaxies. Thus the hypothesis of similarity can be tested, and if it holds it will provide a good value for the distance modulus of the Virgo cluster.

Within individual globular clusters, both dynamic and spectroscopic observations can be undertaken with the FOC. In both cases, due to the crowding of stellar images and to the wide range in brightness found towards the cluster centres, many intriguing questions remain unanswered. Dynamically, the inner parts of the clusters are the most interesting. The detailed velocity distribution of stars in the globular cluster is poorly known, although measured motions are in the range 6-10 km s^{-1}. The radial dependence of this distribution is required to determine the virial mass of the cluster and to constrain theoretical models of the formation and evolution of globular clusters. The high resolution of the FOC will enable proper motions of the component stars to be measured well into regions unresolved in ground-based photographs, and the faint limiting magnitude will extend the velocity distribution down to low-luminosity, low-mass stars.

Velocity measurements will probably throw light on the origin of the X-ray emission detected in some clusters. Accretion onto a collapsed object is the favoured explanation, but whether onto a neutron star or a black hole is a matter of speculation. In the former case, binary systems may even be observable directly - such detections would also give information on the mass-luminosity relation and consequently on the original helium content of the cluster members.

Spectroscopic observations provide direct information on the chemical composition and on the chemical variations induced by evolution. The gradient of metal content can be traced from the outer to the inner parts of galaxies via globular clusters, and the variation of chemical composition of clusters located in different spiral arms or in different parts of nearby galaxies. One might expect to derive UBV diagrams for the individual brightest stars in clusters in M31 in which the largest clusters are barely resolved in ground observations.

Brightness profiles at the centres of elliptical and early-type spiral galaxies are needed to understand the dynamics of these systems. Again, ground-based resolution is inadequate, although some recent observations have suggested the existence of a brightness excess at the centres of some ellipticals suggesting the presence of a central black hole - here the FOC resolving power should be decisive.

For normal galaxies, we expect to be able to classify morphologically galaxies in distant clusters up to a redshift of about 0.8, depending on the amount of colour evolution occurring. The f/96 mode of the FOC will provide sufficient spatial resolution to allow the determination of the core radii of distant galaxies where the small field of view will be no limitation. The high spatial resolution of the FOC may prove to be the deciding factor in making these observations, although the technical feasibility of the measurements will depend on some unanswered questions about the scale sizes and luminosities of distant galaxies. Even for nearby galaxies the constancy of values expected for the core radii are not well understood. Although the aim of such a project would be to use the core radii as standard rods in order to study the redshift dependence of angular sizes and hence estimate q_o we do not have a precise idea of what dynamical evolution might do to the core radii; nevertheless such observations will be useful in understand the evolution of galaxies, if not for cosmology.

2.4. Nuclei of galaxies and high-energy astrophysics

The FOC will greatly improve our knowledge of other galaxies, of the nature of the violent phenomena going on in some of them and of the nature of quasars. Astronomers will be able to observe the detailed optical structure of galactic nuclei with a resolution approaching that of radio interferometers and monitor possible changes in this structure. For example, high-resolution radio studies of galaxy NGC 1275 have recently indicated the existence of bright knots in the nuclear region, the intensities or sizes of which are thought to have changed over the past three years. Optical monitoring of such sources will be possible with the FOC, and the dynamical conditions close to the nuclei of nearby active galaxies will provide strong clues as to the physical processes involved. High-resolution imaging, through filters separating emission lines believed to be produced in different regions, can search directly for structure in Seyferts such as NGC 1068 and NGC 4151 to verify the stratification of the ionisation regions predicted by photoionisation models. The FOC long-slit spectrograph can then be used to search for any velocity structure present while preserving some spatial information. Promising lines might be CIVλ 155 nm and HeIIλ 164 nm which are produced in different regions of ionisation - choosing ultraviolet lines means that contamination from the underlying galaxy spectrum is minimised.

Numerous projects to investigate the relationship of normal galaxies. Seyferts, quasars and BL Lac objects can be undertaken. A typical galaxy cluster around a quasar at z = 1 should be about 1 arcmin across. The 44x44 arcsec^2 field of the FOC at f/48 can be used to search for these galaxies to a level fainter than is obtainable from the ground. Observation of the field in redshifted Lyα and in an adjacent band may enable foreground and background galaxies to be rejected.

One of the most important observational problems related to quasars is the search for an underlying galaxy associated with the quasar - i.e. to search for nebulosity having the morphology and the absorption line spectrum of a galaxy at the same redshift as the quasar. Progress in this area has been slow because the relevant surface brightnesses are very low (Figure 10). It will be important to determine the morphologies of the galaxies underlying the quasar, to understand the relationship between morphological type, radio properties and space density of radio galaxies and quasars. Radio galaxies with extended double structure and well-determined morphologies are nearly all elliptical systems; we can hope to determine whether radio quasars are similarly embedded in elliptical galaxies, and whether the radio-quiet quasars (like the weakly-emitting Seyfert nuclei) are also in spiral or SO galaxies.

Observations connected with radio sources are similarly very exciting. Radio source counts at different frequencies are known to have different slopes, the spatial distribution of steep-spectrum sources indicating a strongly evolving population, while the flat-spectrum and low-luminosity sources appear to be more smoothly distributed. One thing that is badly needed is a complete list of optical identifications to a fainter limit than can be achieved from Earth.

At present a dozen radio galaxies and quasars are known with jets and knots located in the vicinity of the nucleus. Those regions known to emit both optical and radio non-thermal continuum radiation can provide information on the transfer of particles or energy from the nucleus outwards. Observations with the FOC will complement the increasing availability of very deep radio maps and digital devices for direct imaging. Observing in the ultraviolet increases the contrast of the non-thermal jet against the stellar continuum and the increased angular resolution will enable the jets to be followed very close to the nucleus, for example in M87, if scattered light proves to contaminate the innermost knots.

Further out in such radio sources it will be important to continue the search for optical emission associated with the radio lobes. The conditions under which this radiation arises is not understood - it could arise from emission lines, or from synchrotron or inverse Compton radiation. A study of the spatial distribution of the emission compared to that of the radio emission, colours and polarisations will give a better idea of the detailed physical processes involved - all such cases of suspected emission are very faint.

Spectroscopic observation can be used to determine the relationship between the rotation axes of the central galaxies of double radio sources and the extended radio structure. This is important for models of energy flow and radio source evolution, and has proved very difficult to determine from the ground.

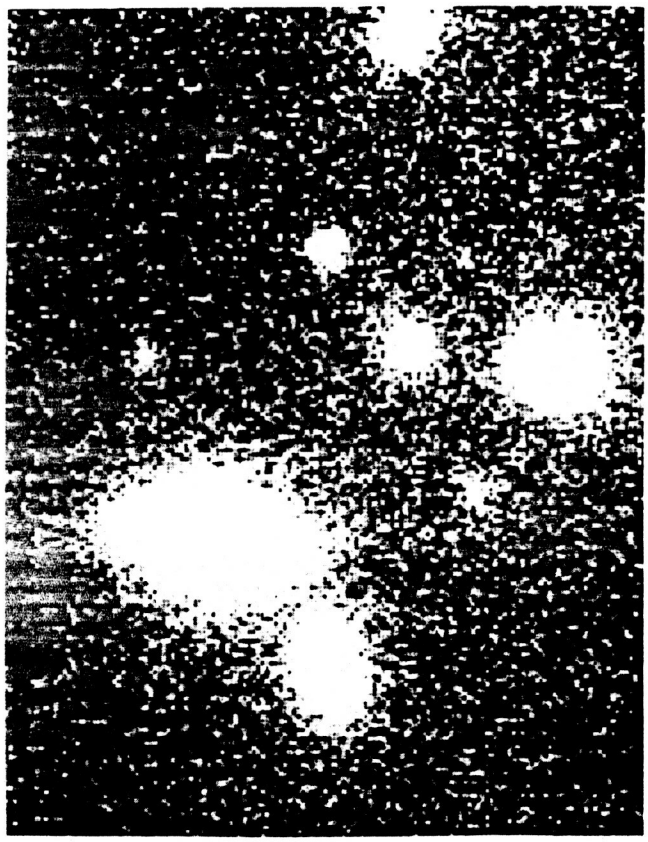

FIG. 29. Imaging of the quasar Ton 256. The central object is Ton 256 exposed sufficiently deeply to show the presence of the galaxy around it. Also seen are the cluster galaxies and foreground stars.

2.5. Solar System Objects

The Space Telescope will enable important observations of planets and satellites to be made that are not feasible in any other way. The very high resolution of the FOC will make it possible to observe features 50 times smaller in area than is now the case under the very best conditions with ground-based telescopes. The FOC will view large areas of a planet synoptically with only gradual changes of lighting or viewing geometry over periods of months, whereas planetary orbiters and flybys are severely limited by orbital constraints to the observation of particular areas (usually small) at particular times. Moreover, the FOC can provide, in an imaging mode, multiple-passband photometry and polarimetry of better

quality than any planetary mission now scheduled. Such observations can frequently be made when the ST is unable to work on fainter objects in the presence of Sun- and Earth-light.

The very high resolution of the FOC can be utilised for planetary imaging by attenuating the optical input and stacking a number of rectified output scans.

A better understanding of planets requires, to a large degree, better observations of their changing features. Dust storms, white clouds, polar caps, and polar hoods evolve on Mars. Faint atmospheric markings circulate around Venus, while Jupiter displays a continuously varying pattern of belts, zones and spots. Little is known about dynamic processes on Uranus and Neptune; but they may well not be placid and featureless at FOC resolution. Recently discovered photometric variations hint that some of the major satellites of the outer planets may also be interesting objects to watch at FOC resolution. Even in view of the recent Voyager results, FOC imaging will further advance our understanding of Jovian dynamics and will also bring Saturn within range of dynamical study. FOC monitoring of Mars during several successive apparitions should advance our knowledge of the atmospheric circulation pattern, dust-cloud generation, regional wind velocities, aeolian transport and white-condensate cloud formation. Imaging photometry and polarimetry will provide data concerning regional surface composition, surface texture and aerosol scattering.

The ST will also allow spatially resolved images of smaller solar system objects to be made. There are numerous objects in the Solar System whose dimensions at opposition are of the order of 1 arcsec or less and which are particularly appropriate for observations with the FOC. As examples we could cite (i) the largest asteroids (among them Ceres, Pallas, Juno and Vesta); (ii) the Galilean satellites; (iii) two of the largest satellites of Saturn (Rhea and Titan); (iv) Uranus, Neptune (and possibly its large satellite Triton) and Pluto.

For the last three planets, there is still the exciting prospect of discovering new satellites as has been the case for Pluto. This search may involve the coronographic mode of the FOC which will also be of use for the study of extended atmospheres around planets and satellites.

The discovery of the ring system around Uranus calls for a thorough search for a small body inside the orbit of Miranda, with approximately half of its mass. Uranus subtends a radius of 2 arcsec, the rings have a radius of 4 arcsec while Miranda orbits at 10 arcsec from the planet. It is therefore only necessary to place Uranus out of the field of view and take a long exposure of the region between the ring and Miranda - ideally the curved path of the suspected satellite would be revealed.

Quite a large number of asteroids can be examined directly for diameter, shape and even surface details. For the largest objects, detailed surface studies can be carried out during a single rotation cycle. For example, Ceres rotates in 9.1 h, its diameter is 1003 km and its maximum apparent diameter is 0.7 arcsec. A surface element of about 30x30 km^2 can be resolved directly with the pixel size of the FOC, and the resolution can be further improved with suitable deconvolution methods and the f/288 mode. Such observations could be combined with polarimetric studies to obtain information on the surface structure.

The combination of all these observations can be used to determine the spin-axis orientations. Ground-based photometry indicates very strange geometrical configurations for some objects, a result which can also be interpreted as the effect of a possible binary nature of some of the asteroids. 624 Hector is one such object; if it is a single asteroid the axial ratio must be at least 6:1, although there are theoretical considerations which suggest a binary nature. A direct f/96 exposure combined with suitable image-processing techniques could resolve this problem unambiguously.

Another project feasible with the FOC is the search for planets around other stars similar to those of our own Solar System. In the case of Barnard's star, long series of observations have failed to reveal the presence of a second stellar mass, and therefore there is fair evidence that the star really is single. The residuals from the linear motion may instead be attributable to at least one planet-like body at an angular distance between 1.5 and 2 arcsec from the star and with apparent magnitude $m_V = 28$. The technique consists of using the coronograph occulting mask to avoid any scattered light from the star's central peak caused by the FOC optics, by the detector faceplate and by the inner walls of the image intensifier. Edge effects and diffraction from the secondary spider are taken up by the apodizing mask. The residual background is not uniform but has a mottled structure which is fixed in position on the detector faceplate. A rotation of the telescope around its optical axis will then cause a rotation of this pattern, while the planet will remain in the same celestial position. The subtraction of the rotated image from the previous one will therefore leave the image of the planet. The FOC is the best instrument on board for this project (even with its poor red response) because of its high angular scale and the very good coronograph.

3. CONCLUSIONS

The FOC is one of the key elements of the European Space Agency's contributions to the Space Telescope programme. The other elements of the active European participation in this programme are: (i) the provision of a major subsystem namely the solar arrays and associated mechanisms and (ii) the participation with ESA provided personnel in the operational activities of the Space Telescope Science Institute.

The FOC is the result of the coordinated efforts of many individuals within ESA, the scientific community and industry. The contributions made by all are gratefully acknowledged.

Astronomical Capabilities of the Faint Object Spectrograph on Space Telescope

R. J. Harms and the FOS Science and Engineering Team

Center for Astrophysics and Space Sciences
University of California, San Diego
La Jolla, California 92093

Abstract

Examples of scientific observing programs planned with the Faint Object Spectrograph on Space Telescope are presented. An overview of the spectrograph design and operation is presented. The expected astronomical performance of the instrument is described in some detail. References for further information are given.

1.0 Introduction

The Faint Object Spectrograph (FOS) is designed to allow spectroscopic analysis of physical conditions in faint and often extremely distant astronomical objects. The Space Telescope (ST) itself provides unprecedented spatial resolution throughout the ultraviolet to near-infrared portion of the spectrum. The excellent image quality is used by the FOS not only to make possible study of fine structures but also to achieve major improvement in limiting magnitudes by suppressing sky background. As described below, the FOS design is matched to the ST-unique capabilities to provide astronomers a flexible instrument with broad spectral coverage, moderate spectral resolution, ultraviolet spectropolarimetry capability, stable and nearly linear photometric response over a large dynamic range, fine temporal resolution, and extremely low background.

Several examples of scientific studies planned by the FOS Investigation Definition Team (IDT) are mentioned in Section 2.0. These programs illustrate the intended applications of the FOS, but form a biased sample emphasizing the predominantly extragalactic interests of the FOS IDT. Section 3.0 describes the FOS design features, modes of operation, and its status as of June 1982. Of greatest interest to potential users, Section 4.0 discusses the anticipated performance of the FOS based on measurements of the flight hardware components. Finally, Section 5.0 lists references where the reader can obtain further information about the FOS.

The FOS is being built by the University of California, San Diego (UCSD) and prime subcontractor Martin Marietta Corporation (MMC) Aerospace Division in Denver, Colorado. Key personnel involved in the FOS program are introduced in Table 1.0-1.

TABLE 1.0-1
Principal FOS Scientists and Engineers

NAME	POSITION	INSTITUTION
Roger Angel	Co-Investigator	University of Arizona
Frank Bartko	Co-Investigator	Martin Marietta Corporation
Edward Beaver	Co-Investigator	Science Applications Inc., University of California, San Diego
Ralph Bohlin	Co-Investigator	Goddard Space Flight Center, Space Telescope Science Institute
Margaret Burbidge	Co-Investigator	University of California, San Diego
Arthur Davidsen	Co-Investigator	Johns Hopkins University
Holland Ford	Co-Investigator	Space Telescope Science Institute
Richard Harms	Principal Investigator	University of California, San Diego
Bruce Margon	Co-Investigator	University of Washington
Louis Ripp	Project Manager	Martin Marietta Corporation
Charles Ross	Project Manager	University of California, San Diego
Eugene Strein	Project Engineer	University of California, San Diego
Joseph Vellinga	Systems Engineer	Martin Marietta Corporation

2.0 Science programs

The light-collecting power of the ST in the ultraviolet spectral region, the sharp imaging capability, and the reduced sky background offer the potential for many exciting observations. In this section, we describe some of the programs planned by the FOS IDT.

Because this paper is primarily an instrumental description, the planned scientific investigations are presented only cursorily. Still, we hope some of the excitement is evident, while the examples illustrate uses of the FOS capabilities.

2.1 Active galaxies. High spatial resolution spectra of Seyfert and active galaxy nuclei are planned to obtain information concerning physical properties (temperatures, densities, and velocities) of the H II regions, dust content, and the nature of the ionization mechanism. Line strengths and profiles of the features listed in Table 2.1-1 will provide information to determine the physical parameters of individual ionized structures. Observations of intensity ratios of the auroral to transauroral line strength ratios listed in Table 2.1-2 will indicate dust content. Finally, measurements of the ultraviolet continuum and line intensities of differently ionized elements will indicate the extent of ionization due to thermal or nonthermal photoionization or due to shocks. All the lines in both tables lie within the spectral range accessible with the FOS.

TABLE 2.1-1
Density Sensitive Features

ION	WAVELENGTH (Å)	CRITICAL DENSITY*
[Ne V]	1575	2.0×10^8
[A V]	2691	1.1×10^8
[A III]	3109	5.8×10^7
[O III]	4363	2.4×10^7
[O III]	5007	6.5×10^5

* At $T = 10^4 K$

TABLE 2.1-2
Extinction Sensitive Transitions

ION	AURORAL/TRANSAURORAL WAVELENGTHS (Å)
[A III]	5192/3109
[A IV]	7300/2854
[A V]	4625/2691
[O II]	7320 - 7330/2470
[Ne III]	3342/1815
[Ne V]	2974/1575

2.2 Quasars. The studies of quasars are grouped in three categories below. The goals of these three broad programs can be summarized as: 1) determine the nature of underlying nebulosity associated with some quasars, 2) determine the physical conditions within quasars, and 3) seek the relationship of quasars with other astrophysical objects.

The spatial resolution of the ST will be exploited in order to analyze the nature of the underlying nebulosity seen around some quasars, and presumably to be seen around more quasars by the ST cameras. Spectra of this nebulosity will test the hypothesis that quasars are embedded in galaxies. The FOS design incorporates special occulting apertures matched to the ST optics to maximize the nebulosity signal to quasar plus sky background noise ratio for these observations. The FOS team also intends to observe asymmetrical wisps and jets associated with some quasars and to compare these data to observations of the optical synchrotron knots in the M87 jet. The ultraviolet continuum emission from the jets will test models which generate relativistic electrons by collision between relativistic protons and cooler denser gas. The data will also provide information about the synchrotron cutoff frequencies of the various knots.

The proposed investigation of physical conditions within quasars uses essentially the same methods as described in Section 2.1 to study Seyfert nuclei. In particular, we will obtain information concerning temperatures and densities from auroral and nebular line strengths, about dust content from auroral to transauroral line intensity observed ratios, and about the high density regions from density-sensitive transauroral line intensities. For highly redshifted quasars, the highly interesting helium abundances from measurements of He I and He II lines will be possible. Indeed, many extreme-ultraviolet lines of astrophysical significance will become observable in highly redshifted quasars. Table 2.2-1 lists some of these features along with the minimum redshift which will bring them into the observing range of the FOS on ST.

TABLE 2.2-1

Significant Quasar Features Observable with FOS for Restricted Redshifts

ION	REST WAVELENGTHS*(Å)	MINIMUM REDSHIFTS OBSERVABLE**
H I	1025.7, 972.5, ..., lim 911.8	0.12, 0.18, ..., 0.26
He I	584.3, 537.0, 522.2, lim 504.4	0.97, 1.14, 1.20, 1.28
He II	303.2, 256.3, 243.0	2.79, 3.49, 3.73
C II	1036.3+, 903.6++, ...lim 508.6	0.11, 0.27, ..., 1.26
C III	977.0, 386.2, 310.2, lim 259.0	0.18, 1.98, 2.71, 3.44
C IV	312.4, 244.9	2.68, 3.70
N I	1134.2++, 963.9++, lim 853	0.01, 0.19, 0.35
N II	1084.0++, 915.6++, 671.0++, 644.6++, ..., lim 418.9	0.06, 0.26, 0.71, 0.78, ... , 1.75
N III	989.8++, 763.3+, 685.0++, 451.9++, ..., lim 261.4	0.16, 0.51, 0.68, 1.54, ..., 3.40
N IV	765.1, 247.2	0.50, 3.65
O I	1039.2+, 1025.8+, 988.8+, lim 910.5	0.11, 0.12, 0.16, 0.26
O II	832.8+, 539.4++, 430.0++, lim 353.1	0.38, 1.13, 1.67, 2.26
O III	832.9++, 702.3++, 507.4++, 373.8++, 305.7, 303.6 2.76, 2.79	0.38, 0.64, 1.27, 2.08,
O IV	787.7++, 608.4+, 553.3+, 279.6+	0.46, 0.89, 1.08, 3.11
O V	629.7	0.83
O VI	1031.9, 1037.6	0.11, 0.11
Ne I	743.7, 735.9, lim 575.0	0.55, 0.56, 1.00
Ne II	462.4, 460.7, 454.6+, 445.0++, ..., lim 302	1.49, 1.50, 1.53, 1.58, ..., 2.81
Ne III	488.1++, 313.0+, 283.2++	1.36, 2.67, 3.06
Ne IV	543.9++, 542.1, 541.1	1.11, 1.12, 1.13
Ne V	568.4++, 480.4++, 358.0++	1.02, 1.39, 2.21
Ne VI	558.6++, 433.2++, 401.1++, 399.8++	1.06, 1.65, 1.87, 1.88
Ne VII	465.2	1.47
Ne VIII	780.3, 770.4	0.47, 0.49
Na II	376.4, 372.1, 301.4, 300.2, lim 262	2.06, 2.09, 2.82, 2.83, 3.39
Na III	378.1	2.04
Na IV	410.4, 408.7	1.80, 1.81
Na V	463.3, 461.0, 451.9	1.48, 1.49, 1.54
Na VI	489.6, 414.3, 311.9	1.35, 1.78, 2.69
Mg II	lim 824.7	0.39
Mg IV	321++	2.58
Mg V	353.1, 351.1	2.26, 2.28
Mg VI	403.3, 400.7, 399.3	1.85, 1.87, 1.88
Si II	lim 759	1.52
Si III	566.5, lim 370	1.03, 2.11
Si IV	457.7, lim 275	1.51, 3.18
S II	912.7, 910.5, 906.9, lim 530	0.26, 0.26, 0.27, 1.17
S III	1021.2, 1015.5++, 1012.5, 735.3, 732.4, lim 354	0.13, 0.13, 0.14, 0.56, 0.57, 2.25
S IV	1073.2, 1062.7, 816.0, 809.7, 753.8, 750.2, 748.4, 744.9, 661.4, 657.3, lim 262	0.07, 0.08, 0.41, 0.42, 0.53, 0.53, 0.54, 0.54, 0.74, 0.75, 3.39
S V	786.5	0.46
S VI	944.5, 933.4, 249.3, 249.0	0.22, 0.23, 3.61, 3.62
A I	1066.7, 1048.2, 894.3, 876.1, lim 786.8	0.08, 0.10, 0.29, 0.31, 0.46
A II	932.0, 919.8, 740.3, 723.4, 671.9, 670.9, 666.0, 661.9, lim 449	0.23, 0.25, 0.55, 0.59, 0.71, 0.71, 0.73, 0.74, 1.56
A III	887.4, 878.7++, 871.1, 637.3, lim 303	0.30, 0.31, 0.32, 0.80, 2.80
A IV	850.6, 843.8, 840.0	0.35, 0.36, 0.37
A V	449.1	1.56

* Blends unresolved by FOS listed at weighted line center

** FOS minimum observable wavelength ≈ 1150Å due to magnesium fluoride cutoff

\+ Lowest wavelength of marginally resolvable blend with FOS

++ Lowest wavelength of a blend only partially resolvable by FOS

NOTE: References for the wavelengths are from National Bureau of Standards (1950), Chemical Rubber Company (1968), Osterbrock (1974), and Bahcall (1979). The data given are sometimes inconsistent but never to a degree which significantly undermines the intent of the table to specify redshift limits for FOS observations.

A specific program to test the hypothesis of cosmological redshifts for quasars involves correlating equivalent widths of the Lα and C IV lines with the far-ultraviolet continuum luminosities of quasars. Presently only high redshift quasars can be observed;

the ST allows low redshift observations in the ultraviolet which should decide the nature of the correlation. We also plan to test for the same correlation in Seyfert galaxies, which if found, would establish both a relationship between quasars and Seyferts as well as the cosmological redshift hypothesis for quasars.

2.3 Galaxy chemical abundances. The FOS IDT has proposed observations of H II regions and planetary nebulae in the Local Group Galaxies in order to determine young and old stellar population abundances respectively as a function of galaxy mass and location within a galaxy. The spatial resolution of the ST will allow extension of these abundance measurements well into the nuclei of these galaxies, while absence of Hg I λ4358 airglow will make possible the detection of far fainter O III λ4363 abundance sensitive (through electron temperature) line intensities than is possible from the ground. Also, observed line strengths of ultraviolet lines such as C IV λ1548 will permit abundance determinations of astrophysically important elements.

2.4 Planetary nebulae. We have proposed to obtain ultraviolet spectra of the central stars of planetary nebulae in the Magellenic Clouds. The well-determined distances will allow accurate luminosities to be derived. The long-baseline ultraviolet spectra should provide good data for fitting model stellar atmospheres from which accurate effective temperatures can be obtained. It will be possible to observe central stars of planetary nebulae ranging in brightness from V = 15.6 to V=22 which will define central star evolution over a period in excess of 30,000 years.

2.5 Time resolved spectrophotometry. Time resolved spectrophotometry of binary X-ray sources at ultraviolet and optical wavelengths can be expected to detect pulsations which will reveal the physical processes occurring when a relatively cool stellar atmosphere is intensely irradiated with X-rays. A series of spectrophotometric data from an X-ray binary serves both to elucidate the physics of the X-ray to optical pulse processing mechanism and to provide a velocity curve for the cool stellar companion from which (with the X-ray source velocity profile) the masses of the cool and X-ray emitting objects can be calculated. This program takes advantage of the FOS capability to obtain spectra at intervals as short as every 30 milliseconds.

Two additional results will be obtained from the data gathered for the program above. Time-integrated spectral profiles at moderate dispersion will discriminate between Roche lobe overflow and stellar wind driven mass transfer processes. Significant lines for this work are C IV λ1548, N V λ1240, and O VI λ1032 (the last not obtainable with the FOS). The second result to be expected from these data is the detection of absorption lines of the X-ray ionized surrounding matter providing information about the X-ray luminosity, circum-source matter density, and the flux variability of galactic X-ray sources on time scales comparable to the recombination times of the nearby interstellar gas -- about 100 years.

A similar study of recently discovered extreme ultraviolet sources such as HZ 43 and Feige 24 should help determine the high temperature end of the degenerate star luminosity distribution. The important inferences on stellar evolution provided by such data will comprise an interesting new test of the weak interaction theory.

2.6 FOS spectropolarimetry. Interstellar polarization was discovered in visible light 30 years ago and within a few years the basic explanation used today had been developed. The angular momentum vectors of spinning elongated or flattened dust particles are aligned in a perpendicular direction by an interstellar magnetic field. Thus the mean grain profile is elongated and the interstellar medium containing thin grains is linearly dichroic. In the 1960's it was found that the wavelength dependence of the linear polarization could be explained by grains of about the same size as those responsible for optical interstellar extinction and so a unified picture emerged. The subsequent discovery of circular polarization tended to confirm this picture.

However, satellite measurements of interstellar extinction in the ultraviolet have revealed added complexity (e.g., Aannestad and Percell, 1973). Two additional grain components seemed to be required -- one to explain the 2200Å extinction peak and another - very small particles - to account for the continued rise in extinction in the far ultraviolet. There are regional variations in the amount of ultraviolet relative to optical extinction. An understanding of the nature of these grain components is an essential prerequisite to elucidating the origin of interstellar dust.

Ultraviolet spectropolarimetry of reddened early type stars will be important in unraveling various aspects of these mysteries. First, the graphite explanation of the 2200Å feature is problematical and will suffice only if the particles are small and virtually spherical (Gilra, 1972). Since spherical particles produce no interstellar polarization, a clear test of this hypothesis is presented. Second, the composition of the very small particles is unknown though it has been suggested that they are the

refractory cores around which the classical dielectric particles accrete. Are these grains elongated and aligned? Only ultraviolet polarization measurements can answer this since small particles produce negligible affects at optical wavelengths. The details of grain alignment mechanisms are still controversial and here we have an unparalleled opportunity to discover many size and composition dependent effects.

Stars other than those exhibiting optical interstellar polarization will also be polarized in the ultraviolet. Electron scattering is important in Be and Of stars. Late type supergiants are also bright enough to be detected. The origin of polarization is a matter of debate; although circumstellar dust seems to play an important role, photospheric effects are also in evidence. Ultraviolet polarimetry will help determine the relative importance of these mechanisms. Compact reflection nebulae can also be examined to find the size and composition of dust.

A completely different mechanism giving rise to linear polarization is the influence of very strong magnetic fields on radiative transfer through the atmosphere of a white dwarf. It is expected that for light frequencies higher than the cyclotron frequency, the linear polarization will not propogate through the atmosphere (Angel, 1978). A cutoff in polarization at short wavelengths thus would give a fairly direct measure of field strength. The strong surface field measurement (by the Zeeman effect) of 2.5 X 10^8G in Grw + 70° 8247 implies a cyclotron frequency corresponding to a wavelength of 4000Å. A drop in linear polarization is seen below this wavelength and measurements below 3000Å should show no recovery. If the effect can be calibrated and checked in well understood objects, determination of polarization cutoff can be used to give a unique measure of field strength in other strongly magnetic white dwarfs.

Another important area of exploration with the FOS polarimeter will be the polarimetric properties of quasars and Seyfert galaxy nuclei using both the ultraviolet response and good spatial resolution of ST. In nearby Seyfert nuclei the forbidden line emission regions just revolved spatially from the ground will be easily resolved the the ST. In NGC 1068, for example, asymmetric dust clouds exterior to the permitted line emission region give rise to strong (10%) net polarization at 3000Å. The wavelength dependence further into the UV will give information on the dust composition, and its spatial and spectral distribution will help show the geometry and dynamics of the galactic nucleus. For the majority of quasars whose polarization is detected, but quite small (about 1%), it is not even known whether scattering processes or synchrotron radiation is responsible. The fact that in radio quasars with double lobes, the polarization and lobe axis are aligned, suggests that the origin is related fairly directly to the quasar geometry. We can expect that studies with the FOS polarimeter and from the ground covering the range 1200Å through the near infrared may lead to an understanding of the origin of polarization and perhaps of the continuum emission itself.

2.7 Cosmology with supernovae. One of the most exciting and difficult observations planned with the FOS will be to obtain spectrophotometric measurements of distant (redshift ≈ 0.3) supernovae in an attempt to determine the cosmological parameter q_o. (This presumes use of similar observations for lower-redshift supernovae to measure H_o.) The concept has been thoroughly discussed in the literature (Wagoner, 1980 and references therein).

The basic idea is simple. If it is possible to measure the cosmological redshift (from that of the containing galaxy), the initial time of explosion (early detection), and the expansion velocity of the supernova photosphere, then the physical size of the emission region can be known as a function of time (practically, limited to an interval about one month). Spectrophotometry combined with sufficient supernova models can fix the observed luminosity. (If the supernova were simply a blackbody, the derivation would be trivial; one obtains apparent luminosity directly, while the spectrally measured temperature and known physical dimensions determine absolute emitted luminosity. The true situation is, of course, more complex.)

Severe theoretical difficulties arise from the uncertainties introduced by intervening interstellar extinction and a complex photosphere (whose effective radius may vary with wavelength). However, the large sampling of information obtained from a given observation (hundreds to thousands of sampled wavelengths) probably can overcome these difficulties. The procedure is especially attractive, however, because cross-checking is available; successive measurements in time sample the supernova at different sizes and temperatures. Of course, observations of several supernovae will be necessary also.

The practical difficulties are also major. At a redshift of 0.3, the blue magnitude of a supernova will be about B = 22 to 23, and its temperature around 15,000K shortly after formation. In one month, it will cool to about 6000K and fade a magnitude. As described in Section 4.0, such an object will be possible but difficult to observe at moderate resolution with the FOS; especially as the supernova fades, it may be necessary to switch

to a low dispersion. In order to reduce the background from the parent galaxy, the ST spatial resolution is clearly essential. (However, we expect detection of the supernovae to arise from ground-based automated monitor surveys.)

It is fair to say that these measurements of redshift 0.3 supernovae lie at the extreme limits of ST + FOS performance. However, success appears possible, and the scientific reward will be large. Astronomers being ever willing to push instrumentation to its limits, we have no doubt others will conduct even more challenging observations on ST.

3.0 Instrument description

The Faint Object Spectrograph is one of four axial scientific instruments on the Space Telescope. Figure 3.0-1 depicts the main features of the FOS. The instrument is divided into two major compartments: an electronics shelf area above and an optics-plus-detector region below. The entire structure is about 1 x 1 x 2 meters.

Light enters the FOS through a pair of entrance ports (shown at lower left of Figure 3.0-1) located about 60mm = 215 arcseconds off the optical axis of the ST. The light from the object of interest then passes through one of two independent optical channels, each of which focuses nearly stigmatic spectral images on the photocathodes of photon-counting Digicon detectors. These channels differ only in the wavelength sensitivity of their respective detectors. At the ST focal surface is placed the FOS aperture wheel, containing eleven sets of single or paired apertures which range in size from 0.1 to 4.3 arcsec projected onto the sky. The optical beam then passes through the polarization analyzer (which includes a clear aperture position). The grazing incidence mirror, a "roof" prism, deflects the beam 22° upward. The reflection is required in order to allow the apertures to be placed near ST optical axis to minimize astigmatism, while meeting packaging constraints within the FOS. The deflected beam passes through an order-sorting filter, when required, in the filter/grating wheel. It is collimated by an off-axis paraboloidal mirror and then both dispersed (except for one imaging position) and focused by the selected element on the filter/grating wheel.

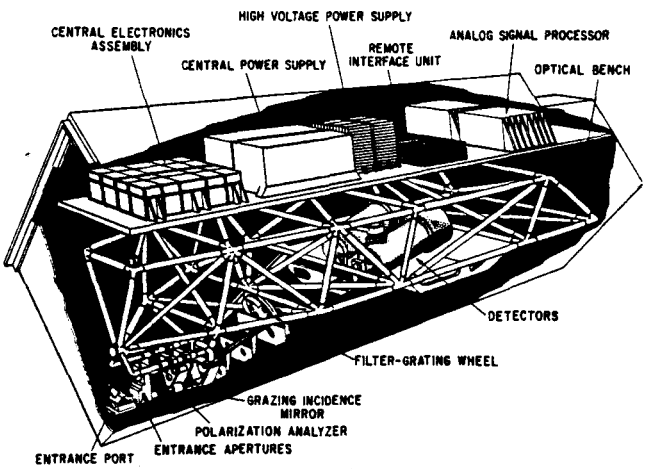

FIGURE 3.0-1. Faint Object Spectrograph: dimensions of the axial ST instrument are about 1 x 1 x 2 meters.

3.1 Optics. The design of the FOS optics is dominated by the desire to maximize throughput efficiency while utilizing the part of the ST focal plane as nearly on-axis as possible. The FOS design has eliminated any need to compensate for ST optical distortions, and has reduced to a minimum the number of optical surfaces. For example, a far-ultraviolet photon suffers only 3 reflections in the FOS before reaching a detector (grazing-incidence mirror, collimator, and focusing grating).

The entrance port has simply two positions to close or open the FOS to external light. The port mechanism also contains mirrors so that, in its closed position, light from the internal spectral calibration lamps can be shone through the optical path for wavelength calibrations.

The entrance aperture mechanism selects one of the twelve aperture sets (in either optical path). Table 3.1-1 lists the various aperture choices provided. The largest aperture, 4.3 arcseconds square, will be used for target acquisition. A variety of apertures from 0.1 arcseconds diameter for spectroscopy of fine spatial structure (e.g. knots in jets such as in M87) to 1.0 arcseconds for spectrophotometry or faint-nebula spectroscopy will enable astronomers to conduct diverse observations with high scientific efficiency. Specialized occulting apertures are intended for the study of faint sources

surrounding bright objects, particularly nebulosity surrounding quasars.

Table 3.1-1 Primary Entrance Apertures

Number	Shape	Size* (arcsec)	Center-to Center Separation(arcsec)	Special Purpose
Single	Round	0.5 dia	N/A	Polarimetry
Single	Round	0.3 dia	N/A	Polarimetry
Single	Round	1.0 dia	N/A	Polarimetry
Blank	N/A	N/A	N/A	Light Shield
Single	Square	4.3	N/A	Target Acquisition
Pair	Square	0.5	3.0	Object & Sky
Pair	Square	0.25	3.0	Object & Sky
Pair	Square	0.1	3.0	Object & Sky
Pair	Square	1.0	3.0	Object & Sky
Single	Rectangular**	0.25 x 2.0	N/A	Extended Objects
Single	Square	2.0	N/A	Surrounding Nebulosity
Single	Rectangular**	0.7 x 2.0	N/A	Surrounding Nebulosity
		Failsafe Entrance Aperture		
Pair	Square	0.5 and 4.3	4.4	Target Acquisition & Spectroscopy

* For rectangular apertures, first dimension is along dispersion, second perpendicular to dispersion.

** With occulter bar which is 0.3 arcsec wide in cross-dispersion direction.

The FOS polarization analyzer allows positioning of any of three elements into either optical path: a clear aperture, a thin-waveplate plus Wollaston prism assembly, or a thick-waveplate plus Wollaston prism assembly. One waveplate is permanently located in front of each Wollaston. The polarimeter is designed so that only a single motor is required to rotate the waveplates and to move either of the Wollaston/waveplate pairs from one entrance port to the other or out of the way. A drum, which is only 1.9 inches in diameter, contains the two Wollaston/waveplate pairs. The Wollastons are permanently fixed to the drum, but the waveplates are mounted in rotatable cylinders inside the drum. The waveplate cylinders have a 16-tooth gear on the outside which meshes with a 17-tooth fixed center gear inside the drum. One revolution of the drum rotates the Wollastons by 360°. The waveplates, however, rotate 382.5°. Each rotation of the drum thus increments the position angle of the waveplate fast axis by a net 22.5°. Sixteen rotations of the drum bring the mechanism back to its original configuration. Figure 3.1-1 is a photograph of the flight polarizer mechanism.

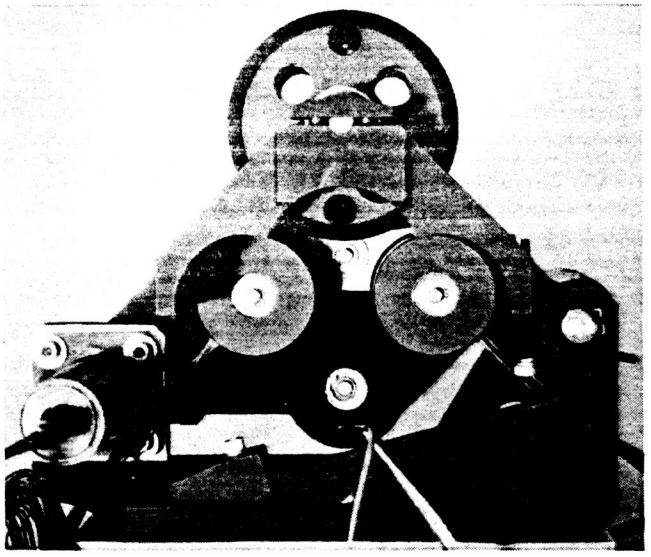

FIGURE 3.1-1. FOS Polarizer Analyzer: upper rotating barrel is about 5 cm diameter.

The filter/grating wheel photographed in Figure 3.1-2 (still with dummy optical elements), allows selection from ten positions in each optical path. Table 3.1-2 presents the dispersion selections available, and describes the filters used in five of the ten positions.

A considerable challenge in the FOS design was the requirement to maintain positional tolerances (initial alignment and stability) in the tens of micrometers for an optical structure over a meter long. Not surprisingly, the FOS optical bench is made of graphite-epoxy. However, as a photograph of the bench (Figure 3.1-3) and a photograph of its joints (Figure 3.1-4) make clear, the geometry is complex. The design selected uses pre-welded invar joints into which are inserted the graphite-epoxy tubes, all designed for near-zero thermal expansion coefficient at the optical compartment operating temperature of 20C.

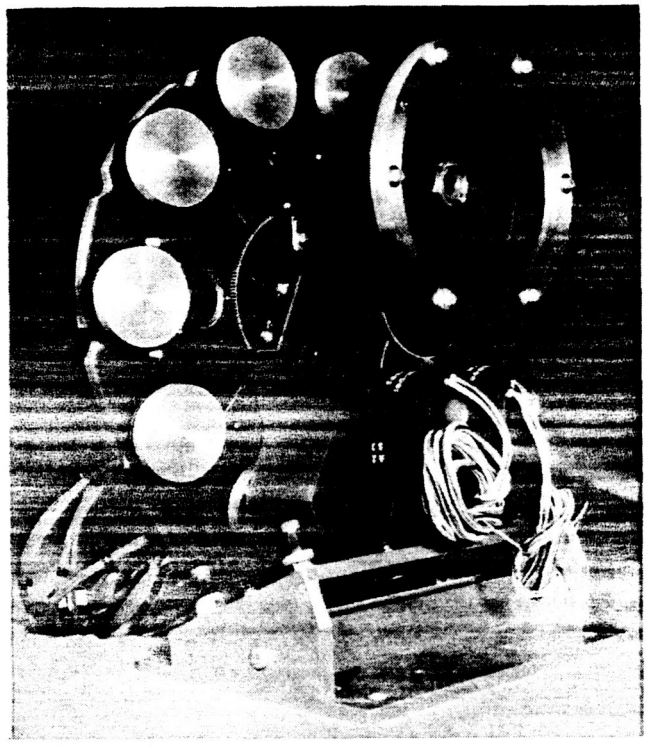

FIGURE 3.1-2 (upper left). FOS Filter/Grating Wheel: outer ring of aluminum caps are disperser locations; inner ring of holes are filter locations.

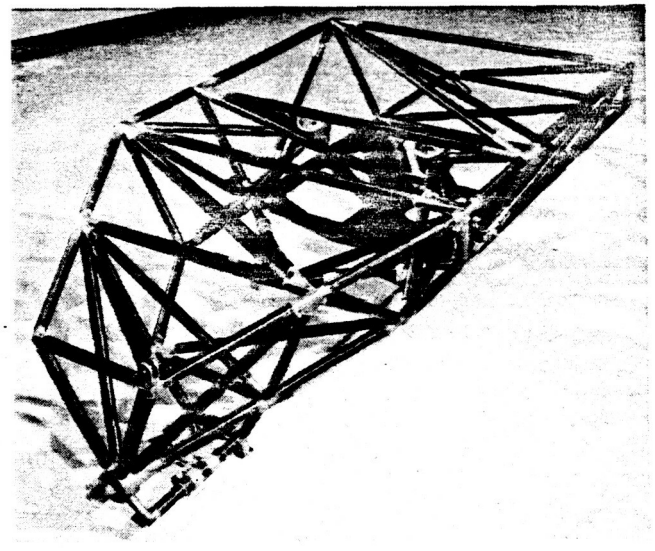

FIGURE 3.1-3. FOS Optical Bench: over one meter long, constructed of invar joints and graphite-epoxy tubes.

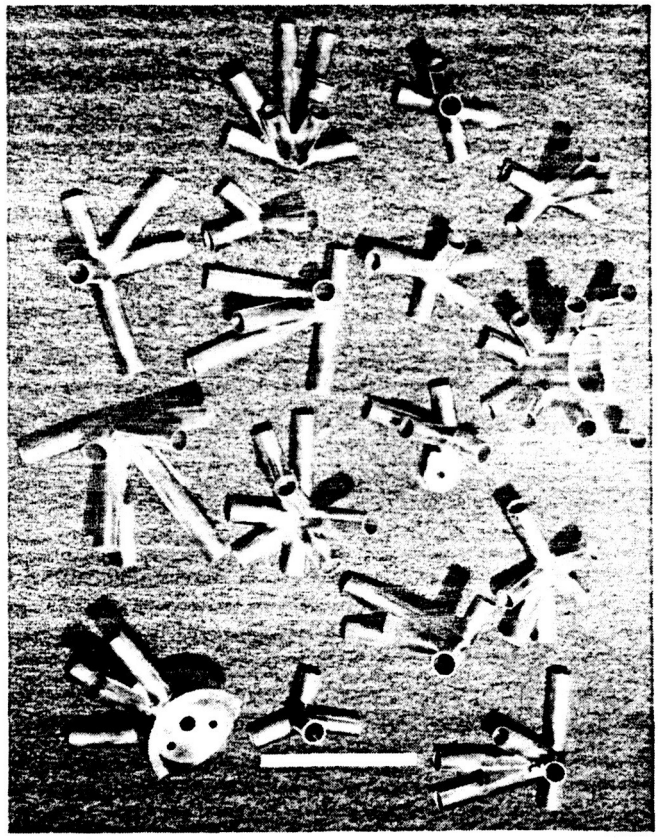

FIGURE 3.1-4. Optical Bench Invar Joints: note geometrical complexity leading to choice of welded joint structure.

Table 3.1-2 Wavelength Coverage of FOS Modes

Element	Resolution at Central Wavelength ($R = \lambda/\Delta\lambda$)	Wavelength (nm) Min	Max
Dispersers			
Grating H13	1200	110	164
Grating H19	1200	153	228
Grating H27	1200	221	329
Grating H40	1200	319	474
Grating H57	1200	459	683
Grating H78	1200	626	931
Grating L16	200	110*	220**
Prism	100	250	700
Grating L60	200	400	800
Mirror	1	110	900

Blocking Filters

Element	Wavelengths (nm) T=1%	T=90%	Minimum Wavelength (nm) Mode	Transmission at Min. Wavelength
FH27 = fused silica	>165	<200	221	93%
FH40 = WG 305	290	340	319	87%
FH57 = GG375 G34	355	425	459	91%
FH78 = OG 530	510	550	626	91%
FL60 = CG375 G34	355	425	400	85%

* Resolution is about 400 at 250 nm.
** Resolution is about 25 at 700 nm.

3.2 Detectors. There are two independent assemblies, one for each optical channel. Each detector assembly consists of a Digicon tube (described in Harms et al., 1979 and references therein), deflection coils, a permanent magnet focus assembly, magnetic shielding, mounting and alignment structure, heat pipes, temperature sensors, hybrid preamplifiers, and connectors.

The two Digicon detector assemblies, designated "red" and "blue", differ only in their photocathode and faceplate materials. The blue detector has a bialkali photocathode (Na_2KSb) deposited on a magnesium fluoride window to cover the wavelength region 115 nm $< \lambda <$ 500 nm. The photocathode of the red detector, trialkali $Na_2KSb(Cs)$ deposited on fused silica, provides an extension of sensitivity to the red, covering the range 180 nm $< \lambda <$ 850 nm. To reduce dark background to the extremely low values required for FOS scientific programs (< .002 counts diode^{-1} sec^{-1}), the detectors are cooled to the temperature range -10C to -28C by means of attached heat pipes.

The Digicons operate by accelerating (to 20-25 KeV) photoelectrons emitted by the transmissive photocathode onto a linear array of 512 silicon diodes. Figure 3.2-1 shows a photograph of a (reject) diode array mounted onto its 5 cm diameter ceramic header containing 520 vacuum-tight electrical feedthroughs. The charge pulse generated in each diode is amplified and counted by one of 512 independent electronic channels, beginning with the hybrid preamplifiers physically colocated with each Digicon. Figures 3.2-2 and 3.2-3 are photographs of the red flight detector, showing the overall detector assembly and the preamplifiers at the aft end.

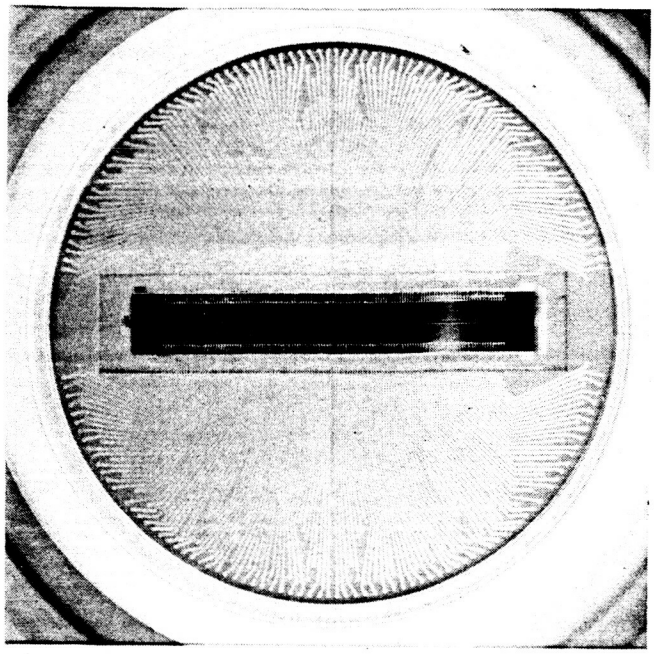

FIGURE 3.2-1. Digicon Array on Ceramic Header: 512-element array is about 2.5 cm long; 5 cm diameter header contains 520 vacuum feedthroughs.

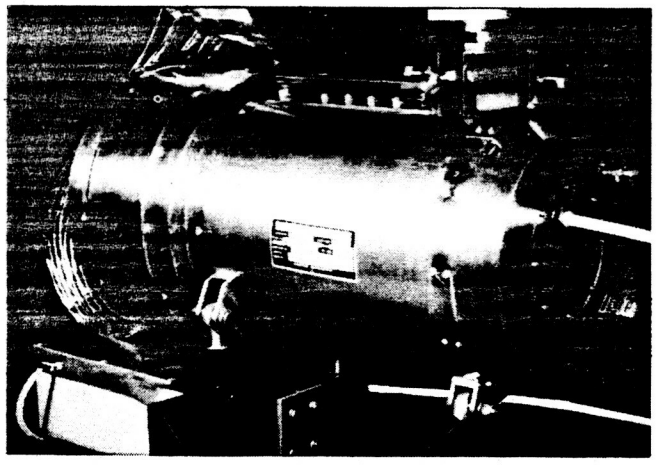

FIGURE 3.2-2. Red Flight Detector: during single-string integration tests at UCSD, 511 of 512 channels are operating.

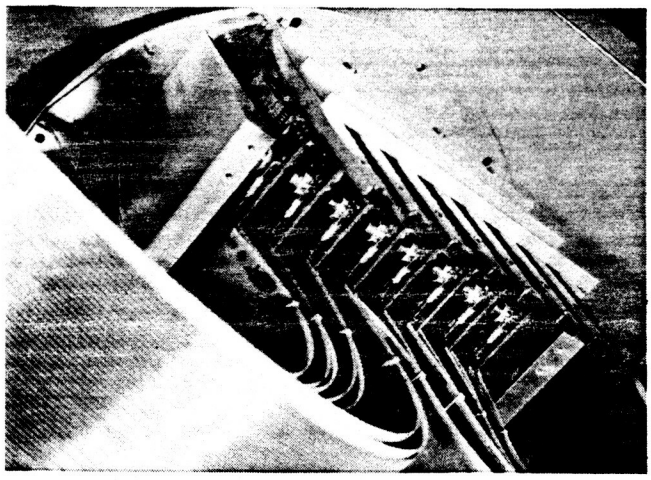

FIGURE 3.2-3. Detector Hybrid Preamplifiers: the 512 preamps fit into back end of detector assembly; set consumes less than 10 watts.

3.3 Control. The FOS receives commands processed through the ST Command and Data Handling (C&DH) computer which controls all ST scientific instrument activity. Internal to the FOS itself are two microprocessor systems, one for each detector system. Each microprocessor (only one can be operating at a given time) controls all the functions needed to operate one side of the FOS such as moving mechanisms, controlling power supplies, scanning the photocathode with the diode array by use of the deflection coils, and accumulating science data. The memory for each microprocessor consists of 24K bytes of read-only memory and 32K bytes of random-access memory. Figure 3.3-1 details the memory usage early in 1982 (still subject to minor evolution). Storage available for science data integration during an observation is adequate for 12K 16-bit data elements, allowing considerable (but finite!) scanning flexibility with the 512-element diode arrays. (The firmware plot packages have been essential for the development and ground-based testing of the FOS.)

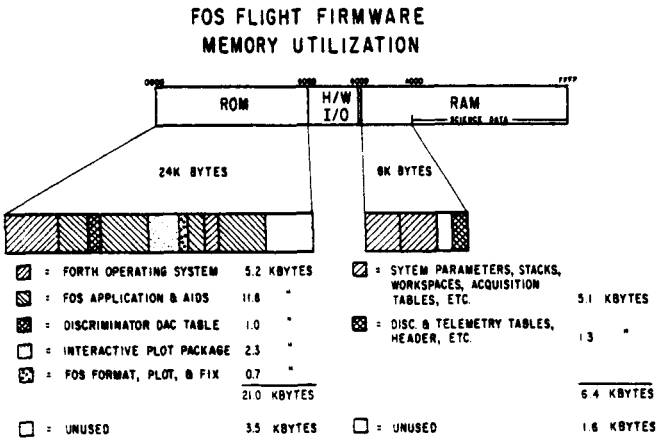

FIGURE 3.3-1. FOS Onboard Control Firmware.

3.4 Operating modes. Because so many FOS parameters are software-selectable under ground-system commands, the possible number of observing configurations truly is astronomical. However, in terms of intended use, the FOS operates in one of six basic modes: 1) target acquisition, 2) spectroscopy, 3) time-resolved, 4) sectropolarimetry, 5) rapid-readout, and 6) time-tagged. Each offers the observer unique advantages (and limitations) for specific purposes.

As might be suspected, acquiring an extremely faint astronomical target in a viewing field of maximum size 4.3 arcseconds square using a one-dimensional detector, can be a nontrivial task. The preferred solution, which should become the usual procedure with increasing ST experience in orbit, will be to know target coordinates and possess ST pointing of sufficient accuracy to allow simply commanding the telescope to the proper position to image the object into the desired FOS entrance aperture. For less benign circumstances, the FOS possesses one position on the filter/grating wheel with a mirror only to provide undispersed images on the detectors as well as onboard software and firmware able to determine small offsets necessary to center a target in a particular FOS aperture, provided that the field is extremely simple. If locating the target requires application of more than the most rudimentary intelligence, the onboard software simply maps the field and depends upon the astronomer (working with the ground data display system) to identify the desired target. The time to acquire a faint target in a complex field can easily be greater than the exposure time to obtain the spectrum; thus, blind offsetting techniques such as are used at ground-based telescopes will be desirable for increased observing efficiency. It is also possible, though not assured, that one of the two ST cameras can be used to assist in target acquisition for the FOS.

The most common use of the FOS will probably be in the spectroscopy mode. Any one of ten possible portions (Table 3.1-1) of the ST image can be usefully observed in any of nine spectral regions (Table 3.1-2). Observations may be virtually as brief as desired (shortest snapshot is less than 50 μsec) or as long as the time-allocation committee will approve. For a typical observation, lasting from a few minutes to a few hours, the data is internally integrated in the FOS in software selectable intervals (now planned to be one minute) between each readout to the ground or ST tape recorders. The frequent readouts result in negligible loss of observing efficiency and protect against catastrophic losses of data.

The time-resolved mode will be used to study objects with known periodicity in about the 50 msec to 100 second range. In this mode, the data is stored in separate memory

locations (slices) corresponding to phase, with four to ten samples per full period being typical. Interruptions of data acquisition to read out each frame of data are set by commands to last an integral number of periods so that each frame of an observation has the same correspondence between phase and slice (so long as the period is correctly known!). Thus, all information should be contained in the last frame. Finally, there exist synchronous and asynchronous submodes; these differ only as to whether or not the initial phase angle is explicity locked to the source at the start of the observation (by commanding the start to occur at a specified Universal Time).

The technique used for spectropolarimetry in the FOS is very similar to that developed for ground-based instruments. A polarizing prism of doubly refractive material is introduced into the spectrophotometer, so as to form twin dispersed images of the slit in opposite senses of polarization at the detector. This analyzer is used at a fixed position, and a waveplate is introduced ahead of it which is turned in 22.5° intervals to analyze for linear and circular polarization. In this way the polarization effects in the dispersing optics following the analyzing prism are of no consequence, and have no effect on the accuracy of the measurement. Two separate waveplates of differing retardation are included in order to allow measurement of linear and circular polarization throughout the ultraviolet region. (It turns out that this allows visible-light operation also.) Any spectral mode may be used with either polarizer waveplate.

There are certain astronomical targets where rapid time variability is suspected, but the precise period of variability is unknown, or aperiodic rapid variabiity is expected. Time-resolved mode is unsuitable for these observations, as the bin folding period must be preset in that mode. Instead, normal FOS data taking is used, but the spectra are read out at very frequent intervals, rather than the approximately 60-sec integration times we anticipate for normal FOS data-taking. The frequency of readout is again set by the observer's requirements, but the shortest possible integration times are limited by various processor overheads. We expect 20 ms is a reasonable estimate of the shortest integrations (the exact minimum overheads are complex because the possibility exists to take "short spectra", ignoring some of the 512 diodes). This rapid-readout capability obviously requires the 1 MHz downlink from ST through TDRSS to the ground (or storage onto magnetic tape within ST).

The time-tagged mode, probably to be the least used FOS mode, will allow study of the most rapid variability possible using the FOS. Periodic or aperiodic variability on timescales in the range of about 10 microsec to 50 msec are well suited to time-tagged study. In time-tagged mode, each of the FOS accumulators counts the 1.024 MHz spacecraft clock rather than sensor counts. When the first photon arrives in a given channel, this counting freezes and further counts are inhibited in that channel. To be of value, time-tagged mode data must normally be read out at high rates, e.g., the 1 MHz telemetry rates, and will produce a very high data rate during its rare usages (estimated 2%-5% of FOS observing time). Note that this produces far more than 2%-5% of FOS data, however; it may (in competition with rapid-readout mode) produce a majority of FOS data to be reduced. The data outputs are each unsigned integers between 0 and 65,535. The selected accumulation time, for reasonable data, must be long enough to allow proper flight software operation, but be less than the clock overflow period, resulting in a range of allowed periods from about 10 msec to 64 msec. The data obtained in this mdoe will be similar in format to that obtained by many X-ray experiments.

3.5 Schedule. The FOS was selected to be a first-generation instrument aboard ST in November 1977, and will be delivered to NASA in April 1983 to support the planned early 1985 launch date for ST. At the time this paper is being written (June 1982), the design of the FOS and the fabrication of all flight hardware components has been completed. Assembly of the instrument is underway (Figures 3.5-1 to 3.5-7), with alignment and acceptance tests soon to follow. Measurements of the flight components have been completed, allowing realistic prediction of the performance to be expected of the FOS in the ST.

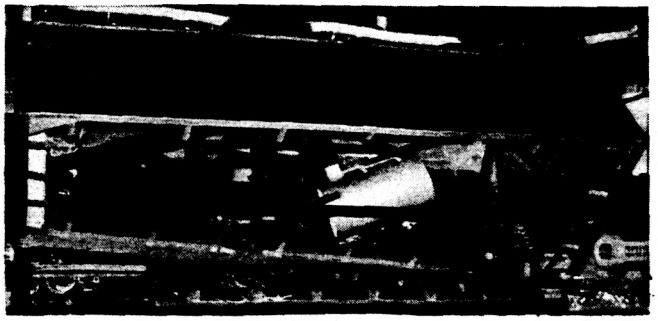

FIGURE 3.5-1. Optics/Detector Compartment during assembly.

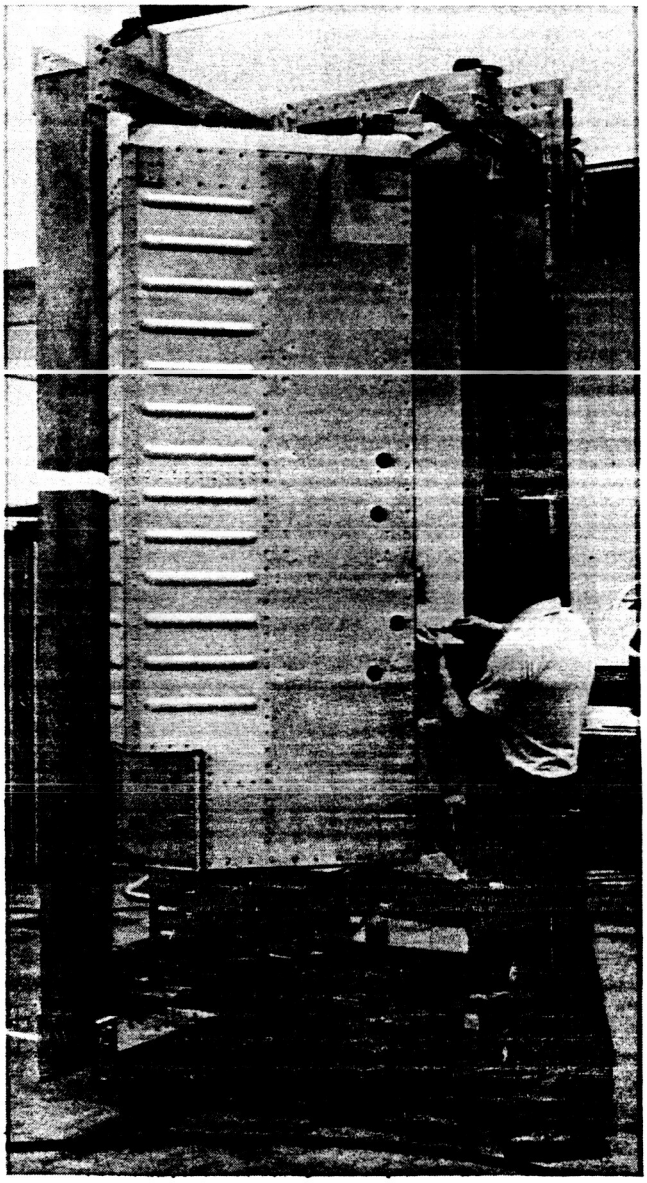

FIGURE 3.5-2. FOS Structure being assembled in its transport frame.

FIGURE 3.5-3. FOS High Voltage Power Supply partially assembled early 1982.

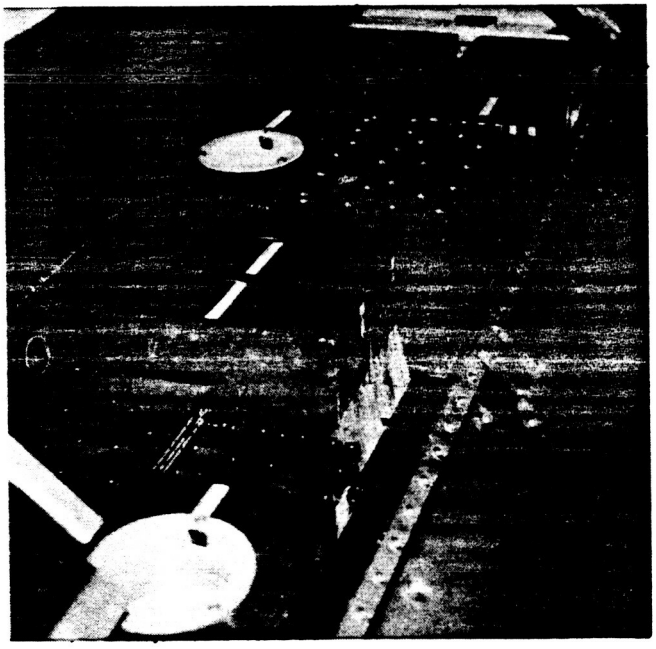

FIGURE 3.5-4. Electronics Bench during assembly.

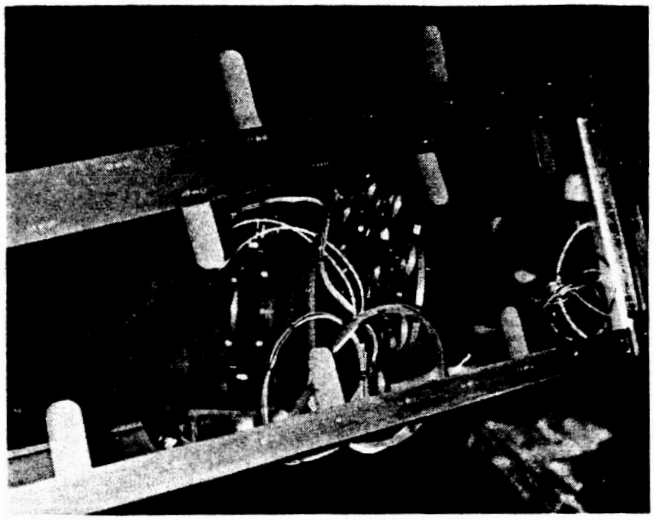

FIGURE 3.5-5. Filter/Grating Wheel being assembled onto optical bench.

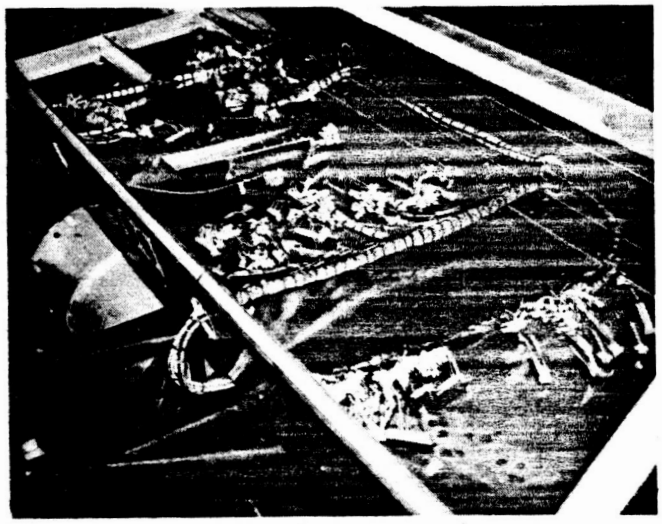

FIGURE 3.5-6. Flight Harness installation, optics bay below, electronics shelf foreground.

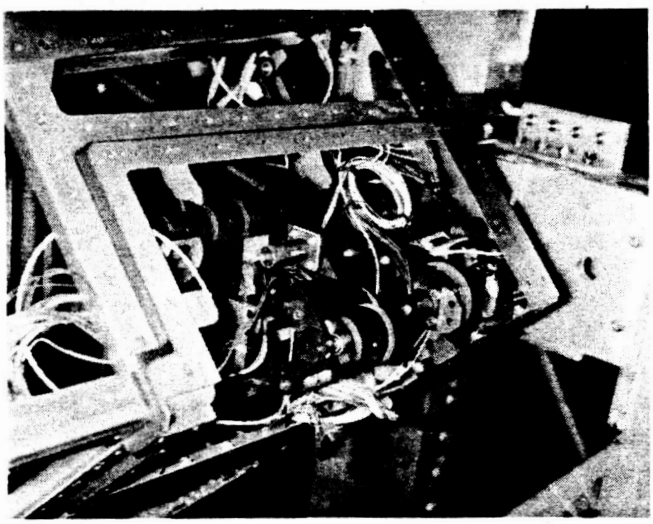

FIGURE 3.5-7. Polarizer and Entrance Port Mechanisms assembled into the FOS.

4.0 Performance

Knowledge of expected performance parameters for the FOS in ST which should prove valuable for planning observing programs are presented in this section. As will be evident, the FOS promises to be a flexible instrument applicable to observations over a wide range of luminosities, including especially faint objects as its name suggests.

4.1 Noise. In order to achieve faint limiting magnitudes, extreme reduction of instrumental background noise sources is essential. The favorable pulse-height-distribution of the Digicons makes false counts due to random analog signals exceeding the discriminator threshold very rare (approximately one such false count per Hubble time constant). The noise sources which can be significant to the FOS are: 1) straylight, 2) fluorescence and phosphorescence due to energetic particle bombardment, 3) thermionic emission, and 4) electromagnetic interference.

The ST itself includes many safeguards against straylight--sun shield, baffles, and high quality optics. The FOS apertures limit incoming light, filters block unwanted short-wavelength photons, while internal baffling must suffice to control other straylight. Unfortunately, no measurements of straylight performance are yet possible, and predictions of straylight performance are not to be trusted (in this author's opinion). Of course, we intend and expect that for most observations straylight will not be a limiting factor. One likely exception can already be identified. Because the FOS is a single-pass spectrometer with broad wavelength sensitivity, ultraviolet spectra of very red objects may suffer strong red straylight contamination. Fortunately, for such observations, the High Resolution Spectrograph can be used.

The sapphire prism and the windowed detectors each contribute unwanted counts due to fluorescence and phosphorescence under energetic-particle bombardment such as will be seen in orbit. Due to this concern, we have measured the light-producing properties of the materials used to manufacture the FOS. Major lot-to-lot variations occur, so the measured samples should come from adjacent parts of the same boule if the actual flight article cannot be tested. In addition to the trapped-particle radiation, decay from materials which become radioactive under such bombardment must also be considered (primarily if it is part of the detector assembly). The sapphire prism light emission is acceptable (both particles and ultraviolet light produce fluorescence) because it is distant enough from the detectors that the direct illumination of the Digicons is small, and it is sufficiently defocused that light transmitted by the optical train is small also. The prism should never produce detectable levels of diffuse straylight background. The detectors are another matter. Fluorescence from the windows would be the major (and unacceptable) source of instrumental background if not suppressed. We use the 512-element diode array as self-anticoincidence detectors, relying on the circumstance that such fluorescence produces a simultaneous (by FOS timescales) burst of photoelectrons. Such bursts can be eliminated by enabling a software-selectable threshold which rejects any frame of data in which the sum of counts over a selected set (generally, all operational) of channels exceeds the software limit. With this burst noise rejection scheme operating, we expect fluorescence to contribute less than 0.001 count/diode/sec outside the South Atlantic Anomaly (SAA). Inside the SAA, such noise may be much greater, and it may not be possible to observe at all (the software may eliminate all data if noise bursts occur too frequently).

The dominant instrumental noise is expected to be the thermionic photocathode emission from each Digicon. During ST operation, the photocathode temperatures are calculated to lie between -10C and -28C. At the warm end of this range, the red Digicon noise has been measured to lie between 0.001 and 0.002 counts/diode/sec. At -10C, the blue detector background is about 0.0005 counts/diode/sec.

Electromagnetic disturbances, if severe enough, can cause the FOS electronics to produce spurious counts. All the ST instruments including the FOS incorporate normal good engineering practice -- single-point grounds to eliminate ground loops, shielding from conducted and radiated electrical fields, etc. -- and, of course, each instrument's production of electromagnetic interference is controlled. Additional protection for the FOS is provided by the burst-noise rejection scheme discussed above. Still, such sources of noise can only be eliminated with certainty at the ST integration level by thorough testing.

Thus, all instrumental background noise sources are expected to be less than our goal of 0.002 counts/diode/sec (outside the SAA).

4.2 Dynamic range. The minimum detectable source levels are set by instrumental background, while the maximum accurately measurable source levels are determined by the response times of the FOS electronics. Figure 4.2-1 compares the detected (apparent) rate to the true input rate for a typical channel of the FOS. The true rate can be derived

from the apparent rate up to at least a true rate of 5×10^4 counts/channel/sec (and, perhaps, to 10^5 counts/diode/sec). This enormous dynamic range, at least 2.5×10^7, means that sources over a range of 18 magnitudes in apparent luminosity can be observed with the FOS. (However, the accessible magnitude ranges are reduced by non-flatness of the spectrum, of course.)

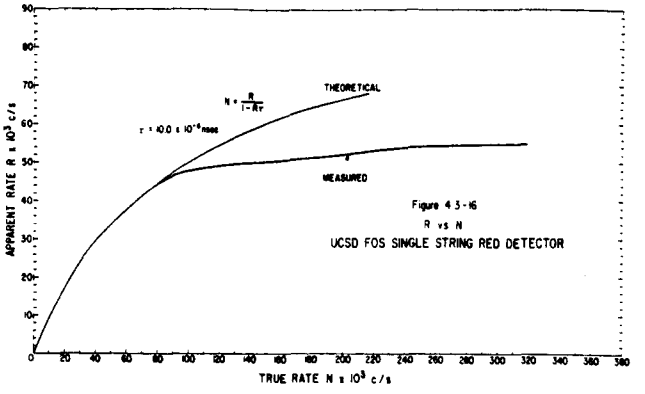

FIGURE 4.2-1. Measured versus true rates.

4.3 Instrument profile. The ability to resolve closely spaced spectral features is related to the instrument response-profile (to monochromatic input) at small separations (the peak), while the ability to detect weak spectral features is limited by the long distance response profile (the wings). The peak of the response profile is dominated by the nearly-50μ width of the Digicon diodes along the dispersion direction. The wings of the profile result primarily from scattered light due to the dispersers. A typical response profile, measured with a 50μ exit slit for one of the flight gratings, is presented in Figure 4.3-1. The results fully meet out desires, with far-field scattered light below 10^{-4} times the peak amplitude. One still remaining uncertainty is that we have not yet been able to measure the profiles of the most ultraviolet gratings, whose scattering properties may be worse.

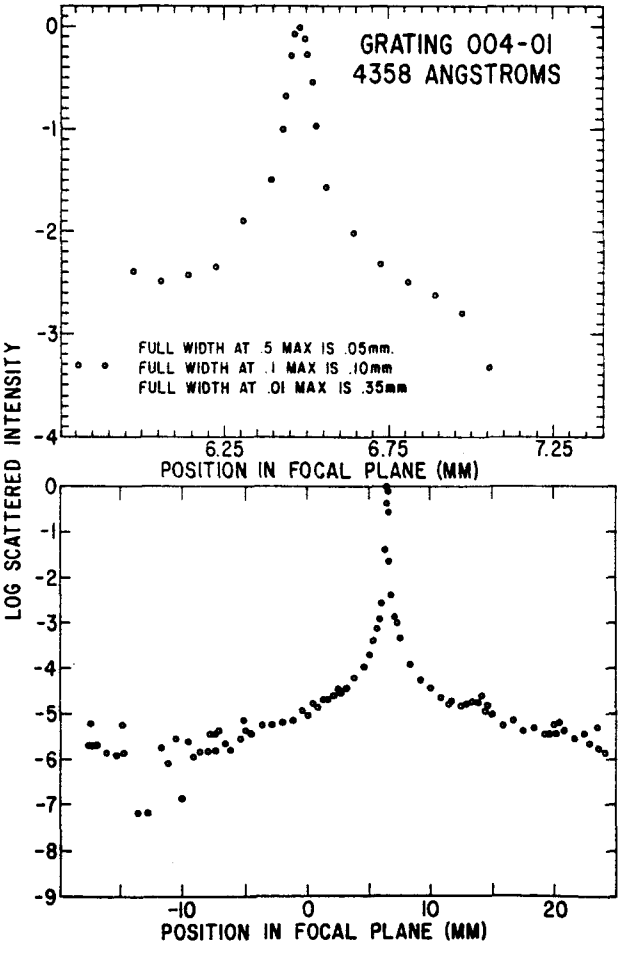

FIGURE 4.3-1. Upper figure displays peak scattered light profile of FOS flight grating; lower figure shows wings of profile. Measurement used 50 micron exit slit to match Digicon diode size.

4.4 Efficiencies. The total sensitivity of the spectrograph is strongly dependent upon the performance of the three least-efficient components in the optical train: 1) the dispersers, 2) the detectors, and 3) the polarizer.

Figures 4.4-1 and 4.4-2 display the fraction of incoming unpolarized light which is directed to the first-order focused spectrum by the moderate-and low-resolution dispersers. The high efficiency of the prism was expected. However, Hyperfine Inc. exceeded even our optimistic expectations in ruling the FOS flight gratings. With peak efficiencies over 50% in the ultraviolet and reaching 75% in the red, these concave gratings are the best produced of which we are aware. Figure 4.4-3 simply illustrates that the grating efficiency is not a strong function of the polarization of the incoming light.

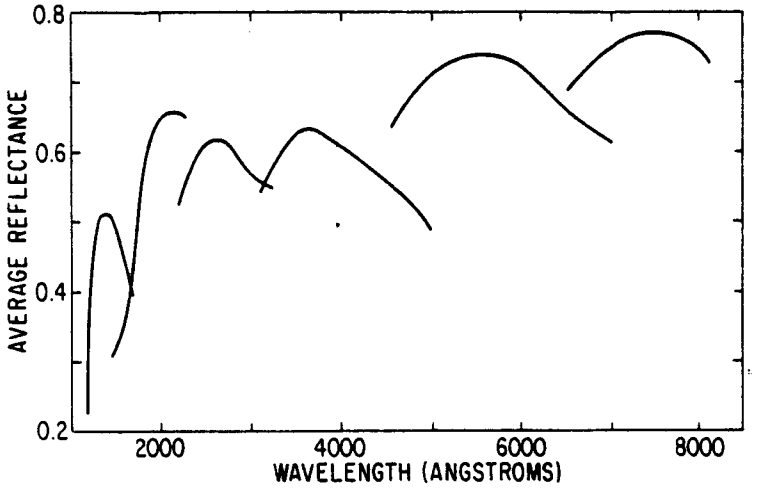

FIGURE 4.4-1. First-order efficiencies of FOS flight moderate-resolution gratings.

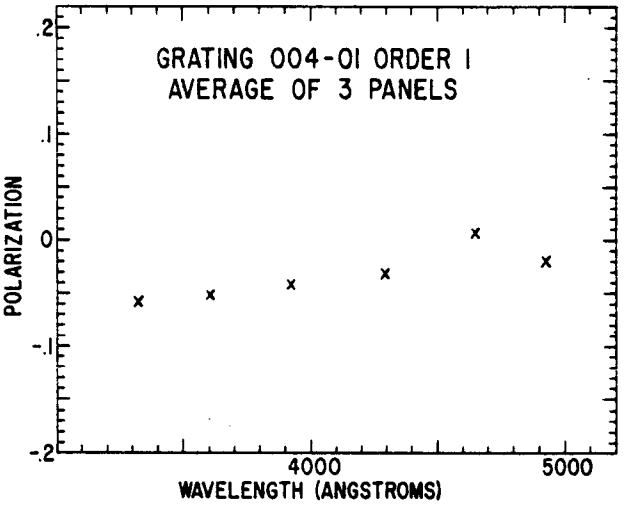

FIGURE 4.4-3. Polarization produced by flight FOS grating.

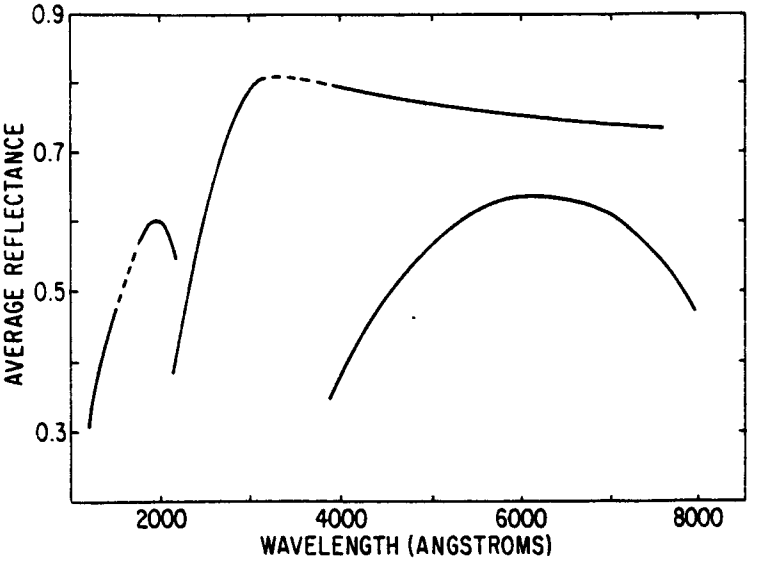

FIGURE 4.4-2. Efficiencies of FOS flight low-resolution dispersers: UV grating, prism, red grating.

The response of the detectors has also been highly gratifying to us. The Digicons, produced by Electronic Vision Systems Division of Science Applications Incorporated, not only meet the stringent background noise requirements discussed in Section 4.1, but provide high quantum efficiency coverage from the magnesium-fluoride cutoff in the ultraviolet to the red photocathode dropoff in the near-infrared. Figure 4.4-4 shows the quantum efficiencies of the two flight detectors. Peak efficiency of the blue Digicon is just under 20%, of the red Digicon about 25%.

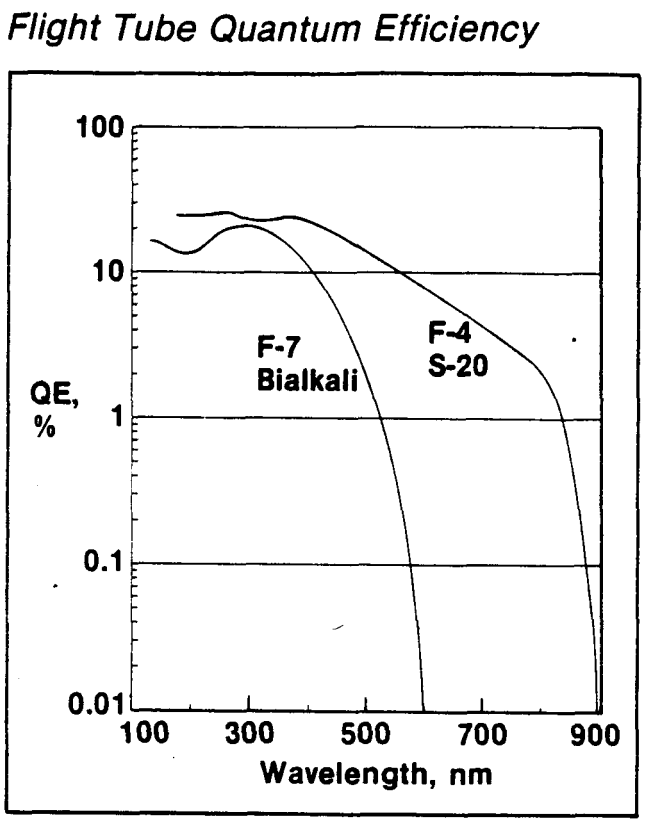

FIGURE 4.4-4. Quantum efficiencies of the two FOS flight detectors. Both produce under 0.002 counts/diode/sec noise at -10C.

The sensitivity of the polarizer depends both upon its throughput efficiency and its modulation efficiency (refer to Angel and Allen, 1982 for a detailed discussion of the FOS polarizer). The transmission efficiency of the complete polarizer rises from about 20% at Lyman α to around 60% at 160 nm, and thence rises more slowly to just over 80% at 240 nm. Because, at any given time, the detector can observe only one of the two spectra produced by the polarizer, another factor of two loss in practical throughput occurs. Finally, Table 4.4-1 lists the modulation efficiencies for each of the two waveplates. Note that the polarizer is sensitive to both linear and circular polarization over nearly the entire wavelength range of the FOS.

TABLE 4.4-1
Retardations of the Flight Waveplates

λ(Å)	Waveplate A δ	Waveplate A Efficiency linear	Waveplate A Efficiency circular	Waveplate B δ	Waveplate B Efficiency linear	Waveplate B Efficiency circular
1175	-108°	.65	.95	-93°	.53	1.00
1200	100°	.59	.98	0°	0	0
1216	215°	.91	.57	90°	.50	1.00
1250	360°	0	0	161°	.97	.33
1300	460°	.59	.98	228°	.83	.74
1350	482°	.76	.85	247°	.70	.92
1400	485°	.79	.82	250°	.67	.94
1450	480°	.75	.87	241°	.74	.87
1500	468°	.65	.95	238°	.76	.85
1600	439°	.85	.98	226°	.85	.72
2537	251°	.66	.94	123°	.77	.86
3650	163°	.98	.29	84°	.45	.99
6328	95°	.54	.99	43°	.13	.68

4.5 System performance. We can combine the measured performance parameters just discussed with the anticipated properties of the ST to calculate the expected on-orbit capability of the ST plus FOS. To indicate the system response, we consider observations using the quarter-arcsecond aperture. Figure 4.5-1 then illustrates the system sensitivity function versus wavelength for spectroscopic and spectropolarimetric observations. For moderate- and low-resolution spectroscopy, Figures 4.5-2 and 4.5-3 convert this into a conservative measure of limiting V magnitudes for a variety of astronomically relevant flux distributions. It is encouraging that acceptable quality (signal/noise = 5) spectra can be obtained in only one hour of integration down to about 22nd magnitude at resolution R = 1200, down to about 24th magnitude at R = 200, and (with the prism) down to nearly 26th magnitude (low and nonuniform resolution). Nor are these truly limiting; heroic observations can go 1.75 magnitudes fainter before instrumental noise dominates the signal. A significant exception to this is in the low-resolution mode. For the cases depicted in Figure 4.5-3, sky background is already significant using the prism at 400 to 500 nm. Of course, use of the 0.1 arcsecond aperture when possible will reduce sky levels another two magnitudes. (Sky brightness is not a problem in the moderate-dispersion mode.)

The polarizer goes less deep, of course. Table 4.5-1 tabulates the achievable accuracies in 10 nm bandpasses for a 15th magnitude A0 star for ultraviolet polarimetry in a 20 minute exposure.

TABLE 4.5-1
Polarization Accuracy for A0 Star, V=15, Exposure Time = 20 Minutes

(Å)	% Accuracy For Linear*	% Accuracy For Circular**
1216	6.4	5.8
1500	1.9	1.5
2000	0.89	0.74
2500	0.66	0.54
3000	0.63	0.58

* Standard deviation in Stokes parameter ratios Q/I and U/I
** Standard deviation in Stokes parameter V

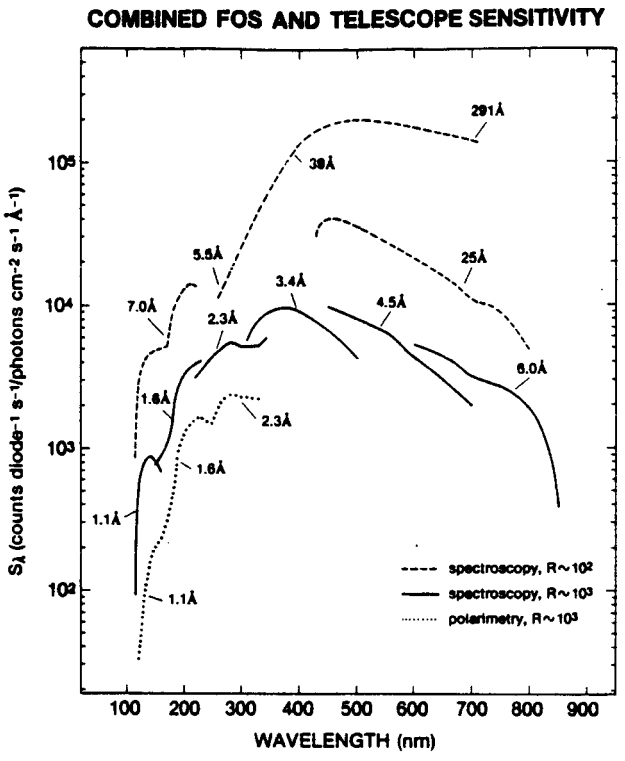

FIGURE 4.5-1. FOS + ST Sensitivity using the quarter arcsecond diameter entrance aperture.

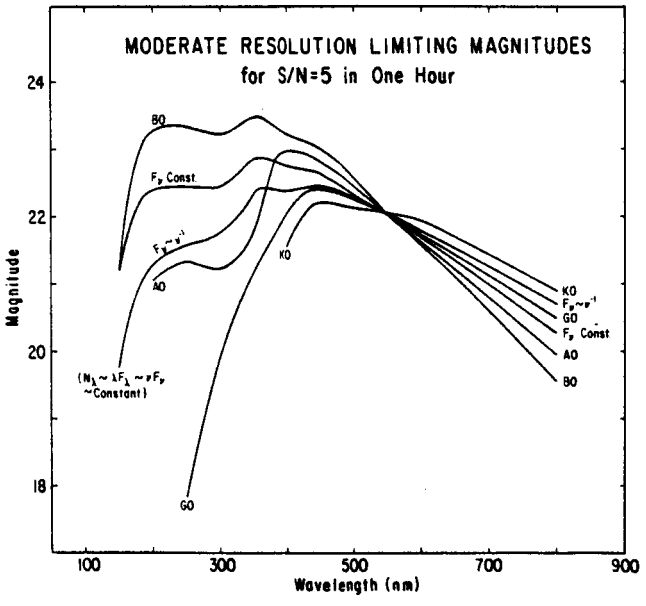

FIGURE 4.5-2. Limiting V Magnitudes for several flux distributions which produce 0.01 counts/sec/diode for moderate-resolution FOS spectroscopy (R=1200). With quarter-arcsecond aperture, night sky is negligible.

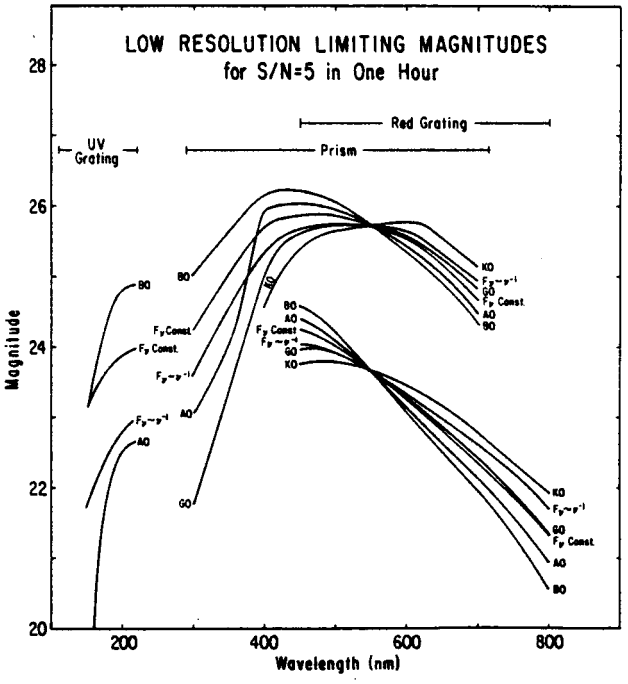

FIGURE 4.5-3. Limiting V magnitudes for low resolution FOS spectroscopy (R=200 for gratings, R strongly varying for prism). With quarter-arcsecond aperture, sky is significant only with the prism between 400 and 500 nm (e.g. for observing 25-26 magnitude objects).

5.0 References

Explicitly cited references are listed below:

1. Aanestad, P. A., Percell, E. N., 1973, Annual Rev. of Astro. and Astrophys., Vol. 11, p. 309.
2. Allen, R. G. and Angel, J. R. P., 1982, Proc. Society of Photo-Optical Instrumentation Engineers, Vol. 331, in press.
3. Angel, J. R. P., 1978, Ann. Rev. of Astro. and Astrophys., Vol. 16, p. 487.
4. Bahcall, J. N., 1980, in Scientific Research with the Space Telescope, IAU Coll. No. 54, NASA CP-2111, p. 215.
5. Gilra, D. P., 1972, The Scien. Results from the Orbit Astro. Obs., A. D. Code, Ed., p. 295 (NASA ST-310).
6. Harms, R. J. et al., 1979, Proc. Society of Photo-Optical Instrumentation Engineers, Vol. 183, p. 74.
7. Moore, C. E., 1950, An Ultraviolet Multiplet Table, Circ. of the NBS 488, Section 1.
8. Osterbrock, D. E., 1963, Planet. Space Sci., Vol. 11, p. 621.
9. Wagoner, R. V., 1980, in Physical Cosmology, Les Houches, Session XXXII, 1979, p. 179.
10. Weast, C. R. ed., 1968, CRC Handbook of Chemistry and Physics, 49th Edition, p. E-71.

Other general references describing features of the FOS include:

1. Bahcall, J. N. and O'Dell, C. R., 1980, in Scientific Research with the Space Telescope, IAU Coll. No. 54, NASA CP-2111, p. 5.
2. Ginaven, R. O. et al., 1981, Proc. Society of Photo-Optical Instrumentation Engineers, Vol. 290, p. 81.
3. Harms, R. J. et al., 1982, Proc. Society of Photo-Optical Instrumentation Engineers, Vol. 331, in press.
4. Leckrone, D. S., 1980, Publ. Astronomical Society of the Pacific, Vol. 92, p. 5.

N82 33303

The High Resolution Spectrograph for the Space Telescope

John C. Brandt

Laboratory for Astronomy and Solar Physics
NASA-Goddard Space Flight Center
Greenbelt, Maryland 20771

and the

HRS Investigation Definition* and Experiment Development** Teams

Abstract

The High Resolution Spectrograph (HRS) in conjunction with the Space Telescope (ST), will extend ultraviolet astronomical spectroscopy to higher spectral, spatial, and time resolutions than previously achieved, as well as to fainter and more distant celestial objects. Other significant advances inherent in the instrument are high photometric accuracy and efficient operation via exposure meter control and real-time rejection of bad data. These capabilities are provided to accomplish the scientific programs of the HRS Investigation Definition Team, which concern the interstellar medium, stellar winds and evolutionary aspects of stellar atmosphere studies, the determination of chemical abundances relevant to stellar evolution, the investigation of quasars and Seyfert galaxy nuclei, and the analysis of the atmospheres of solar system objects, including comets. The HRS will doubtless contribute to many other types of scientific programs as well.

I. Introduction: instrument capabilities

The HRS for the ST has been designed to facilitate certain investigations in ultraviolet astronomy that require instrumental capabilities beyond those available in previous spacecraft such as the International Ultraviolet Explorer (IUE) and Copernicus (OAO-3). The scientific objectives are discussed in Section II.

Spectral resolution

The HRS has three spectral resolution modes, characterized by $R = \lambda/\delta\lambda = 100{,}000$, 20,000, and 2,000. They are referred to here as the "high," "medium," and low" resolution modes, respectively. The HRS high resolution mode provides spectral resolution comparable to that of the coudé spectrographs on large ground-based telescopes and exceeds the resolution of previous ultraviolet observatory instruments. An illustration of the science requirement for the high spectral resolution mode is given in Appendix A. The medium resolution mode provides the same spectral resolution as the OAO-3 U1 channel and slightly exceeds the resolution of the IUE high dispersion spectrographs. The HRS low resolution mode, within its limited wavelength range, provides about ten times higher resolution than the low dispersion IUE spectrographs.

Spectral range

The ST itself is not provided with LiF-coated optics and thus the HRS has not been designed to observe as far into the ultraviolet as OAO-3. However, observations down to 1100 A and perhaps somewhat shorter wavelengths are feasible, so that (for example) it will be possible to observe the 1108 A 0-0 Lyman band transition of molecular hydrogen. The nominal spectral range of the HRS extends up to about 3200 A in the high and medium resolution modes; the low resolution mode is operative up to about 1700 A.

---

*J.C. Brandt, A. Boggess, S.R. Heap, S.P. Maran, A.M. Smith (NASA-Goddard Space Flight Center); E.A. Beaver (University of California, San Diego); J.B. Hutchings (Dominion Astrophysical Observatory); M.A. Jura (University of California, Los Angeles); J.L. Linsky (Joint Institute for Laboratory Astrophysics); B.D. Savage (University of Wisconsin); L.M. Trafton (University of Texas at Austin); R.J. Weymann (University of Arizona).

**R. Melcher, F. Rebar, H.D. Vitagliano, J. Shannon, V. Krueger, J. Yagelowich, E. Devine, K. Flemming, W. Fowler, J.K. Kalinowski (NASA-Goddard Space Flight Center); G. Yurka, W. Meyer, J. Chodil, I. Becker, M. Bottema, H. Eck, T. Kelly, S. Koby, H. Garner, J. Kinsey, V. West (Ball Aerospace Systems Division); D. Ebbetts (University of Wisconsin); D.J. Lindler (Andrulis Research Corporation); R.E. Stencel (NASA Headquarters); F.M. Walter (Joint Institute for Laboratory Astrophysics).

Spatial resolution

The HRS is equipped with two entrance apertures that determine its capability to isolate a target star or a portion of an extended source. They are respectively 2 arc sec and 0.25 arc sec square. The larger slit will be used normally in target acquisition, however either slit may be used for target acquisition or for spectroscopy. (In order to obtain the full capability of the high resolution mode, the small slit will be used to reject light in the wings of the ST point spread function.) For comparision, the IUE large and small entrance apertures are approximately 10 x 20 arc sec (oval) and 3 arc sec (circular), respectively.

Time resolution

The HRS produces spectroscopic data in two ways: (1) by onboard coaddition of spectra over observer-selectable intervals (exposure times), which may be specified as integer multiples of 200 ms (accumulation mode); (2) by generating individual spectra at rapid intervals, which are integer multiples of 50 ms (direct mode). The time resolution in the accumulation mode is the exposure time, which may be as short as 200 ms. The time resolution in direct mode is the interval length, which may be as short as 50 ms. The duration of an observation in direct mode, due to the high data rate, is limited by available capacity of the ST tape recorder, or by the duration of a real-time link to the ground.

Photometric accuracy

The HRS, provided with pulse-counting detectors, is intended to achieve a relative photometric accuracy of 1% in order to enable the detection of weak spectral lines. The dynamic range will be at least 10^7. Separate preamplifiers and postamplifiers are provided for each diode in the 512-channel Digicon detectors, and the threshholds of each preamplifier are separately commandable. In the accumulation mode, HRS flight software cyclically substeps the electron image on the diode array (according to an observer-chosen pattern) during a spectral exposure in order to compensate for the gaps between diodes, to obtain the full spectral resolution of the spectrograph, to smooth out the pixel-to-pixel response, and to acquire needed background (scattered light) data. At intervals during this process, the electron image is shifted along the array by an integer number of diodes; thus photons at a given wavelength are counted with more than one diode alternately during the exposure. This insures that gaps do not occur in the measured spectrum due to the unavoidable presence of a few bad diodes. A comb-addition program accumulates the data in the proper wavelength bins. Periodic calibration of the HRS on standard stars is required to support spectrophotometric observations.

Sensitivity

The high sensitivity of the HRS results from the substantial ST collecting area, the optical design of the spectrograph, and the properties of the pulse-counting detectors. The response of the HRS is summarized in Figure 1. To translate the ST-HRS system performance into astronomers' terms, see Appendix B, where the nominal operating range of the HRS is depicted for several types of stars. To minimize the effects of scattered light, notably from photospheric radiation in cool stars or stellar systems with bright, cool components, the two HRS detectors are solar blind. This is especially true of the CsI-photocathode Digicon, which is provided with a LiF window; this detector, with good sensitivity below about 1800 A, is insensitive even to the longer wavelength ultraviolet radiation.

II. Scientific goals

The scientific goals of the HRS investigation are summarized by five general topics:

- the interstellar medium;
- mass loss by stellar winds and the evolution of the outer atmospheres of stars;
- abundances of the elements and stellar evolution;
- extragalactic sources, including quasars and the nuclei of Seyfert galaxies;
- the solar system - the atmospheres of planets, satellites and comets.

For each general topic area there are several specifically identified goals; each goal can be accomplished by a set of appropriately planned observations, supported in some cases by other ST instruments. Here we discuss four hypothetical observations (not necessarily actual observations to be made by the HRS Investigation Definition Team) that address a few of these goals and which illustrate how the unique capabilities of the HRS are used in such studies.

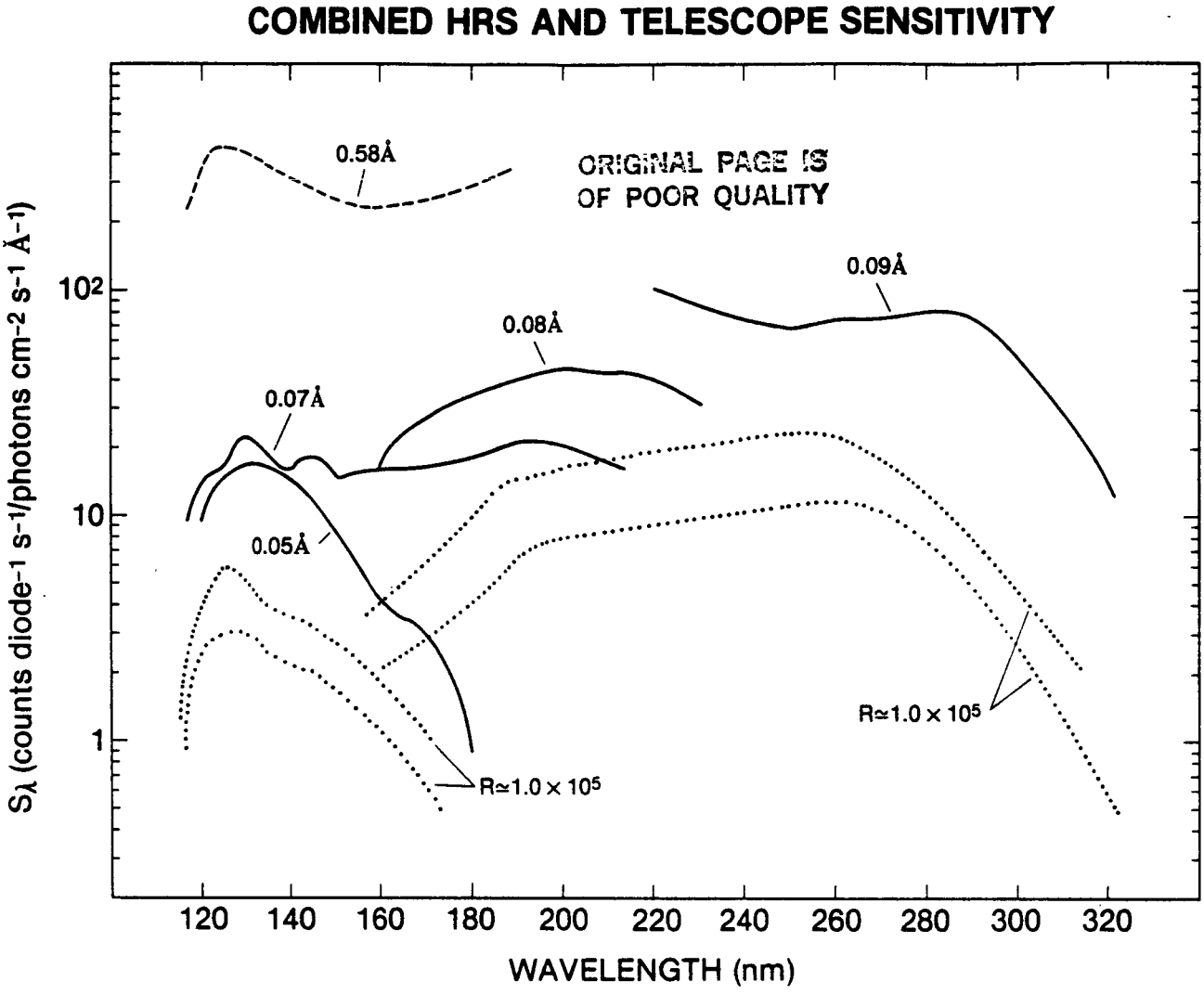

Figure 1 Combined sensitivity curves for the HRS and ST. Spectroscopic modes for R = 2 x 10^3, 2 x 10^4, and 1 x 10^5 are denoted by dashed, solid, and dotted lines, respectively. For R = 1 x 10^5, the two pairs of curves are envelopes connecting the sensitivity maxima and maxima within the echelle orders. Resolving power is approximately constant with wavelength in the echelle mode. Approximate widths of resolution elements are labeled on the curves for the first order modes. The 0.25 arc sec aperture is assumed. The ordinate gives counts per second per diode for an incident flux in photons per cm^2 per second per angstrom (D.S. Leckrone).

2A0311-22 (Observation plan by J.B. Hutchings)

These observations pertain to the topic area of stellar winds and outer atmospheres. The target is an accreting magnetic white dwarf in a binary system (orbital period = 81 min). The goal is to understand the physics of mass flow in this system. The visual magnitude of the target is about 14 and is variable. Emission lines arise from the accretion disk or accretion columns and they show regular variations with a "period" of about 20 min. Brightness variations on a time scale of about 6 min also occur.

A study of the spectral variations requires the relatively high spectral resolution of the HRS "medium" resolution mode, R = 20,000, as well as a time resolution of 1 min, rather high for spectroscopy of such a faint star. The two spectral features to be measured are the C IV and Si IV doublets at 1550 A and 1397 A, respectively, which arise

in the accreting plasma. At this spectral resolution, these features cannot be observed with a single grating setting (HRS carrousel position). If there were no interfering factors due to ST orbital and other operating parameters, each doublet would be observed separately for a suitable interval of about 100 min, i.e., one binary period plus 20% overlap. (If the observations of both features are accomplished within a week of each other the respective orbital phases can be precisely related.) However, if continuous viewing of 100 min is not achievable, the observations of a single feature would be scheduled, e.g., for three 33-min or greater intervals, chosen so as to obtain full orbital phase coverage. Data would be acquired in accumulation mode, with coaddition of spectra in the flight computer every 200 msec. Wavelength calibration, based on a Pt-Ne hollow cathode lamp internal to the HRS, would be accomplished prior to and following each such 33-min interval. The CsTe Digicon and the 2 arc sec entrance slit will be used.

Selected interstellar clouds (Observation plan by M.A. Jura)

These observations pertain to the topic area of the interstellar medium. The targets are stars located beyond clouds that have little molecular hydrogen and the goal is to determine the efficiency of molecule formation on grains as opposed to formation in the gas phase, by means of a search for hydroxyl and water molecules in such clouds. The search for two weak lines (1222.07 A and 1239.73 A) of these molecules requires the HRS high spectral resolution mode, the 0.25 arc sec entrance slit, and high photometric accuracy. In view of this last requirement, the HRS exposure meter program will be commanded to acquire an average of 100,000 counts/diode on specific (observer-chosen) diodes in the CsI Digicon, which will be used for these observations.

Observations in the HRS accumulation mode would be made at each of the two above wavelengths in each of five target stars, as listed below. A wavelength calibration on the Pt-Ne lamp would be secured before and after each observation. As can be seen, the estimated exposure times are rather short:

o	delta Ori V = 2.23	exposure times- O9.5II	25 sec per line
o	epsilon Ori V = 1.70	exposure times- B0Ia	26 sec per line
o	kappa Ori V = 2.09	exposure times- B0.5Ia	30 sec per line
o	30 CMa V = 4.40	exposure times- O9Ib	228 sec per line
o	tau Sco V = 2.84	exposure times- B0V	32 sec per line

Velocity dispersion in the central region of the Andromeda Galaxy (Observation plan by R. Weymann)

These observations pertain to the topic area of extragalactic sources. The target is M31 and the goal is to determine the spatial dependence of the velocity dispersion in the central region of this galaxy. This goal requires high sensitivity, since the target is faint in the ultraviolet, but relatively high spectral resolution (the HRS "medium" resolution mode is appropriate) is needed. Accordingly, the exposure times are long. Because of the high accuracy required in placing the HRS entrance slit for these observations, the ST Wide Field and Planetary Camera (WF/PC) might be used to support the initial target acquisition of the M31 nucleus. High spatial resolution and hence the HRS 0.25 arc sec entrance slit are required. The observations will be made at a single grating setting, a wavelength corresponding to a suitable absorption line near 2800 A, and therefore the CsTe Digicon is specified. Observations at five positions in M31 are specified:

	Location	Exposure Time
A.	On the nucleus	1500 sec
B.	Displaced 0.3 arc sec along M31 major axis	4500 sec
C.	Displaced 0.3 arc sec from nucleus, orthogonally to the major axis	4500 sec
D.	Displaced 0.6 arc sec along major axis, in the same sense as observation B	15000 sec
E.	Displaced 0.6 arc sec from nucleus, in the same sense as observation C	15000 sec

Comet Halley (Observation plan by J.C. Brandt)

These observations pertain to the topic area of the solar system. The target is Comet Halley and the goal is to determine the abundance ratio D/H in this comet. The desired quantity could indicate the relative abundance of deuterium in the solar nebula and might have cosmological implications as well. Accomplishing this goal requires at least moderately high spectral resolution and excellent target-tracking; in the most difficult case, on 10 April 1986 when the comet is only 0.4 AU from the earth, the proper motion of the target will be 343 arc sec during 30 min. The uncertainty in this quantity should not exceed 0.05 arc sec during 30 min. The WF/PC would be used to assist in initial target acquisition and at intervals to confirm or adjust the tracking. The uncertainty in position of the cometary nucleus may be 10 arc sec.

The Lyman-alpha line of deuterium, at 1215.340 A, is about 1/3 A short of the hydrogen Lyman-alpha wavelength; this corresponds to about 5 resolution elements in the HRS medium resolution mode. When the HRS was originally proposed, this was close to a limiting observation: assuming a central hydrogen Lyman-alpha brightness of 40 kilorayleighs (as in Comet Bennett 1969i) and a D/H ratio of about 10^{-4}, with the originally proposed large entrance slit size of 1 arc sec square, we estimated that there will be about 0.013 counts/s/diode if the deuterium line falls on one diode. Comparable count rates were anticipated in the wing of the hydrogen line, from scattered light, and from dark noise. Thus, an exposure time of 10 hrs to achieve a signal-to-noise ratio of 10 in deuterium Lyman-alpha was estimated. Fortunately, this estimate has now been lowered to about 1 hr thanks to the increase in the design size of the large slit, to 2 arc sec, a lower dark count achieved in the flight detectors than had been specified, and a larger currently predicted hydrogen Lyman-alpha flux. In fact, it may be practical to attempt the observation in the high resolution mode, so as to achieve higher sensitivity to the detection of a weak deuterium line.

Zeta Aurigae (Observation plan by R. Weymann)

These observations pertain to the topic area of stellar winds and the outer atmospheres of stars. They illustrate how a subject investigated significantly by IUE gains new dimensions when the target can be examined with the high spectral resolution mode of the HRS. The target is the atmospheric eclipsing binary zeta Aurigae and the goal is to investigate the role of momentum transport by Alfvén waves or other relevant modes in red giant mass loss. To attain this goal, it is necessary to obtain detailed data on the variation of velocity and number density with distance from the star, to supplement the studies of time variations in the intensities of chromospheric lines obtained by IUE. The data can be acquired by high-resolution spectroscopy at various orbital phases over the 972-day orbital period. The presence of the early-type companion star will enable us to observe lines well into the ultraviolet, as seen in the IUE echelle-mode observations reproduced in Figures 2, 3, and 4. In particular, the ultraviolet spectrum allows us to observe abundant ions, so that material leaving the red giant can be studied at all orbital phases.

The observations will be made in the high spectral resolution mode and with the 0.25 arc sec entrance slit. The optimum grating positions can be determined from the available IUE observations; the wavelengths listed below are only illustrative. The data will be taken in accumulation mode; here, the exposure meter control has particular value, since the spectral intensity distribution changes noticeably (see the Figures) with time. One suite of observations corresponding to the following table would be made once every 48 days over a full orbital period. In addition, during the two intervals of deepest chromospheric eclipse, each lasting about 20 days, a suite of observations would be made once every second day.

Illustrative Wavelength	Detector	Exposure
2600 A	CsTe Digicon	10 sec
2604	" "	10
2607	" "	10
2612	" "	10
2000	" "	15
2009	" "	15
2012	" "	15
2022	" "	15
1600	CsI Digicon	50
1603	" "	50
1606	" "	50
1614	" "	50
1400	" "	120

Illustrative Wavelength	Detector	Exposure
1411 A	CsI Digicon	120 sec
1415	" "	120
1420	" "	120
1200	" "	180
1211	" "	180
1216	" "	180
1219	" "	180

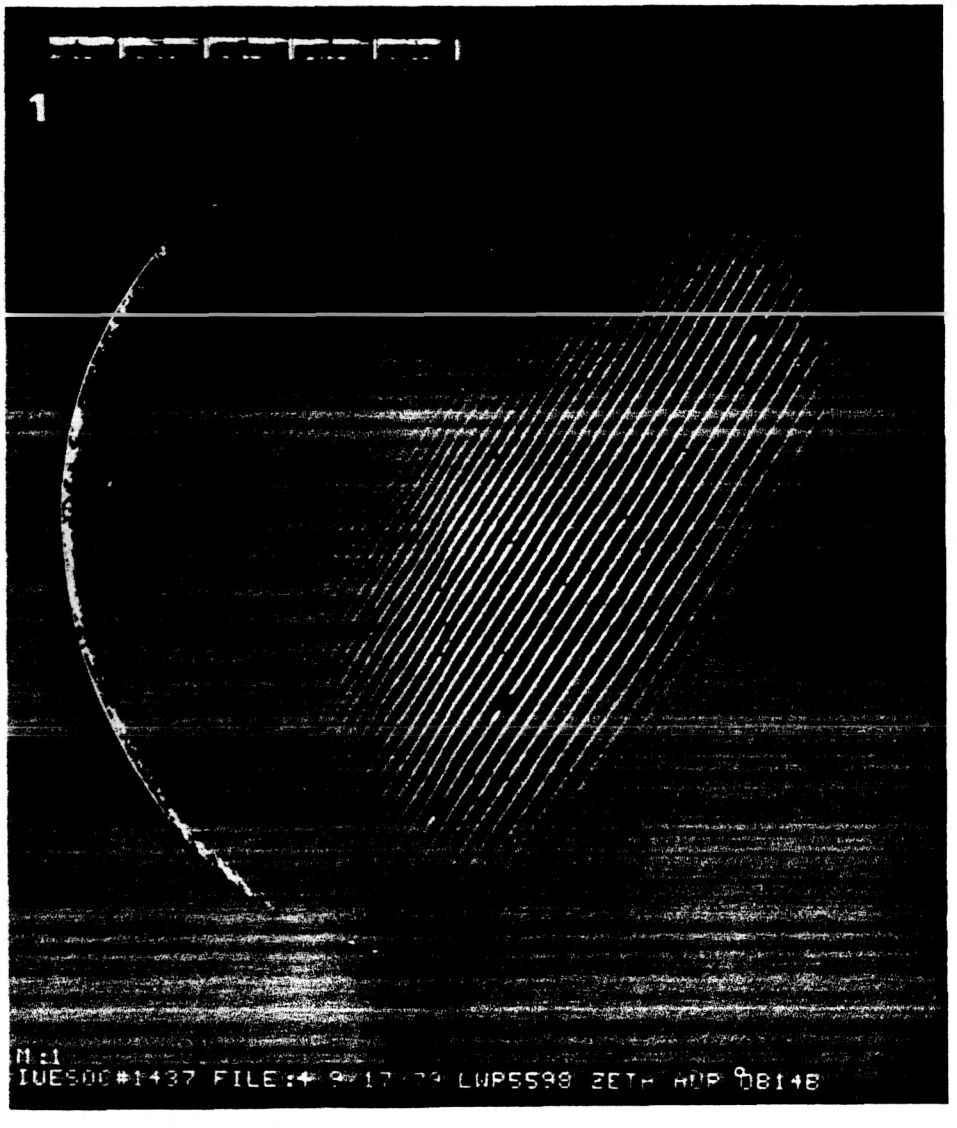

Figure 2 IUE echelle-mode observation of zeta Aurigae on September 16, 1979. The hot star continuum dominates the spectrum and the h and k lines of Mg II with their P-Cygni profiles are conspicuous. Eclipse has not yet begun. (R.D. Chapman)

Note that a suite of observations involves one Digicon change, four major carrousel rotations (counting the motion after target acquisition, to position the echelle for the first spectral measurement) and twelve minor carrousel rotations (to select individual positions of a grating already selected by a major carrousel motion).

It is worth noting that about five atmospheric eclipse binary systems are observable with IUE, but about 100 (according to an estimate by R.D. Chapman) can be examined

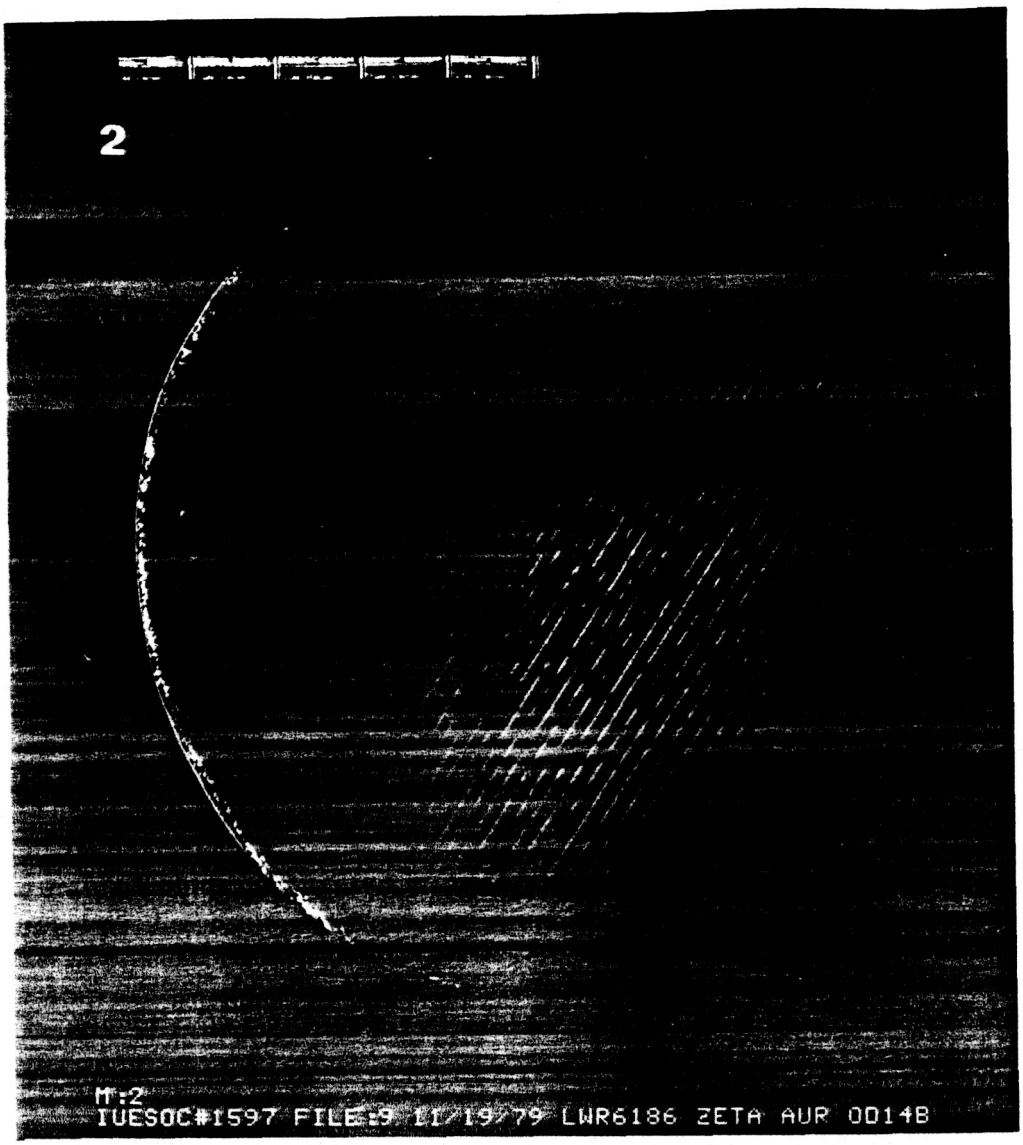

Figure 3 IUE echelle-mode observation of zeta Aurigae on November 19, 1979. The spectrum is now dominated by many absorption lines indicating that eclipse of the hot star by the cool red supergiant has begun. (R.D. Chapman)

with the HRS. This means that a significantly wider variety of atmospheres, corresponding to stars of different spectral types, can be scrutinized by this powerful technique.

III. Implementation of the High Resolution Spectrograph

Requirements

The HRS is required to obtain spectra at resolutions R = 10^5, 2 x 10^4, and 2 x 10^3. The CsI/LiF Digicon detector is to be operative over the spectral range 110 nm - 170 nm in all three spectral resolution modes. Sensitivity further to the red is not desired, for maximum discrimination against scattered light. The CsTe/MgF_2 Digicon is required to be operative over 115 nm - 320 nm in the medium resolution mode and over 170 nm - 320 nm in the high resolution mode; sensitivity further to the ultraviolet is desirable. Spectra are to be measured simultaneously across 500 diodes in the linear array of a detector.

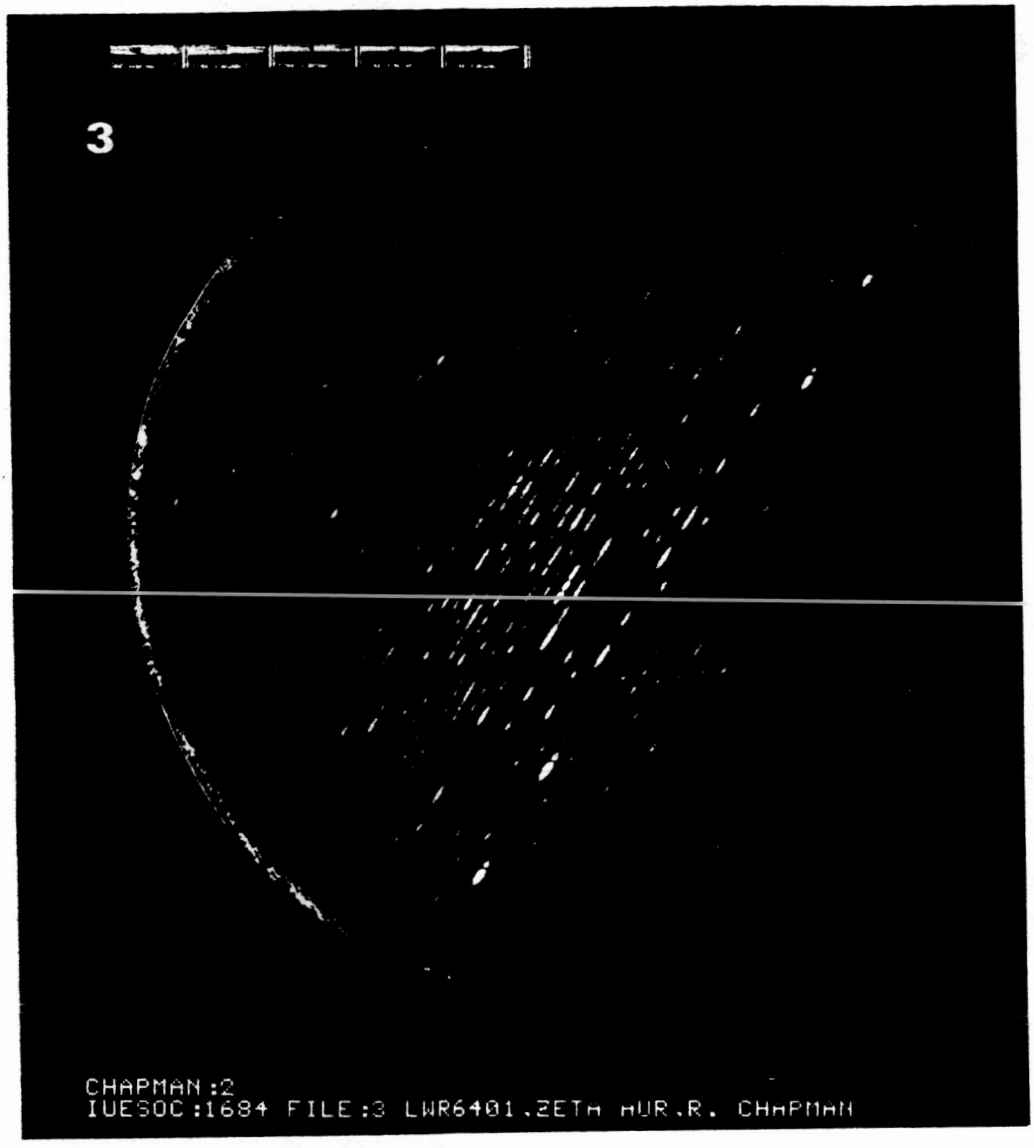

Figure 4 IUE echelle-mode observation of zeta Aurigae on December 16, 1979. The system is at mid-eclipse and the spectrum consists of emission lines from the supergiant. (R.D. Chapman)

The sensitivity goals of the HRS include the following: the total spectrograph system efficiency, in counts/photon, in the medium resolution mode (which employs first order gratings as the dispersive elements) is to exceed 1% throughout the interval 125 nm - 280 nm, with a maximum of at least 3% in the 180 nm - 320 nm range. In the high resolution mode (where an echelle is used), the system efficiency is to exceed 0.4% at the blaze wavelengths throughout the interval 120 nm - 280 nm, with a maximum of at least 1.2% in the 180 nm - 290 nm range.

The HRS system dark noise, outside the South Atlantic Anomaly, is required to be less than 0.01 counts/channel/s at nominal operating temperature.

The derived limiting magnitude requirements on the HRS are as follows. The HRS, in the medium resolution mode, shall achieve a signal-to-noise ratio of at least 10 per channel at a flux maximum near the wavelength of maximum HRS efficiency in a 200-s integration on an unreddened AOV stellar flux distribution corresponding approximately to magnitude V = 15. In the high resolution mode, the same signal-to-noise shall be achieved in a 200-s integration on an unreddened AOV flux distribution corresponding approximately to magnitude V = 12. Here, a telescope throughput (including the effect of

obscuration) of 0.58, corresponding to an effective aperture of 23200 cm^2, a radiation background of 10^{-3} counts/s/channel, and a sky background of less than 10^{-3} photons/cm^2/s/A/(arc min)^2 have been assumed.

The relative response of any two channels in either Digicon is required to remain constant to within 1% over intervals of up to 30 days. It is also required that the background contribution to the total count rate shall be measurable to 1% accuracy through observations of the residual intensities of interstellar lines. The photometric performance of the HRS is further specified with respect to count rates that are randomly distributed in time as follows: at rates up to 10^5 counts/s/channel, the measured rates shall be correctable to the true rates to an accuracy of better than 4%, while for count rates of 1 to 10^4 counts/s/channel, the measured rates shall be correctable to the true rates to an accuracy of better than 1%. Allowance is made for degradation of up to 2% of the channels in each Digicon due to blemishes or other manufacturing defects.

A minimum integration period of 50 ms for a single frame of data (spectrum) is required. Longer integration periods are to be preset with an accuracy of 100 microseconds. The reset time between successive integrations in the accumulation mode is required to be less than 2 ms.

Spatial resolutions of 0.25 arc sec and 2 arc sec are required, and the HRS is required to be capable of providing offset target image positions to the flight computers of sufficient precision to allow centering of a target within the small slit to an accuracy of 0.020 arc sec.

The HRS is required to provide an internal wavelength calibration system operative both in the laboratory and in orbit that is capable of establishing a wavelength scale (given information on the target image position in the entrance slit) accurate to the wavelength equivalent of 0.40 pixels. The HRS is required to remain sufficiently stable so that a single wavelength calibration using one of the Digicons shall be valid over a period of 1 hr.

The HRS is required to be furnished with a light source suitable to enable the pixel-to-pixel relative response to be determined within the spectral range 110 nm - 320 nm for any operative spectral mode of the instrument and for all diodes of the corresponding Digicon.

Optical design

The optical design of the HRS (Figure 5) is based on the principle of making the spectral image at the center of the detector photocathode stigmatic by using off-axis paraboloids as the collimator, camera mirrors, and cross-dispersers. The dispersive elements are five first-order gratings (four high-frequency gratings for various submodes of the medium resolution mode and one for the low resolution mode) and an echelle, used in two high resolution submodes that correspond to the two Digicon detectors. See Tables 1 and 2.

Table 1

Gratings Selected for Flight in the HRS

Number	Application	Radius of Curvature (mm)	Groove Frequency (mm^{-1})	Blaze Angle (deg)	Method of Manufacture
1	First order	∞	6000	unblazed	holographic
2	First order	∞	4960	unblazed	holographic
3	First order	∞	4320	unblazed	holographic
4	First order	∞	3600	unblazed	holographic
5	First order	∞	600	2.2	ruled
6	Echelle	∞	316	63.4	ruled
7	Cross-disperser	2950	197.5	0.7	ruled
8	Cross-disperser	2688	87.8	0.5	ruled

Table 2

HRS Spectral Mode Characteristics

Grating Number	Total Wavelength Coverage (A)	Instantaneous Wavelength Coverage (A)	Nominal Resolving Power	Applicable Detector
1	1050-1700	25	2×10^4	CsI/LiF
2	1150-2100	33	2×10^4	$CsTe/MgF_2$
3	1600-2300	38	2×10^4	$CsTe/MgF_2$
4	2200-3200	43	2×10^4	$CsTe/MgF_2$
5	1050-1700	288	2×10^3	CsI/LiF
6 & 7	1050-1700	6-10	1×10^5	CsI/LiF
6 & 8	1700-3200	9-20	1×10^5	$CsTe/MgF_2$

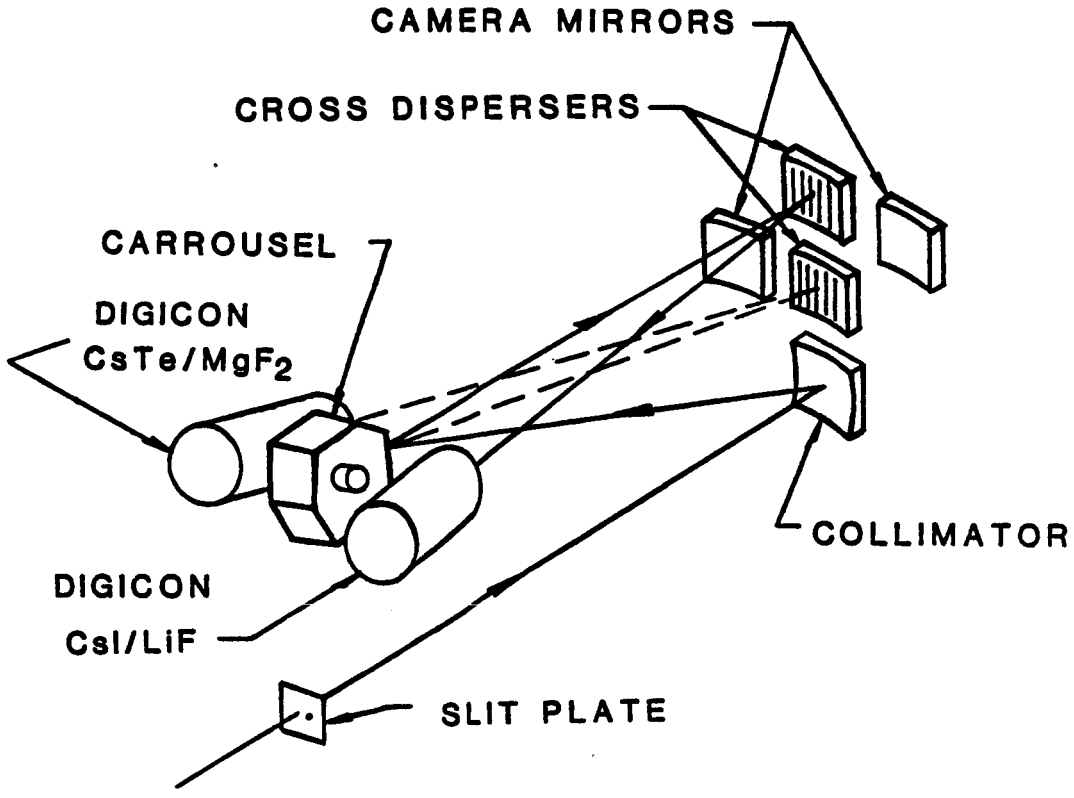

Figure 5 The optical design concept for the HRS.

In the medium resolution mode, one grating provides satisfactory performance over the spectral range of the CsI/LiF detector, but three gratings are required to cover the range of the $CsTe/MgF_2$ detector while still operating each near its optimum blaze. In the high resolution mode, an echelle is used with either of two concave cross-dispersers, depending on the detector. The long wavelength cross-disperser is mounted behind a thin fused quartz window with a short wavelength cutoff near 1600 A to discriminate against second order spectra. A quartz window is also mounted in front of grating No. 4 (see Table 2) for the same purpose.

The two entrance slits are fixed; the ST is moved so as to image the target in one HRS slit or the other. As the HRS slits are about 5 arc min off the ST optical axis, the target image contains appreciable astigmatism and the difference between the tangential and sagittal foci is significant (about 1.2 mm). In order to obtain spectra of precisely defined regions in extended sources, separate sagittal and tangential slit jaws are mounted at the corresponding foci. The collimator, an off-axis paraboloid, is decentered and tilted so that the resulting astigmatism exactly compensates the telescope astigmatism, while the coma remains zero. Thus a beam

collimated to within 0.25 arc sec is produced, which corresponds to a linear aberration at the detector of only about 1.4 micrometer. The last focussing element (camera mirror or cross-disperser) therefore produces the only aberrations of the combined ST-HRS optical train. Thus, spectral image quality is determined by these aberrations, which, off the stigmatic center, are third-order coma and astigmatism resulting from differences in the respective tilts and curvatures of the sagittal and tangential image planes. The detector photocathodes are tilted to achieve optimum imaging in the echelle dispersion direction at all spectral orders in the echellogram, and are positioned to reduce the effects of curvature. These arrangements do not degrade the image quality in spectra from the first order gratings.

The HRS is also provided with plane optics to support four camera modes used for target acquisition. These are summarized in Table 3, where the applicable range is expressed, for purposes of illustration, in terms of the apparent visual magnitude of a star whose spectrum is that of a 3×10^4 °K blackbody. This range (the listed figures are nominal values) is based on a count rate range of 10^2 to 10^5 counts/s.

Table 3

HRS Target Acquisition Modes

Mode	Optical Configuration	Digicon	Applicable Range
N2	Main Acquisition Mirror Camera Mirror B	$CsTe/MgF_2$	V = 13 to 21
N1	G5 in Zeroth Order Camera Mirror A	CsI/LiF	V = 7 to 15
A2	Outer Fused Silica Plate Camera Mirror B	$CsTe/MgF_2$	V = 10 to 18
A1	Inner Fused Silica Plate Double Pass through Outer Plate Camera Mirror A	CsI/LiF	V = -1 to +7

Detectors

There are two Digicon detectors, provided with CsI/LiF and $CsTe/MgF_2$ photocathode/window combinations, respectively. Each is provided with a linear array of 500 diodes, on which the photoelectrons are magnetically focused after acceleration across a 22.5 kV potential. Focussing is via a rare earth permanent magnet assembly. However, electromagnetic deflection coils are provided to allow the desired portion of the photocathode to be imaged on the array. The deflection coils are used to select orders in the echellogram, for substepping during accumulation mode, to sample interorder or other off-spectrum background, and for scanning the field of view during target acquisition. Individual diodes of the linear array are 40 micrometers wide on 50-micrometer centers; their height (dimension perpendicular to the dispersion) is 400 micrometers, which corresponds to 2 arc sec at the ST focal plane.

The Digicons are operated in the digital photon-counting mode. A separate output pulse results from each detected photon and each of the 500 diodes of the linear array is furnished with an independent preamplifier and postamplifier, as are twelve special-purpose diodes located in the Digicon. The latter include smaller diodes (projected size 0.25 arc sec square) used to monitor focus and to map the field of view, gold-overcoated diodes used to monitor particle radiation while the HRS is operating, and long diodes that are oriented parallel to the dispersion and which may be used to evaluate scattered light during spectral data acquisition. The response of a single diode to a 22.5 kV accelerated photoelectron is 5600 electron-hole pairs.

Wavelength calibration lamps

The HRS is provided with two redundant platinum-neon hollow cathode wavelength calibration lamps. The design is based on the successful IUE lamps. Each lamp is furnished with a dedicated entrance slit.

Flat field calibration lamps

Redundant low-pressure xenon lamps, which emit primarily in a resonance line at 147 nm, are used as internal standards for diode-to-diode response calibration and photocathode mapping and as light sources for the operation of locating the photocathode mask edges.

Flight software

During normal flight operations, the HRS will operate under the control of HRS-dedicated software resident in the NSSC-1 computer, a component of an ST subsystem known as the SI C&DH (Science Instruments Control and Data Handling System). Unlike the other ST instruments, the HRS does not contain a microprocessor.

The major tasks of the HRS flight software are to support safing, and to conduct observation initialization, target acquisition, and science data acquisition, as well as to control "regularly scheduled events." Each of these processes will generally be conducted autonomously when the HRS is operating (as opposed to being in "Hold" while another instrument is operating) whether or not a link to the observer and ground controllers is available. However, the flight software is designed to allow observer interaction for target acquisition and spectroscopic observations when appropriate or necessary.

The HRS safing programs operate to detect anomalous conditions (for example, when an engineering or housekeeping parameter is out-of-limits) by reading flags set by the NSSC-1 flight executive program. In response, the safing programs issue a safing command sequence to the HRS when conditions warrant this action. The program also generates telemetry to describe the actions taken and inhibits the HRS flight software from further execution pending commands from the ground.

The function of the observation initialization programs is to configure the HRS in order to perform the desired target acquisition or spectroscopic observations. Features of this functional area are the Observation Control Table (OCT), the Observation Sequence Table (OST), and the Ground Control Observation Sequence Table (GC/OST). The OCT contains nearly all the information necessary to conduct an observation, including the desired configuration of the spectrograph, the specifications for detector substepping, exposure meter control, bad data rejection, etc. An exception is the target coordinates, since the HRS flight software is invoked to conduct an observation only after the ST has locked on the guide stars. The HRS software may request small maneuvers of the ST in the vicinity of the target, but not a slew to the next target. The OST is a buffer that contains the information needed to fill the OCT for each of many observations in a sequence (one at a time). The OST is loaded from the delayed command processor of the ST flight executive program. The GC/OST is an area of memory that may be loaded directly from the ground when a link to the spacecraft is available. It contains an active flag, a "skip-ahead" value, and information in the same format as the OST, although there is room for only a few observation specifications. When a link is available, the GC/OST allows the observer on the ground to adjust the program of exposures on the current target in response to an evaluation of data received from the HRS. The observer cannot interrupt an exposure in progress, but can set the GC/OST active flag so that when the exposure is completed, the HRS flight software will perform the observations that have been newly loaded into the GC/OST. Having finished these new observations, the flight software continues with the original program of exposures on the current target (if the available time-on-target permits), after skipping ahead, when so commanded, to an observer-specified position in the sequence of exposures contained in the OST.

The target acquisition software is used to search for, center on, and/or make a specified offset to a target. Searches are performed in a spiral pattern, one 2-arc-sec square field of view at a time, with a maximum size specified by the observer. The pattern is generated one small slew (of 1.8 arc sec) at a time, by a series of requests from the HRS flight software to the ST flight executive. Unless the observer has specified otherwise, the search terminates and spectroscopic observations begin as soon as the target is located and has been centered in the desired entrance slit. The target acquisition software may also be used to map the field of view or to map a search area consisting of a series of fields of view. (However, the maps are not analyzed by the flight software; they are obtained for analysis by astronomers on the ground.) The acquisition of simple (point-like), stationary targets will generally be done autonomously under flight software control. Unlike IUE, where the images used for target acquisition are constructed in visible light by the IUE fine error sensor, HRS target acquisition is conducted in broadband ultraviolet light.

The target acquisition software can also be used to support observer-interactive target acquisition. For example, an area might be mapped under flight software control, then

after the map is transmitted to the ground, the flight software would await further instructions, such as an observer-initiated request to generate an offset to an adjacent location. In the event that a software-controlled target acquisition process should fail (for example, if no source with flux within observer-specified limits is found in the specified search area), the flight software issues a report and awaits further instructions. It is anticipated that many targets in complex fields and nearly all moving targets will be acquired with the aid of supporting observations by the WF/PC. The HRS, it is anticipated, will be operated almost exclusively as a prime operating instrument; its utility as a serendipity instrument is limited both by the small size of the entrance slits and by the fact that the HRS flight software cannot operate with the limited NSSC-1 memory available to an instrument in serendipity mode.

The science data acquisition software controls the actual taking of spectroscopic data after the observation initialization routines have configured the spectrograph. Among their specific tasks, the science data acquisition programs zero all substep storage bins, perform computations and set parameters related to the doppler shift corrections (see below) and supervise event parades that determine the Digicon deflection coordinates for each (typically 200 ms) integration of an exposure. Other tasks include quality checks on the data frame produced by each integration of an exposure, followed by coaddition and comb addition into appropriate substep bins. Of special interest to the observer, the science data acquisition programs include exposure meter routines. These allow the astronomer to specify "overexposure" and "underexposure" limits, if such are desired. The overexposure feature terminates an exposure on a particular wavelength when the desired number of counts have been accumulated in a specified group of channels. The underexposure feature terminates an exposure when it is determined, early in the anticipated interval of the exposure, that the count rate is less than a specified lower limit. In either case, when the exposure meter software terminates an observation, the flight software reconfigures the HRS for the next planned exposure (typically, at another grating setting) and begins exposing again. Thus, optimum use can be made of the available time on target. To take advantage of this capability, the observer will want to specify a somewhat longer list of spectroscopic exposures than can actually be accomplished assuming that the a priori exposure time estimates are correct. Needless to say, with ultraviolet astronomy currently a forefront research area, such estimates are rarely very accurate.

The doppler shift corrections supervised by the HRS flight software consist of periodic shifts of the substep pattern along the dispersion direction to compensate for the change in the wavelength of a spectral line in the observer's frame due to the changing vector of the Space Telescope's orbital motion. This correction, which is needed only in the HRS high spectral resolution mode, allows the coaddition programs to continue to add counts corresponding to a specific rest-frame wavelength into the same storage bin during a time exposure. The feature can be disabled by observer selection.

The "regularly scheduled events" programs of the HRS flight software invoke instrument safing checks and doppler shift corrections once per min, compute radiation diode and anti-coincidence counter count totals once every 6 s, and record diagnostic flight software variables once every 30 s. In addition, a Standard Header Packet dump is requested at the beginning and end of each exposure.

IV. Status of the HRS development program

The HRS is being developed by NASA-GSFC with Ball Aerospace Systems Division (BASD) as the prime contractor and with scientific direction by the Principal Investigator (J.C. Brandt), assisted by the other members (Co-Investigators) of the HRS Investigation Definition Team and by scientists listed above as members of the HRS Experiment Development Team. Principal engineers in the HRS program at GSFC and BASD compose the majority of the Experiment Development Team. Andrulis Research Corporation is the responsible contractor in the area of science data analysis software.

As of June 1982, virtually all HRS flight components and subsystems have been completed. Testing of the two assembled flight detector subsystems is under way and planning for laboratory calibration of the assembled spectrograph is in an advanced stage. The flight detectors and their performance characteristics are listed in Table 4. The dark counts can be compared with our design specification of 0.01 counts/s; evidently it should be possible to observe much weaker sources with the HRS than was originally anticipated. This is especially important for spectroscopy of extragalactic targets. In general, the detector test results can be summarized as follows: dark counts and distortion are low, resolution is good, diode nonuniformity is less than 1%, signal linearity is satisfactory and no transient response problems have been found. Components used in the detector subsystem, including permanent magnet focus assemblies, deflection coils, and high-voltage resistors all meet or exceed the design specifications. The successful completion of the very difficult hybrid circuit

fabrication for the preamplifiers and postamplifiers is especially noteworthy, as technical difficulties were both anticipated and experienced in their development. Among the preamps, 64 flight units, providing a total of 1024 individual preamplifier circuits for the two Digicons, have passed acceptance tests and 4 flight spare units are being fabricated. Of the 64 corresponding flight postamp units, 52 have been completed and accepted, and another 16 are currently in process of fabrication.

Table 4

HRS Flight Detectors: Summary of Characteristics

Characteristic	D1 (CsI/LiF)		D2 ($CsTe/MgF_2$)	
	1216 A	1473 A	1216 A	2537 A
Quantum Efficiency(%)	16.3*	11.5	12.4	15.2
Dark Signal (counts/s/diode)	3×10^{-4}		1×10^{-3}	
Distortion (μm)	$\pm$15.5		$\pm$34	
Photocathode Nonuniformity (%)**	$\pm$3		$\pm$5	
Photocathode Blemish (No.)	0		6	
Diodes Inoperable	2		4	
Mask/Diode Alignment (deg)	-1.8		+0.44	
Mask/Diode Tilt (deg)	-0.5		-0.16	

*Quantum Efficiency at 1067 A is 10.7%.
**Peak difference across selected sampling lines.

Because of our concern for the successful performance of the hybrid circuits, the elaborate test plan to which all flight units are subject includes electrical measurements, bond pull tests, 96-hour burn-in periods, leak tests, and other modes of inspection. Appropriate screening is conducted on the open packages, during the sealing sequence, and on the final closed packages.

A modest grating development program for the echelle and first-order gratings (both ruled and holographic first-order gratings were fabricated) has been completed and the flight echelle and other gratings have been selected; their characteristics are summarized in Table 1. The program did not succeed in developing an echelle optimized for the HRS; instead, a satisfactory commercial echelle will be used. However, we were most encouraged by the results of both commercial and in-house NASA-GSFC holographic first-order gratings fabrication projects. All optical components have been finished and most have been mounted on the finished graphite-epoxy optical bench. Optical alignment work is under way. The Pt-Ne lamp spectral calibration system, which incorporates hollow-cathode lamps, optics, circuitry and mechanical parts, is nearly finished, and the flat field (low pressure Xe lamps) calibration system is in an advanced stage of construction.

All of the HRS flight mechanical subsystems have been designed and most are completed or in an advanced stage of construction. During normal flight operations, there will be only two moving parts in the HRS, a shutter to close the large entrance slit (the shutter is fail-safe "open") and the grating carrousel. The grating carrousel (Figure 6) is the primary operating mechanism in the HRS. It is used to select acquisition mirrors applicable to various target magnitude ranges, to select the echelle/detector or grating/detector combination applicable to any spectral mode, and to set the echelle or grating position required to observe any desired wavelength in that mode. The shutter mechanism has been completed and tested. The carrousel, its bearings, encoder, motor and support structure have been tested, disassembled, adjusted, and reassembled, and have been vibration-tested.

Figure 6 The HRS carrousel mounted on a vibration fixture with dummy optics.

Engineering test data show that the carrousel positioning short-term repeatability is ±0.1 arc sec of rotation, which corresponds to ±0.05 pixels in the spectrum, a factor of 10 better than our specification. Once positioned, peak-to-peak short-term stability of the carrousel is also ±0.1 arc sec, and the stability over 30 min is ±0.25 arc sec, a factor of two better than our specification. The only other mechanisms in the HRS are used to drive an aperture door and two vent doors. These doors are opened after launch and then are not exercised until such time as the HRS might be serviced by an astronaut or be brought back to the ground. The door drive mechanisms have been designed; motor-gearheads required for the drives are being fabricated.

High voltage supplies for the detectors have been fabricated and encapsulated. They satisfactorily passed functional, thermal and corona tests. Low voltage power supplies for the HRS electronics have been designed and engineering models have passed test. Assembly work on the flight units is under way. The detector electronics box, which incorporate the postamplifier circuits, is being fabricated. The main electronics box has passed breadboard testing and the corresponding flight boards have been fabricated and tested. All flight cables have been designed and are currently being fabricated with the aid of a wooden mockup of the HRS.

We are currently devoting considerable attention to the subject of contamination control. This is especially important for an ultraviolet instrument. The graphite-epoxy HRS optical bench is maintained in a suitably controlled environment (the bench is continuously purged with dry nitrogen, which maintains a relative humidity of less than 10% during periods when technicians are not working with it) and we are monitoring the water content of the bench material and molecular deposits at the surface on a regular basis. Specifically, molecular contaminants are kept at or below 0.5 milligrams per square foot. Paints proposed for thermal control on the permanent magnet focus assemblies are being evaluated under laboratory conditions for total weight loss and vacuum condensable material. The gasket material for the instrument enclosure cover seal has been tested for contamination aspects and found acceptable. Similar tests are scheduled for the vent and aperture door mechanisms.

The flight software has been completed. A few modifications are in preparation for submission through the configuration control process and a flight software user/operator's manual is being completed. Software for ground testing of the HRS is being written; a preliminary design will be completed in the fall of 1982, with the final software due in January 1983.

An extensive requirements document for the HRS Investigation Definition Team science data analysis software has been completed and the software itself is being written. Already, some programs suitable for quick-look data analysis during laboratory tests of the HRS have been completed. We intend to make the data analysis software available to the ST Science Institute and we are encouraging the cognizant authorities to make these programs available to General Observers in the ST Science Data Analysis System.

The categories of HRS science data analysis software under development are: spectral data analysis, target acquisition support and data analysis, quick-look analysis, calibration, reduction, post-reduction analysis, and performance analysis. The software will be implemented in the IUE Regional Data Analysis Facility at NASA-GSFC in addition to being supplied to the ST Science Institute. A data management system is provided to alleviate paperwork, allow timely processing of data, and reduce the chance of operator error. The system makes use of a merged observing log that shows the processing status of HRS observations and that incorporates calibration libraries for the automatic selection of appropriate calibration files.

For quick-look applications, the HRS science data analysis software performs such tasks as unscrambling the detector channel patterns, display of engineering data, display of the science data in terms of counts *vs.* channel number, and crude reductions. Among the reduction processes are response linearization by means of analytic formulae, diode-to-photocathode position mapping by a simple formula, correction for diode nonuniformities by reference to a suitable updated table, correction for photocathode nonuniformities (also with a table), background subtraction (either by substep bin subtraction or by use of background diode counts), wavelength scale determination with analytic formulae, echelle ripple corrections by formulae, and correction for the total ST + HRS wavelength-dependent sensitivity, also by approximate formula. The reduced data are displayed or written as desired. Final data reduction involves similar and additional tasks, but does not invoke approximations when precise calibration information is available.

Laboratory calibration (Proposed plan by D. Ebbets)

Preliminary photographic studies in support of the calibration program are under way. The expected test environment during laboratory calibration of the full 1024-channel (two detectors) flight spectrograph includes the following elements: active thermal control of the HRS optical bench; flight software control; quick-look analysis immediately after each test; hard vacuum whenever the full high voltage is on a detector; spectrograph mounted on an air-supported, isolated table; critical tests done at night when building vibrations are minimal; an ST simulator to emulate the imaging properties of the ST Optical Telescope Assembly; ultraviolet calibration sources, providing the spectra of Pt, Hg, Ar, Xe, *etc.*; availability of an absorption cell, with ultraviolet-transmitting windows, filled with appropriate molecular gases, such as CO and NO.

Calibration tests of the flight Xe flat field lamps will include measurements of the two-dimensional irradiance distribution, checks to verify that there is no vignetting, and adjustments, via an iris, to control the irradiance of each lamp so that the desired photon flux, producing approximately 7000 counts/s/diode, illuminates the detector photocathode. The flight wavelength calibration lamps will be tested to measure the offsets for target wavelength calibration (which result from the displacement between the lamp entrance slits and the target entrance slits); to produce a thorough list of lines measured at high resolution; to determine profiles of lines, including evaluation of multiple components and background between lines; and to support studies of the possible use of the undispersed lamp image to monitor the flux sensitivity of the HRS in target acquisition (i.e., undispersed light) modes.

Calibration of the flight detector systems includes tests and/or determination of dark count, resolution, distortion of format, scattered light, uniformity across individual diodes, diode-to-diode response, channel-to-channel crosstalk, photocathode response spatial variations, paired pulse corrections, and deflection stability. Preliminary results of this program, are as follows. The dark count has a Poisson distribution. With a point source ($<40\mu m$) focused on a central diode, the response (normalized to the central diode) of the two adjacent diodes is less than 2% and the response of the next-to-adjacent diodes is less than 0.1%. Paired-pulse corrections are found to correspond to theoretical calculations very accurately. The deflection stability amounts to $\pm$2.1 micrometers, or only 1/3 substep, over 2.5 hr after a 20-min warm-up period.

Radiometric calibration tests will measure absolute sensitivity versus wavelength for all first order grating modes and echelle blaze function ("echelle ripple") for all applicable orders and wavelengths. All of the medium resolution grating modes will be intercalibrated. The day-to-day stability and repeatability of the calibration will be monitored in the laboratory and checks on secular degradation will be made.

Spectral purity will be calibrated by measuring the resolving power at several wavelengths in each grating mode. Likewise, the instrumental point spread function will be measured as a function of wavelength in each mode. These tests will make use of the ST simulator, spectral lamps that provide narrow emission lines, and the mini-arc (shining through the molecular absorption cell). Several alternate substepping patterns will be used.

The stability and repeatability of the spectrograph will be tested during laboratory calibration to demonstrate compliance with the short-term requirements, to measure the sensitivity to thermal excursions, and to investigate the possibility of long-term changes. This will be accomplished by repeating functional tests of dark count, focus and resolution, photometric stability, and wavelength calibration stability, by making specialized tests of the detector deflection when commanded to the photocathode mask edge for about an hour, and by monitoring the results with the carrousel and deflection positions set to place one spectral line at a defined location for a similar period.

Measurements of stray and scattered light during the laboratory calibration program are designed to detect stray light, to influence final design and placement of light baffles, to ensure that vignetting is avoided, to measure residual stray light after placement of baffles, to measure sensitivity to visible light (i.e., check the solar "blindness"), to demonstrate the effectiveness of the order sorting filters that are used with one first order grating and in one echelle mode, to measure interorder background in echelle modes and out-of-plane background in other grating modes, to calibrate the large dedicated background diodes, to measure "in-order" scattering in all spectral modes, and to search for variations in any of the above with time.

Laboratory calibration of the HRS target acquisition modes cannot be complete, since it is impossible to simulate the interaction with the ST, which will make small angle maneuvers as required by the HRS flight software during the acquisition process. However, the lab work will attempt to demonstrate the functioning of the applicable flight software, test the image-forming algorithms used in data reduction, measure orientations and offsets of entrance slits in Digicon deflection units, calibrate the count rate vs. incident broadband ultraviolet flux in all four camera modes, and demonstrate the ability to discriminate flux differences of 0.5 magnitude over a range of 20 magnitudes.

Wavelength calibration tests will verify the alignment and focus of the optical elements, validate and update the wavelength lookup table that is used to configure the HRS for an observation, provide the wavelength vs. diode number calibration needed for data reduction, and transfer the external wavelength scale to the flight lamps.

Acknowledgments

We thank the ST Instruments Scientist, Dr. David Leckrone, for valuable comments and illustrative computations. We are indebted to Dr. Robert D. Chapman for IUE data on zeta Aurigae and for helpful remarks on atmospheric eclipsing systems.

Bibliography

Bahcall, J.N., and O'Dell, C.R. 1980, The Space Telescope Observatory, in Scientific Research with the Space Telescope, Proc. IAU Colloq. No. 54, NASA CP-2111, p. 5.

Brandt, J.C. et al. 1979, High Resolution Spectrograph for the Space Telescope, in Instrumentation in Astronomy II, Proc. Soc. Photo-Opt. Instr. Eng., 172, p. 254.

Brandt, J.C. et al. 1981, Progress Report on the High Resolution Spectrograph for the Space Telescope, in Ultraviolet and Vacuum Ultraviolet Systems, Proc. Soc. Photo-Opt. Instr. Eng., 279, p. 183.

Leckrone, D.S. 1980, The Space Telescope Scientific Instruments, Pub. Astr. Soc. Pacific, 92, p. 5.

Leckrone, D.S. 1982, Spectroscopic Equipment for the Space Telescope, Phil. Trans., A, in the press.

Longair, M.S. 1979, The Space Telescope and its Opportunities, Q.J.R.A.S., 20, p. 5.

Appendix A

Capabilities of the R = 100,000 Mode

Many important astrophysical problems require resolutions of approximately 10^5 and we present some examples. The first concerns observations of absorption lines in a sharp-lined, chemically peculiar, early-type star. Figure A-1 shows a synthetic spectrum computed for the region around the ionized boron line near 1362.5 A. Figure A-2 shows the same spectrum degraded to the resolving power of IUE ($\lambda/\delta\lambda = 1.2 \times 10^4$). Clearly, much of the intrinsic information is lost. Figures A-3, A-4, and A-5 show the same spectrum as it should appear with the 10^5 mode of the HRS for values of V sin i = 0, 3, and 6 km/sec, respectively. Most of the spectral information is retained at the higher resolution and the use of deconvolution techniques may permit recovery of some of the residual "lost" information.

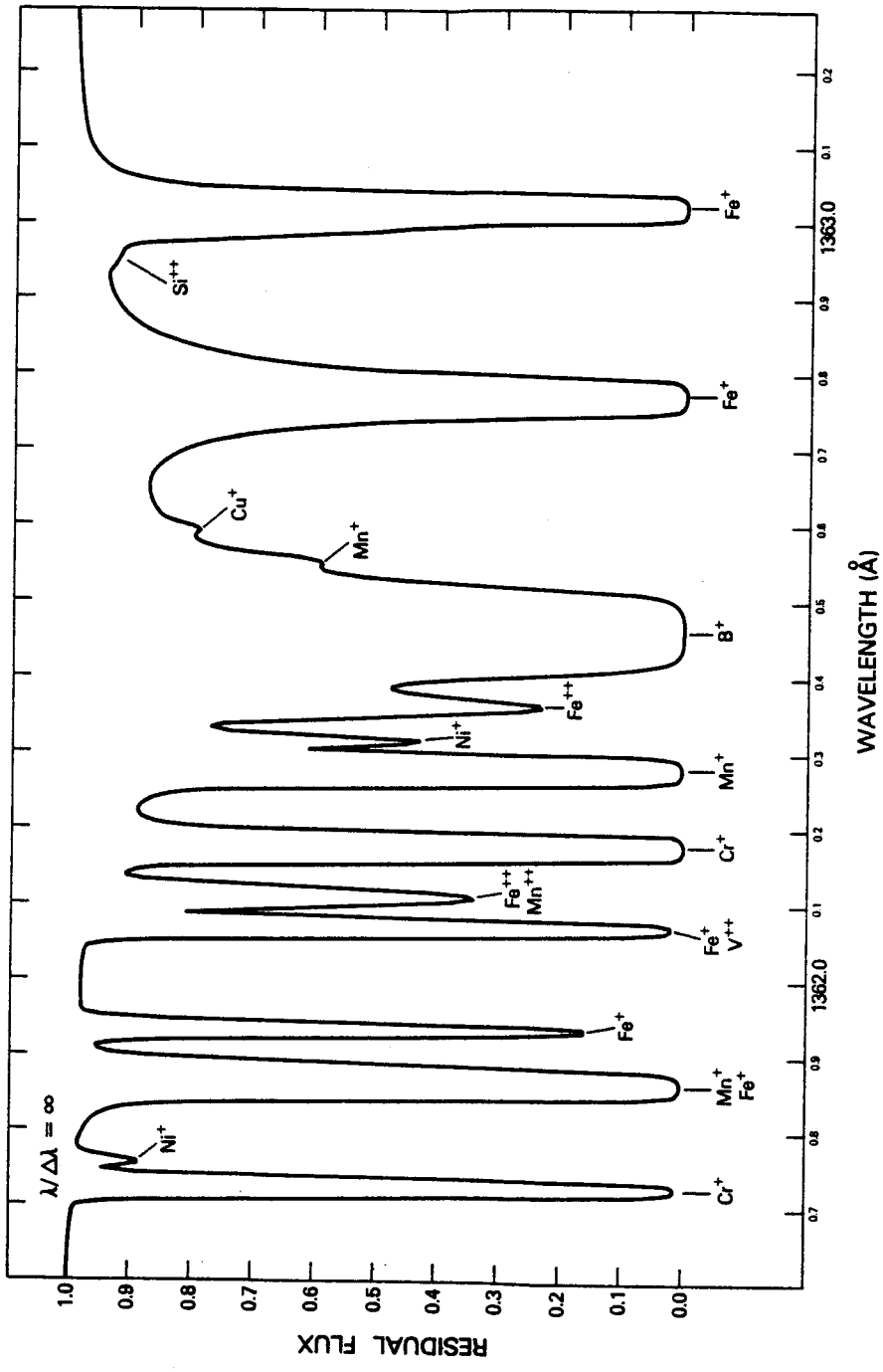

Figure A-1 Theoretical spectrum of a sharp-lined, chemically peculiar star (D.S. Leckrone).

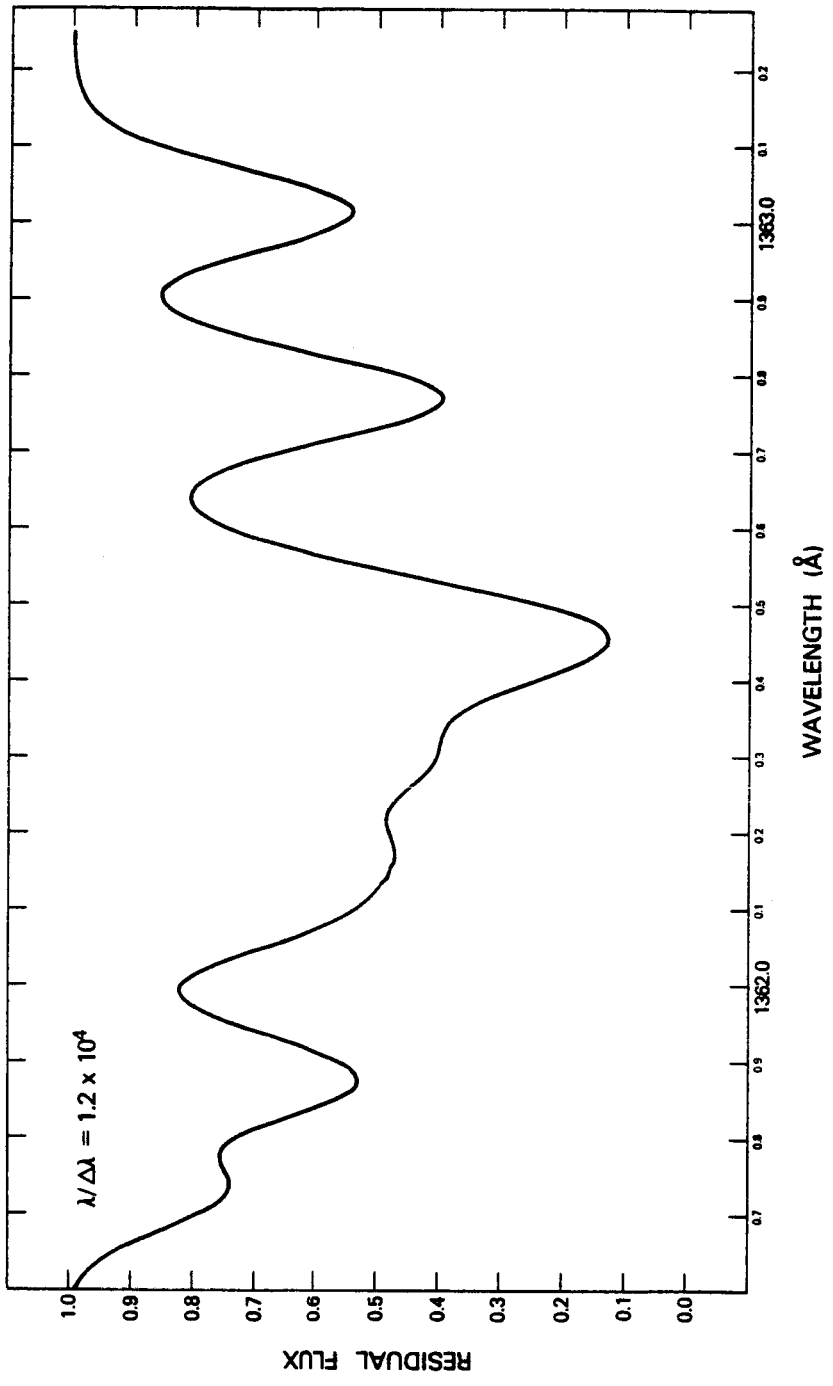

Figure A-2 Spectrum from Figure A-1 convolved with the IUE instrumental broadening function, R = 1.2 x 10^4 (D.S. Leckrone).

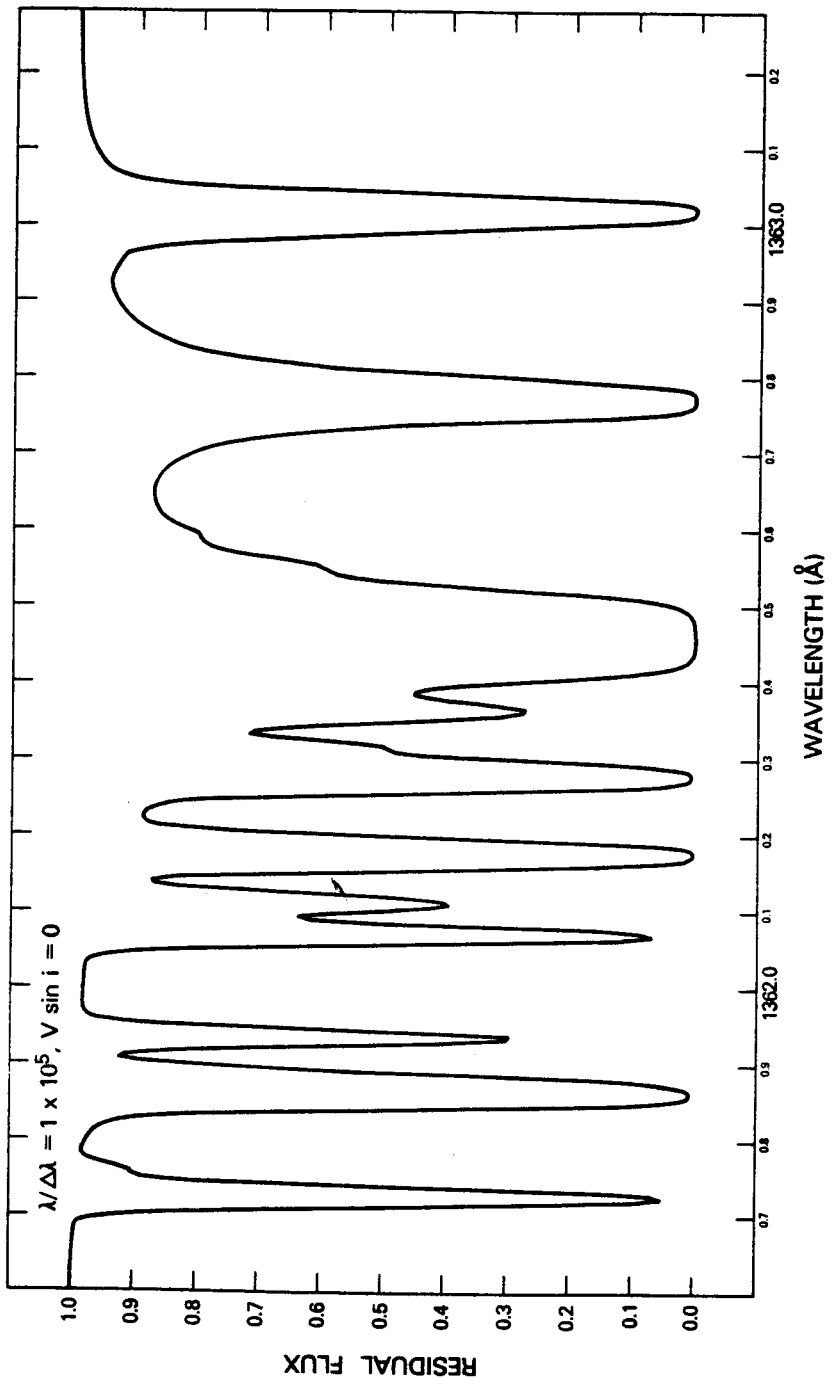

Figure A-3 Spectrum from Figure A-1 convolved with the expected HRS echelle mode instrumental broadening function, R = 1 x 10^5 and with V sin i = 0 (D.S. Leckrone).

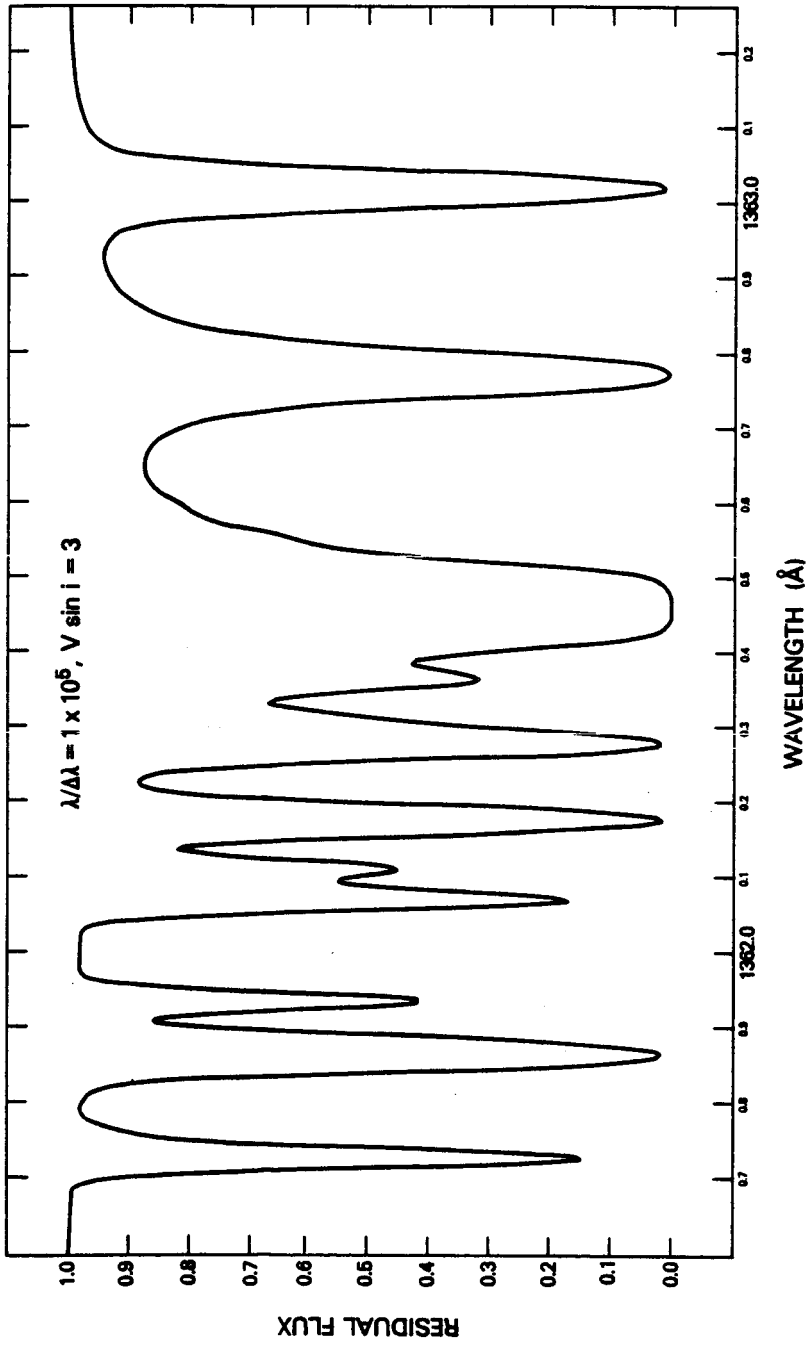

Figure A-4 Same as A-3 with V sin i = 3 km/sec (D.S. Leckrone).

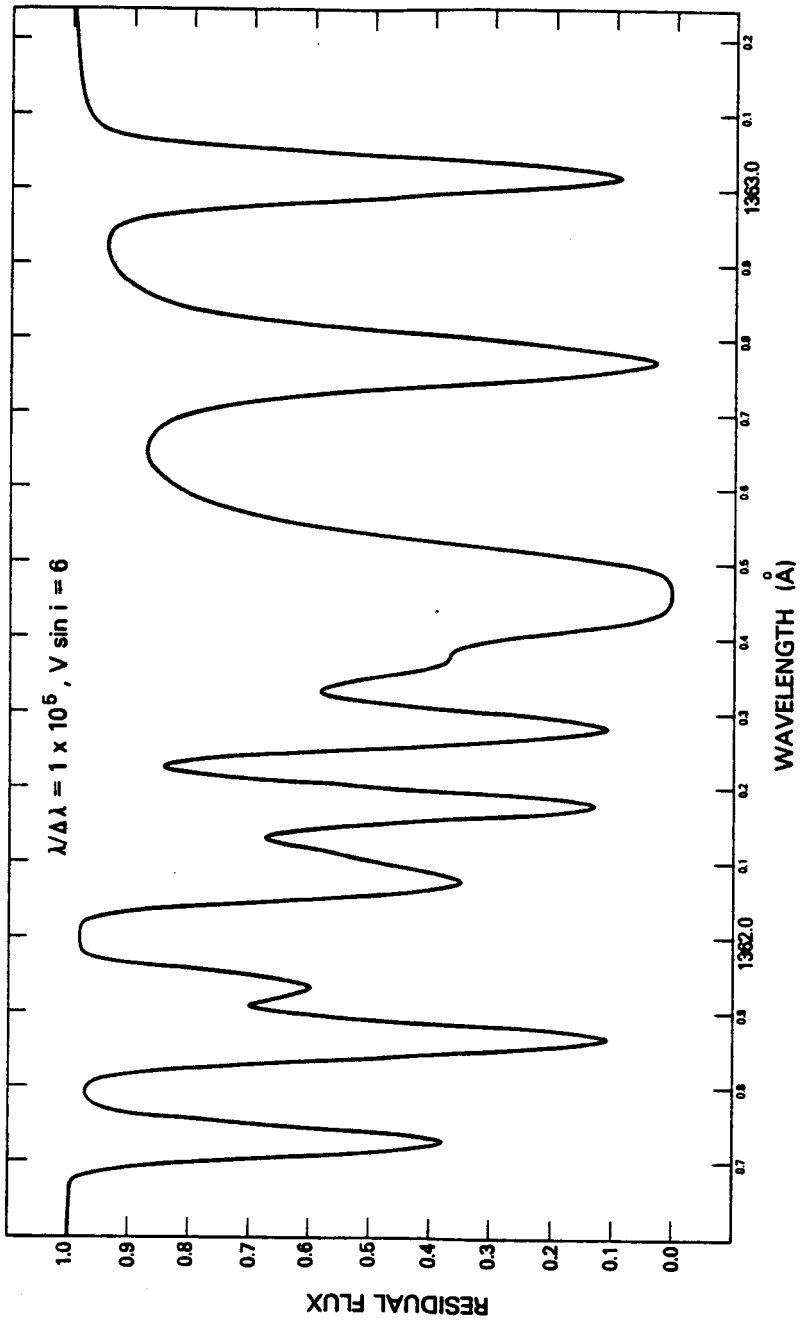

Figure A-5 Same as A-3 with V sin i = 6 km/sec (D.S. Leckrone).

The second example concerns observations of interstellar lines. In Figure A-6, we plot L. Hobbs' (1969) observations of the sodium D2 line in epsilon Orionis at $\lambda/\delta\lambda = 6 \times 10^5$. Also shown is the same information degraded to resolving powers of 120,000 and 22,000. At the lower resolving power, much of the original information is lost, but at a resolving power of approximately 100,000 (here 120,000) the structure is maintained.

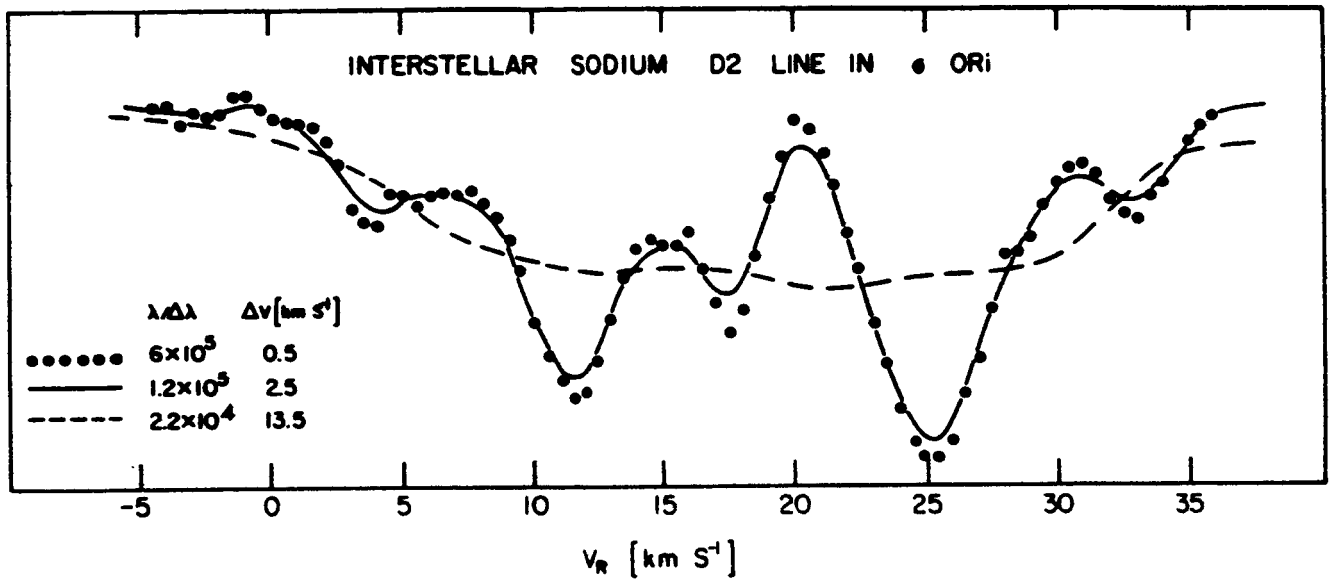

Figure A-6 Profile of the Na D2 line at several resolving powers.

Appendix B

"Limiting Magnitude" Diagrams for HRS Stellar Observations

Detailed planning of observations should rely on the combined ST and HRS sensitivity curves given in Figure 1. However, a qualitative idea of the stars within the capabilities of the HRS is a stimulus for conceiving and planning observational programs.

Figure B-1 (after J.B. Hutchings) represents a limiting magnitude diagram for hot stars. The intrinsic magnitudes shown are in the ultraviolet. The diagram shows the relative capabilities of various ultraviolet spectrographs for a specified "proper exposure." For example, in the $R = 2 \times 10^4$ case, the HRS can observe stars intrinsically 4 magnitudes fainter than IUE. Interstellar reddening has been included in a simple way. As is apparent, many galactic O and B stars are observable at $R = 10^5$.

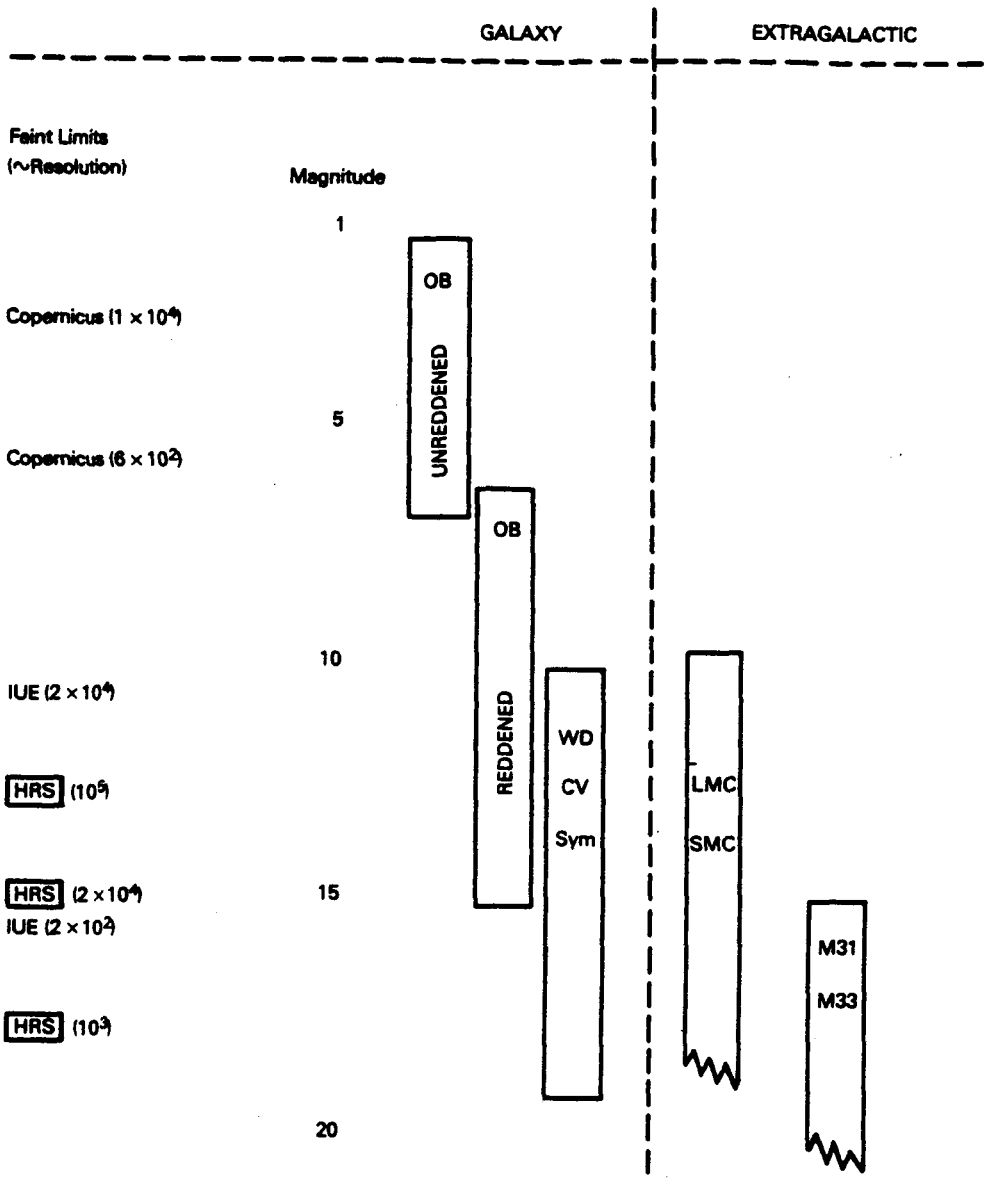

Figure B-1 Limiting ultraviolet magnitude diagram for hot stars (after J.B. Hutchings).

Figures B-2, B-3, B-4, and B-5 show limiting magnitude diagrams for stars of intermediate temperature at wavelengths of 1360 A, 1650 A, 1940 A, and 2500 A, respectively (prepared by D.S. Leckrone). The criterion for Figures B-2, B-3, B-4, and B-5 is achieving a S/N = 20 in a three-hr integration.

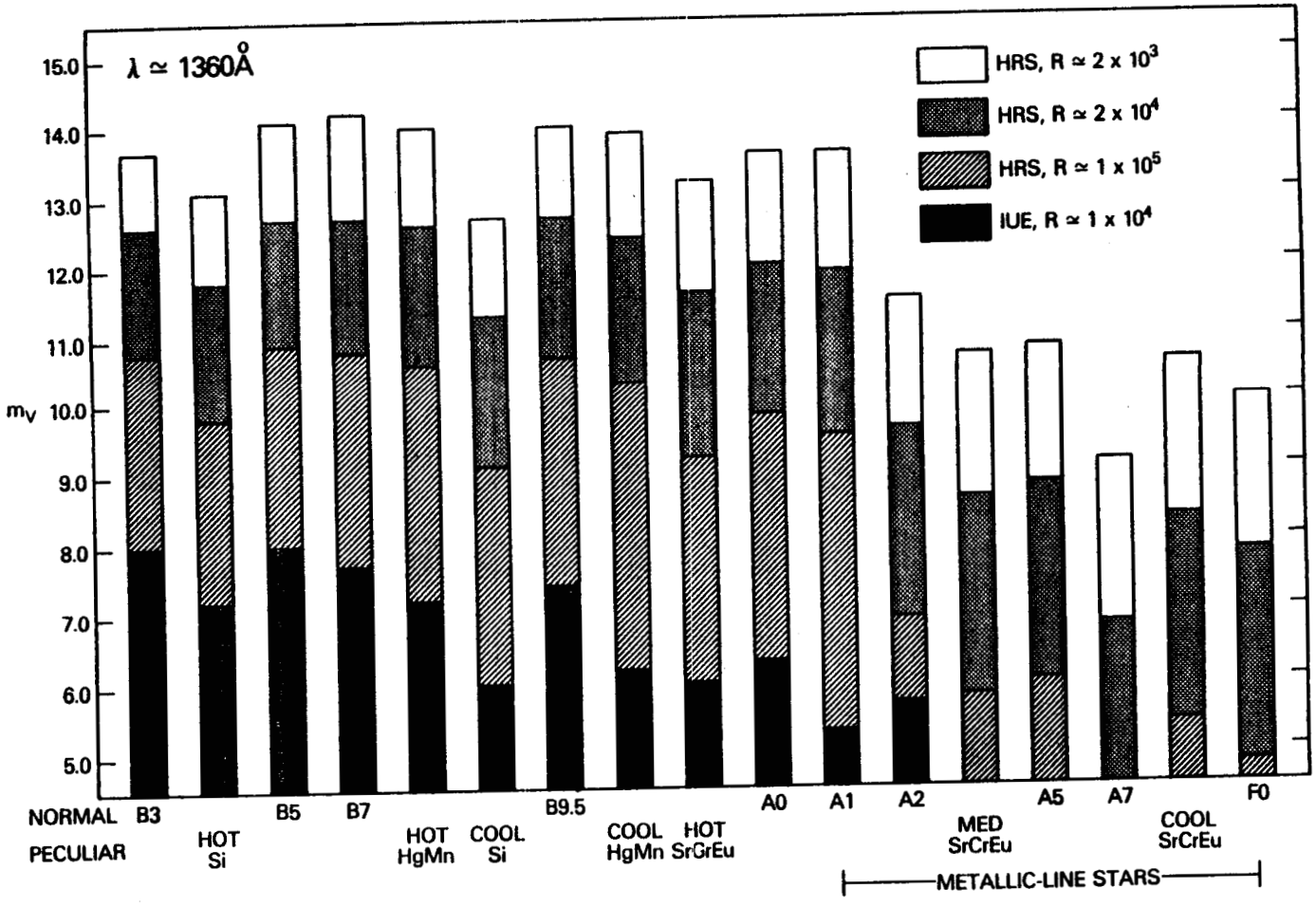

Figure B-2 Apparent visual magnitudes of normal and peculiar B and A-type stars which can be observed at 1360 A in the various HRS modes (and IUE) with S/N = 20 in 3 hrs assuming 0.8 magnitudes/kpc average visual extinction (D.S. Leckrone).

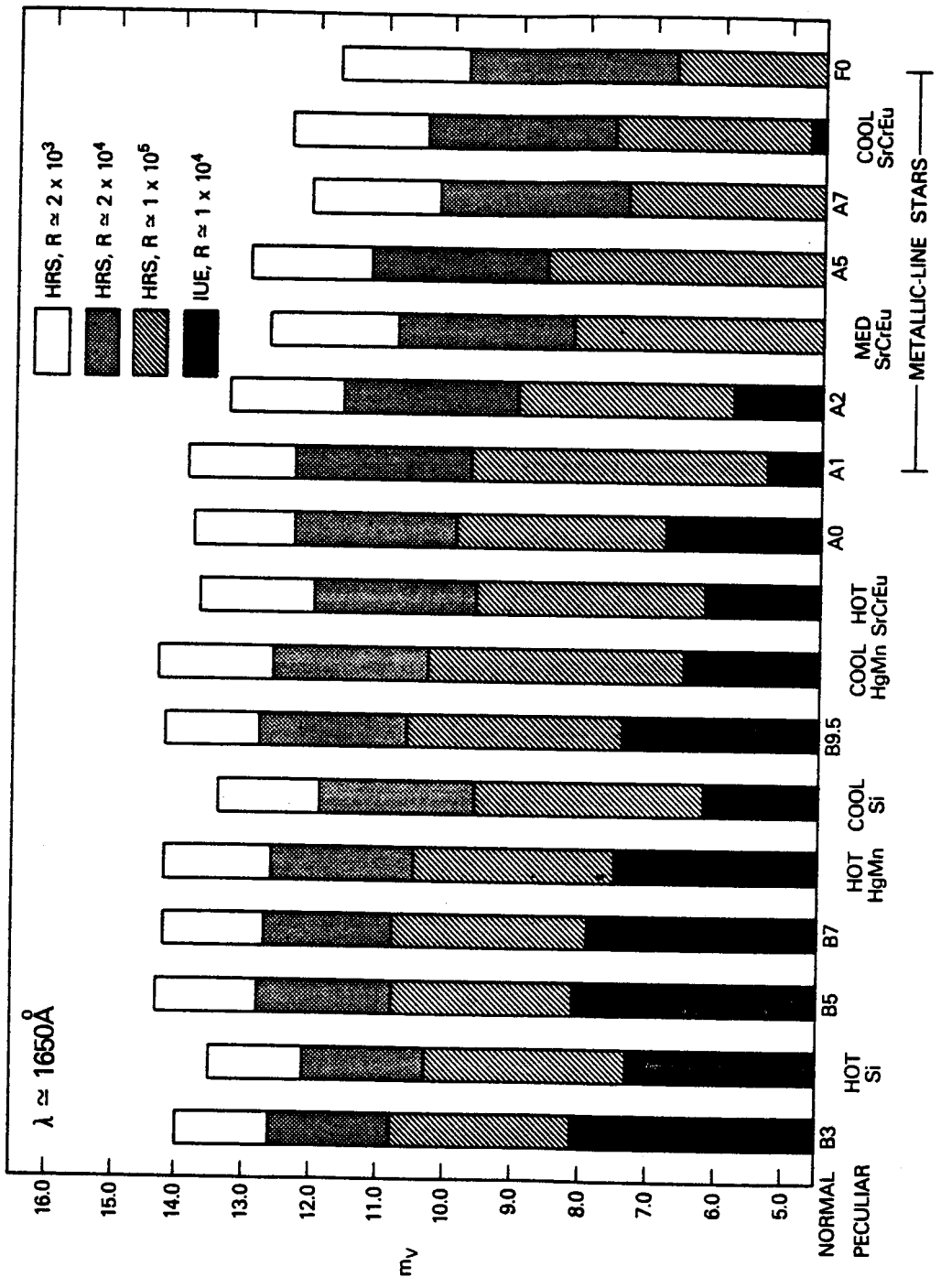

Figure B-3 Same as B-2 for 1650 A (D.S. Leckrone).

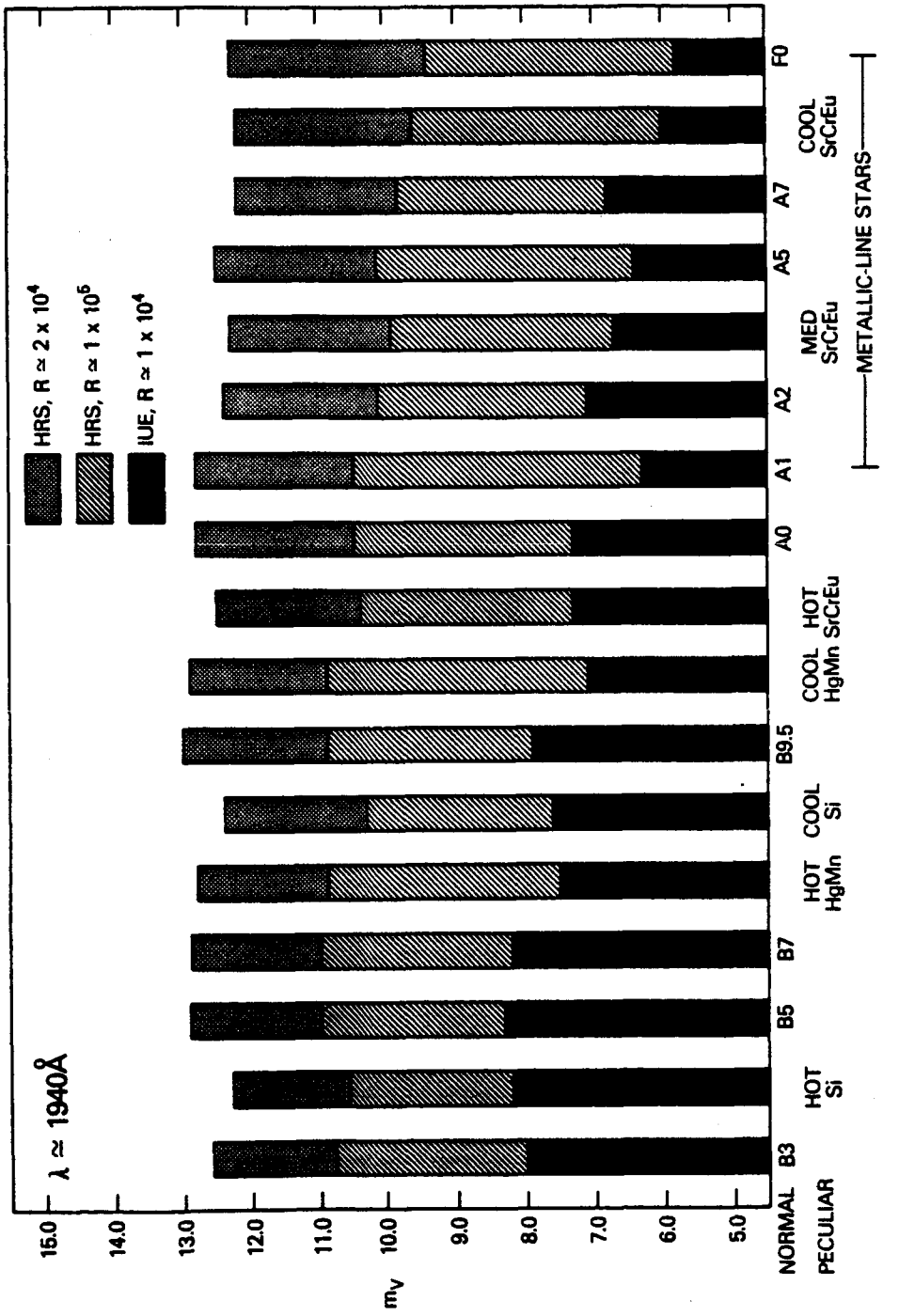

Figure B-4 Same as B-2 for 1940 A (D.S. Leckrone).

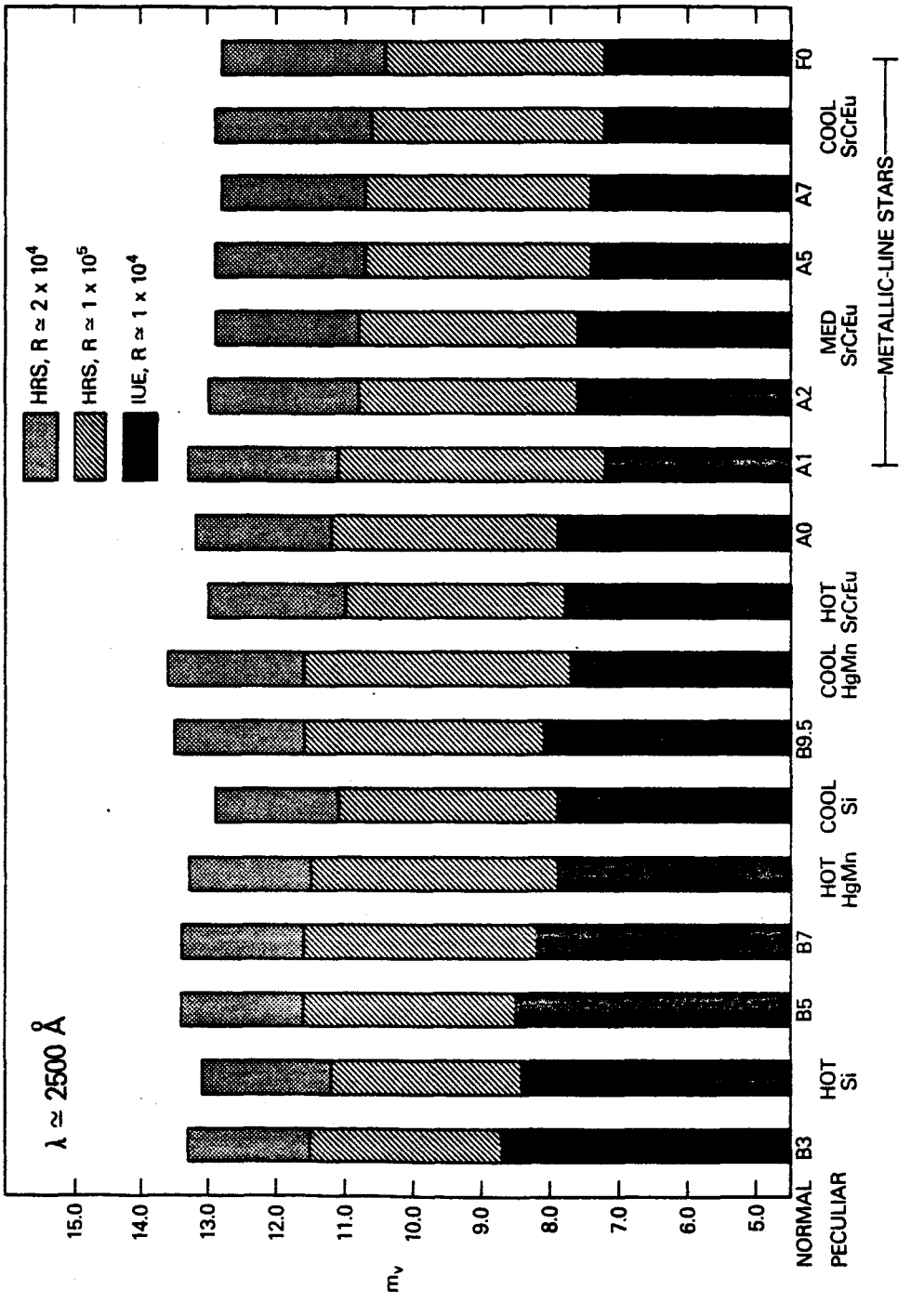

Figure B-5 Same as B-2 for 2500 A (D.S. Leckrone).

Figure B-6 (prepared by J.L. Linsky) gives limiting magnitudes for an emission line in various cool stars. The assumptions used are stated on the figure.

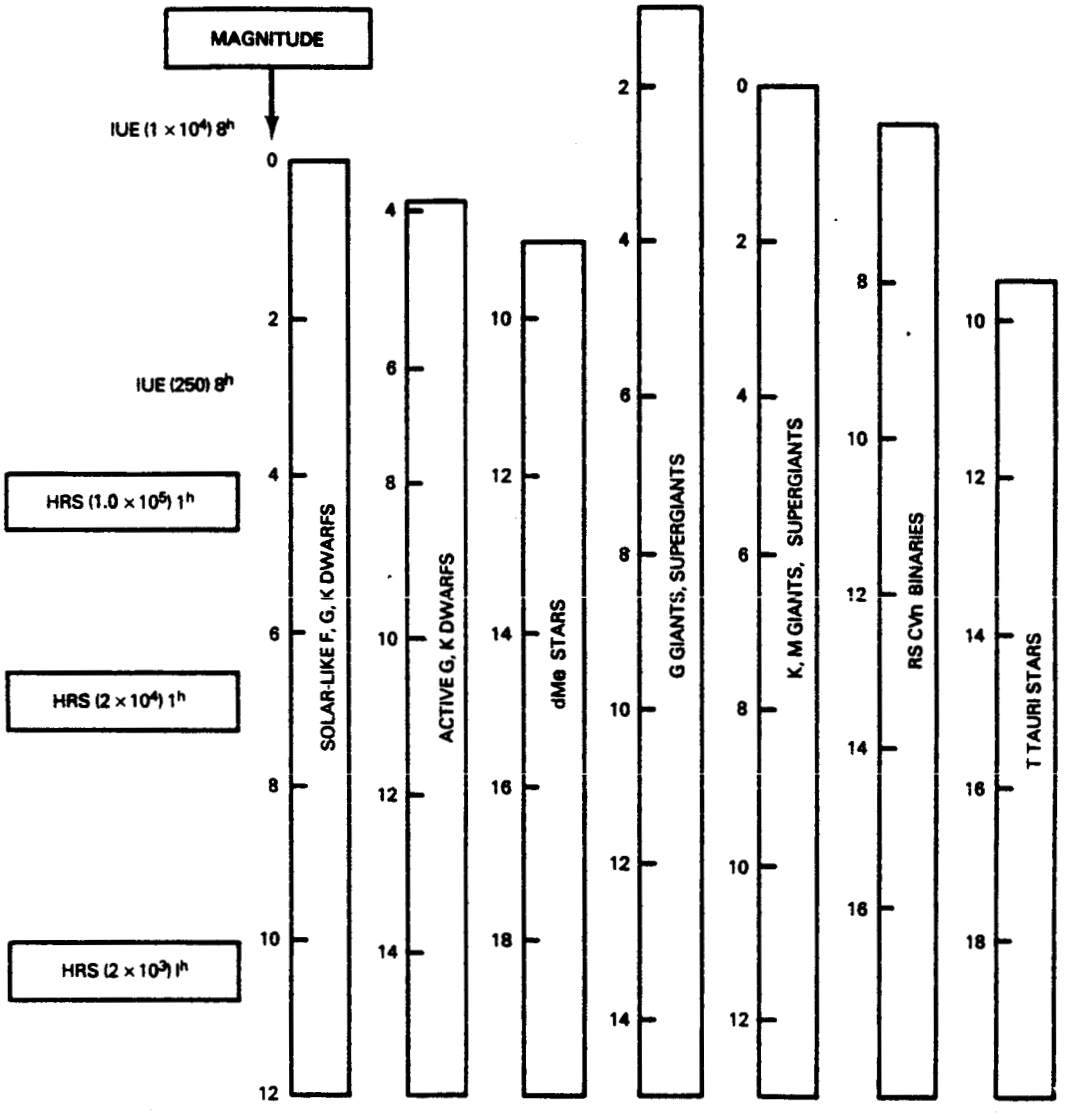

MAGNITUDE LIMITS FOR OBSERVATION OF C IV λ1548 EMISSION LINE WITH S/N = 10 (OR C I λ1657) IN SPECIFIED TIME FOR UNREDDENED STARS

Figure B-6 Visual magnitude limits for observation of selected emission lines in cool stars (J.L. Linsky).

N82 33304

The High Speed Photometer for the Space Telescope

R. C. Bless

Astronomy Department, University of Wisconsin-Madison
Madison, WI 53706

and the HSP Investigation Team

Introduction

Ground-based high speed photometry has developed rapidly over the last decade or so and is yielding significant results concerning a variety of objects, such as cataclysmic variables and the non-radially pulsating white dwarf ZZ Ceti stars; the rings of Uranus were discovered by fast occultation photometry. These observations however, are affected in various ways by the earth's atmosphere which not only limits the observable spectral range, but also introduces scintillation noise which makes it difficult to search for variability at time scales less than about one second. Ground-based observations also require photometer apertures to be several arc seconds in diameter, thus increasing the contribution of the sky background to the signal, or in the case of occultations, increasing the amount of scattered light from the occulting object. An observatory in space, with excellent telescope optics and stable pointing system, is free from these limitations. The High Speed Photometer (HSP) exploits the capabilities of the ST by making photometric measurements over the visual and ultraviolet at rates up to 10^5 Hz and by measuring very low amplitude variability (especially for hotter stars in the UV). A secondary purpose of the instrument is to measure linear polarization in the near UV.

As an example of the striking improvement made possible by the ST, consider occultation observations. Although occultations from a space observatory occur more rapidly than those observed from the ground, the ST makes possible a large increase in the number of occultation opportunities. This is so because the smaller photometry apertures which can be used on ST produce a much improved signal-to-noise ratio. Only a dozen or so stellar occultations useful for investigating planetary atmospheres have occurred over the past two or three decades; from ST the number should increase to one or two per year for each planet. Furthermore, ST offers the possibility of "stationary" occultations, i.e. twice during each orbit the moon appears to be nearly stationary with respect to the celestial sphere. Objects within a box approximately 0°.5 x 0°.03 occulted by the moon will be occulted more slowly than the same objects observed from the ground. Thus over about a twenty year period many objects which the moon occults will undergo a stationary occultation as seen from ST, enabling these events to be observed at a very high signal-to-noise ratio.

In what follows we will present an overview of the HSP, its optics and detectors, its electronics, its mechanical structure, and finally some observational considerations. This should enable the reader to understand enough of the capabilities and limitations of the HSP so that he or she can begin to consider various observing programs which might be carried out with this instrument. Information needed for detailed observational planning, e.g. filter transmission curves, will be available from the ST Science Institute at a later date.

HSP Detectors and Optics

Figure 1 shows a sketch of the arrangement of the detectors and optics in the HSP. There are five detectors in the instrument - four image dissector tubes and one photomultiplier tube. The former are ITT 4012RP Vidissectors, two with CsTe photocathodes on MgF faceplates (sensitive from λ1200 to λ3000) and two with bialkali cathodes on quartz faceplates (sensitive from λ1800 to about λ7000). Each image dissector tube, its voltage divider network, and its deflection and focus coils are all contained in a double magnetic shield within the housing. The photomultiplier is a Hamamatsu R666S with a GaAs photocathode. Three of the image dissectors - the two CsTe and one of the bialkali tubes - are used for photometry. The second bialkali dissector is used for polarimetry, and the photomultiplier along with the bialkali photometry dissector are used for occultation observations. For convenience, we will refer to the photometric, polarimetric, and occultation "modes", but in most respects the operation of the various detectors is identical.

Consider the photometric mode first. Light from the ST enters the HSP through one of three holes in its forward bulkhead. These holes are all centered on an arc about 8 arc min off-axis. After passing through a filter and aperture, the light is brought to a focus on the dissector photocathode by a relay mirror - a 60mm diameter off-axis ellipsoid located about 800mm behind the ST focal surface. The relay mirrors enable a more efficient use to be made of the ST focal plane available to us than would otherwise be possible, i.e. no more than two image dissectors could be placed directly in the focal plane. The

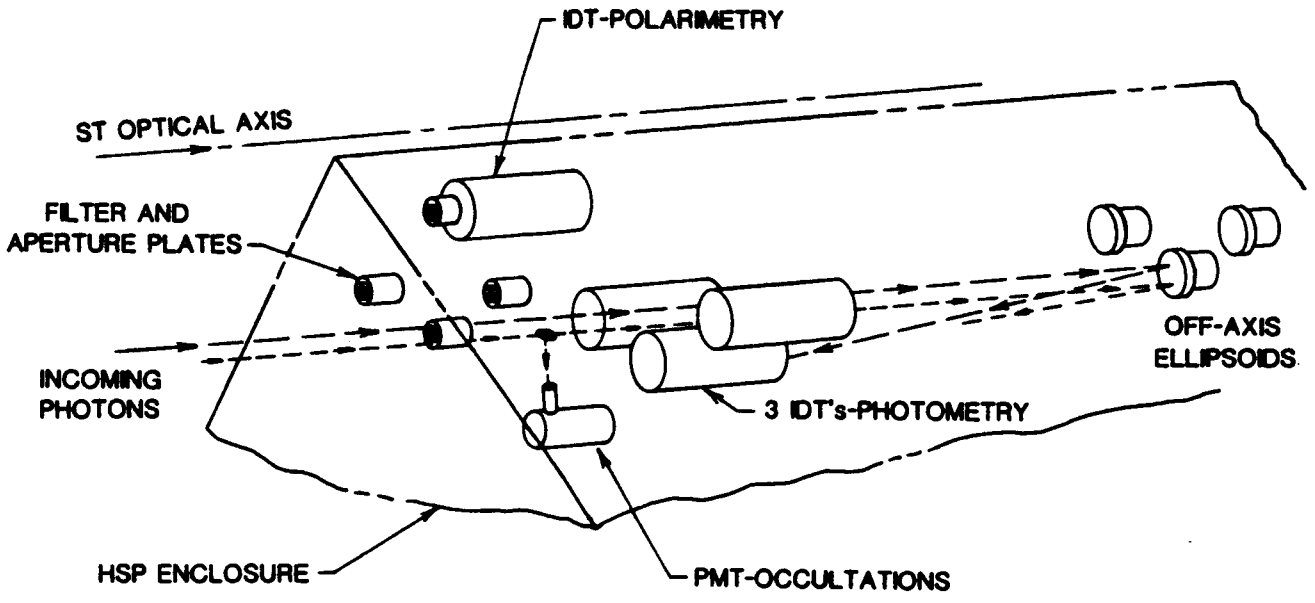

HSP DETECTOR ARRANGEMENT

Figure 1

magnification of the relay mirrors is about 0.65 which converts the f/24 bundle entering the HSP to an f/15.6 at the photocathode, with a corresponding change in scale from 3.58 arc sec/mm to 5.54 arc sec/mm, respectively. The off-axis ellipsoids produce images at the photocathode which are about 0.25 arc sec in diameter. The actual intensity distribution at each image is some combination of the geometrical aberrations and ST point spread function. Since about 70% of the energy in an ST image falls within a circle whose diameter is 0.2 arc sec, it is reasonable to expect that the total image blur will be about $\sqrt{2}$ times larger than the geometric blur. For this reason one set of HSP apertures was made 0.4 arc sec in diameter. Images which encompass 90% or more of the energy, however, are more than 0.5 arc sec in diameter. Addition of the effects of worst case pointing jitter and other uncertainties, led to the choice of 1.0 arc sec for the diameter of the second set of apertures.

The only unusual feature of the HSP's optical system is in its filter-aperture "mechanism" (see Figure 2) mounted behind each forward bulkhead entrance hole. Each plate contains thirteen filters mounted in two rows positioned 36mm ahead of the ST focal plane. At this location the converging bundle of light from the ST is 1.5mm in diameter, well within the 3mm width of each filter. For each filter plate there is an aperture plate located at the ST focal surface which contains 50 apertures arranged in two rows that are positioned directly behind the corresponding rows of filters. Nine of the filters are associated with four apertures - two with diameters of 1 arc sec (280μ) and two with diameters of 0.4 arc sec (112μ); because of space limitations, three more filters are associated with only three apertures. The thirteenth filter, of double width, has five associated apertures, including one of 10 arc sec diameter for object acquisition. The ST is commanded to point so that the objects' position in the ST focal plane coincides with the particular filter-aperture combination desired. Light from the object is then focussed on the dissector cathode by the relay mirror. The resulting photoelectrons are magnetically focussed and deflected in the forward section of the image dissector so that the photocurrent is directed through a 180μ aperture (corresponding to 1 arc sec on the sky). This aperture connects the forward section of the detector with the 12 stage photomultiplier

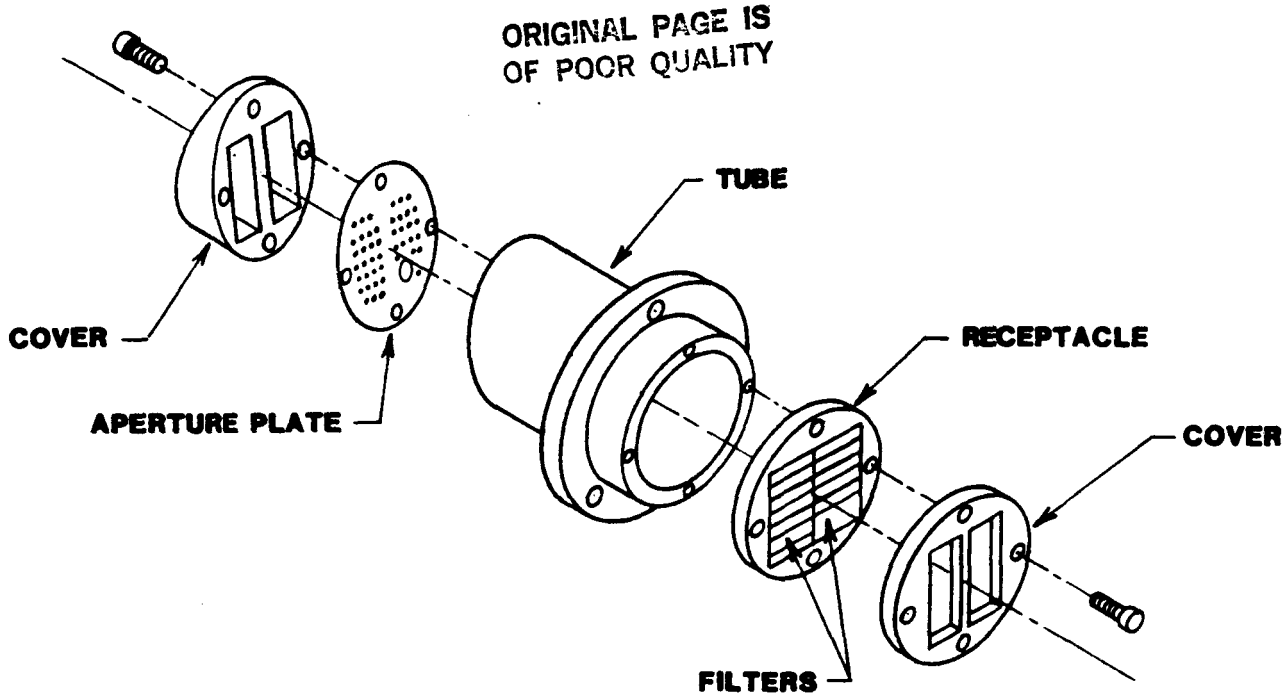

HSP FILTER/APERTURE TUBE CONFIGURATION

Figure 2

section. Thus with no moving parts, 27 different filter-aperture combinations are available for each photometry detector in the HSP.

All of the filters are multi-layer interference filters of Al and MgF_2 evaporated on MgF_2 substrates for the far ultraviolet, or on suprasil quartz for the near UV. The visual filters consist of Ag and MgF_2 layers deposited on glass. Their general characteristics are listed in Table 1. Some filters are common to all three photometry image dissectors for the sake of redundancy as well as to enable all three channels to be tied together photometrically. Other filters define bandpasses similar to those flown on previous space observatories while yet others are similar to some in the Wide Field and Faint Object Cameras.

To operate in the so-called occultation mode, light from the target object passes through a filter (in this case clear glass) and on through a 1 arc sec aperture after which it strikes a Ag-MgF_2 beam splitter at 45° to the incident beam. The mirror reflects red light to the photomultiplier via a red glass filter and a Fabry lens. The beam splitter passes a spectral band in the blue on to a relay mirror and to an image dissector. Occultation observations can therefore be made at about λ8200 and λ3200 simultaneously. Single bandpass occultation observations can of course be made with any of the filter-aperture combinations available.

Finally in the polarimetric mode radiation (only about 4 arc min off-axis) passes through a filter-aperture assembly directly to the image dissector; no relay mirror is used. The filter assembly contains only four near UV filters (see Table 1) across which are four strips of 3M Polacoat each with its polarizing axis 45° from its neighbor's. The aperture plate contains one arc sec apertures only, two for each filter-polarizer combination. Linear polarization at each of the four bandpasses is measured by observing through each of the four polaroids in succession.

Table 1

HSP Filters

Photometry λ	Photometry FWHM	Photometry λ	Photometry FWHM	Polarimetry λ	Polarimetry FWHM
1200	200	3400	(u)	2175	200
1400	200	4100	(v)	2450	300
1550	200	4700	(b)	2800	300
1700	200	4860	Hβ	3400	300
1800	300	5500	(y)		
2175	200	5500	V		
2450	300	6200	R		
2800	300	1800-7000			
1200-3000					
1800-3000					

FWHM = full-width at half maximum transmission

Electronics

Figure 3 shows a block diagram of the HSP electronics. All five detectors have identical electronic subsystems with the obvious exception of the photomultiplier, which does not have amplifiers to drive focus and deflection coils needed in the image dissectors. The high voltage power supplies are 8-bit programmable to provide negative DC voltages between 1500 and 2500 volts for the detectors. One benefit of this programmability is that it provides a means of extending the dynamic range of the detectors in their analog (current-measuring) mode. The preamplifiers, located near their respective detectors, provide a voltage gain of about 7. Their output is received by pulse amplifier/discriminators which amplify and detect pulses above a threshold set by an 8-bit binary control input, enabling the signal-to-noise ratio to be optimized for any high voltage setting. All detectors can be operated in either a pulse counting or current mode. In the former mode data can be taken in integration times as short as 10μsec, commandable in 1μsec intervals to any longer time. The delay time between successive integrations can be any value, including zero. Pulses separated by about 50nsec or more can be separately detected so that count rates of up to 2×10^5 Hz can be accomodated with a dead-time correction of no more than one percent. In the analog mode a current-to-voltage converter measures detector current outputs over a range of 1 nA to 10μA full scale in 5 decade gain settings selectable by discrete command inputs. Full scale output is 10 V. The amplifier output is converted to a 12-bit digital value by an A/D converter. The shortest observation times range from 4ms in the 1 nA range to 0.4ms in the 10μA range.

The five identical detector controllers perform those functions which relate to a specific detector, i.e. they receive a sequence of parameters and instructions from the system controller necessary for an observation and science data collection. Each contains an I/O port, a storage latch, two pulse counters, and a multiplexer. Detector parameters are received from the system controller through the I/O port and are stored in eight one-byte latches. These latch outputs are used to control focus and deflection amplifiers, high voltage power supplies, discriminator thresholds, analog gain settings, etc. A 1.024 MHz clock signal, received through the I/O port, supplies a signal to the A/D converter and synchronizes sampling start and stop control signals to the two pulse counters. It can also be used as a test input to the counters. The outputs of the two pulse counters, the A/D converter, and the eight one-byte latches are multiplexed and transmitted through the detector controller bus I/O port to the system controller.

As its name implies, the system controller's functions have to do with the instrument as a whole rather than with a specific detector. These functions include serial command decoding and distribution, detector controller programming, science data acquisition and formatting, serial digital engineering data acquisition and formatting, and interfacing with the ST command and data handling system through redundant remote modules and redundant science data interfaces. The system controller consists of an Intel 8080 microprocessor, memory, and various I/O ports. Direct memory access is provided to allow rapid data transfer through the science and engineering data ports, and for acquisition of science data from the detector controllers and rapid storage in memory. An 8K byte ROM block is provided for the microprocessor program storage. The remaining memory is composed of six 4K blocks of RAM which may be configured in any order. Four K of the RAM are allocated for the microprocessor system, 16K as a buffer for science data storage, and 4K as spare block. Each buffer can be used independently or alternately in sequence. The spare block may be used to replace any other 4K block which becomes defective. In contrast to the detector controllers, the system controller is dual standby redundant.

The power converter and distribution system converts the input +28V DC bus power from the ST to secondary DC outputs required by all other subsystems and provides power input switching and load switching for independent operation of individual detector electronics and heaters. The DC-DC converters essential to overall instrument operation are standby dual redundant. Converters which power electronics associated with only one detector are not redundant. With three detectors and their electronics on simultaneously the power consumption is about 135W.

HSP Structure

The HSP is aligned and supported in the ST at three registration points (see Figures 4 and 5). Two of these (one forward and one aft) have ball-in-socket fittings, and the third point (in the forward bulkhead) provides tangential (rotational) restraint. The mechanical loads (including a pre-load to keep the HSP in alignment) are transmitted from the instrument to the telescope structure through the three registration points. The two ball-in-socket fittings, the electronics boxes, and the optical and detector system are all mounted directly to a box beam and baseplate, the main structural elements of the HSP. The box beam runs the length of the instrument thereby connecting the two forward and aft fittings and carries the preload. The baseplate (actually a milled-out lattice structure) is attached to the box beam and provides stiffness to the structure. Four internal bulkheads on each side of the box-beam and baseplate form ten bays for the electronic boxes which are mounted on the baseplate. In addition to giving mechanical support to the electronics and to the wire harness, the baseplate provides a high conductance path between electronic modules as well as a radiating surface. The optics and detectors are mounted to (but thermally isolated from) the box-beam on the side opposite the baseplate, and at the forward end of the instrument. Detectors are not actively cooled and are expected to range in temperature between -15°C and 0°C for "cold" and "hot" orbits, respectively. Over an orbit their temperatures will change by no more than 0.1°C. The total weight of the HSP is 273 kg.

Observing with the HSP

Consider now an observation one could make with the HSP. Suppose it is desired to do photometry on a star in several wavelength bands in the ultra-violet. The observing program (including the required guide stars), planned well ahead of time according to a schedule to be established by the ST Science Institute, will be translated to the appropriate ST and HSP commands, checked to see that no operational constaints are violated, and transmitted to the ST where it will be stored until the specified execution time. The ST will then acquire the guide stars in such a way that the program star falls within the 10 arc sec aperture of the specified image dissector. A 20 x 20 raster scan is

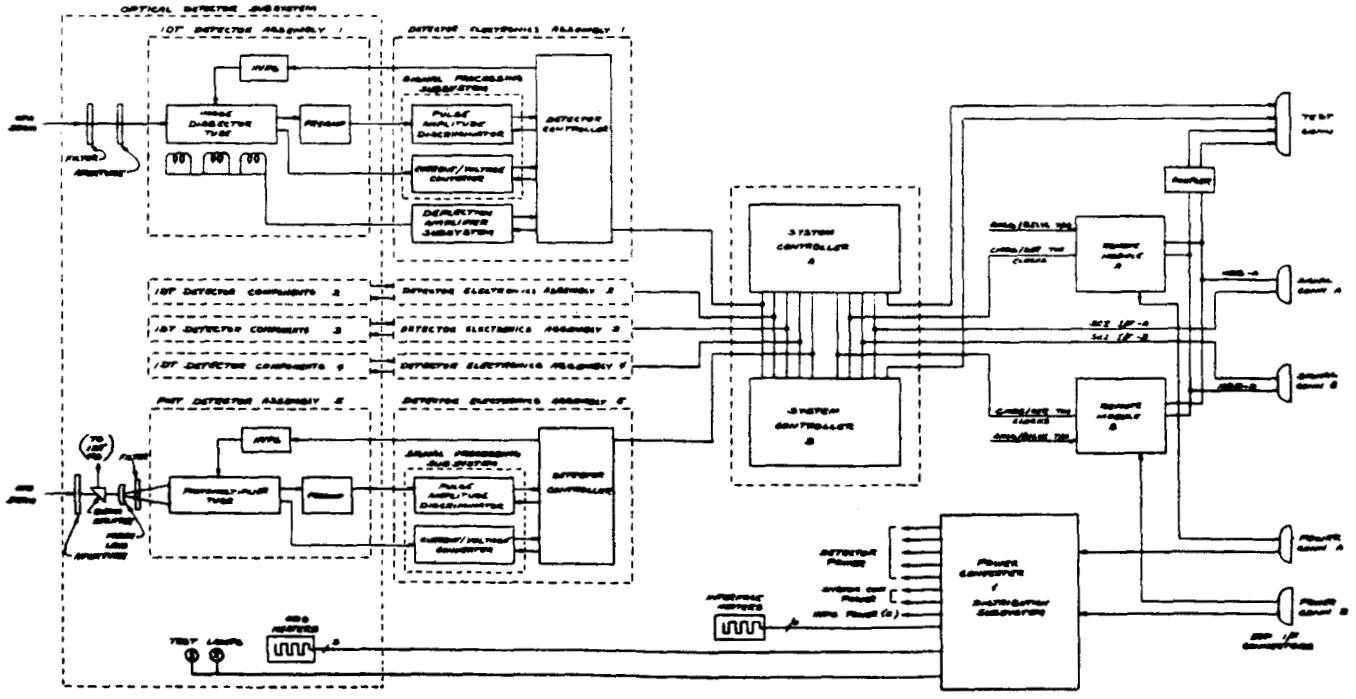

Figure 3 - HSP Electronics Block Diagram

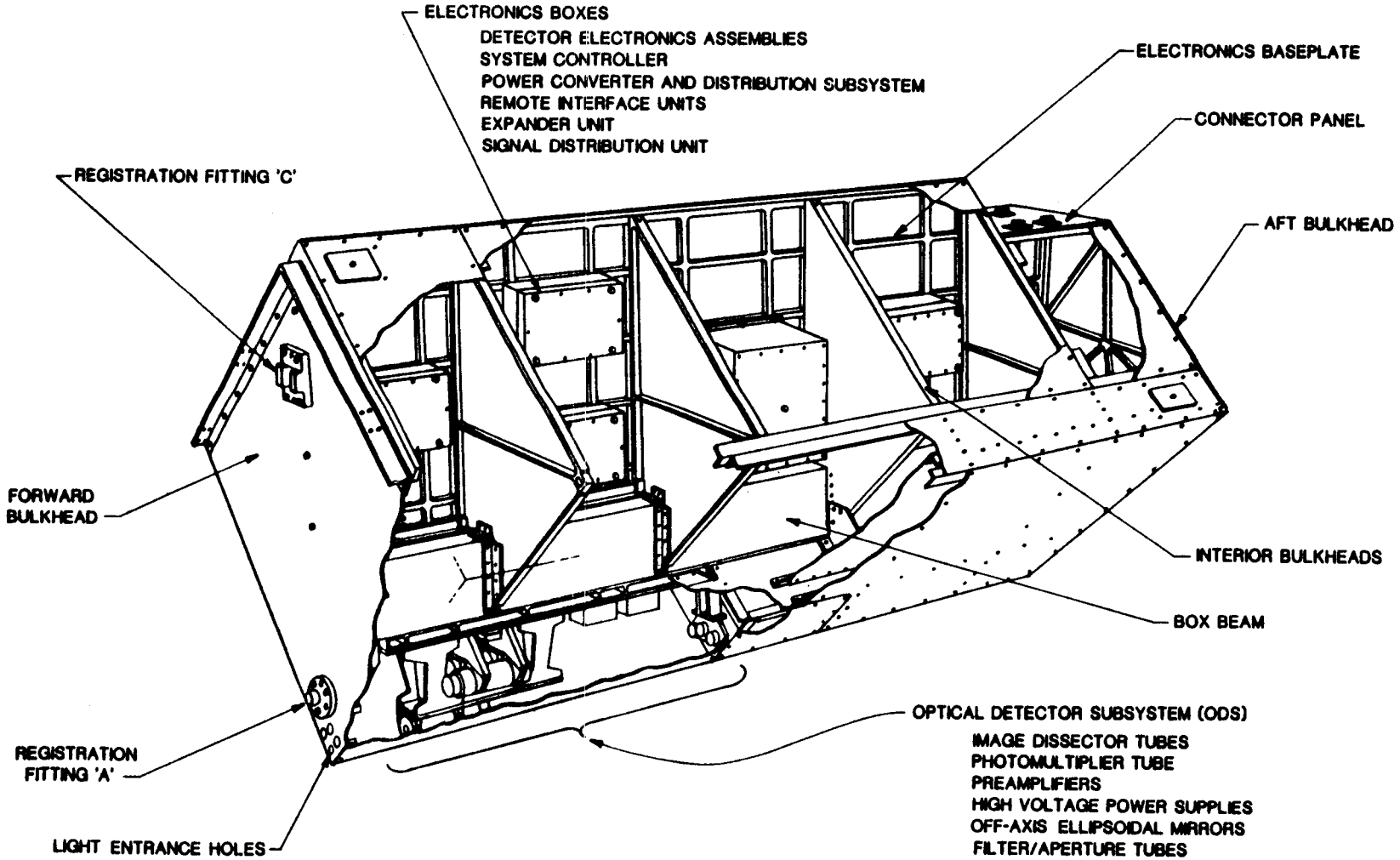

HIGH SPEED PHOTOMETER

Figure 4

performed by the dissector. If the star field is simple so that the program star is the brightest object or the only object within a specified magnitude interval, the centroid location of the star is found automatically and the correct offset to the first filter-aperture combination is calculated. This offset is passed to the ST pointing control system and the small maneuver is carried out. The program star is now in the correct aperture, the detector parameters properly set, and the observation begins. If a measurement of the sky background is required, it can be made through one of the three other apertures corresponding to the same filter. Apertures in a given row are 7.5 arc sec apart so generally one aperture should be suitably located for a background measurement. The ST pointing is not changed; the dissector is simply commanded to collect photoelectrons from the point on the photocathode corresponding to the selected sky aperture.

In many instances the HSP will not require the pointing stability of which the ST is capable, e.g. when doing photometry on a bright star for which integration times are short. It may then be possible to carry out a photometry sequence with the desired filter-aperture combination under gyroscopic control rather than under the control of the full fine guidance system. This would shorten considerably the time required to carry out such observations. This and other operational possibilities, e.g. observing while the ST passes through the trapped radiation in the South Atlantic Anomaly, will have to be investigated after launch.

The minimum time required for the image dissector beam to be deflected from one location to another is about one msec. Should star and sky data be required at integration times shorter than that two alternatives are available; either background observations can be taken before and after the high speed data run, or if a second dissector contains a filter identical with or relatable to the filter used for the program star, two dissectors can collect data simultaneously, one from the star, one from the sky, with integration times for each detector as short as 14 μs. This is only slightly slower than the shortest 10 μs integration time possible when only one detector is collecting data. The 10^5 Hz data collection rate (in which a data word is 8 bits long rather than the usual 16) would fill the HSP buffers in only 0.16 sec. However, data at this rate can be transferred continuously to the on-board tape recorder for about 15 minutes where it will be stored until its contents are transmitted to the ground.

Most observations will be made by commands stored on-board the ST. About 10-15% of the time, however, it is expected that it will be possible to make interactive observations in real-time. This will be useful in many circumstances. For example, if the program star is in a crowded field it may not be possible to acquire it by means of the automatic finding routine described earlier. Instead, the raster scan would be displayed on the ground where the observer would indicate the program object with a cursor after which its position would be transmitted to the ST. Also, in real time one could change an amplifier gain or command a move to another filter-aperture combination should it be desirable to do so. Of greatest interest, perhaps, is the possibility of moving to another target star if, for example, the first one was in a quiescent rather than an active phase. In any case, all such changes must be checked beforehand to insure that no spacecraft constraints are violated by any of the possible program options. Furthermore, the end point of a series of real-time observations must be fixed in position and time regardless of whatever intervening adjustments are made. Despite these restrictions this mode should be of considerable use to HSP users interested in observing flare stars, etc.

The HSP contains no calibration lamps; its final radiometric calibration will be established by observing stars with known spectral energy distributions. A good estimate of the instrument's sensitivity can be gotten from the specification that in 2000 sec it be able to measure a 24^m star in the V band with a signal-to-noise ratio of 10. Typical image dissector dark counts and currents are less than 0.1/sec and 1 pA, respectively.

Several data processing routines are being developed to aid HSP observers. All of these may be used during real-time observing episodes as well as after the normal observational mode. They include converting the observed digital or analog signals to relative or absolute fluxes, background subtraction, data smoothing, determination of color indices, etc. Various data processing operations will be available for use on time series data, e.g. synchronous co-addition, fast Fourier transform, and auto-correlation routines.

The HSP is the simplest of the instruments on the Space Telescope. It has, however, certain unique capabilities which we hope astronomers fully exploit in the years ahead.

ORIGINAL PAGE
BLACK AND WHITE PHOTOGRAPH

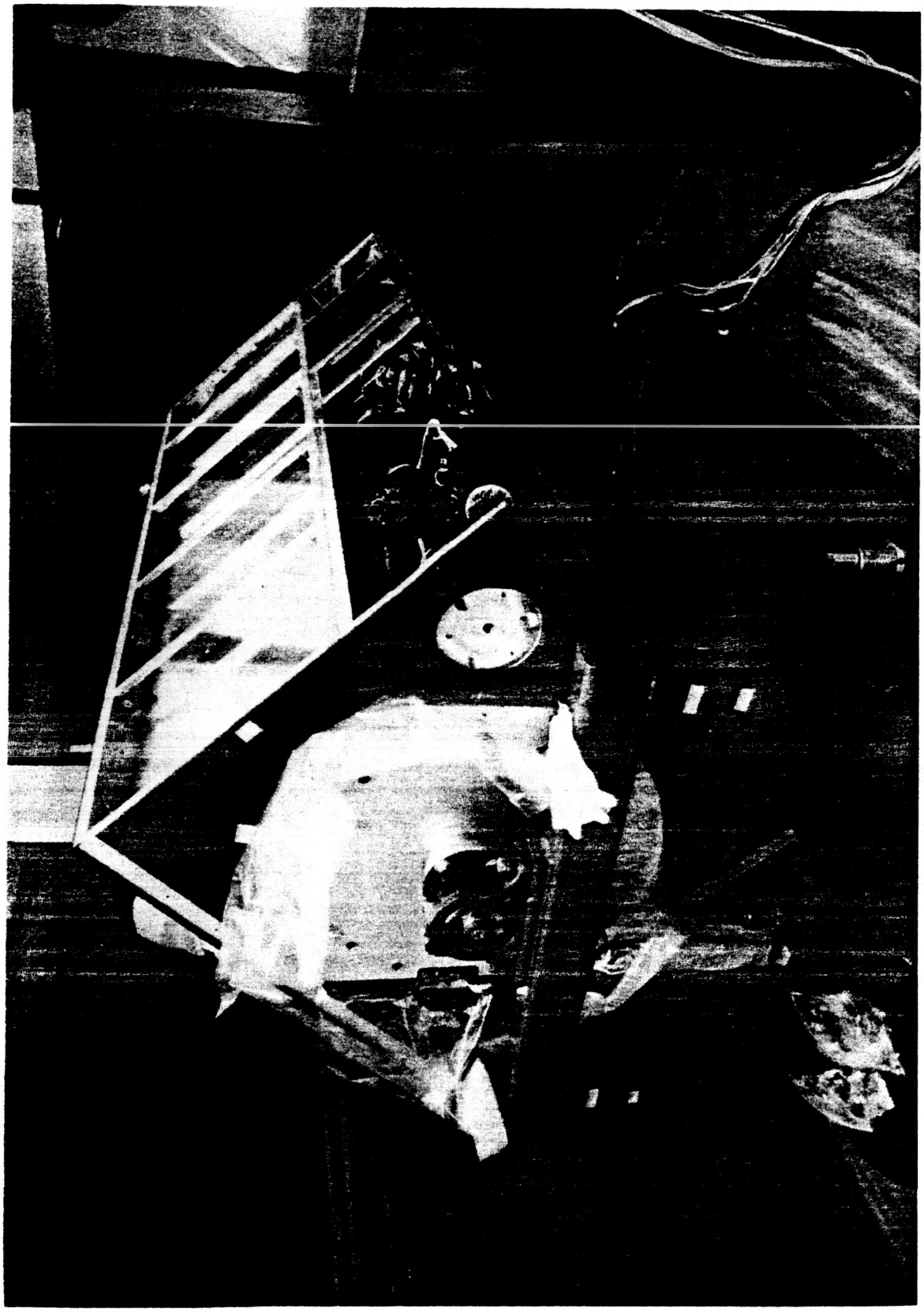

Figure 5 - The HSP in final assembly at the University of Wisconsin. The instrument, its ground support equipment, and its software were designed and constructed by the staff and students of the University's Space Science and Engineering Center and the Space Astronomy Laboratory of the Astronomy Department.

D9

N82 33305

Astrometric Observations with the Space Telescope

R. L. Duncombe
Department of Aerospace Engineering

G. F. Benedict, P. D. Hemenway, W. H. Jefferys, P.J. Shelus
Department of Astronomy

University of Texas at Austin
Austin, Texas 78712

ABSTRACT

Astrometry with the Space Telescope (ST) is performed using one of the Fine Guidance Sensors (FGS). The FGS, which is based on a pair of Koester's prism interferometers, one for each axis, is capable of measuring the position of one object relative to another with an accuracy of 0.002 arcseconds. Astrometric Data Reduction Software (ADRS), which will be available to the astrometric user of ST, is described. Finally, we discuss the kinds of problems the Space Telescope Astrometry Team plans to investigate using ST.

Astrometric Observations with the Space Telescope

The NASA/ESA Space Telescope (ST) will have the capability of measuring relative positions of stars within its field of view with an accuracy of 0.002 arcseconds rms. The magnitude range of ST astrometry is from 9-17 without filters, and may be extended to about the 4th magnitude with filters. The astrometric measurements are made with the Fine Guidance Sensors (FGS). Two of the FGS are used to control the pointing of the Space Telescope, and the third FGS (which may be any one of the three) will be available for astrometric measurements.[1-5]

Each FGS views a 90° sector of an annulus comprising the outer portion of the ST focal plane (Figure 1). Each sector of the annulus will henceforth be referred to as a "pickle"; each pickle is four arcminutes wide with a maximum chord length of about 18 arcminutes. The quoted measurement accuracy refers to the relative positions of two objects visible in the same pickle.

A schematic diagram of the FGS is shown in Figure 2. Each FGS contains an optical beam splitter, two orthogonal Koester's prism interferometers (one for each axis) and their associated photomultiplier tubes. Two beam deflectors, called "star selectors", rotate to bring the light from an object anywhere in the FGS field of view into the 3-arcsecond square aperture of the FGS detector assembly. If the object is exactly on the axis of the interferometer, the signal from each of the two photomultipliers associated with that axis will be equal, and the difference of the two signals will be zero. If the object is off-axis, the difference provides a non-zero error signal that measures how far off-axis the object is. Circuitry within the FGS itself then repositions the star selectors and brings the object back onto the interferometer axis, nulling the error signal. The relative position of two objects in the FGS field of view can be calculated from the angles θ_A, θ_B, $\Delta\theta_A$, and $\Delta\theta_B$ shown in Figure 3, which are given by the star selector positions.

When used as an astronomical instrument, the FGS has several modes of operation. In the lock-on mode, the interferometers are successively nulled on different objects within the same pickle. From the star selector readings, the relative positions of the objects are obtained. Secondly, there is the multiple star mode. In this mode, the target object is moved diagonally across the aperture of the FGS. As the object moves across the aperture, the error signal in each axis varies, tracing out the instrumental "transfer function" (see Figure 4). The transfer function can be analyzed to detect duplicity of stars, and to measure the relative positions of the two components. Finally, there is the moving target mode. In this mode, used for tracking moving objects such as minor planets, the FGS is kept locked on the object and the position of the object is sampled periodically.

The process of astrometric calibration will provide a means of determining the capabilities and limitations of ST astrometry. First, a calibration field (for which groundbased observations are available) will be measured with the FGS for zero-order plate scale and field distortion effects. Because no field is known which contains relative star positions accurate to 0.002 arcsec over 18 arcmin, overlapping plate techniques will be used to determine the field distortions to within a scale factor. Then a moving target, such as an asteroid, will be used to determine the scale to within the measuring accuracy of the FGS.[6] Finally, a sample of multiple and suspected single stars will be scanned with

the FGS to determine transfer functions and thence brightness distributions. Minimally broadened observed transfer functions will yield a good estimate of the ST-FGS instrumental transfer function.

It can be seen from the foregoing that there are certain serious restrictions on the use of the FGS for astrometry. First, two of the FGS are required for Space Telescope guidance, so only one is left free to make astrometric measurements. Second, the FGS is not an imaging instrument, but measures the positions of the objects in its field of view one at a time. The FGS cannot "see" an object but only "sense" its presence after moving to its approximate coordinates. Hence, the area of the pickle must be inventoried in advance and observations must be pre-planned in order to direct the FGS aperture in turn to each object to be measured.

Since the pointing and control of the Space Telescope is an engineering function, the data from the FGS come down the engineering data link. The data path from the ST FGS to the Science Institute is as follows: The signal from the FGS passes through the support systems module (SSM), is transmitted via the tracking and data relay satellite system (TDRSS), to the NASA communication ground station (NASCOM) and hence to the payload operations control center (POCC), where the astrometry data are stripped out of the engineering data stream. The astrometry data then go via the science operations ground system (SOGS) to the Space Telescope Science Institute (STScI).

Astrometric Data Reduction Software

To assist the astrometric user of the Space Telescope, a library of astrometric data reduction software modules (ADRS) will be available. The ADRS is based on the user selecting from a menu-like list of software modules, called "filters", to be applied to the data. Each module performs a well-defined operation on the data file, producing a new data file on which further operations may be performed. The user may select from among standard operations available to any operating system (for example, creation and deletion of files, editing and combining files, copying, saving and renaming files), and special modules created for astrometric purposes. The operating system of the computer also provides a facility for the user to define and name a sequence of operations in which one filter follows another. An on-line "help" facility is provided to give assistance to the user as needed.

In designing the software, a standard file format has been adopted, which is flexible and allows astrometric data to be structured in a hierarchical fashion for convenient processing (Figure 5). Individual data items are identified by alphanumeric identifiers that may be defined by the user or by the system. Special modules are provided which allow the user to take arbitrary data files and format them in this standard fashion for further processing by the software.

A number of specifically astrometric software modules are being written. These include modules for conversion among the various coordinate systems (e.g., instrumental, gnomonic, equatorial, and conversion among gnomonic coordinate systems with different tangential points), for the determination of the mean position of an object from the sequence of encoder readings which were obtained ("centroiding"), and for the correction of the data for various effects, both instrumental (optical distortion, "tilt", etc.), and physical (e.g., differential aberration due to vehicle motion as well as the motion of the Earth). The precession module will assume the new IAU76 precession constants as the default case.

For analysis of data taken in the multiple star mode, a special module is being written at Lowell Observatory for the analysis of transfer function data. This module will be capable of providing position angle and separations of double stars which have separations of greater than approximately 0.03 arcseconds.

The core of the ADRS system is the REDUCE module. REDUCE obtains a user-specified file which contains the reduction model for the current field. The reduction model can be quite arbitrary, involving any combination of linear, tilt and distortion terms, as well as color and magnitude terms (although these are not expected to be significant for ST). In addition, provision is made for the inclusion of any other terms the user may desire. There is, in principle, no limitation on the nature of the terms that may be part of the reduction model. The specification of each model to be included in the reduction is very simple; the names of the observations and parameters are declared, and the appropriate equation of condition is written down. The user may also use predefined models; a selection of standard models will be provided at the STScI for general use.

REDUCE writes a least-squares overlapping-plate reduction program[8-10] which is specifically tailored to the definition of the model specified. Either solution by use of traditional normal equations or using orthogonal transformations of the condition equations can be specified. Analytical derivatives are calculated for each of the terms in the model, and subroutines are provided to compute them. This program is then given to the compiler, and executable code is produced.

REDUCE may be used for overlapping plate solutions using arbitrary user-specified models, including parallax and proper motion solutions, astrometric binary solutions, visual binary solutions, functional fits to single and multidimensional data and orbital calculations. REDUCE will be used to determine calibration parameters and to perform data analysis tasks.

These programs, which will be available to the astrometric user of the Space Telescope, may be complemented by any additional programs the observer may wish to prepare for the analysis of data.

Scientific Program

ST astrometry is capable of accuracies from 2 to (more typically) 10 times greater than traditional groundbased astrometry. Such accuracies open up many exciting areas for research.

Parallaxes will be measurable with an accuracy of 0.001 arcsecond or better, bringing objects like RR Lyrae stars and Cepheid variable stars within range of the trigonometric parallax method. Improvements in the parallaxes of fundamental calibrators (e.g., the Hyades and Pleiades) will be possible. It may be possible to investigate systematic errors in ground-based parallaxes more thoroughly, thus improving their usefulness. The central stars of some planetary nebulae will be within range, and the parallaxes of other objects of particular astrophysical interest can be improved.

In double star astrometry, the separation range of 0.02-1.0 arcseconds is difficult to observe from the ground. As a consequence, the statistics of double stars in this range are poorly known. It will be possible with ST to obtain information on this every time the telescope is pointed, if a scan of a star in the third FGS is made routinely. The frequency with which such scans will actually be made is an operational question which has not been decided at this point. However, nothing in principle prevents a significant amount of statistical data on this very important question from being gathered. In addition, it will be possible to obtain visual orbits for some stars which are known spectroscopic binaries. This may be important in improving our knowledge about stellar masses, since the number of directly observed stellar masses is still very small.

Another very exciting area of research is the search for planets of nearby stars using the astrometric method. We estimate that about a dozen stars are likely prospects for the detection of planetary objects using ST astrometry.

Star clusters and stellar systems are another area of great interest for ST astrometry. Observations with ST (probably with the Wide Field Camera) may be used to measure the motions of stars within clusters, to detect the effects of tidal forces on the cluster and of mass segregation within the cluster. The latter is facilitated by the fact that the extreme sensitivity of the ST will make it possible to observe stars at the lower end of the main sequence. Proper motion information on stars in clusters can be obtained in a fraction of the time required for groundbased astrometry. It may even be possible to detect proper motions in nearby galaxies.

A major contribution by ST to fundamental astrometry is made possible by the ESA decision to launch an astrometric satellite, HIPPARCOS. The HIPPARCOS instrumental system of bright (to about 9th magnitude) stars will provide a "solid body" reference frame with an overall unknown rotation. Two separate problems with common solutions must be distinguished. One, to determine the rotation of the HIPPARCOS instrumental system, and two, to tie the actual coordinates of the HIPPARCOS instrumental system to some fundamental or absolute coordinate system. Using its capability to measure precise angular distances between objects of disparate magnitude, the Space Telescope can be used to tie the HIPPARCOS system to: a) an absolute coordinate system derived from radio interferometric observations using radio sources which have discrete optical counterparts, b) very distant and, hence, relatively motionless objects such as QSO's and c) a dynamical system such as that defined by the motions of selected minor planets.[11]

Observations of bodies in the solar system will provide more information on the gravitational fields of the planets than has been obtainable from the ground. In particular, inter-satellite angular distances measured with the FGS will provide data good to 5 km at the distance of Jupiter and 10 km at the distance of Saturn. Long term observations of the satellite systems discovered by Voyager spacecraft may provide observational answers to some of the celestial mechanics questions raised by the very short interval fly-by observations.

Exotic, "non-standard" astrometric measurements include the gravitational deflection of light by Jupiter, the measurement of optical proper motions in quasars, and other projects, limited only by the imagination of the user and the true capabilities of the instrument after launch.

We believe that the astrometric potential of ST is one of the factors which make astrometry one of the more exciting areas in modern astronomy, a position not generally held in the previous generation.

Acknowledgements

The support of the National Aeronautics and Space Administration, under NASA contract NAS8-32906, is gratefully acknowledged. The authors would like to thank their colleagues on the Space Telescope Astrometry Team, Drs. Otto Franz, Laurence Fredrick and William van Altena, for numerous conversations and considerable assistance.

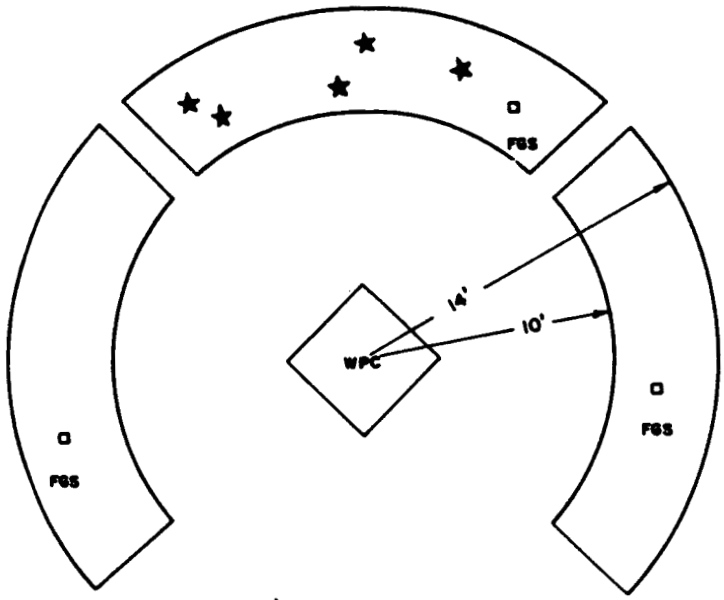

Figure 1: ST focal plane, showing location of FGS field of view.

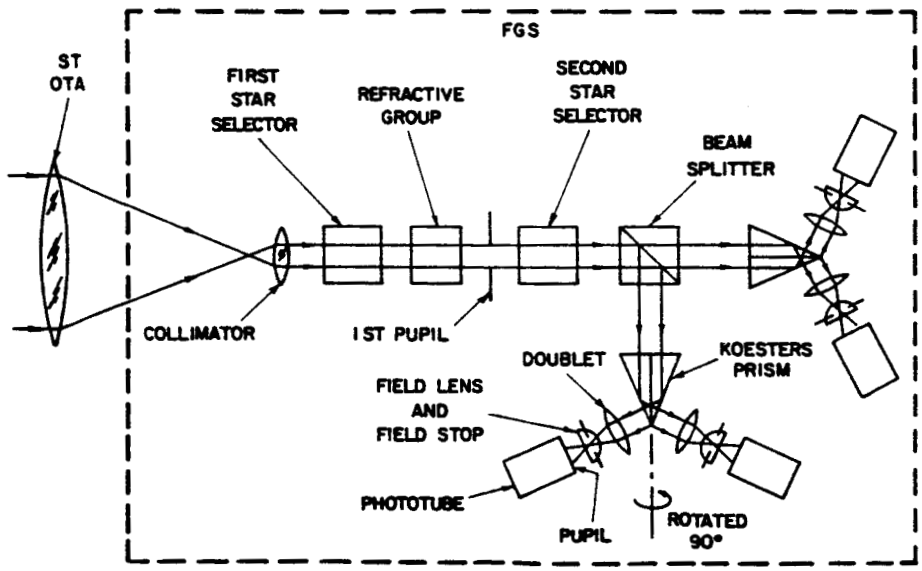

Figure 2: Schematic diagram of the FGS.

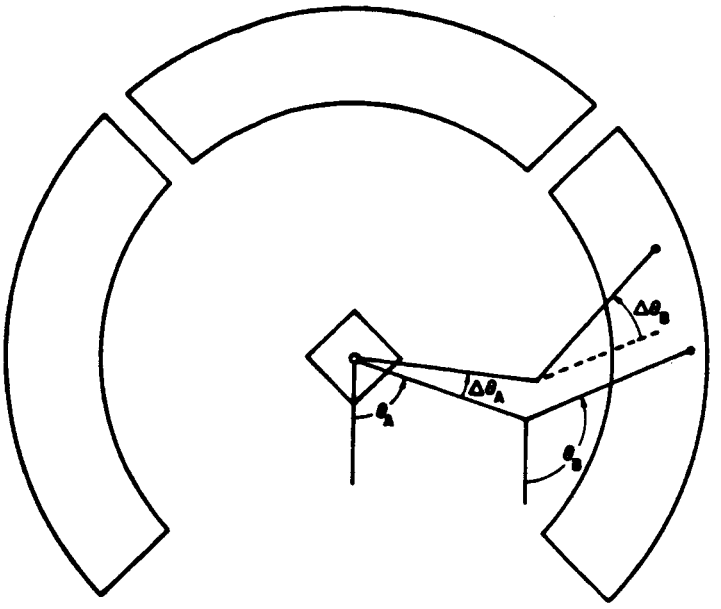

Figure 3: Geometry of the star selector coordinates.

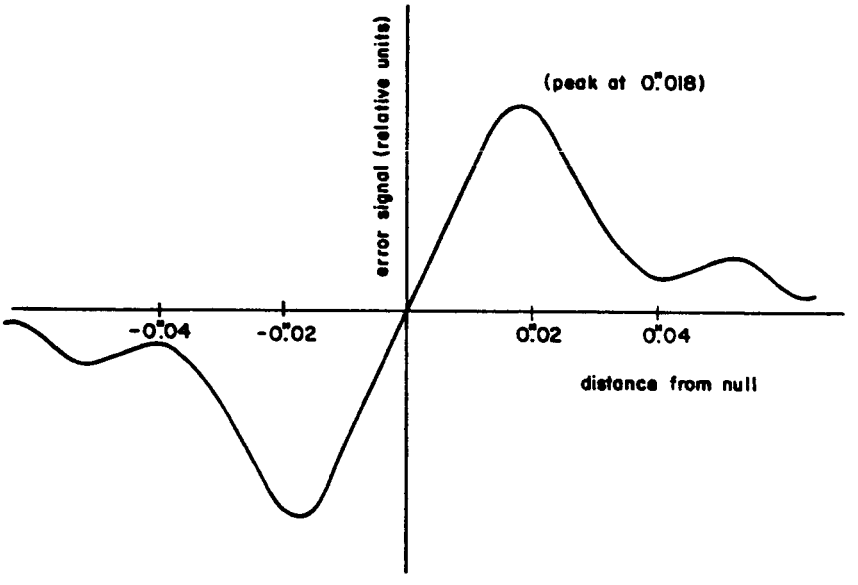

Figure 4: FGS transfer function.

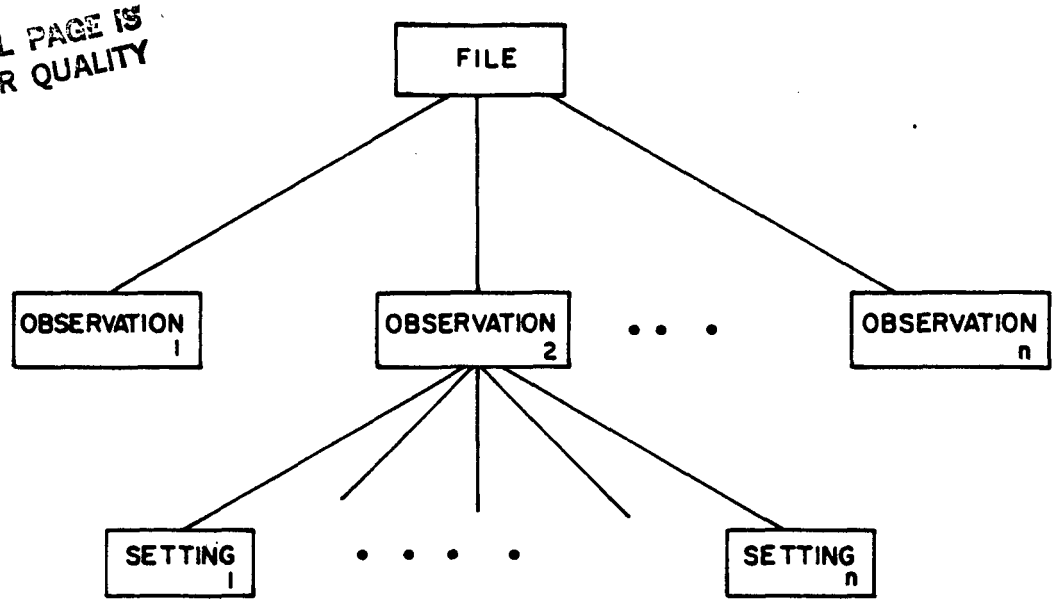

Figure 5: Structure of astrometry data files.

References

1. van Altena, W.F., Franz, O., Fredrick, L.W., 1974, IAU Symposium #61:283-293, "Astrometry with the Large Space Telescope".

2. Jefferys, W.H., 1978, Colloquium on European Satellite Astrometry, Padova, pp.111-115, "Space Telescope Astrometry".

3. van Altena, W., 1978, IAU Colloquium #48:561-571, "Space Telescope Astrometry".

4. Jefferys, W.H., 1980, Celestial Mechanics, 22:175-181, "Astrometry with the Space Telescope".

5. Jefferys, W.H., 1980, Highlights of Astronomy, 5:789-794, "U.S. Space Telescope: Astrometric Capabilities".

6. Hemenway, P.D., 1978, BAAS, 10:458, "Initial Considerations of Minor Planet Astrometry with Space Telescope".

7. Jefferys, W.H., Benedict, G.F., Hemenway, P.D., Shelus, P.J., 1982, BAAS, 14:581, "Space Telescope Astrometry Software".

8. Jefferys, W.H., 1979, A.J., 84:1775-1777, "On the Overlapping Plate Method in Astrometry".

9. Jefferys, W.H., 1980, A.J., 85:177-181, "On the Method of Least Squares".

10. Jefferys, W.H., 1981, A.J., 86:149-155, "On the Method of Least Squares II".

11. Hemenway, P.D., Jefferys, W.H., Shelus, P.J., and Duncombe, R.L., 1982, "Fiducial Reference for the HIPPARCOS Reference System" presented at the Colloquium on the Scientific Aspects of the ESA Space Astrometry Mission, Strasbourg, France, 22-23 February, 1982, (in press).

Reflections on the Space Telescope

M.S. Longair

Royal Observatory
Blackford Hill, Edinburgh EH9 3HJ, Scotland

1. Introduction

There have been a number of occasions in the history of astronomy when individuals or teams of scientists have awaited with anticipation the first results from a new telescope, knowing full well that they were about to uncover worlds which had never before been seen by man. One thinks of Galileo and his first observations of the Moon and the planets, of the pioneers of radio astronomy who first found that there exist discrete radio sources, of Dr Giacconi and the Einstein X-ray observatory, of the first Voyager pictures of Saturn, and so on. These moments when new observational horizons are suddenly opened up are among the greatest peaks of intellectual excitement which scientists ever experience and are comparable to those supreme moments when suddenly a new physical theory of obvious validity is discovered. We are all in the same position with respect to the Space Telescope. It is a tribute to the vision of the originators of this project that these moments of revelation are to be available not just to a small group of favoured scientists but to the whole astronomical community.

I have entitled this paper "Reflections on the Space Telescope" because it is a personal view of the significance of the project for modern astronomy. Besides inevitable personal bias, the range of topics considered is bound to be incomplete because of the rapid development of the subject. Nonetheless I believe it is worthwhile trying to set the stage for the types of question which are most important for the advance of astronomy and astrophysics. Because of the huge demand for observing time, we will all be trying to guess what the Time Allocation Panel will consider to be of the very highest scientific importance and consequently those programmes which self-evidently must be supported. I will then try to indicate how rapidly the scene can change by looking at some advances in astrophysics over the last 5 years which illustrate how, even since the time when the Space Telescope project was approved, the big issues have changed. If one was to write a proposal today for the use of Space Telescope, it would look rather different from one made, say, 5 years ago which is indeed what many of us have done. Then I will raise a number of my personal concerns about the project and finally look at some historical paradigms for the Space Telescope project.

2. Current Understanding of Astronomy and Cosmology

It is very rash to attempt to summarise the concensus of scientific opinion on such a grand scale. I hope I will be forgiven for reproducing my own version of the current state of knowledge in the form of a single table. This was produced for a recent semi-popular lecture and I am only too aware of its deficiencies. Obviously, it is biassed towards fields in which I have non-zero knowledge. Thus, it excludes substantial areas which will be very important for studies by the Space Telescope, in particular many aspects of Solar System studies, planetary atmospheres, etc. For reasons of brevity, these have been relegated to the heading "Problems of star formation". However, I am the last to underestimate the importance of understanding, for example, the physics of planetary atmospheres, an understanding of which may well be crucial for the continuance of life as we know it on Earth. However, my reasons for excluding topics such as that is that I want to look at the very broad issues of astronomy and cosmology. What are the broad areas in which there is general agreement on the state of knowledge and what are the most important questions to be addressed and, we hope, answered by observations with the Space Telescope. The first half of Table 1 indicates what I believe to be areas of consensus about astronomy and astrophysics and the second half lists fundamental problems associated with each area. I will expand on these topics in the following sections.

2.1 The basic physics of stars and stellar evolution

Many aspects of the physics of stellar structure and stellar evolution are among the most exact of astrophysical sciences. The facts that we can understand the evolution of stars on the main sequence and onto the giant branch in considerable detail is a great triumph of astrophysics. Most people would agree that the overall picture is probably correct but there are some significant worries. Perhaps the most immediate problem is that of our own Sun which must be a bench-mark for any theory of stellar structure. The

Table 1

What we know about astronomy and cosmology

1. The basic physics of stars and stellar evolution are understood.

2. Stars form in obscured dense regions of interstellar space embedded within giant molecular clouds.

3. The interstellar medium contains many phases and is not in equilibrium. Matter is circulated through the interstellar medium following processing in stars.

4. Galaxies are the basic building blocks of the Universe.

5. Most large scale high energy phenomena in galaxies are associated with the nuclei of active galaxies which contain a massive compact object, probably a black hole.

6. The hot big bang model of the Universe provides the most convincing framework within which to conduct astrophysical cosmological research.

What we need to know about astronomy and cosmology

1. Stars and stellar evolution
   - (i) The Solar neutrino problem.
   - (ii) Is stellar evolution in globular clusters really understood?
   - (iii) What determines mass loss rates during stellar evolution?
   - (iv) What are the progenitors of the various end points of stellar evolution?

2. Star formation
   - (i) What determines the rate of star formation and its dependence on density, temperature and chemical composition?
   - (ii) What is the initial mass spectrum and its dependence on density, temperature and chemical composition?
   - (iii) What is the precise sequence of events which take place during star formation and how are they related to what we observe?

3. Interstellar medium
   - (i) What is the rate of enrichment of the interstellar gas by the mass loss of stars of different types?
   - (ii) What is the distribution of fragile primordial elements such as D, ^{3}He, ^{4}He, ^{7}Li throughout the interstellar gas in our Galaxy?
   - (iii) What is the distribution of those isotopes which are sensitive tracers of the mechanisms of element formation in the Galaxy?

4. Galaxies
   - (i) What are the basic parameters which define the properties of a galaxy besides its mass?
   - (ii) What are the dynamical properties of the stars in elliptical galaxies?
   - (iii) What is the nature of the dark or hidden matter?

5. Active Galaxies
   - (i) Can we find definitive proof of black holes in active galactic nuclei?
   - (ii) How is energy extracted from an accreting compact object in a useful form?
   - (iii) What can we learn about the behaviour of matter in strong gravitational fields?
   - (iv) How are high energy particles accelerated and ejected as collimated beams from active nuclei?

6. The hot big bang
   - (i) What are the value of H_o and q_o?
   - (ii) What is the value of Ω and is it equal to $2q_o$?
   - (iii) What is the physical nature of the cosmological evolution of quasars, radio sources and galaxies in general?
   - (iv) Is there a cut-off at $z \sim 4$ and does it correspond to the epoch of galaxy formation?
   - (v) What can we learn about the formation of galaxies from observations of quasars and galaxies over the redshift range $0 < z < 3$?
   - (vi) What is the chemical abundance of the primordial material from which galaxies formed?
   - (vii) How do these problems constrain the very early stages of evolution of the Universe and its relation to Grand Unified Theories of elementary particles?

Solar neutrino problem is still with us despite intense efforts over the last 10 years to understand why there appears to be only about one third the flux of neutrinos observed compared with the predictions of the best models of the Solar interior. This is not the appropriate place to review possible solutions to this problem but it should suffice to say that, until it is understood, the Solar neutrino problem will remain a major worry for stellar evolution.

There are other major concerns about the comparison between the theory and the observed H-R diagrams for globular clusters. There remain fundamental problems of calibration of the H-R diagrams which introduce important uncertainties into the precise location of the main-sequence termination point. In addition, the internal scatter within the data on a particular cluster make the precise determination of the locus of stars on the H-R diagram difficult. There is accumulating data which suggest that the H-R diagrams of well studied clusters do not agree particularly well with the theoretical models.

A second major area of uncertainty is the role of mass-loss at various stages in the star's evolution. Once stars evolve off the main sequence, mass-loss must occur at various later stages if we are to explain the existence of horizontal branch stars, their ultimate evolution to the tip of the giant branch and the formation of planetary nebulae. Great advances have already been made with IUE in understanding mass-loss phenomena but there is still a very long way to go. Not only are the results of these studies important for stellar evolution, they are also crucial for understanding the chemical evolution of the interstellar gas.

A third major area of current uncertainty is what determines the ultimate object which forms at the end point of stellar evolution. What are the properties of the star which determine whether a white dwarf, a neutron star or a black hole will form when the star has used up all its nuclear fuel? The whole question may also be asked the other way around - what are the progenitors of the various end points of stellar evolution which we can now observe? Which stars become type I and type II supernovae, neutron stars or black holes? Why are the properties of type I supernovae so uniform? These are very fundamental questions of stellar evolution which bear upon the evolution of galaxies as a whole.

2.2 Star formation

One of the great achievments of recent years has been the understanding that stars form in dense obscured regions of interstellar space, these regions being embedded in very much larger diffuse clouds, the giant molecular clouds. Regions such as the Orion Nebula have been shown to be the seats of much greater activity than had been previously expected with the discovery of bipolar outflows of hot molecular hydrogen and other species. We can actually observe stars at very early stages in their evolution through their intense infrared radiation, although it is not yet clear exactly what stage this represents i.e. whether nuclear burning has actually switched on or not.

There are many basic questions to which we do not, however, have clear answers. For example, how does the rate of star formation depend upon the temperature, density and chemical composition of the interstellar gas from which stars form? What is the spectrum of masses of stars which form, i.e. the initial mass function, and its dependence on local physical conditions? While some of these questions are best answered by infrared observations, many of them can be addressed by optical and near infrared observations which can be carried out with the Space Telescope.

These basic questions are of central importance for our whole picture of galaxy formation and evolution. The dependence of the star formation rate upon physical conditions largely determines the luminosity of a galaxy at all stages in its evolution and thus determines the observability of galaxies even in their earliest phases of evolution.

2.3 The interstellar medium

It was once thought that the interstellar gas was a rather simple medium but now we know that it has a multi-phase, non-equilibrium structure. Phases of virtually all densities and temperatures are known, from cool giant molecular clouds inside which are embedded high density cool regions, through diffuse intermixed ionised and neutral hydrogen to a hot diffuse phase which is responsible for the high excitation absorption lines seen in the spectra of bright stars by IUE and the diffuse Galactic soft X-ray emission. What makes the picture complicated is the fact that the phases are not truly in equilibrium with one another. The hot phase is continuously heated by supernova remnants and the cool dense phases are strongly influenced by the shock waves and ionisation fronts associated with newly formed stars. A recent discovery which testifies further to the non-equilibrium nature of the interstellar medium is that of the neutral carbon CI line at submillimetre wavelengths. This has been observed at much greater strength than is

expected theoretically and in general terms, the solution to the problem of its existence must be that the neutral phase is not in equilibrium with the ambient radiation field.

There is thus the whole question of defining more precisely the properties of the "violent interstellar medium". In addition, there are some observations of special significance for cosmology. Paramount among these is the determination of the deuterium abundance and its variation with location in the Galaxy. The consensus of opinion is that most of the deuterium is synthesised early in the hot big bang and this accounts for the high abundance observed wherever we look in the Universe. However, because it is destroyed whenever it is processed through stars, it is also a sensitive measure of how much processing any piece of interstellar gas has undergone. It is generally believed that most interstellar matter has undergone some processing through stars and therefore if there are regions where much processing is believed to have taken place and deuterium still observed, a source of additional unprocessed material is needed. These topics are of great importance for the question of the infall of primordial material into our own Galaxy.

Of course, everything which one writes about our own Galaxy applies equally strongly to observations of nearby galaxies where it is simpler to take a global view of the interstellar medium.

2.4 Galaxies

Galaxies are the basic building blocks of the Universe and they come in a very wide variety of shapes, sizes and masses. However, it is becoming apparent that they are probably simpler objects than astronomers have any right to expect. I say this on the basis of the fact that many of the properties of galaxies seem to correlate with their masses. What type of galaxy one ends up with may well result simply from placing a self gravitating system of stars in different gaseous or galactic environments. This realisation, which has only come about over the last 5-10 years, gives me hope that we may be able to understand the various effects which give rise to the diversity of galactic phenomena we observe today and not have to construct a separate theory to explain each object in the Universe. I regard the verification or disproof of this concept as among the most important endeavours of extragalactic astronomy.

In addition, there are many things which we do not yet understand. One major spanner which has been thrown in the works is that we now know that for many elliptical galaxies, the observed flattening cannot be attributed to rotation. This evidence, in conjunction with the facts that the shapes and principal axes of elliptical galaxies can change with radius, indicates that the internal velocity distribution of stars in elliptical galaxies is much more complex than one might naively hope. Of course, when one realises that the gas of stars is collisionless, there was never any real reason to expect the velocity dispersion to be isotropic and Maxwellian at every point in an elliptical galaxy. Nonetheless, it raises many new issues concerning the orbits of stars in self-gravitating configurations and has resulted in some beautiful new theoretical studies by Schwarzschild and his collaborators. These investigations urgently require a firm observational basis from which to proceed to the proper modelling of the velocity distribution in galaxies. Among the items which have gone out the window with this new understanding is the idea that one can appeal to axial symmetry in working out the properties of galaxies; in fact elliptical galaxies are likely, in general, to be triaxial systems.

A second major problem area is that of the hidden or dark matter in galaxies. It has become clear over the last few years that not all the mass in galaxies is visible. The problem first came to light many years ago in the study of rich clusters of galaxies where there was not enough mass in the visible parts of galaxies to account for the gravitational binding of the cluster. This problem has remained and to it has been added the fact that ordinary galaxies have the same problem. To oversimplify grossly, the rotation curves of many giant spiral galaxies appear to remain constant out as far as can be determined. In the simplest approximation, this can be explained by a spherical mass distribution in which the mass interior to radius R increases as R, $(M(\leq R) \propto R)$. In addition, studies of the rotation curve of our own Galaxy and the velocity dispersion of globular clusters suggest that its rotation curve is also flat out to about 100 kpc. Now the luminous matter in galaxies falls off much more rapidly than this and so there must be some form of dark matter which dominates the mass distribution in the outer region, the "dark halo". Again to generalise rather sweepingly, it appears that on all scales from that of Sc galaxies to groups and clusters of galaxies and probably beyond, most of the matter is unobservable at present, other than by its gravitational influence. The discrepancy between the visible and invisible matter is agreed to be about a factor of 10 and possibly greater on the largest scales. Nobody is certain, however, about the form this hidden mass may take, the possibilities ranging from massive neutrinos to massive black holes.

The Space Telescope will provide evidence on this question in a number of different ways. Besides rotation curves for galaxies and velocity dispersions for their satellites, observations of the stellar luminosity function will indicate whether part of the mass discrepancy could be attributed to ultra-low mass stars or Jupiter-like objects which might be present in large numbers in the Galaxy. The discovery of further gravitational lensing quasars can set limits to the numbers of massive objects in the haloes of galaxies.

2.5 Active Galactic Nuclei

Under this heading, I include all the "exotic" active galactic nuclei which have come to dominate so much of astronomical thinking over the last 20 years. I therefore include quasars of all sorts, Seyferts galaxies of all types, N galaxies, BL Lac objects, etc. It is now appreciated that virtually all large scale high energy phenomena in the Universe are associated with activity in galactic nuclei. Even the largest scale radio sources with sizes up to 6 Mpc have their origin in active galactic nuclei on scales less than 1 pc in size. The major theoretical advance has been the realisation that there exist perfectly plausible physical processes by which active nuclei can liberate the vast energies required to power even the most luminous active nuclei. The picture of accretion onto massive compact objects is a very attractive source of energy and seems capable in principle of dealing with even the greatest energy demands.

There remain many problem areas, some of which stretch our current understanding of physics to its very limits. Let me indicate some of the basic questions to which I would like to know the answers.

(i) Can we find definite proof of massive black holes in galactic nuclei? There are some remarkably persuasive arguments but what one really wants is a combination of dynamical evidence on the presence of a compact mass at the galactic centre combined with evidence such as that recently obtained on NGC 4151 on the location and velocity of clouds more-or-less bound to the galactic nucleus.

(ii) How is the energy extracted from the central compact object? Here we need improved modelling in conjunction with very high angular resolution observations of the light distribution and spectra of active nuclei. In particular, there is a continuing need to try to relate optical activity in the nucleus with evidence on the production of ultr-arelativistic particles.

(iii) In these objects, we have a unique opportunity of studying the physics of matter in strong gravitational fields. We have some evidence that, in the case of NGC 4151, we may be looking to within 10 times the gravitational radius of the black hole and then we might hope to be able to observe directly phenomena associated with the dynamics of matter close to black holes.

(iv) What is the origin of the high energy particles in active galactic nuclei? How is the material accelerated and then ejected in the form of a collimated beam, as is required from radio observations of superluminal velocities and extended double structure?

A beautiful example of the type of programme I have in mind is the recent study of NGC 4151 carried out by a large international collaboration with IUE. Virtually all who have worked on active galactic nuclei have hoped that one day some significant correlation would turn up among the variability data which would provide real clues to the origin of activity in active nuclei. To be honest, I have not been particularly convinced by any of the "correlated activity" reported in active nuclei and it was always possible to argue that the situation was too complex or that the time scales which could be investigated were all wrong.

Perhaps the most remarkable result in NGC 4151 is a "hysteresis" effect whereby there is observed to be a strong correlation between the variability of the non-thermal continuum radiation and the intensity of the broad CIV line but with a time delay such that the intensity of the lines respond to increases and decreases in the continuum with a time lag.

It is interesting to note how the various observed properties result in information about the central object and its environment. The crucial pieces of evidence are (i) the time delay between the increase in continuum and the broad line emission of 5-10 days and (ii) the width of the broad line regions, $\Delta v \sim 10\text{-}20{,}000$ km s^{-1}. The first figure tells us the distance of the broad line region from the nucleus and incidentally is rather convincing evidence for the photoionisation models. In the second case, a significant fraction of the broad line velocity is turbulent or rotational, in either case, the velocity acting as a probe of the potential field of the nucleus. We can then use Kepler's law to measure the mass of the nuclear source.

$$\left(\frac{M}{M_\odot}\right) = \frac{r}{3}\left(\frac{v}{c}\right)^2$$

where r is measured in km. Inserting r = 5 light days and v ∿ 10,000 km s^{-1}, we end up with $M \sim 10^8 M_\odot$.

We may speculate why it is that the brightest Seyfert 1 galaxy in the sky turns out to have such convenient properties and end up with the sort of massive black holes which have been discussed for some time. We should look at the problem of investigating other active nuclei by the same technique. In the most luminous quasars, for example, we may expect much more massive black holes because according to the formula for the Eddington limiting luminosity

$$L \sim 10^{38}\left(\frac{M}{M_\odot}\right) \text{ erg } s^{-1}$$

and even with 100% efficient energy conversion luminosities of 10^{47} erg s^{-1} require $M > 10^9 M_\odot$. The velocity widths we observe in quasars are of the same order as those in NGC 4151 and hence the delay time will scale as the mass of the black hole. This sum suggests time scales of several years for quasars or very short time scale variations for similar phenomena in the nuclei of galaxies such as our own. The interesting point is that the range of time scales over which we could observe such phenomena for a wide range of active nuclei are from hours to years and so it is feasible to carry out similar programmes for other exotic nuclei. It will, however, require the dedicated efforts of many astronomers to make the observing time on the Space Telescope available.

The nature of the central accretion disc was also hinted at by these observations. The far ultraviolet radiation may be due to a roughly black-body component at a temperature of ∿ 30,000K. One can then estimate the surface area of the black-body emitter which could produce the far ultraviolet flux. Again, the intriguing part of the story is how naturally physical scales of ∿ 10 times the Schwarzschild radius came out. We need to see how well this whole story will survive scrutiny by further theoretical investigation and further data collection.

This is exactly the type of programme which is ideally suited to the unique capabilities of the Space Telescope. High angular resolution brings a large number of Seyfert galaxies within range of observation.

2.6 The hot big bang model of the Universe

Perhaps the greatest advance in cosmology over the last 20 years has been the evidence which has accumulated in favour of the hot big bang model of the Universe. Up till 1965, there had been persuasive evidence for the evolutionary character of the Universe but no direct evidence that the Universe had passed through a hot dense phase. In 1965, the discovery of the microwave background radiation and the subsequent discoveries of the Planckian nature of its spectrum and its isotropy were powerful evidence that the Universe had once been very hot and the radiation had had time to become thermalised. A natural way in which this could have come about is in the standard hot big bang model in which the Universe cools from a very high temperature, high density phase. Supporting evidence for this picture came from the abundance of ^{4}He which seems to have roughly the same universal abundance wherever it can be observed in the Universe and in exactly the proportions predicted by the theory.

More recently the case has become even stronger with the realisation that all the light elements which are rapidly destroyed in stellar interiors, D, ^{3}He, ^{4}He, ^{7}Li, can also be synthesised in the non-equlibrium conditions in the early stages of the hot big bang. What is remarkable is that it is possible to account for the observed abundances of all these species by a single hot big bang model which has density parameter in the range $\Omega \sim 0.03 - 0.1$. (i.e. $q_o \sim 0.015$-0.05). This is quite remarkable evidence that the Universe went through a hot dense phase and it is independent of the evidence provided by the microwave background radiation.

The importance of these discoveries is that, if the whole picture survives detailed scrutiny, we can use the hot big-bang framework for pursuing yet more difficult fundamental problems of cosmology. In particular, we can treat seriously the three basic problems of the hot big-bang, namely (a) the origin of the baryon asymmetry in the Universe (b) the origin of the isotropy of the Universe and (c) the origin of the fluctuations from which the fine-scale structure of the Universe evolved. Until recently, cosmologists supposed that these properties had to be ascribed to the initial conditions from which the Universe evolved - a totally unsatisfactory situation. We now begin to have the glimmering of an understanding of how these features might come about in evolutionary cosmologies at very early epochs. These possibilities have come about thanks to advances in elementary particle physics and the properties of the favoured schemes for unifying

all the elementary forces of physics. Again, this is not the place to review the way in which this may come about but it is important to note that some of the classical observations which have been made by astronomers may have profound implications for the very early structure and evolution of the Universe.

At the same time, there have been a number of major advances in describing the large scale properties of the Universe. Among these I would count as particularly significant:

(a) The use of cross-correlation functions to describe the large scale distribution of galaxies in the Universe: these studies have been completed for very large samples of galaxies in two dimensions and have now been made in 3-dimensions for samples of bright galaxies by Davis and his colleagues. Among the most remarkable results of studies of this type has been the discovery of the "great holes" in the Universe. The fact that these phenomena exist poses a particular challenge for the theory of galaxy formation.

(b) Evidence for the evolution of astrophysical objects over cosmological time scales. The evidence for evolution over cosmological time scales has been convincing for some time for active systems such as quasars and strong radio sources. These studies are now getting down to the details of how various classes of object evolve with cosmic epoch. The only problem with these studies is that they concern the evolution of rather exotic objects whose astrophysics are not properly understood.

I find particularly intriguing the evidence which is now accumulating for the evolution of the ordinary stellar component of massive galaxies with cosmic epoch.

Let me list some of the pieces of evidence:

(i) Gunn, Hoessel and Oke have shown that a number of giant elliptical galaxies at $z > 0.5$ have much bluer spectra than those at small redshifts.

(ii) Gunn has shown that for bright elliptical galaxies there is evidence for changes in the colours out to redshifts of 0.5 such that the galaxies are "bluer" than a $z = 0$ galaxy would appear redshifted by the appropriate amount.

(iii) Van der Laan and Windhorst have shown that faint radio galaxies which they infer have redshifts of about 0.5 to 1 are bluer than low-redshift galaxies of the same type.

(iv) Infrared-optical studies of radio galaxies by Simon Lilly and myself have shown evidence of strong evolution of the optical-infrared colours of the stellar component of those giant elliptical galaxies which are strong radio sources in the 3CR catalogue.

It is intriguing that most of these cosmological evolutionary changes in the properties of galaxies are in the same sense. Remarkably one of the simple models of galaxy evolution by Bruzual can account for many of the features of these observations. These are models in which, say, half of the gas in a galaxy forms into stars in the first 10^9 years and then the remaining gas forms into stars at an exponentially decreasing rate thereafter. Now, I do not claim that this is what is actually going on but the models are useful illustrations of the types of modification to standard galaxy models necessary to explain these observations.

Despite these real advances in astrophysical cosmology, there remain many stubborn problems which we must try to resolve. In no particular order, these are:

(a) What are the values of the basic parameters which describe the dynamics of the Universe, H_o, Hubble's constant and q_o the deceleration parameter? Despite years of the most difficult observation and analysis, there is no consensus about the values of either of these parameters. The range 50 to 100 km s^{-1} Mpc^{-1} spans the reasonable range of values of Hubble's constant appearing in the literature but there is no consensus on whereabout in this range it lies. There are excellent prospects that, with Space Telescope, this situation will improve through the use of distant Cepheid variables and through the use of supernovae either as classical standard candles, which Type I seem to be, or through the more physical Baade-Wesselink-Wagoner technique.

For q_o, in the sense of a global value of the deceleration of the Universe as a whole, I have less confidence that we will find a meaningful value by the classical redshift-magnitude relation. As mentioned above, we have strong reasons to believe that cosmological evolutionary effects are influencing the colours and absolute properties of distant galaxies and, until we can understand these thoroughly, we cannot hope to produce a reliable estimate of q_o.

(b) What is the mean density of matter in the Universe? I separate the question of the determination of the density parameter $\Omega (= 8\pi G\rho/3H_o^{-2})$ from that of estimates of q_o

because the relation $\Omega = 2q_o$ only holds if general relativity (with zero cosmological constant) is correct and, in general, this is a rather restricted set of possibilities. We ought to try to decide from observations whether or not $\Omega = 2q_o$ and this would give us more confidence that we are proceeding along the correct lines. Unfortunately the independent determination of Ω and q_o is so difficult that many cosmologists adopt the easy way out and suppose general relativity to be correct so that a good value of either q_o or Ω will do.

In fact Ω is probably easier to measure than q_o because we can use the classical methods of mass determination in astronomy but apply them on a grand scale to measure the gravitating mass in large representative volumes of space. The volume of space often used for this purpose is the Local Supercluster which corresponds to a volume of dimensions $\sim$ 20-30 Mpc. On the largest scale, various versions of the cosmic virial theorem can be used. Generally, these results ($\Omega \sim 0.1 - 0.5$) turn out to be somewhat larger than the value determined from the primordial nucleosynthesis of the light elements ($\Omega \sim 0.03 - 0.1$). There is not necessarily any fundamental contradiction between these values because the latter refers only to the baryonic component of the Universe whereas the former refers to all forms of matter including massless particles, massive neutrinos, primordial black holes, etc which would not influence the synthesis of the light elements provided their total mass density is not much greater than $\Omega = 1$. Perhaps the most intriguing aspect of this work is that it gives us an estimate of how much mass could be hidden on the largest scale in the Universe.

(c) What is the physical significance of the strong evolution observed in radio sources, quasars and now the stellar component of elliptical galaxies? All the evidence suggests that evolutionary effects in quasars and galaxies are strong and occur over relatively short cosmological time scales. We need to understand the physical causes of these evolutionary effects. The fact that these effects are observed at relatively small redshifts suggests that with the Space Telescope, we may be able to see much stronger effects occurring in the more distant past.

The basic problem here is that there is no theory of quasars and radio sources which is sufficiently secure for it to be used to predict what the relation between the galaxy and its active nucleus should be. We can all hazard guesses as to how it comes about. The central black hole is fed by gas and, possibly stars, from the surrounding galaxy and grows until it becomes a quasar-like object when its mass is $\sim 10^8 M_\odot$ and there is a ready supply of fuel. But it is not at all clear how ideas like these can be put into a form which provides quantitative relations between galaxy and quasar evolution. We need more physical understanding of quasar, radio galaxy and galactic evolution to be able to put flesh on this question. We have seen how these studies are now possible out to redshifts $z \sim 1$ and I am optimistic that we will gain great insights from studies of these objects in this redshift range as well as by studying those at the largest redshifts with Space Telescope.

(d) Is there a redshift cut-off in the distribution of quasars at redshifts $z \sim 4$ and is this related to the epoch of galaxy formation? The evidence that there is cosmological evolution of the stellar component of galaxies is relatively recent but we have known about the evolution of radio sources and quasars for much longer and these objects can be observed at much greater redshifts than ordinary galaxies. The evolutionary effects for quasars and radio sources are very large indeed corresponding to an increase in the comoving space density of sources by a factor of 10^3-10^4 between redshifts of 0 and 2-3. Whatever the nature of the evolution, something drastic is occurring over this redshift interval.

We have known for a long time that this evolution had to converge at redshifts of the order 2-3 but it is not clear whether or not there is a cut-off at a redshift $z \sim 3.53$, the upper-limit to known quasar redshifts until recently.

The most persuasive evidence that such a cut-off might exist came from Osmer's searches for large redshift optically selected quasars in which he expected to find 9 recognisable quasars on grism plates in the redshift range $3.5 < z < 4.7$ whilst none were found. Various explanations could be advanced for such a cut-off:

(a) There might be intervening dust in the discs of galaxies. By a redshift of 3.5, a large fraction of the celestial sphere is covered by the discs of galaxies and one can arrange parameters so that the optical depth becomes about 1 at $z \sim 3.5$.

(b) There may be a lack of Lyman-continuum photons or gas around large redshift quasars in which case the characteristic Lyman-α line would not be present to be observed.

(c) Galaxies may only condense out of the intergalactic gas at $z \sim 4$.

(d) It may take considerable time to grow the massive black holes needed to power the most powerful quasars. It could be that at $z > 4$, there are quasars but they have not grown to the stage at which they are hyperluminous.

(e) Perhaps in the young galaxies, there is so much dust and gas that all the emission of the quasar is absorbed and reradiated in the infrared waveband.

It is easy to devise tests of various aspects of these hypotheses which can be undertaken by Space Telescope.

We have been working on the interpretation of the radio source counts and V/V_{max} tests for radio selected objects and we have some hints that there may indeed be a cut-off which would suggest that the "obscuration" theories may not be correct. However much more work is required to make the argument a strong one.

Remarkably, enough, just after Osmer's paper appeared, Ann Savage and her colleagues in Australia identified a quasar which turned out to have redshift $z = 3.78$ earlier this year. All this tells us is that the redshift cut-off, if it exists may not be very abrupt but then, no-one really believed it should be sharp anyway. It was one of those ironical coincidences which often happen in astronomy that this discovery was made through the optical identification of a flat spectrum radio source at exactly the same time that the UK Schmidt team in Australia took the first high dispersion prism plates with a new prism, one of the main objectives of which was to find quasars with redshift $z \sim 4$. The initial search was unsuccessful but, with the discovery of a quasar with $z = 3.78$, we are confident that there are many more large redshift quasars to be found. Space Telescope will be one of the most important tools for identifying those distant quasars and investigating the reality of this cut-off.

(e) What are the processes by which galaxies and clusters first formed? If one is an optimist, as most cosmologists have to be, it may be that studies of quasars and possibly galaxies over the redshift range 0 to 3 will provide us with real clues to the processes by which galaxies and clusters first formed. There are various tests one can think of which might give us clues to the overall dynamical evolution of the large scale structure of the Universe. For example, one particularly nice test will be to compare the covariance function for galaxies at a redshift $z \sim 1$ with that at the present epoch. We should be able to see directly how the covariance function has evolved over a significant cosmological time frame and thus test directly the way in which gravitational condensation in the expanding Universe takes place. However, it is unlikely that we will get much evidence of this type at very large redshifts.

Many cosmologists believe that most of the basic processes which are responsible for the condensation of galaxies and clusters into bound systems occurred in the redshift range $5 < z < 1500$. A cynic might argue that it is remarkably convenient for the theorist or speculator to push these processes to a redshift range which is very difficult for observation and thus diminish the possibilities for confronting theory with observed fact.

In principle, if there exist discrete objects in this redshift range, we should be able to investigate their properties and physical conditions along the line of sight to them. However, I believe it may prove very difficult to find such objects. Clearly, they would have to be highly luminous objects to be observable and the best objects for this purpose, the quasars, show at least a convergence in their distribution, if not a cut-off, at redshifts about 4. In addition, there is the awkward fact that the comoving volume per unit interval of redshift decreases as $z^{-1.5}dz$ and so even if the comoving space density of sources remains constant, the probability of finding large redshift objects decreases.

If we cannot use discrete objects, we only have the integrated properties of these objects to look for i.e. diffuse emission from a background of sources or emission and absorption features in the background radiation. Distortions of the spectrum of the microwave background might provide some information but at present the evidence suggests that these distortions must be rather small.

I am not at all optimistic about studying this redshift interval on the basis of what we know. I suspect we need a new discovery to make progress in this area.

My best bet at the moment would be to look for aspects of current theories of galaxy formation which are potentially testable over the redshift range within which galaxies and quasars will be observable. The classical scenarios of galaxy formation (which are basically maintained in more recent studies involving massive neutrinos) may be divided into the adiabatic and isothermal pictures. The basic physical difference between these pictures is that in the former, all fine scale structure is washed out by various damping

mechanisms in the early Universe ($z > 1500$) so that the largest scale structures form first; in the latter, the small scale structure forms first and large scale systems form later by hierarchial clustering. The epoch at which the system first formed may be roughly estimated by equating the mean density of the system which forms first to the mean density of the Universe at that epoch. It is therefore clear that the basic difference is between models in which galaxies form late in the Universe ($z < 5$-10) and those in which the first structures formed much earlier, $z \sim 20$-1000. They also correspond to models in which galaxy formation takes place by fragmentation of large systems or by hierarchial clustering of smaller objects. It is rather pleasant that the two basic models result in two very different pictures and this certainly gives me some hope that we may be able to disentangle how the large scale structure of the Universe came about by direct appeal to observation.

Of course, in addition to these broad pictures, we can appeal to astrophysical processes associated with the formation of the discrete objects themselves. It is virtually certain that the formation of all types of galaxy involves dissipation by radiation and in the most massive systems, the dissipation may result in the emission of strong X-ray and ultraviolet radiation as shock waves heat up the matter collapsing into "pancakes" in the adiabatic theory. This is a potential source for heating and ionising the intergalactic gas discussed by Zeldovich, Sunyaev and their colleagues.

Another possible source of heating appears in a recent model by Ostriker in which it is argued that if galaxies undergo a period of rapid early star formation, which produces much of the heavy elements, the result of the large number of supernovae will be to drive a high temperature shock front out through the surrounding intergalactic medium. Ostriker has proposed that the collision of the blast waves from different galaxies results in a new generation of galaxy formation, much in the same way that the collision of supernova shells may result in high compressions and enhanced star formation. It is an important question whether or not this process could occur on a sufficiently large scale to account for the "cell-like" structure observed in the distribution of galaxies. Again, this process occurring at redshifts $z \sim 5$-10 may result in detectable ultraviolet radiation. One might see bright "sheets" on the sky where the dissipation has taken place.

If I were forced to express a personal opinion on which model I would favour, I am attracted to the adiabatic picture for two basic reasons. First, it naturally explains why strong evolutionary effects should be observable rather late in the Universe. Since objects only form at redshifts $z \sim 5$-10, it is natural that we should see very strong evolutionary effects over this redshift range. Second, the model provides a direct explanation for the large scale holes in the Universe. I am not implying that it is not possible to explain this phenomenon in other models, but it is much less a basic prediction of the other models. If my guess were correct, then it would have the consequence that galaxy formation is brought within the range of observationally accessible redshifts at essentially all wavelengths and this would be a very exciting prospect.

(f) How secure are our ideas about the chemical composition of the primordial material from which galaxies and clusters formed? Proceeding yet further back in time, a crucial cosmological datum provided by ultraviolet astronomy has been the cosmic abundance of deuterium. It cannot be overemphasised how important the abundance of the elements, D, ^{3}He, ^{4}He, ^{7}Li are for the hot big bang model. They provide totally independent evidence from that of the observation of the microwave background radiation that the Universe went through a very hot, dense phase. They also provide us with the possibility of determining the mean baryonic mass density in the Universe as well as a number of important constraints on elementary particle physics.

Deuterium will just be observable by the High Resolution Spectrograph of the Space Telescope and it is of obvious importance to study the constancy or variability of this species in a wide variety of different cosmic environments including comets, the interstellar gas, the Galactic centre etc.

(g) What can the astronomer do about the questions now being raised by particle physicists about the very early evolution of the Universe ($10^{-44} > t > 10^{-5}$ seconds)? It is remarkable how rapidly what a few years ago would have been regarded as wild speculation can become orthodoxy. Whilst Grand Unified Theories are not yet an essential part of every undergraduate astronomer's course, things are moving in that direction. These ideas address themselves directly to the three fundamental questions which I listed at the very beginning of the present section (which is still 2.6!). In turn, these are derived from conclusions which are drawn from astronomical observations plus the best theory we have available. It is our job to subject these observations and the best astrophysical theory to the most searching of scrutiny because there are fundamental issues at stake, some of which may only be addressed by appeal to what happened in the first 10^{-44} second in the Universe. Each part of the picture within our observable

Universe must be tested and all the questions raised above under headings (a) to (f) should receive convincing answers before we can proceed back to the earliest stages.

2.7 Conclusions

It will have been apparent that essentially all the major issues I have highlighted in the above summary can be addressed in a unique manner by the Space Telescope. In addition, you will have noticed that many of the issues involve observations in wavebands other than the optical and ultraviolet. Thus, all astronomers, no matter what their wavelength persuasion, will have a vested interest in the success and results of the Space Telescope. It will also be noted how the whole picture interlocks like a giant jigsaw. If one part of the picture changes, it has repercussions far beyond its immediate significance. This, of course, is one of the great attractions of astronomical research. The ultimate synthesis into a grand cosmological picture is the work of a huge number of separate lines of investigation.

3. Concerns about the Space Telescope Scientific Programme

I will indicate some of the questions which I believe we ought to be addressing as a community in order to reap the maximum scientific advantage from the Space Telescope.

3.1 The rapid evolution of modern astronomy

The immense strides which have been taken in the last 30 years in modern astronomy must represent one of the greatest periods of advance ever in astronomy. It is remarkable how rapidly advances have been made even over a period as short as the last five years, i.e. from the time the Space Telescope project was approved. It is worthwhile recalling some of the major advances which have taken place over that period. To select some prominent events:

(i) The International Ultraviolet Explorer (IUE);
(ii) The Einstein X-ray Satellite Observatory;
(iii) The Very Large Array;
(iv) The Voyager I and II missions to Jupiter and Saturn.

It is difficult now to imagine our view of astronomy without these observatories and the huge contributions they have made to our knowledge of astronomy. Equally the description of the major problems of astronomy and cosmology which I presented in Section 2 is largely based upon recent understanding of these problems. I would have written a rather different picture five years ago. Then, we did not know about the double quasar which is convincingly demonstrated to be a gravitational lens, or the convincing demonstration of superluminal velocities in 3C273, or about precessing relativistic jets in SS433, and so on.

I believe the period up to the launch of the Space Telescope will be one of equally rapid evolution of our subject and we must be in a position to respond to these new challenges in the programmes proposed. My reason for seeing major advances in the next few years is largely based upon the widespread use of highly efficient electro-optical devices on most of our large telescopes. These have made possible many programmes which would have been essentially impossible by traditional techniques. They enable us to address the basic questions in a much more systematic and quantitative form than has been possible previously.

We must therefore ensure that the maximum flexibility is built into the procedures by which observing programmes are selected for observation by the Space Telescope. It would be wrong to judge the importance of the programmes by what were seen to be the essential questions in 1977 or 1982.

3.2 The need for systematic observations

At the recent Vatican Study Week on Astrophysical Cosmology, I made a list of some of the most important observational results which formed the basis for our present understanding of the Universe and the objects which populate it. I reproduce this as Table 2.

You will notice that all of these result from large and systematic studies. In other words, rarely in astronomy does one make a single simple observation which results in a quantum leap in our understanding. As soon as such a phenomenon is observed, the immediate question is "How common is it among similar objects of its class?" and true understanding only comes from further systematic studies. Perhaps the most striking exception to this rule is the discovery of the microwave background radiation but I would argue that there is no other member of its class available for observation in cosmology!

Table 2

Some studies described during the Vatican Study Week

The covariance function for galaxies
The three dimensional distribution of galaxies
The luminosity-velocity dispersion relation
Evolution of giant elliptical galaxies
Distances of nearby galaxies
Surveys of radio quiet quasars
Radio galaxy identifications
X-ray counts for quasars and active galaxies
D, ^{3}He, ^{4}He, ^{7}Li abundances

Therefore, I firmly believe that the way forward is through the pursuit of systematic studies in all the fields selected for observation by Space Telescope. It may of course be that we are lucky and another single great discovery will be made which at a stroke answers some of the profound problems which I have described above. Realistically speaking, however, such a discovery is most likely to come out of the systematic studies, as for example, happened in the cases of quasars, pulsars, X-ray binaries, etc.

This is not a trivial question when one considers how many observing programmes there are and the finite life of the telescope. I would make a plea that certain large scale programmes of observation should be undertaken in a systematic way in order to ensure that many of the basic programmes are carried out. An excellent recent example of the importance of these studies is the IUE collaboration on NGC 4151. In total about 80 8 hour shifts have been devoted by the consortium to its study and the discovery of the correlated activity would not have been achieved without the agreement of many astronomers that this object was of unique importance. None of the astronomers involved would have dreamed of such an important result before the shifts were allocated and yet it has paid huge dividends. I recall that at the Princeton meeting on "Scientific Research with the Space Telescope", Dr Sargent suggested that we would really learn something about active nuclei if all the observing time on Space Telescope were dedicated to observations of NGC 4151, 3C 273 and M 87. I am sure every astronomer will have his own favourite objects to replace these active galaxies.

My personal hope is that large bodies of astronomers will appreciate the importance of devoting adequate time for systematic studies with Space Telescope and form consortia who will enable these projects to be carried out. Indeed, one could speculate whether or not a large portion of the time on Space Telescope might not be allocated in this way. This brings me naturally to the next point which concerns how much science one will be able to achieve.

3.3 The time available on Space Telescope

It is becoming clearer what the observing constraints will be for Space Telescope and how to optimise ones observing programme to make best use of the time available. The basic constraints are set by the requirement that the telescope be adequately shielded from sunlight and the bright Earth and the fact that the slew rate of the telescope is roughly the rate at which a minute hand moves around a clock face. This means that for any substantial exposure you have to be on the darkside of the Earth and hence that individual exposures are limited to less than about 40 minutes per orbit. One can, of course, achieve long exposures by adding together successive orbits.

There are thus advantages in working in relatively small fields and avoiding changing guide stars as much as possible. Even when one does this, it is important to look at how long it takes to achieve limiting performance of the telescope. For example, the Wide Field Camera will probably be able to achieve about $V \sim 28$ in a single 40 minute exposure. This is the sort of magnitude one would want to achieve to measure Cepheid variables in galaxies of the Virgo cluster. Suppose you wanted to measure the distances of 10 galaxies in the Virgo cluster by measuring the light curves of their Cepheid variables. Then, using, say, 10 epochs per galaxy, one would require 100 half orbits. In terms of useage of the telescope, this would correspond to about 150 hours of telescope time or roughly 6 days. In fact since the average time for science will only be about 30-35%, it is more likely that this would take about 10 days of real time.

The point of this example is to show that some of the most important programmes which push the capabilities of the system to the limit are very time consuming. At the other extreme, planetary observations could easily flood the whole community with data in a very short time.

However one does the sums, Space Telescope observing time will be a very scarce commodity

and it is plain that observing time should only be granted to those programmes which not only are of the highest scientific importance but also make most effective use of the available time. Thus, I believe we should not necessarily be looking to achieve limiting performance all the time. We will get a better scientific balance by limiting the numbers of very long exposures to certain crucial observations. The advantages of diffraction limited performance and the opening up of the ultraviolet waveband for imaging and high sensitivity spectroscopy will be such as to produce vast amounts of important data in half orbit observations.

3.4 Ground based back-up

I have two main concerns here. First, there is the question of whether we have appropriate ground based material to be compared with the superb quality of data which we will receive from the Space Telescope. My own experience of trying to accumulate suitable high quality material for the programmes I would like to carry out with Space Telescope has been that it requires a huge effort to get it all together. One really needs access to the same types of instruments which will be flown on Space Telescope. Nowadays, digital spectrographs are in general use world-wide but CCD and IPCS cameras are not yet available to all users on large telescopes. There is so much which can be done from the ground with these devices that I hope they are fully exploited before the time comes to request Space Telescope time.

My second concern relates to the image processing facilities which will be available to the user at his home institute for the analysis of the science data. Most of the world leading institutes now have their own image processing facilities but there is at present little standardisation and one worries about the technical feasibility of astronomers analysing their data effectively at their home institution. There are many data processing systems and we must ensure that there is not excessive duplication of effort. We have tried to avoid this in the UK by developing a national system for astronomical image processing, "Starlink", with linked VAX computers and one would hope that such a system might be expanded internationally and thus take some of the pressure off the facilities at the Space Telescope Science Institute.

3.5 The Space Telescope Science Institute

Finally, I should mention the singular importance of the Space Telescope Science Institute, currently under construction at John Hopkins University, Baltimore. This will become one of the great astronomical centres of the world. However, it will be remembered by most of us for the service it provides to us as users in being able to capitalise fully on the unique capabilities of the Space Telescope. We must provide Dr Giacconi and his team with every support in accomplishing a most difficult but vital task.

4. Conclusion - a historial paradigm for the Space Telescope

Reflecting on the Space Telescope project, one tries to think of historical paradigms which may illuminate the sort of progress we might hope to make with such a facility. For me, the closest historical parallel is with Tycho Brahe and the construction of his great observatory on the island of Hveen near Denmark in the period 1576 to 1586. For me, Tycho Brahe is one of the greatest of scientists. In many ways we should consider him to be the father of modern astronomy. Unlike other geniuses of the period, such as Kepler and Newton, he was a brilliant instrument designer and observer. He appreciated the importance of making systematic observations over long periods. He aimed to achieve the ultimate accuracy possible and to that end designed and constructed the most advanced instruments of his time for the measurement of the positions of the stars and planets. All these instruments used the naked eye, Galileo's discovery of the telescope being still 30 years in the future. He was the first astronomer to take into account effects such as the refraction of light in the Earth's atmosphere and the flexure of his large instruments under gravity both of which would lead to systematic errors in his measurements over the sky. He was the first astronomer to understand the importance of systematic and random errors in his observations. These are now all part of standard scientific practice but it took a genius like Tycho Brahe to appreciate their importance at a time which predates the work of Galileo and Newton.

In the end, Tycho Brahe achieved an accuracy of 2 arcmin in his observations of the stars and planets from systematic observations over a period of 20 years. This represented an order of magnitude improvement over all previous work. His final catalogue listed the positions of 777 stars which represents more than 75% of the stars which can be observed with the naked eye from the latitude of Denmark. In addition, the motions of the Sun and the planets on the sky were systematically measured over a period of up to 20 years.

All this would have been impossible without adequate sponsorship and this was provided by King Frederick II of Denmark who, realising the scientific prestige of Tycho Brahe,

prevented him "brain-draining" to Germany by making him an offer he could not resist. He was offered the island of Hveen for the purpose of building the best observatory possible and was provided "with sufficient endowments to enable him to carry out astronomical observations in the most effective way". In fact, the whole enterprise was an expensive undertaking, the great observatory at Hveen having cost Frederick II "more than a tun of gold", according to Tycho, which is probably equivalent to about $5-10 million at todays prices.

One cannot but be struck by the similarities between Tycho's great project and the Space Telescope project. Both projects were supported by enlightened agencies for the advancement of pure science; both projects increased the precision of astronomical observations by an order of magnitude or more over what was possible previously; for both projects, a dedicated science institute was created; the durations of the projects were similar; both projects utilised the ultimate in scientific technology available to them.

We can only hope that the ultimate scientific return from the Space Telescope will be as great as that of Tycho's observatory. From Tycho's observation, Kepler was able to show that the orbit of Mars was not a circle but an ellipse with the Sun located at one focus. This conclusion could not have been drawn from previous work since the discrepancy between the best fitting circular orbit and the observed orbit was only 8 arcmin i.e. a 4σ discrepancy which Kepler rightly considered to be unacceptable, so strong was his confidence in Tycho's observations. He then went on to derive all three of his Laws of Planetary Motion from Tycho's observations of the movement of the Sun and planets against the background of fixed stars. In turn, Newton derived from Kepler's laws, his Law of Gravity which must rank as one of the greatest intellectual achievements of all time. In his analysis, the fact of elliptical rather than circular orbits was crucial as confirmation of the inverse-square nature of the law of gravity. Note, however, that this would not have been possible without the brilliant observational data of Tycho Brahe. If we achieve with Space Telescope anything which even remotely approaches the fundamental importance of that great discovery, Space Telescope will have achieved real greatness.

References

The sources of material described in this review are so vast that I have made no attempt to reference every fact. Detailed discussion of most of the topics can be found in the following volumes:

M.S. Longair and J. Warner (eds), 1979. "Scientific Research with the Space Telescope", IAU Colloquium No. 54, NASA Special Publication CP-2111.

F. Macchetto, F. Pacini and M. Tarenghi (eds), 1979. "Astronomical Uses of the Space Telescope", ESA/ESO Workshop, ESA Special Publication.

G.O. Abell and P.J.E. Peebles (eds), 1980. "Objects of High Redshift", IAU Symposium No. 92, D. Reidel Publishing Company.

C. Hazard and S. Mitton (eds), 1979. "Active Galactic Nuclei", Nato Advanced Study Institute, Cambridge University Press.

S.M. Fall and D. Lynden-Bell (eds), 1981. "The Structure and Evolution of Normal Galaxies", Nato Advanced Study Institute, Cambridge University Press.

D. Sugimoto, D.Q. Lamb and D.N. Schramm (eds), 1981. "Fundamental Problems in the Theory of Stellar Evolution", IAU Symposium No. 93, D. Reidel Publishing Company.

D. Hanes and B. Madore (eds), 1980. "Globular Clusters", Nato Advanced Study Institute, Cambridge University Press.

R. Balian, P. Encrenaz and J. Lequeux, (eds), 1975. "Atomic and Molecular Physics and the Interstellar Matter", Les Houches Summer School No. 26, North-Holland Publishing House.

A.G. Davis Philip and D.S. Hayes (eds), 1982. "Astrophysical Parameters for Globular Clusters", IAU Colloquium No. 68.

D.S. Heeschen and C.M. Wade (eds), 1982. "Extragalactic Radio Sources", IAU Symposium No. 97, D. Reidel Publishing Company.

H.A. Brück, G. Coyne and M.S. Longair (eds), 1982. "Astrophysical Cosmology", Proceedings of Vatican Study Week, Publications of Pontifical Academy of Sciences.

The reader is also referred to recent issues of "Annual Reviews of Astronomy and Astrophysics" for up-to-date authoritative surveys of many of the topics referred to in this review.